Size-selective Synthesis of [*n*]Cycloparaphenylenes and Related Benzenoid Macrocycles

By

Jacob Keith Istre

A thesis submitted to the Graduate Faculty of Auburn University

in partial fulfillment of the

requirements for the Degree of

Master of Science

Auburn, Alabama

May 6, 2023

Approved by

Dr. Bradley Merner, Chair, Associate Professor of Chemistry

Dr. Rashad Karimov, Associate Professor of Chemistry

Dr. Stewart Schneller, Professor of Chemistry

Dr. Byron Farnum, Associate Professor of Chemistry

Abstract

This work begins with a discussion of the currently existing methods for the *π*-extension of nonplanar aromatic systems with a focus on reactions pertaining to the *π*-extension of cyclophane-based molecules. Completing the first chapter is a synthesis of "[*n*]PQPPs", a new model system developed for the purpose of modeling *π*-extension on *para*-linked curved benzenoid systems, particularly with the goal of investigating reactions for use with [*n*]cycloparaphenylenes.

The second chapter includes a review of the history of [*n*]cycloparaphenylene synthesis and the key methods that are in use for the construction of these nanohoop structures, which represent the smallest possible cross section of armchair carbon nanotubes. After this summary of the field, I report my size-selective synthesis of [6], [8], and [10]cycloparaphenylenes from a cyclohex-2-ene-1,4-diol-containing key intermediate building block, along with an attempted synthesis of [5]cycloparaphenylene which fell short only at the final step. A pathway is then proposed for the completion of [5]CPP based on previous results in our lab.

The third and final chapter of this document follows this with a summary of the existing strategies for the functionalization of [*n*]CPPs, including publications in which the functional groups are installed early in the sequence and carried through the steps as well as late-stage modifications of existing cycloparaphenylenes. Ending this chapter is a concise synthesis of an octamethoxy derivative of [12]cycloparaphenylene, which is proposed as a precursor to a wide cross section of a [12,12]carbon nanotube.

Acknowledgements

This project would not have been possible without my Research Advisor, Dr. Bradley L. Merner. Thank you for your direction and for your willingness to keep explaining all the details when I had dumb questions. Special thanks to the Department of Chemistry and Biochemistry Chair, Dr. Doug Goodwin, for his leadership in the department and investment in the graduate students. I am also indebted to my advisory committee members for their input and guidance: Dr. Rashad Karimov, Dr. Stewart Schneller, and Dr. Byron Farnum. Many thanks also to my current and former lab mates for their team work, encouragement, and feedback all along the way.

I can't go without thanking my wife, Sarah, and my daughter, Holly, for motivating and supporting me. You are the reason I do what I do. Finally, I offer thanks to the God who created science and reason for the ability to seek and discover answers in the world around us. "He is before all things, and in Him all things hold together." – Colossians 1:17

Table of Contents

List of Figures

List of Abbreviations

[*n*]CPP	[*n*]cycloparaphenylene
[*n*]PQPP	[*n*]-para-quinquephenylophane
[*n*]PTPP	[*n*]-(3,3")-para-terphenylophane
APEX	annulative pi extension
Ar	arene or aryl
Bpin	pinacolatoboron
CNB	carbon nanobelt
CNT	carbon nanotube
Cod	1,5-cyclooctadiene
CyJohnPhos	2-(Dicyclohexylphosphino)biphenyl
DBU	1,8-Diazabicyclo(5.4.0)undec-7-ene
DCM	dichloromethane
DDQ	2,3-Dichloro-5,6-dicyano-1,4-benzoquinone
DFT	Density Functional Theory
DMAc	N,N-dimethylacetamide
DMP	Dess-Martin periodinane
FVP	Flash Vacuum Pyrolysis
Grubbs II/G-II	Grubbs' second generation catalyst
Hoveyda-Grubbs II/HG-II	Hoveyda-Grubbs second generation catalyst
HPLC	high pressure liquid chromatography
LDA	lithium diisopropylamide
n-BuLi	*n*-butyllithium
NMR	nuclear magnetic resonance
PAH	polycyclic aromatic hydrocarbon
RCM	ring-closing metathesis
S-Phos	2-Dicyclohexylphosphino-2′,6′-dimethoxybiphenyl
TBAF	tetrabutylammonium fluoride
TEMPO	2,2,6,6-Tetramethylpiperidinyloxyl
TES	triethylsilyl
THF	tetrahydrofuran
TsOH	para-toluenesulfonic acid
X-Phos	2-Dicyclohexylphosphino-2′,4′,6′-triisopropylbiphenyl

CHAPTER 1 "PQPPs": A NEW MACROCYCLIC CURVED AROMATIC SYSTEM FOR THE DEVELOPMENT OF *π*-EXTENSION REACTIONS ON *PARA*-PHENYLENE-BASED STRUCTURES

1. INTRODUCTION

For well over six decades, the synthesis of curved aromatic *π*-systems has been a field of strong interest to the community of organic chemists due to their interesting spectroscopic properties compared to their planar counterparts, along with their potential applications in several burgeoning areas of scientific advancement, such as drug delivery and materials science. Nonplanar aromatic hydrocarbons can be placed into three major categories (**Figure 1**). The first category is the [*n*]circulenes. When the central ring of the [*n*]circulene is not equal to six (*i.e.,* a hexagon) the structure of the fully encircled (with benzene rings) polygon takes on a nonplanar or warped structure. Central rings smaller than six carbons yield bowl-shaped structures (*e.g.* corannulene or [5]circulene) with positive curvature, while larger rings induce negative curvature and typically adopt a saddle-like shape. A second category of curved aromatic systems is found in the [*n*]helicenes, which consist of a string of four or more angularly, *ortho*-fused benzene rings. The interaction between atoms at opposing ends of these strands of aromatic rings, which are trying to occupy the same regions of space, causes them to twist away from planarity into a helical shape, hence their name. Finally, the third and most important category, as it pertains to this work, is seen in the [*n*]cyclophanes. This class of compounds is defined as a macrocyclic structure that contains a central aromatic ring system that is tethered at two non-adjacent positions. Essentially, the tether pulls on the ends of the aromatic ring(s) and bends the sp^2 hybridized atoms out of planarity. Before discussing the synthesis of a new class of cyclophanes that contain a nonplanar *p*-quinquephenylophane (PQPP) unit, a brief discussion of the limited *π*-extension reactions available is in order.

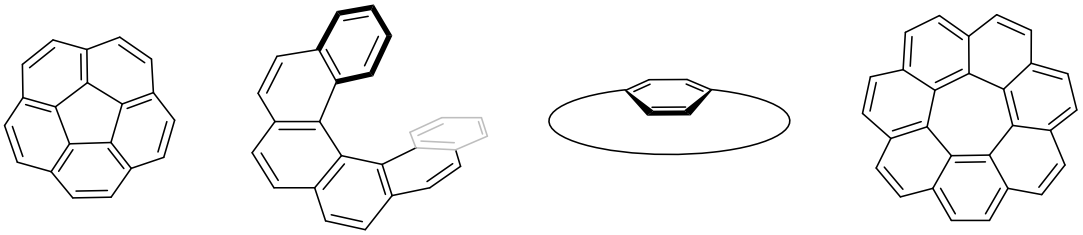

1.1: corannulene ([5]circulene) **1.2: [6]helicene** **1.3: [*n*]paracyclophane** **1.4: [7]circulene**

***Figure 1**: Examples of the three categories of curved aromatics*

1.1 Cyclophanes as models for [*n*]cycloparaphenylenes and platforms for the development of *π*-extension reactions

1.1.1 Relevant classes of cyclophanes

In order to introduce this new class of cyclophanes, which we have dubbed *para*-quinquephenylophanes ([*n*]PQPPs), it will be helpful to place them into the context of other types of macrocyclic benzenoid systems that have been reported. The first and simplest of these classes is the [*n*]*para*cyclophanes. These cyclophanes consist of a benzene ring that has been connected by an aliphatic chain/tether at the *para* positions. A strained member of this kind of cyclophane, [6]paracyclophane (**2.4**), was reported by Tobe and coworkers in 1986 (**Figure 2**).[1] A second type of cyclophanes which is highly relevant to our discussion is the [*n*](3,3")*para*-terphenylophanes ([*n*]PTPPs) which were first reported by Merner and co-workers in 2015.[2] That synthesis, which will be shown in more detail below, was not only suitable for generating a bent phenylene unit that is calculated to have a higher strain energy than a monomer unit of [4]CPP in the case of macrocycle **2.5**, but these compounds come with built-in directing groups in the form of the alkoxy tether, which allows for the straightforward functionalization that can facilitate the development of *π*-extension reactions of the curved aromatic system.[2,3,4]

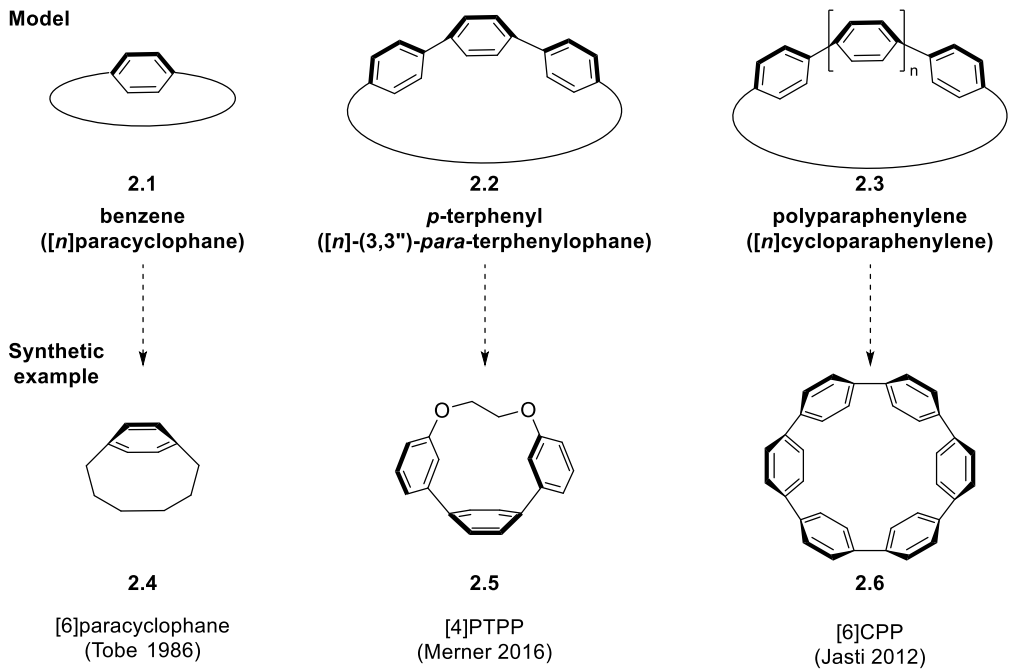

***Figure 2**: Models of the types of cyclophanes and the corresponding synthetic examples*

The third class of compounds to be discussed here are the [*n*]CPPs (*e.g.,* **2.3** and **2.6**), which are not truly cyclophanes in the traditional sense, but are included in this list because of their similarity to the other cyclophanes mentioned and because of their relevance to the development of *π*-extension chemistry

and Chapter 2 of this thesis. [*n*]CPPs represent the smallest diameter-defining cross-section of armchair carbon nanotubes (CNTs) and have been touted as key intermediates in the highly challenging bottom-up synthesis of uniform-diameter CNTs. One of the most strained examples of the [*n*]CPPs, [6]CPP (**2.6**), is shown in **Figure 2**. This highly strained homolog was reported by Jasti and coworkers in 2012,[5] followed by an even more strained homolog ([5]CPP) in 2014. It should be noted that Yamago and co-workers reported a synthesis of [5]CPP at almost the same time as Jasti and co-workers.[6,7]

1.1.2 π-Extension reactions of p-terphenyl-based macrocycles: models for [n]CPPs

The uniquely designed construction of the [*n*]PTPP system (*i.e.* the curved, central *para*-phenylene unit, which is adjacent to arene units that can be selectively functionalized) makes it a great platform for the development of annulative *π*-extension reactions that will form new 6-membered rings, which constitute new polycyclic aromatic hydrocarbon (PAH) systems. These molecular scaffolds can effectively act as model systems for the testing of *π*-extension strategies that can later be used for elaboration of curved, extended *π*-systems. Furthermore, the size of the macrocycle can be modified to investigate the amount of curvature—and therefore strain energy—the central benzene ring can withstand and still undergo annulation. This allows the various sizes of macrocycle to act as model systems for the different sizes of [*n*]CPPs, depending on the strain energy contained within the bent, central *para*-phenylene. Since one of the over-arching goals of the bottom-up synthesis of CNTs or CNT fragments is to convert a benzenoid system to a larger, non-planar PAH, the use of the [*n*]PTPPs as macrocyclic, strained model systems is relevant.

In 2018, our group published a report detailing the use of a homologous series of [*n*]PTPPs as platforms for annulative *π*-extension via the Scholl reaction.[4] Outlined in **Figure 3A** is the synthesis of a bent PAH which is a sidewall segment of an [*n,n*]CNT. Using a well-established sequence of reactions (discussed in detail below), several of the macrocyclic systems were synthesized with varying tether lengths (*n* = 7 to 12). Alkoxy-directed regioselective bromination of the tethered aryl unit with molecular bromine produced tetrabrominated [*n*]PTPP derivatives in high yields, followed by Suzuki coupling with 4-*tert*-butylphenylboronic acid to give **3.3a-f**. The Scholl reaction takes place under the mediation of iron(III) chloride to give cyclodehydrogenation products **3.4A** and **3.4B**, forming not only a curved sidewall segment of a nanotube, but also a bent [5]helicene unit. While most attempted cyclodehydrogenation reactions for this purpose have had limited success, it was discovered that the key to obtaining the desired PAH was in the amount of strain energy inherent in the central benzenoid *para*-phenylene ring. It was calculated that a strain energy of 4.3 kcal/mol or less would allow for the successful Scholl reaction, furnishing **3.4A** versus the rearrangement product **3.4B** when the strain energy is greater than 4.3 kcal/mol. A thorough investigation of this reaction revealed that the rearrangement reaction likely takes place after the first

(desired) annulation as the increase in strain energy upon the second annulation is significantly higher than the first C-C bond formation. .

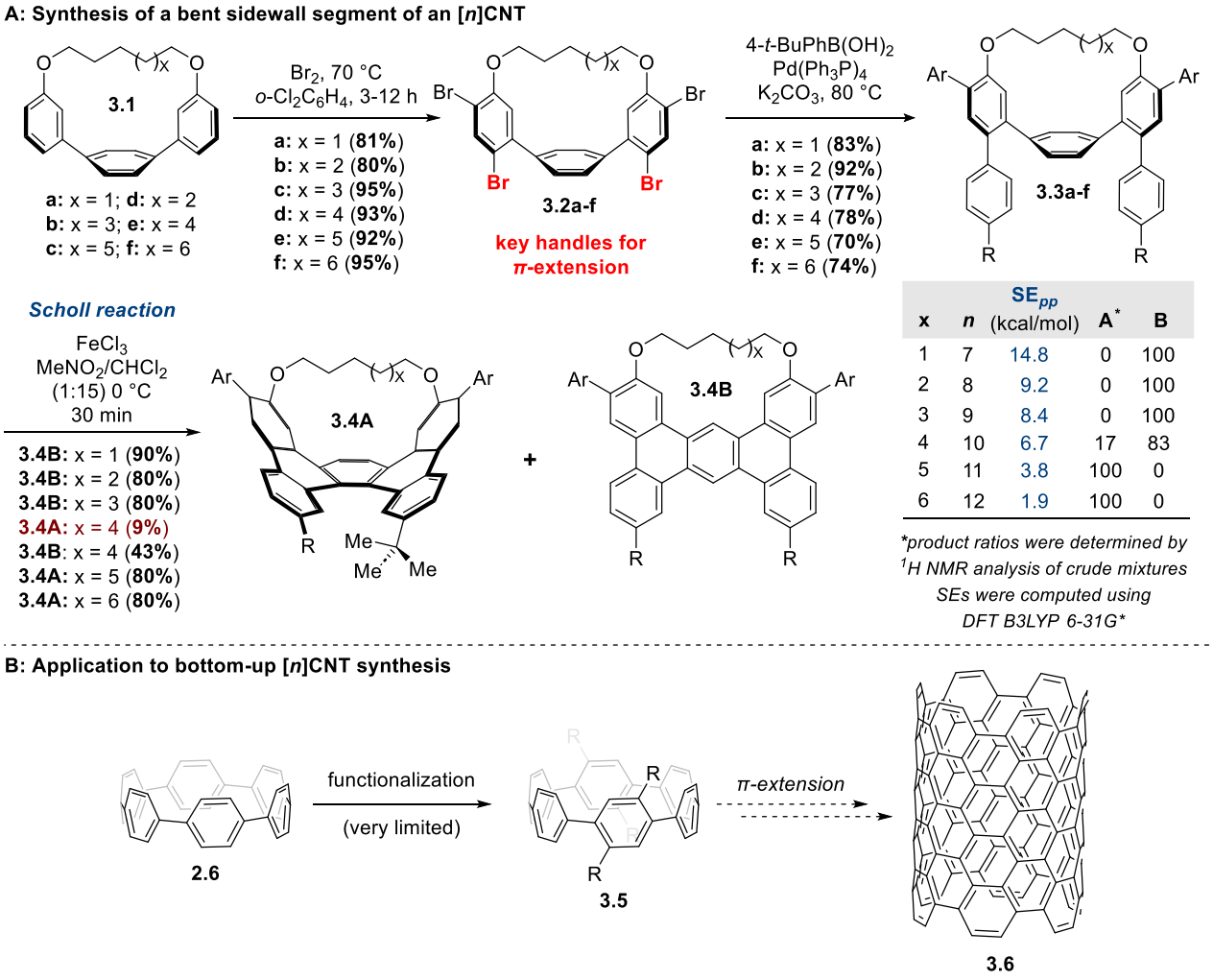

***Figure 3**: Synthesis of bent [n]CNT segments from [n]PTPPs via the Scholl reaction and potential application to the synthesis of [n]CNTs*

1.1.3 The [n]PQPPs as another useful model system for the development of π-extension reactions

The [*n*]PTPPs have clearly been shown to function as useful precursors for the synthesis of curved PAH structures. However, the aforementioned *π*-extension strategy has some limitations. Specifically, as discussed above, the cyclodehydrogenation annulation reaction only works on a central ring that has less than 4.3 kcal/mol strain energy. Thus, alternative annulation methods need to be discovered and investigated, with the most desirable tactic being to perform a late-stage modification of pre-constructed

macrocyclic systems. In 2022, Merner and co-workers reported a new strategy for *π*-extension that involves the treatment of an aryl alkyne (installed via Grignard reaction with an *α*-ketol derived from the common diol precursor of PTPPs) with iodine monochloride at –78 °C to generate a bent phenanthrene subunit that contains both an aryl and vinyl iodide functional handles, which can be used, in theory, for further functionalization.[8] This synthesis will be discussed in detail later, but the general idea is presented in **Figure 4**.

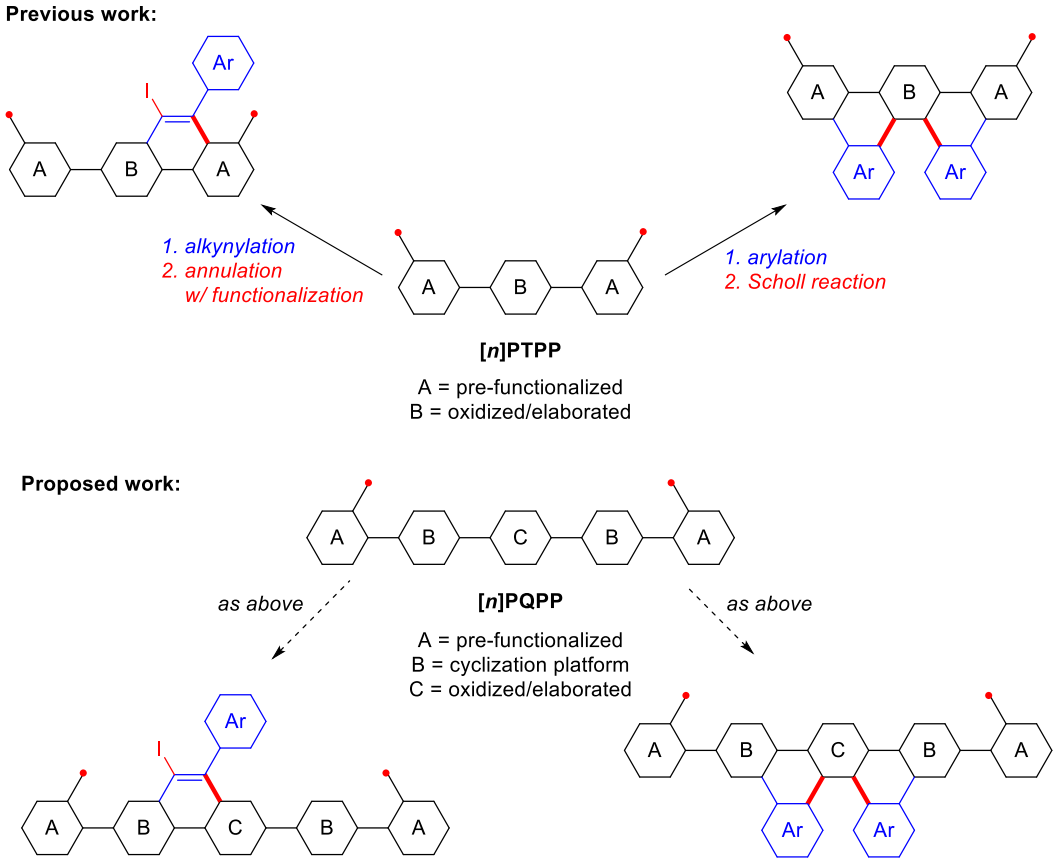

***Figure 4**: General methodologies for π-extension of [n]PTPP and [n]PQPP model systems*

Figure 4 shows the general strategy for converting tethered macrocyclic poly-*para*-phenylenes into PAH units. Rings at the terminal end of the poly-*para*-phenylene systems are pre-functionalized due to the presence of alkoxy directing groups. Also in each system, the central benzene ring can be oxidized and elaborated through a multi-step process before aromatization to install suitable functionality to enable skeletal building reactions and elaboration of the poly-*para*-phenylene units . The key difference between the two classes of macrocycles, aside from the *meta* vs *ortho*-oriented tether connection, is the presence of rings **B** in the PQPP system. These additional rings are projected to act as a platform for annulation, provided appropriate functionality (*i.e.* aryl or arylethynyl groups) on the **A** and **C** rings, which provides a

reasonable hope of creating a much larger *π*-extension product than is possible with PTPPs. For example if the arene unit installed during the alkyne addition reaction is a naphthalene ring, it can be subjected to cyclodehydrogenation to continue the pi-extension of the PQPP unit. Furthermore, because the [*n*]PQPPs contain a sequence of three *para*-substituted curved benzene rings, they act as a more accurate model for CPPs, which is the ultimate goal of this project.

1.2 Examples of *π*-extension reactions on pre-existing strained aromatic units

1.2.1 [n]Circulene-centered π-extension strategies

After multiple publications detailing the multifaceted chemistry of corannulene,[9] including several π-extension strategies, the group of Lawrence Scott outlined a procedure for the synthesis of a [5,5] carbon nanotube (CNT) from a corannulene endcap (**Figure 5**).[10]

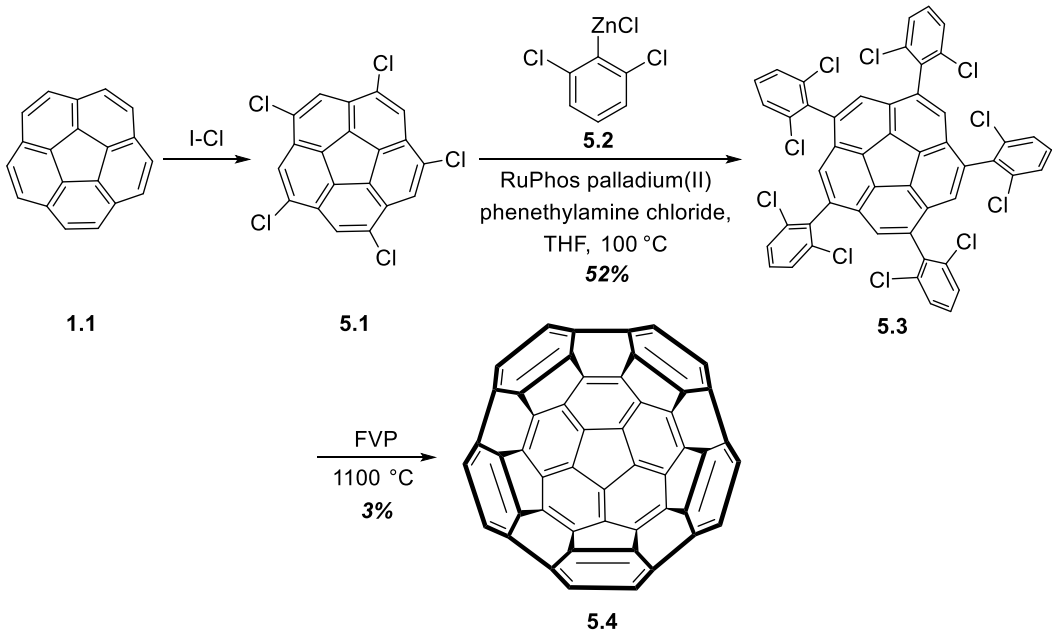

***Figure 5**: Synthesis of an ultrashort [5,5] single walled CNT*

Starting from corannulene (**1.1**), direct chlorination by iodine monochloride forms intermediate **5.1** (pentachloroannulene), which is then subjected to Negishi coupling with 2,6-dichlorophenylzinc chloride (**5.2**) to yield intermediate **5.3** in 52% overall yield (**Figure 5**). Flash vacuum pyrolysis (FVP) of **5.3** at 1100 °C gave the desired nanotube (**5.4**) in 3% yield. Though the yield of the last step was low, only **5.4** was obtained, and this result set the precedent for bottom-up chemical syntheses of CNT targets.

Another synthesis beginning from a corannulene derivative was published by Itami and co-workers, in collaboration with the Scott group, in 2017.[11] Penta(Bpin)corannulene (**6.1**) underwent fivefold Suzuki coupling with 2-bromo-2'-chlorobiphenyl (**6.2**) under dipalladiumtris(dba) catalysis with S-Phos as ligand, giving **6.3** in 76% yield followed by Pd-catalyzed direct arylation with DBU and DMAc to give penta[6]helicene corannulene **6.4** in 10% yield (**Figure 6**).

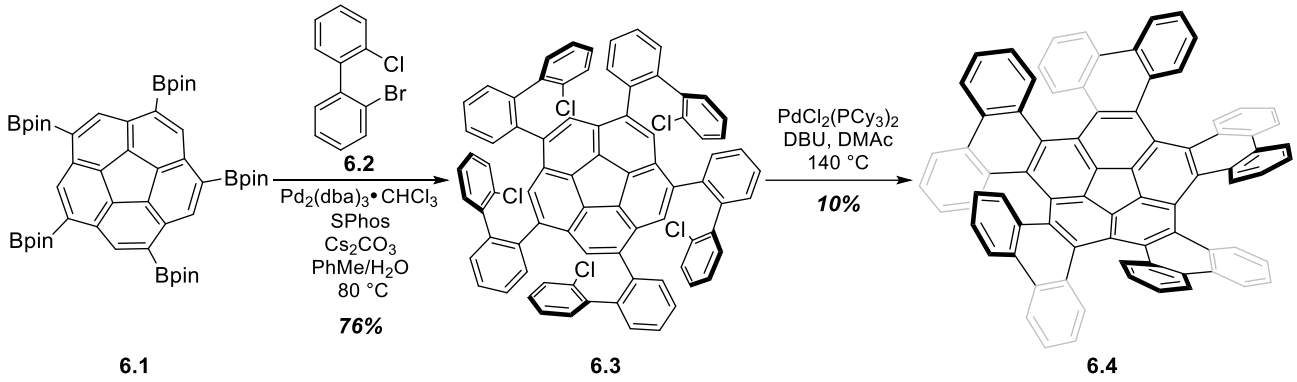

***Figure 6**: Synthesis of quintuple-[6]helicene corannulene*

In 2018, the Miao and coworkers added two highly warped nanographenes to their burgeoning library of circulene-based molecules.[12] From moderately warped diketone **7.1**, a divergent strategy gave two highly distorted *π*-sheets, **7.2** and **7.4,** synthesized in 29% and 23% overall yield, respectively (**Figure 7**). Beginning from the diketone, a Ramirez reaction followed by fourfold Suzuki coupling to each brominated position gave intermediate **7.4**, which was subjected to a DDQ-mediated Scholl reaction to give twisted structure **7.5** in 63% yield. To obtain a more symmetrical nanographene, diketone **7.1** was treated with lithiated fluorene to give the addition product, which was then dehydrated using TsOH to give **7.2** in 64% overall yield. Scholl reaction of this intermediate produced saddle-shaped structure **7.3** in 45% yield.

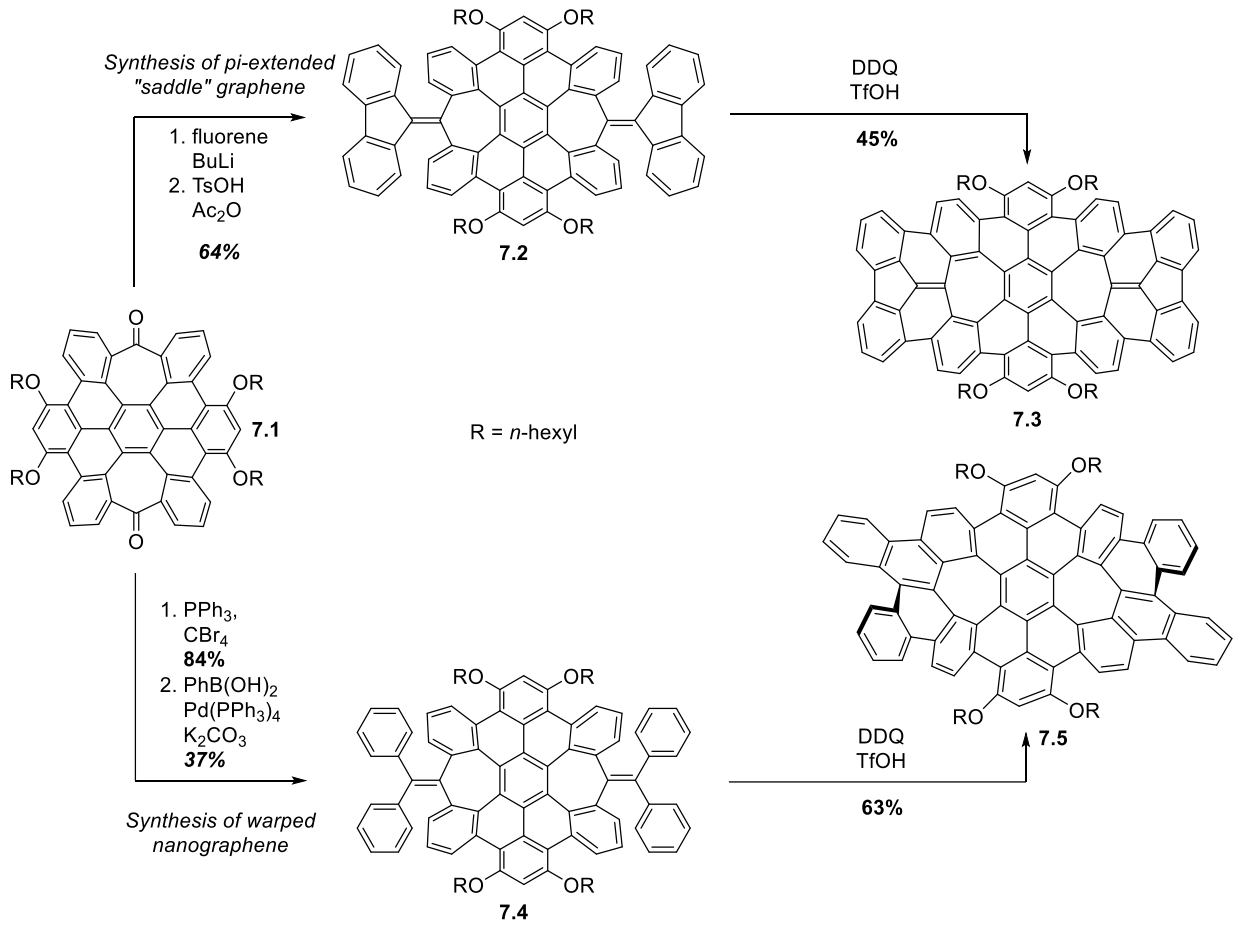

***Figure 7**: Synthesis of π-extended saddle graphene and warped nanographene from the same curved aromatic precursor*

1.2.2 [n]CPP-centered π-extension strategies

The primary class of macrocyclic benzenoid systems, aside from the [*n*]PTPPs discussed above, that have be subjected to the development of *π*-extension reactions are the [*n*]cycloparaphenylenes ([*n*]CPPs). These molecules, also known as 'carbon nanohoops', represent the smallest cross-section of armchair CNTs. Each *para*-phenylene subunit of an [*n*]CPP is connected to the adjacent ones by single bonds to the *para* positions, forming a macrocyclic loop of curved benzene rings. A more detailed conversation about the synthesis of [*n*]CPPs will be forthcoming in Chapter 2, but for this portion of the thesis, we will highlight some uses of CPP derivatives as templates for *π*-extension. These examples are quite limited (the two included below are the only confirmed reports of *π*-extension of existing CPPs, to my knowledge), underscoring the pressing need for innovation in the field of bottom-up CNT synthesis.

The first of these examples was reported by the group of Jasti and co-workers. Using a strategy that the same group had reported for the synthesis of [6]CPP in 2012, the Jasti group reported the synthesis of nanobelt-based segments within [*n*]CPP core structures, in 2016. The most strained of these pi-extended nanohoops is shown in **Figure 8**.[13] Starting from 1,4-dibromobenzene (**8.1**), sequential aryllithium addition to two equivalents of intermediate **8.2** followed by silylation of tertiary alcohols and alkene isomerization produced **8.3** in 38% overall yield. Macrocyclization through a previously established Suzuki protocol with 1,4-bis-Bpin-2,5-divinylbenzene (**8.4**) furnishes macrocycle **8.5** in 11% yield. Desilylation with TBAF, then aromatization using mild reductive conditions, tin(II) chloride and HCl, gives vinylated [6]CPP **8.6** as a *π*-extension precursor. Ring-closing metathesis with Grubbs' second-generation catalyst gave *π*-extended CPP **8.7** in 28% yield. Though the low overall yield is a downside to this synthesis, the resultant PAH segment installed within the [6]CPP framework represents one of the first such structures to come from a pre-functionalized [*n*]CPP derivative.

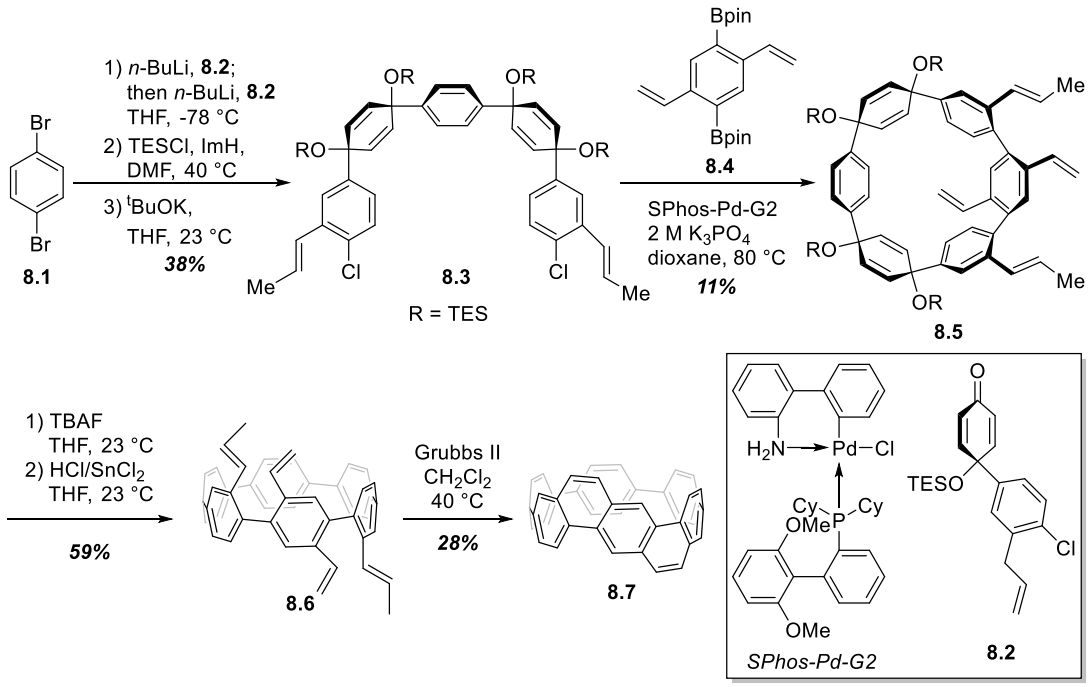

***Figure 8**: Synthesis of a π-extended CPP from an olefinated [6]CPP derivative*

In 2019, the Miao group published the synthesis of two new carbon nanobelts, which are shown below in **Figure 9**. One of these is an armchair segment of a CNT (representing [12,12]CNT), and the other is a segment of chiral [18,12]CNT.[14] Following synthesis of the functionalized nanohoops via a simple five-step elaboration from *p*-quinone-2,5-dibenzyl ether to make **9.1a** and **9.3a**, similar to what had been previously reported by Jasti and Bertozzi (addition of aryllithium, methyl protection, borylation of bromides,

macrocyclization, aromatization), benzyl groups were cleaved and replaced by triflate handles, which underwent Suzuki reaction with (3,4-dipropoxyphenyl)boronic acid to yield **9.1c** and **9.3c** in 12% and 7% yield, respectively, over 3 steps. Cyclodehydrogenation under Scholl conditions ($FeCl_3$ or DDQ/$Sc(OTf)_3$), gives nanobelt **9.2** in 21% yield and chiral nanobelt **9.4** in 66% yield. These molecular targets represent a significant step forward in the field of CNT synthesis and *π*-extension of existing bent aromatic structures and are particularly significant, as these examples represent the first to employ [*n*]CPPs as diameter defining templates for CNT synthesis.

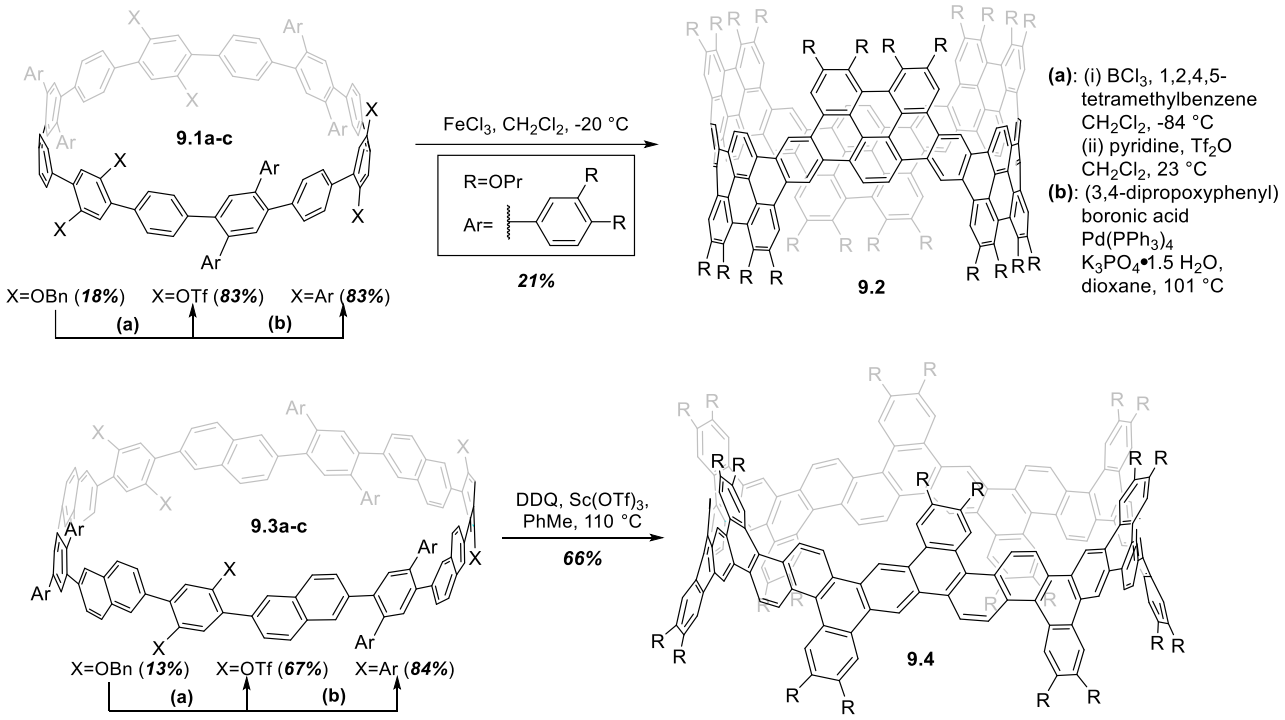

***Figure 9**: Synthesis of two CNBs from π-extension of nanohoops*

The limited number of examples that have been presented above has not been done so with any sort of selection criteria – these are representative of the state of the field of *π*-extension reactions upon strained aromatic systems. This clearly speaks to the need for the development of new strategies *π*-extension of strained benzenoid and small PAH-based structures and the need for synthetic innovation in this area.

1.3 Research Objectives of the Merner Laboratory

1.3.1 Development of model systems to represent [n]CPPs and subsequent π-extension strategies

Given the limited number of methods for synthesizing substituted, highly strained [*n*]CPP derivatives, the first order of business in our research program was to create a new class of molecules that could effectively act as models for [*n*]CPP monomer subunits. Toward this goal, the [*n*](3,3")*para*-terphenylenophanes ([*n*]PTPPs) were envisioned. These macrocyclic structures would consist of a central *para*-phenylene unit, where most of the molecule's strain energy is located, and adjacent arene units containing a *meta*-substituted alkoxy tether between them to induce strain in the system (*see right*) and to direct substitution reactions at these rings. The strain imposed upon the central ring can be modulated based on the length of the tether to simulate various sizes of [*n*]CPPs and their associated *para*-phenylene ring strain.

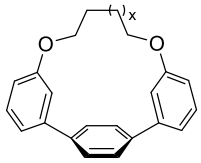

***1**: [n]PTPP*

1.3.2 Discovery of new π-extension reactions for strained aromatic systems

Once the model PTPPs had been produced on a sustainable scale, the next step was to devise a plan for *π*-extension of the systems. To this end, the PTPP core structure will need to be functionalized in a predictable way, preferably through late-stage modification of the completed macrocyclic backbone. Following this, suitable reactions will need to be found which match two criteria: the reactions must 1) allow for *π*-extension of existing aromatic structures, and 2) be powerful enough to induce additional strain while still being mild enough to avoid destruction of the macrocyclic core or rearrangement of the strained aromatic rings to a planar configuration.

1.3.3 Application of the newly developed π-extension strategies to [n]CPPs

After a suitable strategy has been established based on the model system(s), it is then hoped that the model reactions can be employed on one or more [*n*]CPPs to yield π-extended CNBs. This is a challenging synthetic endeavor, as the late-stage modification of [*n*]CPPs is very limited, with only two examples: a selective bromination by Yamago, *et al* and a strategy involving an intermediate transition metal complex of [9]CPP published by Itami (see Chapter 3 for details).[15] Thus, a strategy for the late-stage functionalization of a pre-arene unit would be suitable, or introducing the necessary functional groups at an early stage of the [*n*]CPP synthesis must be developed. In the case of the latter, the functional groups

need to be reasonably robust in order to survive the several synthetic steps that include aryllithium/Grignard additions, cross-coupling, and aromatization reactions.

1.4 Relevant Previous Research in the Merner Group

In order to synthesize the [*n*]PTPPs, a non-cross-coupling protocol was developed for the synthesis of the envisioned macrocycles.[2] From suitable tethered diaryl-dialdehydes, a simple 4-step procedure (later streamlined to become more efficient; see **Figure 11**) gave the desired 1,4-diketone intermediates in high overall yield (**Figure 10**). In the initial report, the dialdehydes (**10.3**) are the product of a two-fold Williamson ether synthesis between 3-hydroxybenzaldehyde and the desired dihaloalkane. These dialdehydes then undergo addition by vinylmagnesium chloride followed by ring-closing metathesis using Grubbs' second-generation catalyst. Hydrogenation with H_2 gas and palladium on carbon, then oxidation of the alcohols with Dess-Martin reagent gives the desired macrocyclic diketones (**10.4**) without cross coupling and with only two chromatographic steps.

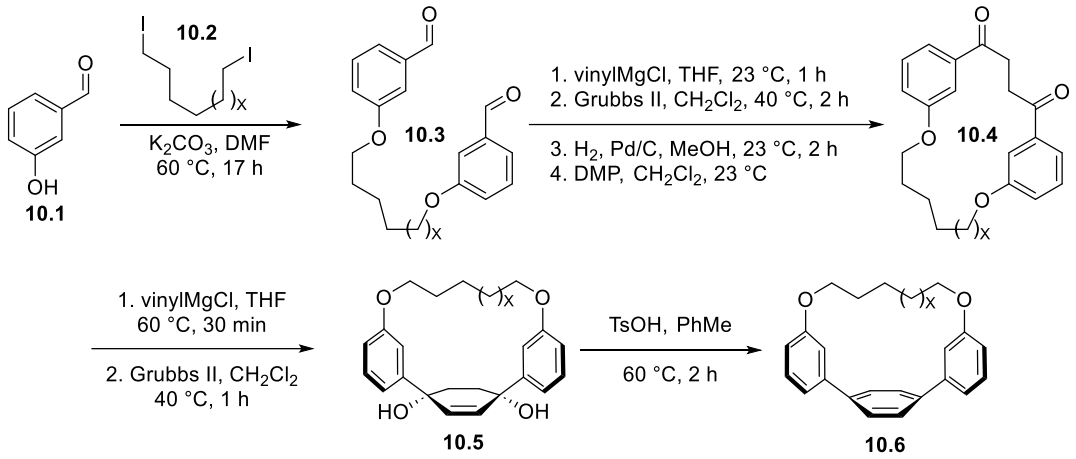

***Figure 10**: First-generation synthesis of [n]PTPPs*

These intermediates are now ubiquitous in our lab, spreading even beyond the *π*-extension work into natural product synthesis as the starting material to synthesize cyclobutene-containing structures.[16] After isolation of the macrocyclic diketone, diastereoselective Grignard addition of two vinyl groups followed by ring-closing metathesis provides cyclohex-2-ene-1,4-diol as the *syn* diastereomer. Due to the conformation of the macrocycle, Grignard addition to the 1,4-diketone is highly selective for the *syn* diol product, allowing for diastereoselectivity ratios of over 20:1 for more strained macrocycles. Finally, a

dehydrative aromatization reaction using TsOH (for less strained systems) or a milder version that employs the Burgess reagent, furnishes [*n*]PTPPs in good yield. The synthesis reported in Figure 10 is taken from the initial synthetic report of this class of macrocyles. Since then, some modifications to the synthetic approach have been developed. Most notably, a switch from the standard palladium-catalyzed hydrogenation to a transfer hydrogenation using sodium borohydride and the already-present Grubbs-type catalyst. These modifications are seen in the synthetic discussion presented below.

Notably, the smallest of the [*n*]PTPPs (with only 4 total atoms in the tether, hence the name [4]PTPP) necessitated a modified process in the final stages due to the large amount of strain energy imposed on the central benzene ring (**Figure 11**).[3] Dialdehyde **11.1** (from 3-hydroxybenzaldehyde and 1,2-dibromoethane) was treated with vinylmagnesium chloride, followed by a ring-closing metathesis and transfer hydrogenation in one pot, and concluding with oxidation of the secondary alcohols by the action of Dess-Martin reagent to afford diketone **11.2** in 15% overall yield. Next, another treatment with vinyl Grignard and subsequent ring-closing metathesis gave **11.3** in 59% yield. Under the standard aromatization conditions (Burgess reagent in toluene, 80 °C), only trace amounts of the desired [4]PTPP were observed, along with partially dehydrated intermediate **11.4**. Switching solvent to tetrahydrofuran and lowering the temperature, along with careful management of Burgess reagent stoichiometry, allowed for optimization of the reaction to prefer **11.4** over the interesting carbamate product **11.5**, which comes from an unexpected reaction of the Burgess reagent.

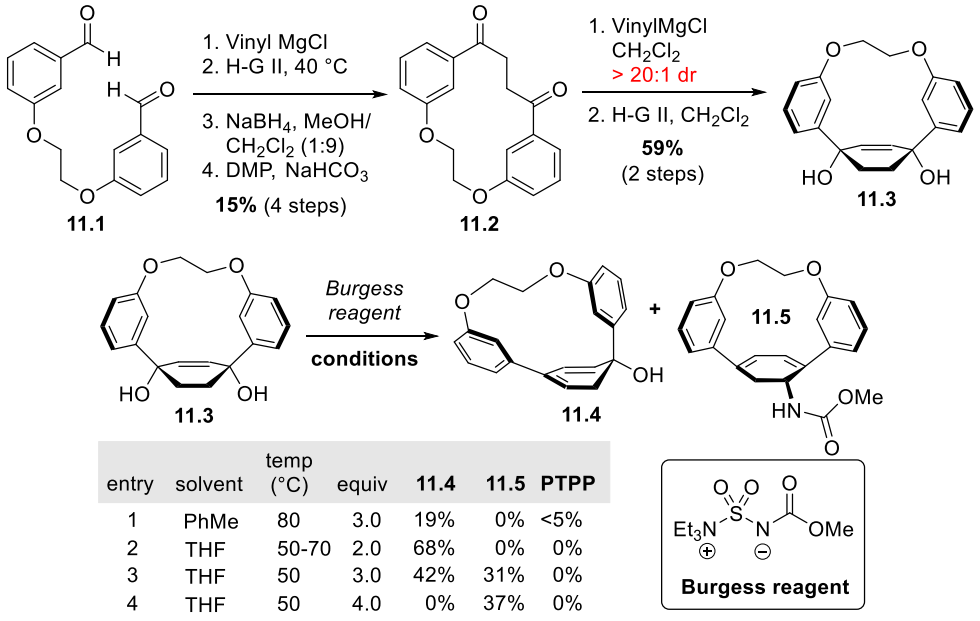

entry	solvent	temp (°C)	equiv	11.4	11.5	PTPP
1	PhMe	80	3.0	19%	0%	<5%
2	THF	50-70	2.0	68%	0%	0%
3	THF	50	3.0	42%	31%	0%
4	THF	50	4.0	0%	37%	0%

***Figure 11**: Synthesis of partially dehydrated intermediate for [4]PTPP*

Conversion of the alcohol in **11.4** to the corresponding acetate **12.1**, followed by elimination with LDA resulted in aromatization to afford **12.2** (**Figure 12**). The central *para*-phenylene ring that is created in the last two steps of the synthesis contains a strain energy of 43 kcal/mol, which is larger than the calculated SE per *para*-phenylene unit of [4]CPP (SE_{pp} = 36 kcal/mol).[17] The total SE imposed on 12.2 in during the aromatization of **11.4** is 51.3 kcal/mol, which is higher than the SE induced per *para*-phenylene unit in the Jasti and Yamago syntheses of [5]CPP (SE_{pp} = 43.7 kcal/mol).[7] This work provides cautious optimism that the aromatization and cyclophane-based strategy developed for 12.2 can be employed in the synthesis of [4]CPP, a synthetic target that has yet to be synthesized.

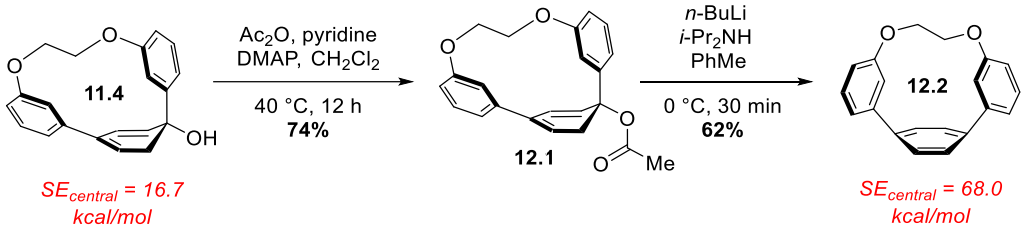

***Figure 12**: Completion of the synthesis of [4]PTPP*

In 2022, Merner and co-workers reported an *π*-extension reaction of a macrocyclic benzenoid system that involves an iodine monochloride-mediated alkyne annulation reaction at low temperature. This reaction is capable of inducing additional strain to the already bent central *p*-phenylene unit of an [8]PTPP and forging a twisted, chiral phenanthrene unit which is functionalized with another aryl group and a vicinal vinyl iodide in the K-region of the newly formed PAH.[8] After synthesis of the cyclohexene-1,4-diol intermediates **10.6** as discussed above, allylic oxidative rearrangement by the action of TEMPO-based oxoammonium salts converts these substrates into *α*-ketol intermediates **13.1a-c** (**Figure 13**).[18] Grignard addition of various alkyl, alkenyl, alkynyl and aryl groups to α-ketols **13.1c** (**x** = 3) afforded a series of 1,2-diol products **13.2c**, which were subjected to aromatization by TsOH or Burgess reagent to afford functionalized [8]PTPPs. Ten examples (**13.3a-j**) have been reported with overall yields ranging from 25-73% yield.

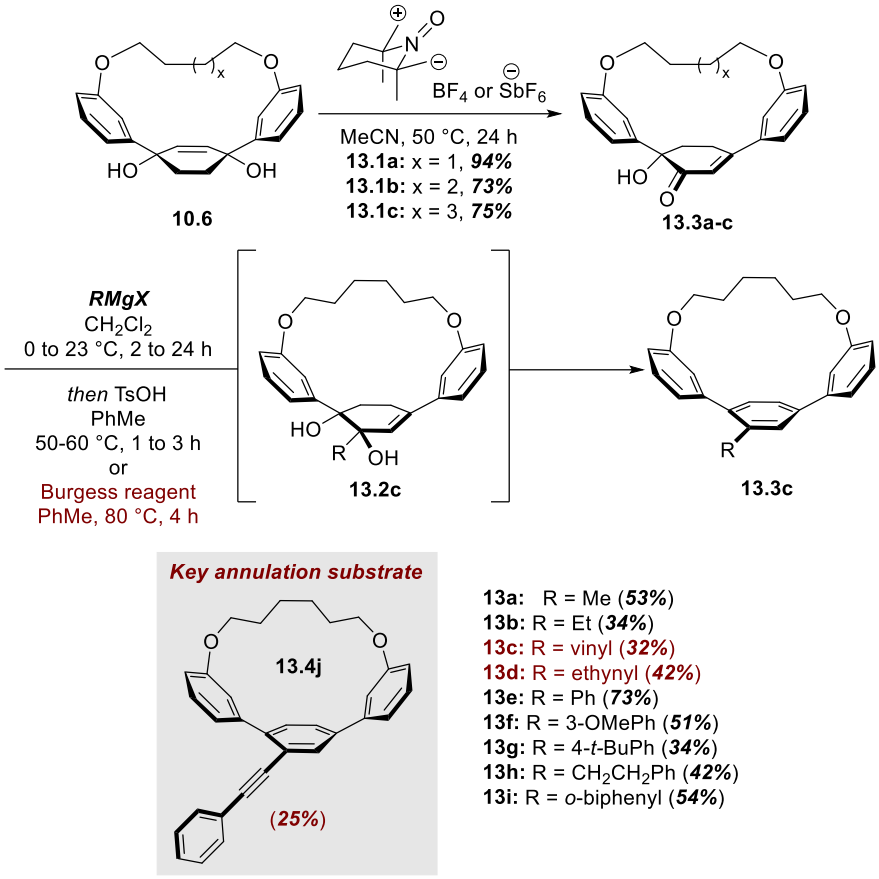

***Figure 13**: Synthesis of alkynylphenyl[8]PTPP, a key annulation substrate*

Unfortunately, attempts at oxidative arylation using the Scholl reaction on materials with arene substituents (**13.3e-i**) did not afford the desired *π*-extended products. Surprisingly, all materials subjected to Scholl conditions underwent rapid decomposition (< 1 h) and no tractable products were isolated. However, based on the reports from the Chalifoux lab of alkyne benzannulations mediated by iodine monochloride to generate phenanthrene systems containing adjacent arene and iodine substituents in the K-region,[19] the indicated phenylethynyl-substituted material (**13.3j**) was subjected to the conditions. This reaction proved to be successful, with an 82% yield of *ortho*-annulated (relative to the alkoxy tether) curved phenanthrene (**14.1**) . *Para*-annulated product **14.2** was not observed, and DFT calculations indicated that the *ortho*-annulation product was the less strained of the two regioisomers, which is opposite of the unstrained model system. It is likely that the steric congestion is outweighed by conformational constraints of the macrocycle, forcing annulation onto the *ortho* position by the iodonium intermediate. This report represents an advancement in the field of *π*-extension reactions on curved aromatic systems. It is envisioned that a similar reaction performed on a suitably functionalized/substituted [*n*]CPP could lead to the same *π*-extension reaction and potentially produce a short CNT (see Chapter 2).

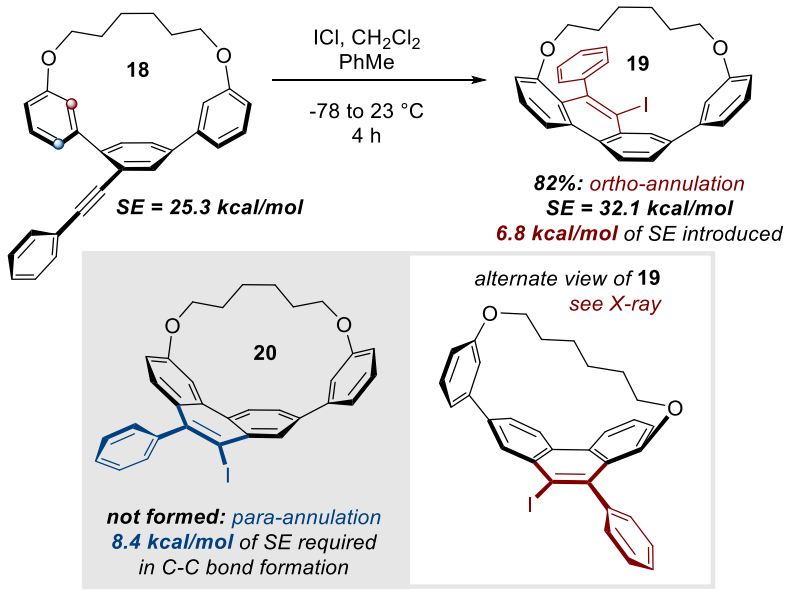

***Figure 14**: Iodine monochloride-mediated annulation of alkynylated [8]PTPP*

1.5 Synthesis of "PQPPs": Another Model System for the Development of π-Extension Reactions of [*n*]CPPs

As has been shown, the central arene units of [*n*]PTPPs are suitable models for the individual *p*-phenylene rings in [*n*]CPPs. At the same time, there are still one major drawback of the [*n*]PTPPs: the arene backbone only contains a single *para*-phenylene ring system. Thus, their usefulness in portraying reaction conditions suitable in [*n*]CPPs may be limited to a single annulation reaction or annulation of a single para-phenylene ring. That is, they will not shed much light onto the prospects of subsequent annulation reactions and the construction of larger PAH units or CNB segments. To address this gap, a new model system was envisaged: the *para*-quinquephenylenophanes, or "PQPPs", as they are referred to here. These molecules, as the name implies, contain five benzene units rather than three; the middle three phenylenes are *para*-linked while the other two are tethered by an alkoxy chain at their *ortho* positions. This change in the arene backbone allows for the investigation of reactions that can be used on a more [*n*]CPP-like framework. We believe that [*n*]PQPPs are a useful model system for the discovery of π-extension reaction conditions that will be applicable to [*n*]CPPs.

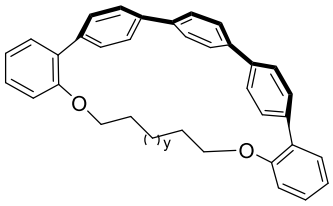

***2**: [n]PQPP*

The first goal for the synthesis of [*n*]PQPPs is to obtain a dialdehyde structure that is analogous to the first intermediate in the [*n*]PTPP sequence. The aryl tether is introduced first from a suitable dibromoalkane in a classic Williamson ether synthesis procedure with 2-iodophenol (**15.1**) in anhydrous DMF, giving tethered diiodide **15.3a-c** in excellent to quantitative yield in the same way as the dialdehyde

is generated for the [*n*]PTPPs (**Figure 15**). Following this step is a Suzuki reaction with 4-formylboronic acid (**15.4**) and tetrakis(triphenylphosphine)palladium(0) in a mixed solvent system, which gives dialdehydes **15.5a-c** in 84-97% yield. These dialdehydes are suitable precursors for the key 4-step procedure to synthesize macrocyclic 1,4-diketones.

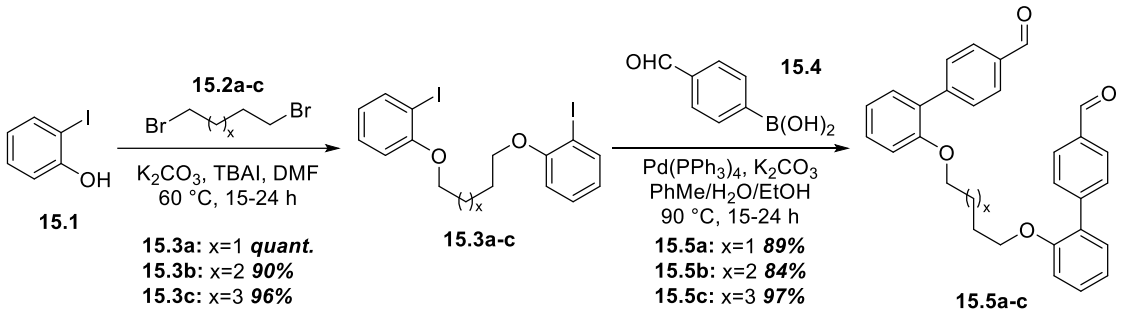

***Figure 15**: Synthesis of dialdehyde intermediates for [n]PQPPs*

Once the pure dialdehydes were prepared on multigram scale, they were subjected to the streamlined macrocyclic 1,4-diketone procedure developed in our laboratory. First, a Grignard reaction with vinylmagnesium chloride in anhydrous dichloromethane at 0 °C gave allylic diol intermediates **16a-c**, which was directly treated with Hoveyda-Grubbs second-generation catalyst in a dilute solution of dichloromethane at reflux (**Figure 16**). After this reaction was completed, the mixture was concentrated and then dissolved in a 1:7 solution of methanol/dichloromethane and treated with sodium borohydride at room temperature to reduce the resultant double bond formed during the RCM reaction by transfer hydrogenation. It should be noted that the same portion of catalyst used for the RCM reaction was employed in the transfer hydrogenation reaction to afford **16.2a-c**. Lastly, the crude diol was oxidized by the action of Dess-Martin periodinane, and finally purified by flash column to give the desired macrocyclic 1,4-diketones (**16.3a-c**) in good yield over 4 steps with only a single chromatographic purification. This established sequence is a staple in our lab and was highly effective in my work to produce the key intermediates in the [*n*]PQPP synthesis.

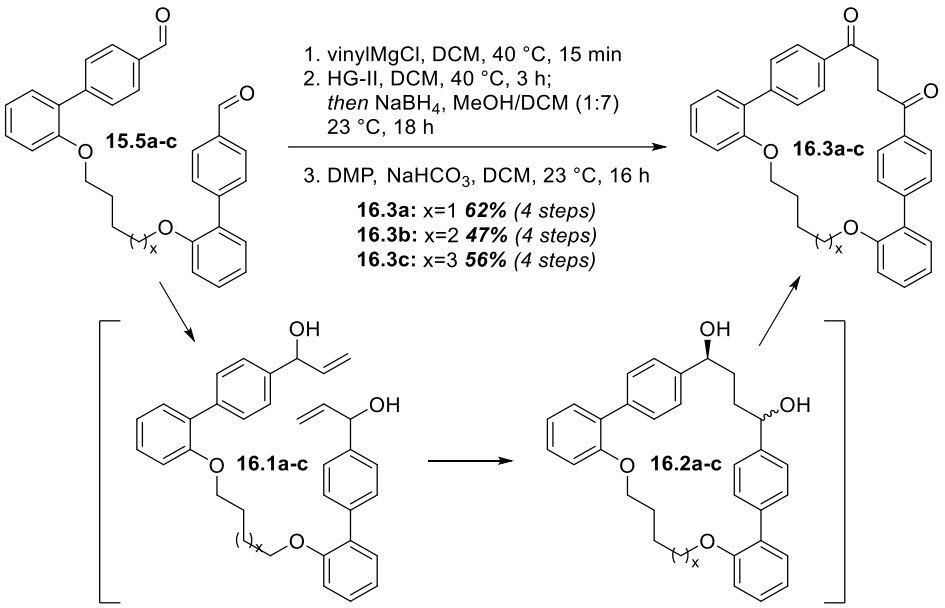

***Figure 16**: Four-step synthesis of macrocyclic diketones*

Once the 1,4-diketone intermediate was obtained, it was once again treated with vinylmagnesium chloride in dichloromethane, this time at 40 °C (**Figure 17**). These conditions were optimized by previous students to give the greatest diastereoselectivity for the addition of the vinyl groups. *Syn* addition is already preferred by the reaction due to the conformation of the macrocycle, which partially obstructs the opposite face of the carbonyl, but these conditions were found to be more effective for *syn*-selective addition in other systems.

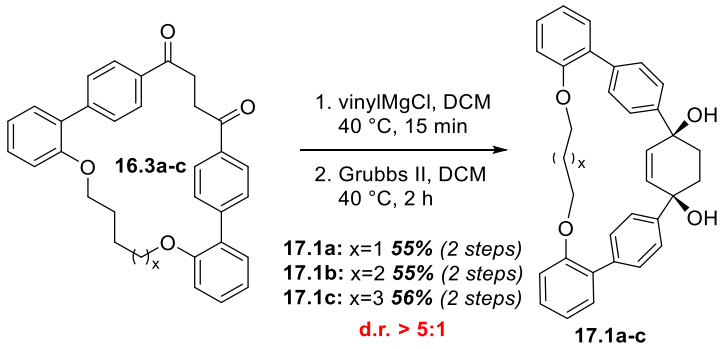

***Figure 17**: Synthesis of the cyclohex-2-ene-1,4-diol intermediates*

In this case, the diastereoselectivity ratio for each homologue was greater than 5:1 (*syn*:*anti*), determined by ^{1}H NMR analysis of the crude mixture. Because only the *syn*-vinyl groups are suited for ring-closing metathesis, any *anti* product is not useful for the next step, but the diastereomers were not

separable by flash chromatography. Therefore, the crude mixture of diols was subjected to Grubbs second generation catalyst to give the cyclohex-2-ene-*syn*-1,4-diol products **17.1a-c** in 55-56% yield.

The final step of the synthesis is the dehydrative aromatization using TsOH in toluene. Each of the homologues underwent clean conversion to the target [*n*]PQPP (*n* = 6, 7, and 8, **2a-c**). The smallest and most strained macrocycle (*n* = 6) resulted in a lower yield, possibly due to the higher strain leading to a more challenging aromatization step. Regardless, the targets had been achieved and a new model system for the [*n*]CPPs had been constructed.

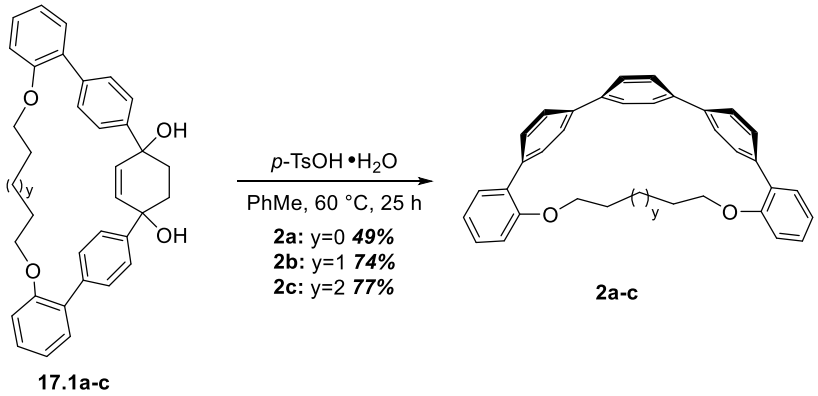

***Figure 18**: Completion of [n]PQPP synthesis*

Strain energies for the [*n*]PQPP systems were calculated. The geometry for each [*n*]PQPP was optimized with Avogadro software and then *Gaussian*. Next, a frequency calculation was performed, and the overall energy of each molecule was determined. Using an isodesmic reaction outlined below, the macrocyclic molecules were opened with ethane, and the geometries were re-optimized (ergo, the molecule –particularly the aromatic regions–becomes linear), then frequency calculations were re-obtained for each homolog. This process was a good approximation for removing the strain energy from the molecule.

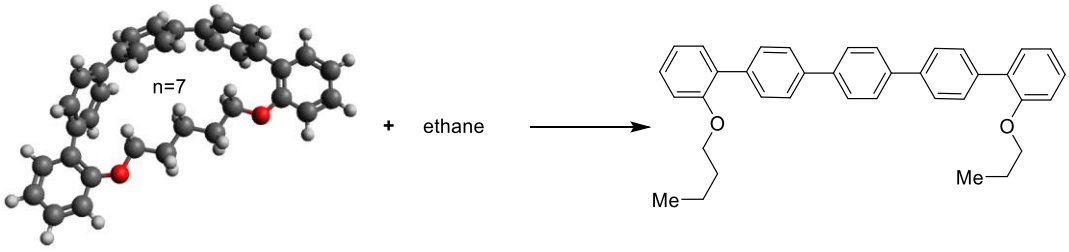

***Figure 19**: Isodesmic reaction of [7]PQPP*

Computational results are summarized in the following table and figure, with *n* = 7 homologue used as an example for the calculations.

N=7 PQPP			
	PQPP	ethane	open system
ZPE	0.555135	0.075241	0.632204
E_{corr}	0.585213	0.078710	0.667673
H_{corr}	0.586158	0.079654	0.668617
G_{corr}	0.493330	0.052131	0.558237
RHF+ZPE_{corr}	-501.661695	-9.755179	-581.459711
RHF+E_{corr}	-501.631617	-9.751711	-581.424241
RHF+H_{corr}	-501.630673	-9.750766	-581.423297
RHF+G_{corr}	-501.723501	-9.778290	-581.533678
SCF	-1502.216830	-79.830420	-1582.091915
Overall SE: 0.044665 Hartrees = **28.0277166 kcal/mol**			
Overall SE for [*8*]PQPP = 19.6146953 kcal/mol			
Overall SE for [*6*]PQPP = 36.1583586 kcal/mol			

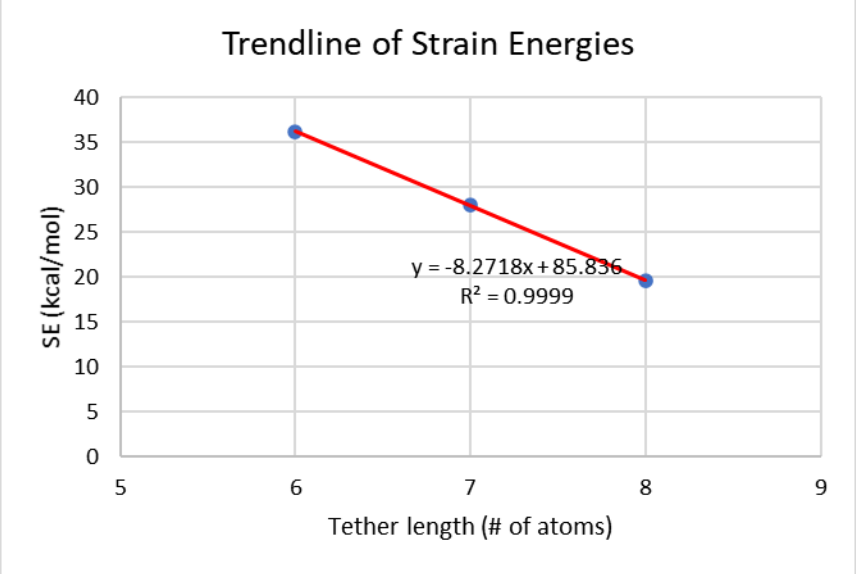

To conclude, the strain energy of three homologous [*n*]PQPPs were calculated using an isodesmic reaction to simulate removing the strain from the macrocycle. Just like other strained aromatic systems such as the CPPs, strain energy is found to increase proportionally to the decrease in macrocycle size. For the three homologues in question, the relationship is linear. This process was not only successful in uncovering the strain energies of relevant bent macrocycles; it also meets the expectation inherent in the system, and was therefore an accurate strategy. All calculations were performed using *Gaussian*, with the B3LYP/6-31G(d) DFT level of theory and basis set, starting from coordinates produced by Avogadro optimized geometries. Ideally, the localized strain of the central and peripheral rings would also be calculated, but this was beyond my ability at the time and I no longer have access to the supercomputer for *Gaussian*.

In summary, three homologous compounds ([*n*]PQPPs) were synthesized as an additional model system for the testing of *π*-extension reactions which can then be transferred to use on CPPs. Each of the three homologues was obtained in nine total steps with a good overall yield, and strain energies for the system were calculated.

1.6 Future Work

To recount the chapter in brief, we set out to create another effective model system for the testing of *π*-extension reactions for CPPs, seeking to find an appropriate moiety to act as an analog for longer polyphenylene chains. A proper model was found in the [*n*]PQPPs, which were synthesized in 9 simple steps from commercial starting materials. As this work continues, the next step will be to test the established *π*-extension sequences used for the [*n*]PTPPs (*i.e.* directed bromination/arylation/Scholl reaction or TEMPO allylic oxidation/aromatization/alkyne annulation. Another potentially promising area of research for these substrates involves the use of the alkoxy groups as directing handles for the regioselective functionalization of the terminal arene units. Depending on the added functional groups, and in concert with the elaboration of the central benzene unit, this could lead to controllable *π*-extension. The primary focus, however, is to merge the conditions and strategies discovered in the PQPP work with a CPP synthesis in a way that allows the new techniques and reactions to aid in the main goal of bottom-up CNT synthesis. This, in part, is the theme of the following chapter.

Beginning from the cyclohex-2-ene-1,4-diol intermediate from the [*n*]PQPP synthesis, an allylic oxidation-type rearrangement using the boron tetrafluoride salt of TEMPO results in *α*-ketol compound **F1.2** in moderate yield. From this step, two pathways emerge. For the first, a simple addition using aryl Grignard reagent is projected to result in arylated 1,3-diol **F1.3,** in which many different aryl groups could be installed in order to choose the desired option for subsequent *π*-extension reactions such as cyclodehydrogenation. If a *meta*-biphenyl unit was chosen, one could envision an annulation of both benzene rings onto the PQPP

backbone in the next step. Alternatively, treatment of *α*-ketol **F1.2** with arylethynyl Grignard (or else a two step sequence of ethynylmagnesium chloride followed by Sonogashira reaction with the desired aryl boronate) would likely result in **F1.4**, a precursor to the iodine monochloride-mediated alkyne annulation published by our group last year on the [*n*]PTPPs, upon which reaction would give annulation product **F1.5**. The resulting iodine handle could be treated with arylboronic acids or esters to yield bisarylated phenanthrene unit **F1.6** as a precursor for additional potential annulation reactions.

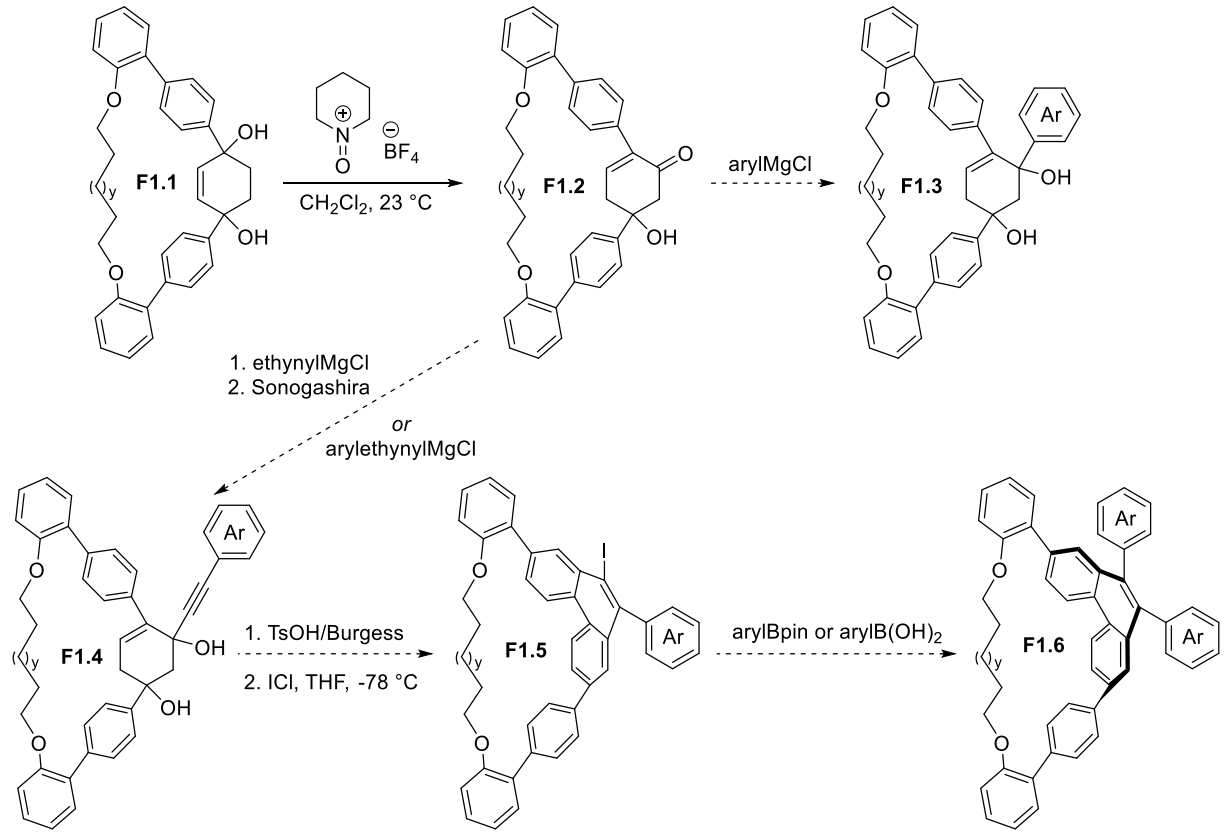

***Figure F1**: Preparation of annulation substrates from [n]PQPPs*

After preparation of the annulation precursors through the sequences outlined in **Figure F1**, the final stages would involve the final annulative *π*-extension APEX reactions. From diol **F1.3**, a dehydrative aromatization with tosic acid or Burgess reagent, then Scholl reaction would result in triphenyl-containing benzenoid macrocycle **F2.1**. Depending on the substituents on the newly installed aryl ring, there may be some potential additional *π*-extension to follow after this step. In like manner, phenanthrene-containing benzenoid macrocycle **F1.6** could be reacted under Scholl conditions to give a cyclodehydration product. For example, a lofty target would be compound **F2.2**, the result of a potential Scholl reaction of **F1.6**, if the installed aryl groups are both “1-naphthyl”. In that case, a wide carbon nanobelt fragment could be envisioned as the product of the reaction, with the Scholl reaction performing up to five aryl-aryl bond

formations. Due to the strain-induced rearrangement common in Scholl reactions of strained benzenoid macrocycles, an iterative process may be necessary, with an earlier Scholl reaction on compound **F1.5**, then coupling of the second aryl unit followed by another Scholl reaction.

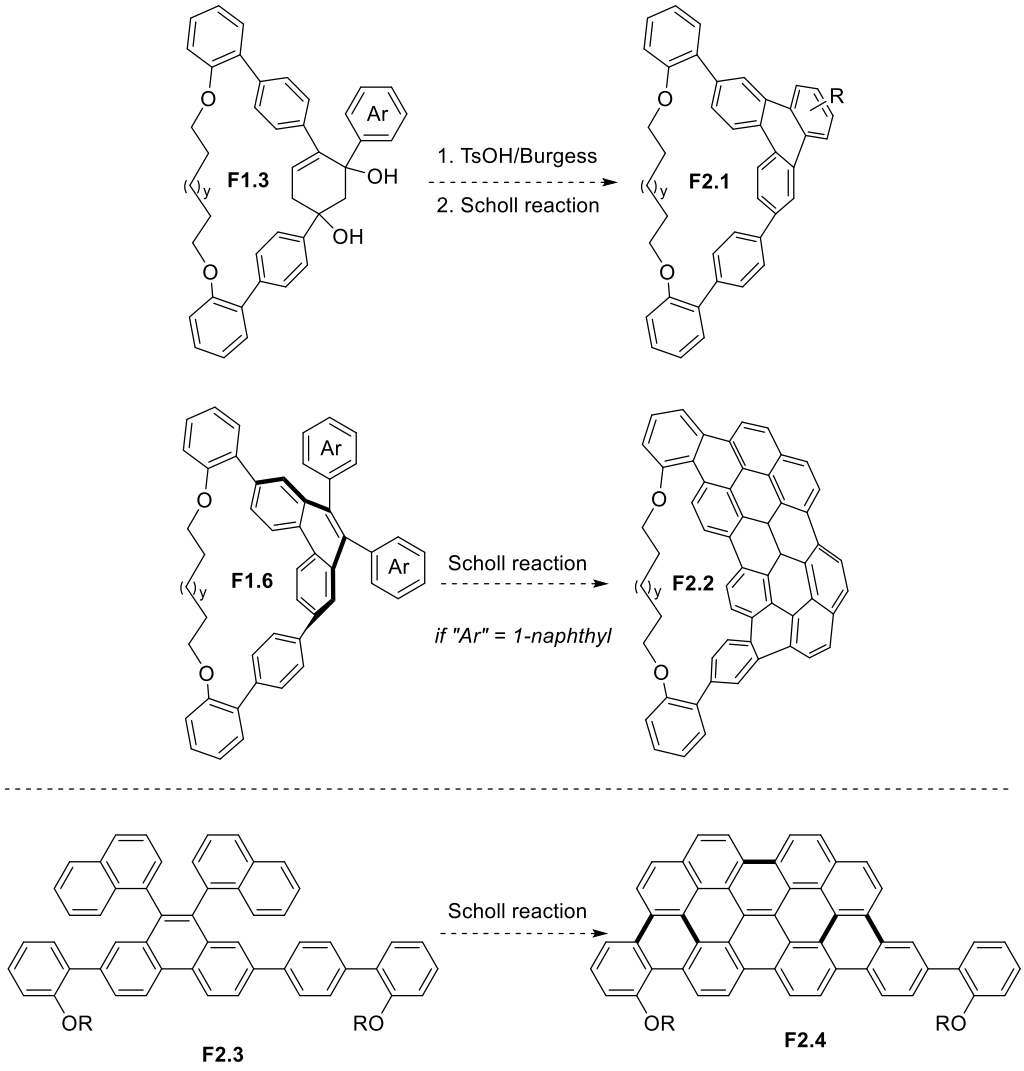

***Figure F2**: Annulative π-extension (APEX) of [n]PQPP templates*

1.7 REFERENCES

1. “Synthesis, structure, and reactivities of [6]paracyclophanes.” Tobe, Y., *et al*. *Tetrahedron* **1986,** *42,* 1851.

2. “A non-cross-coupling approach to arene-bridged macrocycles: Synthesis, structure, and direct, regioselective functionalization of a cycloparaphenylene fragment.” Mitra, N. *et al*. *Organic Letters*, **2015**, *17*, 2700.

3. “A Macrocyclic 1,4-Diketone Enables the Synthesis of a p-Phenylene Ring That Is More Strained than a Monomer Unit of [4]Cycloparaphenylene.” Mitra, N. *et al*. *Organic Letters,* **2016**, *18*, 3278.

4. “π-Extension of Strained Benzenoid Macrocycles Using the Scholl Reaction.” Saha, N. *et al*. *Organic Letters,* **2018**, *20*, 6855.

5. “Bending Benzene: Syntheses of [*n*]Cycloparaphenylenes.” Hirst, E. and Jasti, R. *Angewandte Chemie International Edition*, **2012,** *51*, 2474.

6. “Synthesis and characterization of [5]cycloparaphenylene.” Kayahara, E. *et al*. *Journal of the American Chemical Society* **2014**, *136*, 2284.

7. “Efficient room-temperature synthesis of a highly strained carbon nanohoop fragment of buckminsterfullerene.” Evans, P. *et al*. *Nature Chemistry* **2014**, *6*, 404.

8. “Synthesis of a Bent, Twisted, and Chiral Phenanthrene via an Iodine Monochloride-Mediated, Strain-Inducing π-Extension Reaction.” Saha, N. *et al*. *Organic Letters*, **2022**, *24*, 1038.

9. “A Rational Chemical Synthesis of C_{60}.” Scott, L. *et al*. *Science*, **2002**, *295*, 1500.; “Aromatic π-Systems More Curved Than C_{60}. The Complete Family of All Indenocorannulenes Synthesized by Iterative Microwave-Assisted Intramolecular Arylations.” Steinberg, B. *et al*. *Journal of the American Chemical Society* **2009**, *131*, 10537

10. “A Short, Rigid, Structurally Pure Carbon Nanotube by Stepwise Chemical Synthesis.” Scott, L. *et al*. *Journal of the American Chemical Society* **2012*,*** *134,* 107.

11. “A Quintuple [6]Helicene with a Corannulene Core as a C_5-Symmetric Propeller-Shaped π-System.” Kato, K. *et al*. *Angewandte Chemie International Edition* **2017**, *57*, 1337.

12. A: “Towards Negatively Curved Carbons.” Pun, S.H. and Miao, Q. *Accounts of Chemical Research*. **2018**, *51*, 1630.; *also see* “Synthesis, Structure, and Properties of Tetrabenzo[7]circulene.” Gu, X. *et al*. *Organic Letters*, **2017**, *19*, 2246.; “A Dipleiadiene-Embedded Aromatic Saddle Consisting of 86 Carbon Atoms.” Pun, S.H. *et al*. *Angewandte Chemie International Edition* **2017**, *57*, 1581.; “Synthesis, Structures, and Properties of Heptabenzo[7]circulene and Octabenzo[8]circulene.” Pun, S.H. *et al*. *Journal of the American Chemical Society*, **2019**, *141*, 9680.; “A Twisted Nanographene Consisting of 96 Carbon Atoms.” Cheung, K.Y. *et al*. *Angewandte Chemie International Edition* **2017**, *57*, 9003.

13. “Iterative Reductive Aromatization/Ring-Closing Metathesis Strategy toward the Synthesis of Strained Aromatic Belts.” Golder, M. *et al*. *Journal of the American Chemical Society* **2016**, *138*, 6577.

14. “Armchair and Chiral Carbon Nanobelts: Scholl Reaction in Strained Nanorings.”Cheung, K. Y. *et al*. *Chem* **2019**, *5*, 838.

15. a) “Bromination of Cycloparaphenylenes: Strain-Induced Site-Selective Bis-Addition and Its Application for Late-Stage Functionalization.” Kayahara, E. *et al*. *Angewandte Chemie International Edition* **2017**, *57*, 10428; b) “η6-Cycloparaphenylene Transition Metal Complexes: Synthesis, Structure, Photophysical Properties, and Application to the Selective Monofunctionalization of

Cycloparaphenylenes." Kubota, N. *et al. Journal of the American Chemical Society* **2015**, *137*, 1356.

16. "A macrocycle directed total synthesis of di-*O*-methylendiandrin A." Barnes, T.H. *et al*. *Chemical Communications* **2020,** *56,* 8747.

17. "Theoretical Studies on the Structures and Strain Energies of Cycloparaphenylenes." Segawa, Y. *et al*. *Organic Letters* **2010,** *12,* 2262.

18. "Carbamoyl Functionalized Bent para-Phenylenes via an Unexpected Reaction of the Burgess Reagent with α-Ketols." Jackson, S. N. *et al*. *Journal of Organic Chemistry* **2021**, *86*, 3667.

19. "Bottom-Up Synthesis of Soluble and Narrow Graphene Nanoribbons Using Alkyne Benzannulations." Yang, W. *et al*. *Journal of the American Chemical Society* **2016**, *138*, 9137.; "Highly Regioselective Domino Benzannulation Reaction of Buta-1,3-diynes To Construct Irregular Nanographenes." Yang, W. *et al*. *Angewandte Chemie International Edition* **2018**, *57*, 14773.

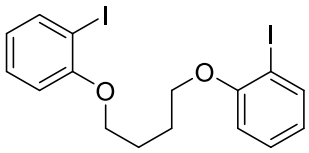

n=6 diiodide (15.3a): 2-iodophenol (1.00 g, 4.55 mmol), 1,4-dibromobutane (0.27 mL, 2.27 mmol), potassium carbonate (950 mg, 6.82 mmol) and tetrabutylammonium iodide (94.0 mg, 0.254 mmol) were added to a round-bottom flask under nitrogen atmosphere, then dissolved in anhydrous dimethylformamide (40 mL) and stirred 18 h at 60 °C. Reaction was cooled to 23 °C, then quenched by addition of 1 M HCl and extracted with ethyl acetate (3 x 30 mL). Combined organics washed with DI water (3 x 50 mL) and brine, then dried over $MgSO_4$, filtered, and concentrated under reduced pressure. Residue was purified by flash chromatography (18 x 2.5 cm, 5-8% ethyl acetate/hexanes) to yield yellow crystalline solid (1.14 g, quantitative). R_f = 0.58 (8% ethyl acetate/hexanes). ^{1}H NMR (500 MHz, $CDCl_3$) δ 7.77 (d, *J* = 7.7 Hz, 2H), 7.47 – 7.20 (m, 2H), 6.84 (d, *J* = 8.2 Hz, 2H), 6.71 (t, *J* = 7.7 Hz, 2H), 4.14 (h, *J* = 2.6 Hz, 4H), 2.13 (q, *J* = 3.3 Hz, 4H). ^{13}C NMR (126 MHz, $CDCl_3$) δ 157.69, 139.66, 129.70, 122.68, 112.37, 86.93, 68.87, 26.29;

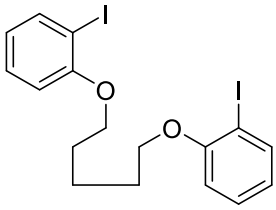

n=7 diiodide (15.3b): 2-iodophenol (1.00 g, 4.55 mmol), 1,5-dibromopentane (0.31 mL, 2.27 mmol), potassium carbonate (950 mg, 6.82 mmol) and tetrabutylammonium iodide (84.0 mg, 0.227 mmol) were added to a round-bottom flask under nitrogen atmosphere, then dissolved in anhydrous dimethylformamide (40 mL) and stirred 18 h at 60 °C. Reaction was cooled to 23 °C, then quenched by addition of 1 M HCl and extracted with ethyl acetate (3 x 30 mL). Combined organics washed with DI water (3 x 50 mL) and brine, then dried over $MgSO_4$, filtered, and concentrated under reduced pressure. Residue was purified by flash chromatography (9 x 2.5 cm, 0-8% ethyl acetate/hexanes) to yield yellow crystalline solid (1.04 g, 90%). R_f = 0.35 (5% ethyl acetate/hexanes). ^{1}H NMR (500 MHz, $CDCl_3$) δ 7.77 (d, *J* = 7.8 Hz, 2H), 7.39 – 7.20 (m, 2H), 6.82 (d, *J* = 8.2 Hz, 2H), 6.70 (t, *J* = 7.7 Hz, 2H), 4.07 (td, *J* = 6.3, 2.2 Hz, 4H), 1.96 (q, *J* = 6.7 Hz, 4H), 1.87 – 1.67 (m, 2H). ^{13}C NMR (126 MHz, $CDCl_3$) δ 157.56, 139.43, 129.42, 122.39, 112.09, 86.78, 68.97, 28.80, 22.94; HRMS (ESI) $[C_{17}H_{18}O_2I_2Na]^+$: *m/z* = 530.9275, calcd. 530.9294.

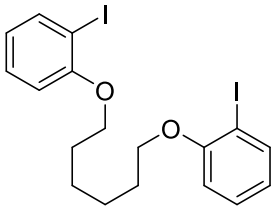

n=8 diiodide (15.3c): 2-iodophenol (2.00 g, 9.10 mmol), 1,6-dibromohexane (0.69 mL, 4.55 mmol), potassium carbonate (1.90 g, 13.70 mmol) and tetrabutylammonium iodide (336 mg, 0.910 mmol) were added to a round-bottom flask under nitrogen atmosphere, then dissolved in anhydrous dimethylformamide (60 mL) and stirred 22 h at 60 °C. Reaction was cooled to 23 °C, then quenched by addition of 1 M HCl and extracted with ethyl acetate (3 x 50 mL). Combined organics washed with DI

water (3 x 80 mL) and brine, then dried over $MgSO_4$, filtered, and concentrated under reduced pressure to yield yellow crystalline solid (2.27 g, 96%). R_f = 0.57 (5% ethyl acetate/hexanes). ^{1}H NMR (500 MHz, $CDCl_3$) δ 7.77 (dd, *J* = 7.7, 1.7 Hz, 2H), 7.48 – 7.19 (m, 2H), 6.81 (dd, *J* = 8.2, 1.5 Hz, 2H), 6.70 (td, *J* = 7.5, 1.5 Hz, 2H), 4.05 (t, *J* = 6.3 Hz, 4H), 1.91 (p, *J* = 6.3 Hz, 4H), 1.72 – 1.60 (m, 4H). ^{13}C NMR (126 MHz, $CDCl_3$) δ 157.60, 139.41, 129.41, 122.34, 112.12, 86.78, 68.95, 29.01, 25.74; HRMS (ESI) $[C_{18}H_{21}O_2I_2]^+$: *m/z* = 522.9631, calcd. 522.9626.

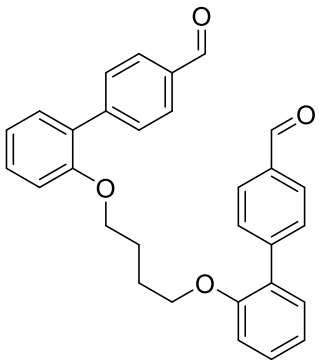

n=6 dialdehyde (15.5a): (Toluene, ethanol, and water were purged with N_2 for at least 30 minutes.) Diiodide **15.3a** (1.14 g, 2.31 mmol) in toluene (15 mL), potassium carbonate (700 mg, 5.08 mmol) in water (10 mL), 4-formylphenylboronic acid (936 mg, 6.24 mmol), tetrakis(triphenylphosphine)palladium(0) (261 mg, 0.231 mmol) and ethanol (5 mL) were all combined in a round-bottom flask under N_2 and condenser, then stirred 24 h at 90 °C. Reaction cooled to 23 °C and diluted with DI water, then extracted with dichloromethane (4 x 25 mL). Combined organics were dried over $MgSO_4$, filtered, and concentrated under reduced pressure. Residue was preabsorbed onto SiO_2 and purified by flash chromatography (18 x 2.5 cm, 80-100% dichloromethane/hexanes, then 1-3% acetone/dichloromethane) to yield brown solid (924 mg, 89%). R_f = 0.38 (100% dichloromethane). ^{1}H NMR (500 MHz, $CDCl_3$) δ 10.01 (d, *J* = 2.2 Hz, 2H), 7.86 (dd, *J* = 8.2, 2.2 Hz, 4H), 7.68 (dd, *J* = 8.2, 2.2 Hz, 4H), 7.34 (dt, *J* = 9.4, 4.7 Hz, 4H), 7.15 – 7.01 (m, 2H), 6.89 (d, *J* = 8.2 Hz, 2H), 3.96 (h, *J* = 2.5 Hz, 4H), 1.82 (p, *J* = 3.0 Hz, 4H). ^{13}C NMR (151 MHz, $CDCl_3$) δ 192.05, 155.80, 145.15, 134.82, 130.78, 130.16, 129.71, 129.43, 129.27, 128.04, 121.08, 112.44, 68.02, 26.12.

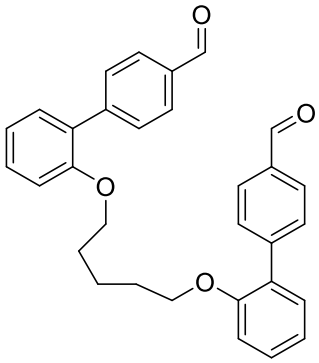

n=7 dialdehyde (15.5b): Toluene, ethanol, and water were purged with N_2 for at least 30 minutes.) Diiodide **15.3b** (1.01 g, 1.98 mmol) in toluene (19.0 mL), potassium carbonate (602 mg, 4.36 mmol) in water (14 mL), 4-formylphenylboronic acid (804 mg, 5.35 mmol), tetrakis(triphenylphosphine)palladium(0) (230 mg, 0.198 mmol) and ethanol (7 mL) were all combined in a round-bottom flask under N_2 and condenser, then stirred 24 h at 90 °C. Reaction cooled to 23 °C and diluted with DI water, then extracted with dichloromethane (4 x 25 mL). Combined organics were dried over $MgSO_4$, filtered, and concentrated under reduced pressure. Residue was preabsorbed onto SiO_2 and purified by flash chromatography (18 x 2.5 cm, 80-100% dichloromethane/hexanes, then 2-5% acetone/dichloromethane) to yield brown solid (769 mg, 84%). R_f = 0.40 (100% dichloromethane). ^{1}H NMR (500 MHz, $CDCl_3$) δ 9.99 (s, 2H), 7.98 – 7.77 (m, 4H), 7.74 – 7.58 (m, 4H), 7.50 – 7.31 (m, 4H), 7.07 (td, *J* = 7.5, 1.0 Hz, 2H), 6.97 (dd, *J* = 8.2, 1.0 Hz, 2H), 3.94 (t, *J* = 6.3

Hz, 4H), 1.72 (dq, *J* = 8.0, 6.4 Hz, 4H), 1.54 – 1.35 (m, 2H). ^{13}C NMR (126 MHz, $CDCl_3$) δ 192.35, 156.16, 145.39, 134.99, 131.02, 130.44, 129.98, 129.66, 129.51, 121.27, 112.77, 77.52, 77.27, 77.02, 68.47, 28.90, 23.07; HRMS (ESI) $[C_{31}H_{29}O_4]^+$: *m/z* = 465.2063, calcd. 465.2066.

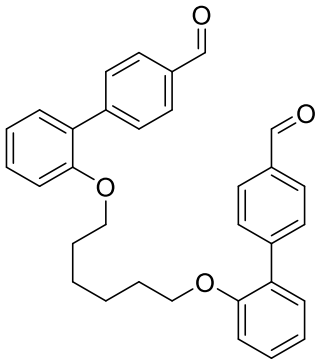

n=8 dialdehyde (15.5c): Toluene, ethanol, and water were purged with N_2 for at least 30 minutes.) Diiodide **15.3c** (807 mg 1.55 mmol) in toluene (14 mL), potassium carbonate (471 mg, 3.41 mmol) in water (9.00 mL), 4-formylphenylboronic acid (627 mg, 4.18 mmol), tetrakis(triphenylphosphine)palladium(0) (180 mg, 0.155 mmol) and ethanol (4.5 mL) were all combined in a round-bottom flask under N_2 and condenser, then stirred 18 h at 90 °C. Reaction cooled to 23 °C and diluted with DI water, then extracted with dichloromethane (4 x 25 mL). Combined organics were dried over $MgSO_4$, filtered, and concentrated under reduced pressure. Residue was preabsorbed onto SiO_2 and purified by flash chromatography (18 x 2.5 cm, 90-100% dichloromethane/hexanes, then 2-5% acetone/dichloromethane) to yield brown solid (717 mg, 97%). R_f = 0.40 (100% dichloromethane). ^{1}H NMR (600 MHz, $CDCl_3$) δ 10.00 (s, 2H), 7.86 (d, *J* = 8.2 Hz, 4H), 7.69 (d, *J* = 8.3 Hz, 4H), 7.45 – 7.29 (m, 4H), 7.06 (td, *J* = 7.5, 1.1 Hz, 2H), 6.98 (dd, *J* = 8.3, 1.1 Hz, 2H), 3.95 (t, *J* = 6.3 Hz, 4H), 1.69 (t, *J* = 6.2 Hz, 4H), 1.44 – 1.33 (m, 4H). ^{13}C NMR (151 MHz, $CDCl_3$) δ 192.32, 156.24, 145.44, 135.03, 131.00, 130.46, 129.96, 129.69, 129.49, 121.22, 112.77, 68.47, 29.27, 25.98; HRMS (ESI) $[C_{32}H_{31}O_4]^+$: *m/z* = 479.2216, calcd. 479.2222.

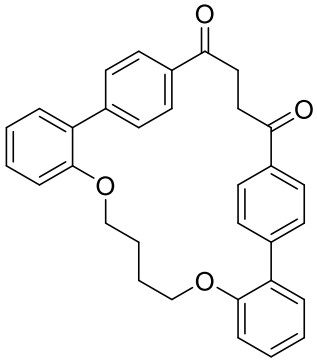

n=6 diketone (16.3a): Dialdehyde **15.5a** (200 mg, 0.446 mmol) was dissolved in anhydrous dichloromethane (40 mL) in a flame dried round bottom flask under N_2, then vinylmagnesium chloride (0.63 mL, 1.20 mmol) was added dropwise at 0 °C. Reaction was warmed to 23 °C, then quenched with DI water (20 mL) and 1 M HCl (20 mL) and extracted with dichloromethane (3 x 25 mL). Combined organics were washed with sat. sodium bicarbonate (30 mL) and brine (30 mL), then dried over $MgSO_4$, filtered, and concentrated under reduced pressure. Residue was taken up in dichloromethane (30 mL, 15 mM), then Hoveyda-Grubbs second-generation catalyst (7.0 mg, 0.011 mmol) was added. Reaction stirred at 40 °C for 1.25 h, then was cooled to 23 °C and concentrated under reduced pressure. Residue was taken up in methanol/dichloromethane (1:7 mixture, 40 mL), then sodium borohydride (85.0 mg, 2.23 mmol) was added under N_2. Reaction stirred 18 h at 23 °C and was quenched with 1 M HCl (20 mL), then extracted with dichloromethane (3 x 20 mL). Combined organics were washed with sat. sodium bicarbonate (20 mL) and brine (20 mL), then dried over $MgSO_4$, filtered, and concentrated under reduced pressure. Finally, residue was taken up in dichloromethane (40 mL) with sodium

bicarbonate (187 mg, 2.23 mmol) and Dess-Martin reagent (378 mg, 0.892 mmol) and stirred 22 h at 23 °C. Reaction was stirred with a 1:1 solution of 10% sodium thiosulfate and sat. sodium bicarbonate (30 mL) for 1 h, then extracted with dichloromethane (3 x 20 mL). Combined organics were dried over $MgSO_4$, filtered, and concentrated under reduced pressure. Residue was purified by flash chromatography (5 x 1.5 cm, 40% ethyl acetate/hexanes) to yield light brown solid (131 mg, 62% yield over 4 steps). R_f = 0.44 (40% ethyl acetate/hexanes). ^{1}H NMR (500 MHz, $CDCl_3$) δ 7.81 (dd, *J* = 8.4, 2.6 Hz, 4H), 7.58 (dd, *J* = 8.4, 2.6 Hz, 4H), 7.44 – 7.29 (m, 4H), 7.06 (td, *J* = 7.5, 2.4 Hz, 2H), 7.03 – 6.99 (m, 2H), 3.97 (q, *J* = 3.4 Hz, 4H), 3.37 (d, *J* = 2.6 Hz, 4H), 1.78 (q, *J* = 3.3 Hz, 4H). ^{13}C NMR (126 MHz, $CDCl_3$) δ 200.50, 156.11, 143.85, 134.90, 130.90, 130.19, 130.11, 129.71, 128.21, 121.58, 113.43, 69.00, 35.40, 26.75; HRMS (ESI) $[C_{32}H_{29}O_4]^+$: *m/z* = 477.2060, calcd. 477.2066.

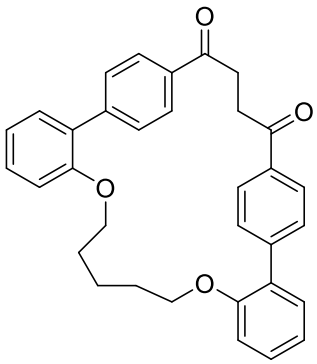

n=7 diketone (16.3b): Dialdehyde **15.5b** (1.50 g, 4.81 mmol) was dissolved in anhydrous dichloromethane (50 mL) in a flame dried round bottom flask under N_2, then vinylmagnesium chloride (6.83 mL, 12.98 mmol) was added dropwise at 0 °C. Reaction was warmed to 23 °C, then quenched with DI water (40 mL) and 1 M HCl (30 mL) and extracted with dichloromethane (3 x 40 mL). Combined organics were washed with sat. sodium bicarbonate (30 mL) and brine (30 mL), then dried over $MgSO_4$, filtered, and concentrated under reduced pressure. Residue was taken up in dichloromethane (320 mL, 15 mM), then Hoveyda-Grubbs second-generation catalyst (75.0 mg, 0.120 mmol) was added. Reaction stirred at 40 °C for 3 h, then was cooled to 23 °C and concentrated under reduced pressure. Residue was taken up in methanol/dichloromethane (1:7 mixture, 160 mL), then sodium borohydride (914 mg, 24.1 mmol) was added under N_2. Reaction stirred 18 h at 23 °C and was quenched with 1 M HCl (40 mL), then extracted with dichloromethane (3 x 50 mL). Combined organics were washed with sat. sodium bicarbonate (40 mL) and brine (40 mL), then dried over $MgSO_4$, filtered, and concentrated under reduced pressure. Finally, residue was taken up in dichloromethane (75 mL) with sodium bicarbonate (2.02 g, 24.05 mmol) and Dess-Martin reagent (4.00 g, 9.62 mmol) and stirred 18 h at 23 °C. Reaction was stirred with a 1:1 solution of 10% sodium thiosulfate and sat. sodium bicarbonate (50 mL) for 1 h, then extracted with dichloromethane (3 x 40 mL). Combined organics were dried over $MgSO_4$, filtered, and concentrated under reduced pressure. Residue was purified by flash chromatography (10 x 2.5 cm, 45% ethyl acetate/hexanes) to yield light brown solid (758 mg, 47% yield over 4 steps). R_f = 0.39 (40% ethyl acetate/hexanes). ^{1}H NMR (500 MHz, $CDCl_3$) δ 7.91 – 7.80 (m, 4H), 7.67 – 7.53 (m, 4H), 7.40 – 7.28 (m, 4H), 7.06 (td, *J* = 7.5, 1.1 Hz, 2H), 6.98 (dd, *J* = 8.2, 1.0 Hz, 2H), 3.84 (t, *J* = 6.0 Hz, 4H), 3.39 (s, 4H), 1.71 – 1.60 (m, 4H), 1.37 (tt, *J* = 9.1, 6.5 Hz, 2H). ^{13}C NMR (126 MHz, $CDCl_3$) δ 200.08, 156.38, 143.83, 134.77, 130.75, 130.49, 130.07, 129.74, 128.17, 121.77, 114.37, 69.42, 35.56, 29.45, 23.11; HRMS (ESI) $[C_{33}H_{31}O_4]^+$: *m/z* = 491.2234, calcd. 491.2222.

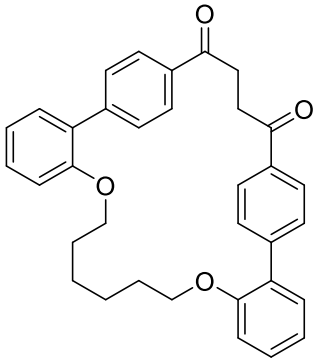

n=8 diketone (16.3c): Dialdehyde **15.5c** (1.49 g, 3.11 mmol) was dissolved in anhydrous dichloromethane (40 mL) in a flame dried round bottom flask under N_2, then vinylmagnesium chloride (3.90 mL, 7.78 mmol) was added dropwise at 0 °C. Reaction was warmed to 23 °C, then quenched with DI water (20 mL) and 1 M HCl (20 mL) and extracted with dichloromethane (3 x 30 mL). Combined organics were washed with sat. sodium bicarbonate (30 mL) and brine (30 mL), then dried over $MgSO_4$, filtered, and concentrated under reduced pressure. Residue was taken up in dichloromethane (210 mL, 15 mM), then Hoveyda-Grubbs second-generation catalyst (49 mg, 0.078 mmol) was added. Reaction stirred at 40 °C for 3 h, then was cooled to 23 °C and concentrated under reduced pressure. Residue was taken up in methanol/dichloromethane (1:7 mixture, 80 mL), then sodium borohydride (600 mg, 15.6 mmol) was added under N_2. Reaction stirred 18 h at 23 °C and was quenched with 1 M HCl (40 mL), then extracted with dichloromethane (3 x 30 mL). Combined organics were washed with sat. sodium bicarbonate (20 mL) and brine (20 mL), then dried over $MgSO_4$, filtered, and concentrated under reduced pressure. *Some impurities removed by crude flash chromatography at this stage (15 x 2.5 cm, 40-60% ethyl acetate/hexanes).* Finally, residue was taken up in dichloromethane (50 mL) with sodium bicarbonate (966 mg, 11.50 mmol) and Dess-Martin reagent (2.37 g, 5.60 mmol) and stirred 26 h at 23 °C. Reaction was stirred with a 1:1 solution of 10% sodium thiosulfate and sat. sodium bicarbonate (50 mL) for 1 h, then extracted with dichloromethane (3 x 30 mL). Combined organics were dried over $MgSO_4$, filtered, and concentrated under reduced pressure. Residue was purified by flash chromatography (5 x 2.5 cm, 30% ethyl acetate/hexanes) to yield light brown solid (880 mg, 56% yield over 4 steps). R_f = 0.53 (40% ethyl acetate/hexanes). ^{1}H NMR (600 MHz, $CDCl_3$) δ 8.11 – 7.83 (m, 4H), 7.70 – 7.55 (m, 4H), 7.42 – 7.29 (m, 4H), 7.06 (td, *J* = 7.5, 1.0 Hz, 2H), 7.00 (dd, *J* = 8.3, 1.0 Hz, 2H), 3.93 (t, *J* = 6.1 Hz, 4H), 3.43 (s, 4H), 1.80 – 1.61 (m, 4H), 1.36 (dt, *J* = 8.0, 3.7 Hz, 4H). ^{13}C NMR (126 MHz, $CDCl_3$) δ 199.17, 156.33, 144.05, 134.29, 130.68, 130.30, 130.17, 129.74, 128.13, 121.37, 113.18, 69.27, 35.44, 29.87, 26.99; HRMS (ESI) $[C_{34}H_{33}O_4]^+$: *m/z* = 505.2394, calcd. 505.2379.

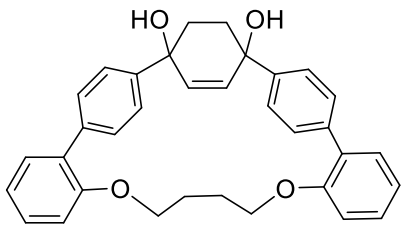

n=6 cyclohexenediol (17.1a): Vinylmagnesium chloride (0.14 mL, 0.257 mmol) was added dropwise to a stirring 40 °C solution of diketone **16.3a** (45.2 mg, 0.095 mmol) in anhydrous dichloromethane (10 mL) under N_2 in a flame dried flask. After 20 minutes, the reaction was cooled to 23 °C and quenched with DI water (5 mL) and 1 M HCl (5 mL), then extracted with dichloromethane (3 x 10 mL). Combined organics were washed with sat. sodium bicarbonate (5 mL) and brine (5 mL), then dried over $MgSO_4$, filtered, and concentrated under reduced pressure. Crude NMR confirmed d.r. of 9:1 (*syn:anti*), then residue was taken up in

dichloromethane and stirred at 40 °C while Grubbs second-generation catalyst (1.6 mg, 0.002 mmol) was added. After 30 minutes, reaction was concentrated under reduced pressure. Residue was purified by flash chromatography (8 x 0.5 cm, 5-15% acetone/dichloromethane) to yield white solid (26.5 mg, 55%). R_f = 0.13 (10% acetone/dichloromethane). ^{1}H NMR (500 MHz, $CDCl_3$) δ 7.59 (d, *J* = 2.6 Hz, 8H), 7.39 (d, *J* = 7.7 Hz, 2H), 7.31 (t, *J* = 8.0 Hz, 2H), 7.14 – 7.00 (m, 4H), 6.25 (d, *J* = 2.6 Hz, 2H), 4.04 (d, *J* = 6.9 Hz, 2H), 3.94 – 3.80 (m, 2H), 2.38 – 2.05 (m, 4H), 1.97 – 1.75 (m, 6H). ^{13}C NMR (126 MHz, $CDCl_3$) δ 156.34, 144.61, 137.64, 135.26, 131.05, 130.90, 129.69, 128.88, 125.44, 121.77, 114.12, 73.19, 69.83, 37.46, 27.21; HRMS (ESI) $[C_{34}H_{32}O_4Na]^+$: *m/z* = 527.2194, calcd. 527.2198.

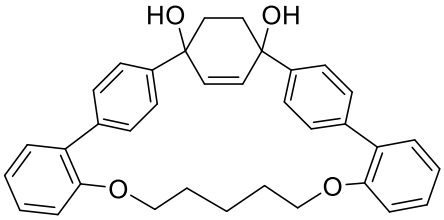

n=7 cyclohexenediol (17.1b): Vinylmagnesium chloride (0.06 mL, 0.100 mmol) was added dropwise to a stirring 40 °C solution of diketone **16.3b** (18.0 mg, 0.037 mmol) in anhydrous dichloromethane (3 mL) under N_2 in a flame dried vial. After 20 minutes, the reaction was cooled to 23 °C and quenched with DI water (3 mL) and 1 M HCl (2 mL), then extracted with dichloromethane (3 x 5 mL). Combined organics were washed with sat. sodium bicarbonate (3 mL) and brine (3 mL), then dried over $MgSO_4$, filtered, and concentrated under reduced pressure. Stored in freezer overnight, then residue was taken up in dichloromethane and stirred at 40 °C while Grubbs second-generation catalyst (0.6 mg, 0.0007 mmol) was added. After 2 h, reaction was concentrated under reduced pressure. Residue was purified by flash chromatography (8 x 0.5 cm, 8-15% acetone/dichloromethane) to yield white solid (10.6 mg, 55%). R_f = 0.13 (10% acetone/dichloromethane). ^{1}H NMR (500 MHz, $CDCl_3$) δ 7.56 (d, *J* = 2.6 Hz, 8H), 7.42 – 7.35 (m, 2H), 7.34 – 7.22 (m, 2H), 7.05 (td, *J* = 7.6, 2.3 Hz, 2H), 6.99 (dd, *J* = 8.1, 2.4 Hz, 2H), 6.22 (d, *J* = 2.6 Hz, 2H), 4.29 – 3.75 (m, 4H), 2.21 (dd, *J* = 12.3, 8.8 Hz, 2H), 2.17 – 2.09 (m, 2H), 1.98 (dd, *J* = 12.5, 8.8 Hz, 2H), 1.68 (tt, *J* = 14.0, 7.2 Hz, 4H), 1.49 (q, *J* = 7.9 Hz, 2H). ^{13}C NMR (126 MHz, $CDCl_3$) δ 156.60, 144.44, 137.95, 134.94, 131.25, 130.76, 129.73, 128.92, 125.37, 121.62, 114.35, 72.90, 69.20, 36.85, 29.66, 22.65. HRMS (ESI) $[C_{35}H_{34}O_4Na]^+$: *m/z* = 541.2354, calcd. 541.2355.

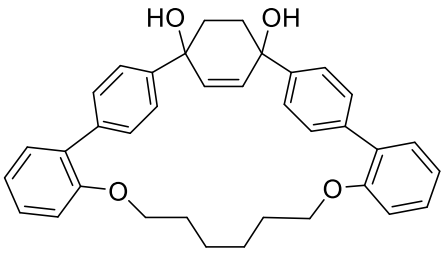

n=8 cyclohexenediol (17.1c): Vinylmagnesium chloride (2.13 mL, 4.27 mmol) was added dropwise to a stirring 40 °C solution of diketone **16.3c** (860 mg, 1.706 mmol) in anhydrous dichloromethane (20 mL) under N_2 in a flame dried flask. After 20 minutes, the reaction was cooled to 23 °C and quenched with DI water (20 mL) and 1 M HCl (15 mL), then extracted with dichloromethane (3 x 20 mL). Combined organics were washed with sat. sodium bicarbonate (15 mL) and brine (15 mL), then dried over $MgSO_4$, filtered, and concentrated under reduced pressure. Residue was taken up in dichloromethane and stirred at 40 °C while Grubbs second-generation catalyst (29 mg, 0.0341

mmol) was added. After 30 minutes, reaction was concentrated under reduced pressure. Residue was purified by flash chromatography (18 x 2.5 cm, 10-15% acetone/dichloromethane) to yield white solid (507 mg, 56%). R_f = 0.13 (10% acetone/dichloromethane). ^{1}H NMR (600 MHz, $CDCl_3$) δ 7.64 (d, *J* = 8.4 Hz, 4H), 7.61 (d, *J* = 8.4 Hz, 4H), 7.39 (dd, *J* = 7.5, 1.7 Hz, 2H), 7.31 (td, *J* = 7.8, 1.7 Hz, 2H), 7.05 (td, *J* = 7.4, 1.0 Hz, 2H), 6.99 (d, *J* = 8.2 Hz, 2H), 6.17 (s, 2H), 4.01 (dt, *J* = 8.6, 5.9 Hz, 2H), 3.93 (dt, *J* = 8.5, 5.3 Hz, 2H), 2.27 – 2.20 (m, 2H), 2.11 (s, 2H), 2.04 – 1.98 (m, 2H), 1.79 – 1.67 (m, 4H). ^{13}C NMR (126 MHz, $CDCl_3$) δ 156.38, 144.34, 144.18, 138.14, 137.40, 131.09, 130.94, 129.73, 128.76, 128.49, 125.56, 125.11, 121.12, 113.30, 112.97, 69.02, 36.27, 29.69, 26.70, 21.72.

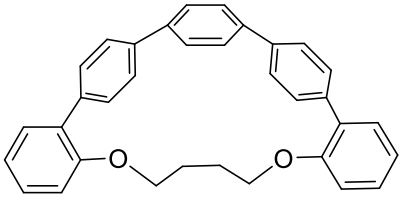

n=6 PQPP (2a): *p*-toluenesulfonic acid (16.0 mg, 0.084 mmol) was added to a 60 °C solution of macrocyclic cyclohexene-1,4-diol **17.1a** (7.4 mg, 0.014 mmol) in toluene (1 mL). Reaction was cooled to 23 °C and concentrated under reduced pressure. Residue was purified by flash chromatography (8 x 0.5 cm, 40-70% dichloromethane/hexanes) to yield fluorescent white solid (3.2 mg, 49%). R_f = 0.67 (100% dichloromethane). ^{1}H NMR (600 MHz, $CDCl_3$) δ 7.67 (s, 4H), 7.59 – 7.55 (m, 4H), 7.47 (dd, *J* = 7.5, 1.8 Hz, 2H), 7.33 – 7.27 (m, 4H), 7.25 – 7.20 (m, 2H), 7.11 (td, *J* = 7.5, 1.2 Hz, 2H), 6.90 (dd, *J* = 8.1, 1.2 Hz, 2H), 2.94 – 2.85 (m, 4H), 0.86 (ddd, *J* = 7.8, 5.0, 3.2 Hz, 4H). ^{13}C NMR (126 MHz, $CDCl_3$) δ 157.20, 139.87, 138.51, 135.36, 134.30, 130.40, 128.98, 128.92, 128.27, 127.05, 123.14, 119.63, 71.72, 25.75; HRMS (ESI) $[C_{34}H_{29}O_2]^+$: *m/z* = 469.2171, calcd. 469.2168.

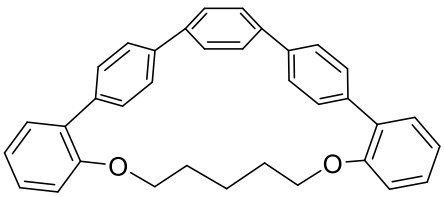

n=7 PQPP (2b): *p*-toluenesulfonic acid (8.5 mg, 0.045 mmol) was added to a 60 °C solution of macrocyclic cyclohexene-1,4-diol **17.1b** (4.6 mg, 0.01 mmol) in toluene (2 mL). Reaction was cooled to 23 °C and concentrated under reduced pressure. Residue was purified by flash chromatography (8 x 0.5 cm, 40-70% dichloromethane/hexanes) to yield fluorescent white solid (3.2 mg, 74%). R_f = 0.50 (100% dichloromethane). ^{1}H NMR (500 MHz, $CDCl_3$) δ 7.66 (d, *J* = 2.5 Hz, 4H), 7.62 (dd, *J* = 8.3, 2.4 Hz, 4H), 7.52 (d, *J* = 7.6 Hz, 2H), 7.40 (dd, *J* = 8.3, 2.4 Hz, 4H), 7.29 – 7.21 (m, 2H), 7.19 – 7.12 (m, 2H), 6.92 (dd, *J* = 8.1, 2.2 Hz, 2H), 2.94 – 2.77 (m, 4H), 0.99 (p, *J* = 7.4 Hz, 4H), 0.28 (h, *J* = 5.2 Hz, 2H). ^{13}C NMR (126 MHz, $CDCl_3$) δ 157.01, 139.98, 139.10, 135.65, 134.73, 130.61, 128.98, 128.65, 128.30, 127.01, 123.45, 119.89, 71.87, 31.36, 20.28; HRMS (ESI) $[C_{35}H_{31}O_2]^+$: *m/z* = 483.2318, calcd. 483.2324.

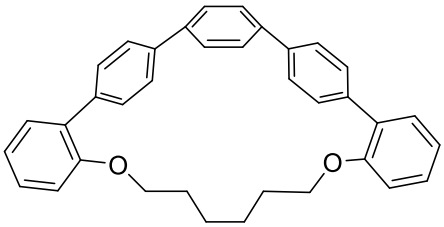

n=8 PQPP (2c): *p*-toluenesulfonic acid (23.0 mg, 0.121 mmol) was added to a 60 °C solution of macrocyclic cyclohexene-1,4-diol **17.1c** (16.0 mg, 0.020 mmol) in toluene (3 mL). Reaction was cooled to 23 °C and concentrated under reduced pressure. Residue was purified by flash chromatography (8 x 0.5 cm, 40-70% dichloromethane/hexanes) to yield fluorescent white solid (11 mg, 77%). R_f = 0.72 (100% dichloromethane). ^{1}H NMR (600 MHz, $CDCl_3$) δ 7.72 (s, 4H), 7.70 – 7.66 (m, 4H), 7.52 (dd, *J* = 7.5, 1.8 Hz, 2H), 7.47 – 7.39 (m, 4H), 7.32 – 7.24 (m, 2H), 7.18 (td, *J* = 7.5, 1.2 Hz, 2H), 6.99 (dd, *J* = 8.0, 1.2 Hz, 2H), 2.93 – 2.85 (m, 4H), 0.99 (dq, *J* = 14.0, 7.1 Hz, 4H), 0.39 (dt, *J* = 10.6, 3.4 Hz, 4H). 13C NMR (126 MHz, CDCl3) δ 157.25, 139.61, 138.95, 136.19, 135.31, 130.58, 129.05, 128.94, 127.88, 126.73, 123.83, 121.07, 73.10, 30.98, 26.06. HRMS (ESI) [C36H33O2]+: *m/z* = 497.2458, calcd. 497.2481.

CHAPTER 2 SELECTIVE SYNTHESIS OF [6], [8], AND [10]CYCLOPARAPHENYLENES

2. INTRODUCTION

As mentioned in Chapter 1, [*n*]cycloparaphenylenes ([*n*]CPPs) are often viewed as the shortest possible cross-sections of single-walled armchair carbon nanotubes (CNTs) and have been a desirable target for chemical synthesis for several decades. The first successful synthesis of an [*n*]CPP was reported in 2008 by recent Nobel laureate Carolyn Bertozzi and a postdoctoral researcher in her lab (at the time), Ramesh Jasti. In this proposal, a newly developed method will be discussed for the synthesis of these strained nanohoops, along with a proposal for *π*-extension toward higher-order subunits of CNTs. While several strategies now exist for the gram-scale synthesis of these [*n*]CPPs, including significant contributions from the Jasti, Itami, and Yamago groups, along with a high volume of publications discussing the electrochemical properties of such molecules and their heterocyclic derivatives, very little is known about their elaboration into *π*-extended structures such as carbon nanobelts (CNBs) or CNTs. The strategies that have been developed in our laboratory and were pursued during my graduate studies are hypothesized to provide a highly useful methodology for the *π*-extension of [*n*]CPPs.

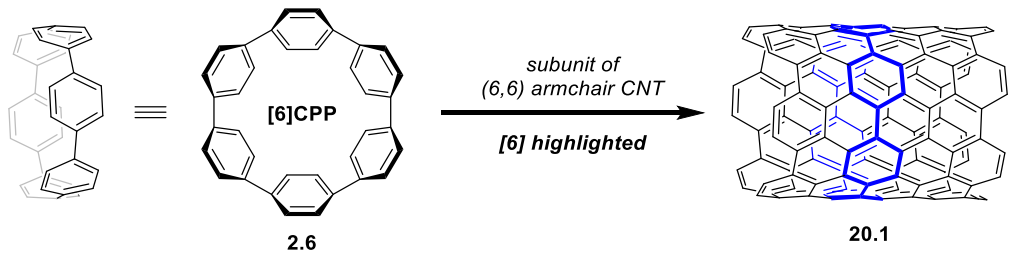

***Figure 20**: Mapping [6]CPP onto a [6,6]CNT segment*

The primary goal of this research is to establish a protocol for the bottom-up synthesis of CNTs via targeted *π*-extension of existing CPP frameworks. Existing procedures for the creation of [*n*]CPPs are divisible into three categories, which will be discussed in detail below. These methods include: 1) the Jasti method, which uses a cyclohexadiene subunit as the L-shaped precursor; 2) the Itami method, which uses a cyclohexane in similar fashion; and 3) the Yamago method, which is known colloquially as the 'Pt-square' assembly. Although these techniques are demonstrably effective for the synthesis of [*n*]CPPs, their application to any higher-order nanobelts or CNTs has only recently been established (see **Figure 9**, Chapter 1). Therefore, synthetic innovation in the area of p-extension reactions of curved benzenoid systems is required. In this chapter, I will describe how a cyclohex-2-ene-1,4-diol subunit—already a well-

established moiety in the Merner lab[2,3]—can act as the L-shaped precursor for [*n*]CPPs. The advantage that this system offers over the precursor subunits that have been employed by Jasti, Yamago and Itami, is that they can be functionalized at a later stage to facilitate the introduction of functional group and substituents that can be used for p-extension of the macrocyclic benzenoid framework. Merner and co-workers have recently reported the synthesis of a highly strained benzenoid macrocycle containing one of the most strained *para*-phenylene units known using a cyclo-2-ene-1,4-diol unit as a precursor[3] and a have recently-published a strategy that enables *π*-extension of a strained p-terphenyl-containing macrocycle.[4]

To this day, the functionalization of cycloparaphenylenes has been extremely limited for a multitude of reasons. The difficulty with functionalizing [*n*]CPPs, is that you have *n* equivalent benzene rings. A single substitution is possible, but very difficult, and controlling subsequent reactions is even more difficult. Another one of these causes is the limitation placed on the system by the inherent strain energy present in the molecule. High strain energy within the macrocyclic structure and individual benzene rings warps the structure and makes functionalization more difficult and less predictable than in a planar analog. Because of this, the number of known reactions that are suited for these types of functionalizations is quite low in the case of strained *π*-systems.

One of the challenges associated with performing late-stage substitution reactions on [*n*]CPPs is that they are susceptible to macrocyclic ring-opening and rearrangement reactions that result in the release of strain energy. Functional groups which would perhaps otherwise be inert or robust find themselves decomposing in milder reaction systems due to the altered conditions, leading to unexpected reaction failure or undesired byproducts. For example, acid-mediated dehydration reactions or Lewis-acid conditions such as the Scholl reaction often lead to rearrangement, as discussed later in Chapters 2 and 3. To avoid this problem, mild and neutral conditions must be used in the relevant steps (such as dehydration using the Burgess reagent rather than TsOH), with the goal of avoiding strain-releasing macrocyclic rearrangement or ring opening.

This chapter will describe a new strategy that has been developed for the size-selective synthesis of [*n*]CPPs using cyclohex-2-ene-1,4-diols as key intermediates and L-shaped building blocks for macrocycle assembly. This pre-arene subunit has been employed in the synthesis of highly strained benzenoid macrocycles, and here I will discuss how they have been used to furnish [6], [8], and [10]cycloparaphenylenes. Moreover, the conversion of macrocyclic cyclohex-2-ene-1,4-diols to selectively functionalized *p*-terphenyl-containing macrocycles has been reported by Merner and co-workers (see Chapter 1), and our hope is that the macrocyclic intermediates of [*n*]CPPs that will be discussed below can be employed in subsequent *π*-extension reactions and ultimately the synthesis of size-selective CNBs.

2.1 Timeline of successful [*n*]CPP synthesis

Though the pursuit of viable syntheses of [*n*]cycloparaphenylenes has spanned nearly a century, the first successful report of a [*n*]CPP structure to succumb to chemical synthesis came in 2008.[20] In this paper, Bertozzi and Jasti reported the synthesis of [9], [12], and [18]CPP via a "shotgun approach" using L-shaped, cyclohexa-2,5-diene-1,4-diol subunits in a Suzuki macrocyclization reaction. This started the scramble to make increasingly smaller nanohoops. Two years later, in 2010, [8]CPP was synthesized by the group of Shigeru Yamago using a "platinum square"-type precursor, which was converted to the CPP via reductive elimination.[21] In 2011, Jasti published the synthesis of [7]CPP, and just a year later [6]CPP was also reported by Jasti and co-workers.[22,23] Finally, in 2014, Yamago and Jasti both reported their independent syntheses of [5]CPP just a few weeks apart.[6,7] Roughly nine years have now passed since this most strained [*n*]CPP was reported. During the interim, several selective syntheses of known [*n*]CPPs have been reported, including gram-scale preparation, most of these coming from the aforementioned research groups and the laboratories of Kenichiro Itami.[24] As is plain from the drawing below, [4]CPP is an enormously strained molecule. It is perhaps no surprise that this molecule still eludes synthetic chemists for now, but this is a target that will continue to inspire synthetic innovation.

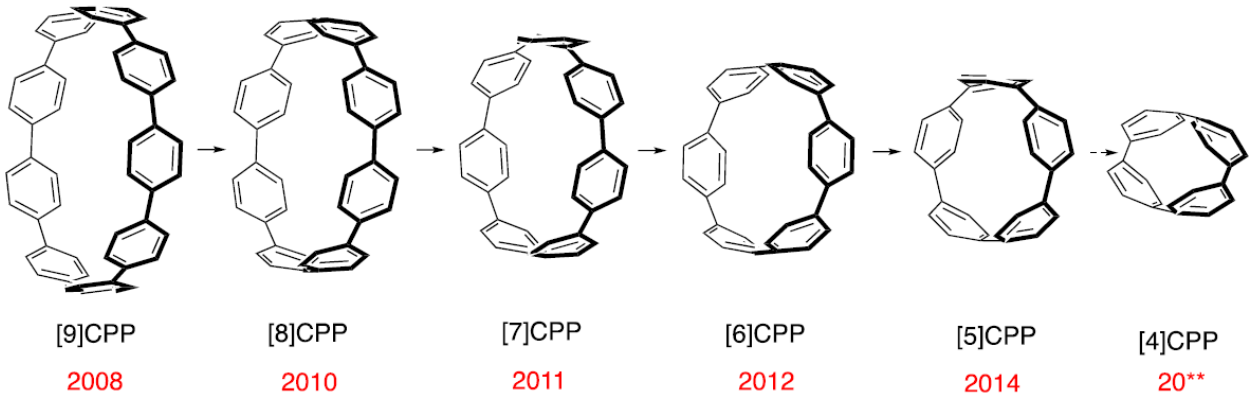

***Figure 21**: Timeline of [n]CPP synthesis*

2.2 Existing strategies for the synthesis of [*n*]CPPs

There exist three primary strategies for creating CPPs, pioneered by Jasti, Itami, and Yamago, respectively. The Jasti approach uses a *syn*-1,4-dimethoxycyclohexa-2,5-diene subunit, which is combined with other subunits via Suzuki-Miyaura cross coupling to obtain the desired number of *para*-phenylene units, followed by macrocyclization (also utilizing cross-coupling or directed arylation) and aromatization to afford CPPs

(**Figure 22A**). The Itami group takes a similar approach, using a *syn*-1,4-dihydroxycyclohexane unit instead of a diene unit (**Figure 22B**). These *syn*-1,4-diol precursor groups, or "L-shaped subunits", allow assembly of the macrocycles without interference from excessive strain by pushing the aromatization step until the end. The third route, reported by Yamago, *et al*, employs a unique platinum square precursor, with the arene subunits connected by Pt atoms at the vertices (**Figure 22C**). A reductive elimination affords [*n*]CPP or analogous macrocycle. The first half of this chapter will focus on the methods employed by these three groups in the formation of [*n*]CPPs as developed individually by the chemists. Afterward, I will spend some time discussing the adaptation and potential improvement made by our work over and above the currently existing pathways to the curved benzenoid structures.

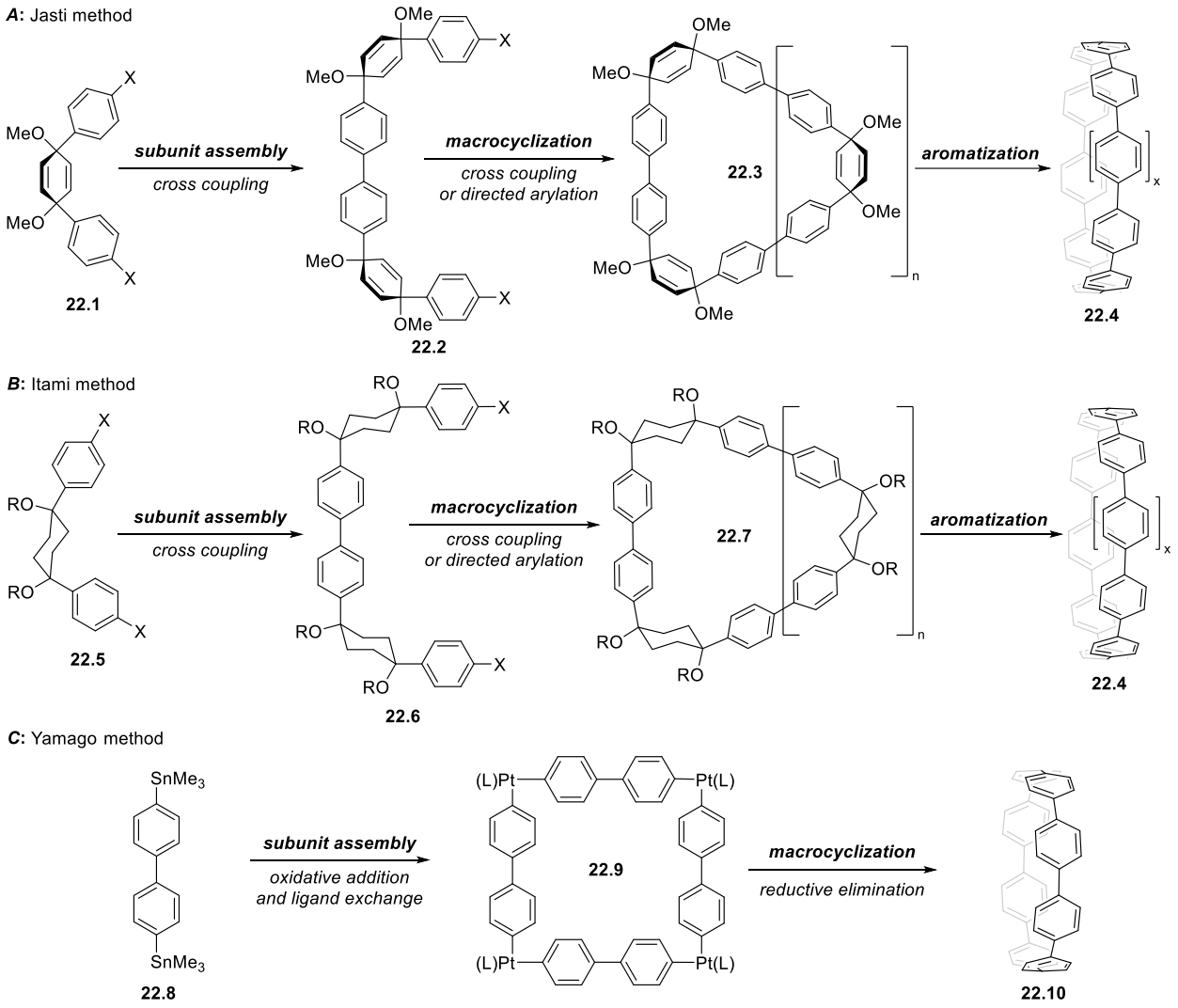

***Figure 22**: Three general strategies for synthesizing [n]CPPs*

2.2.1 Jasti method for size-selective synthesis of [n]CPPs

As the first and most prolific chemist to uncover the path to the [*n*]cycloparaphenylenes, Jasti has reported a vast number of syntheses of these macrocycles. The general outline of his strategy is shown below (**Figure 22A**). After synthesizing the L-shaped subunit via aryllithium addition to a quinone-based substrate, the subunits are combined into a U-shaped system **22.2**. This can then be converted into the relevant macrocycle **22.3** by either cross coupling with another block, directed arylation, or in the case of [5]CPP, oxidative boronate coupling. Treatment of the macrocycle with the proper aromatization conditions produces the desired [*n*]CPP.

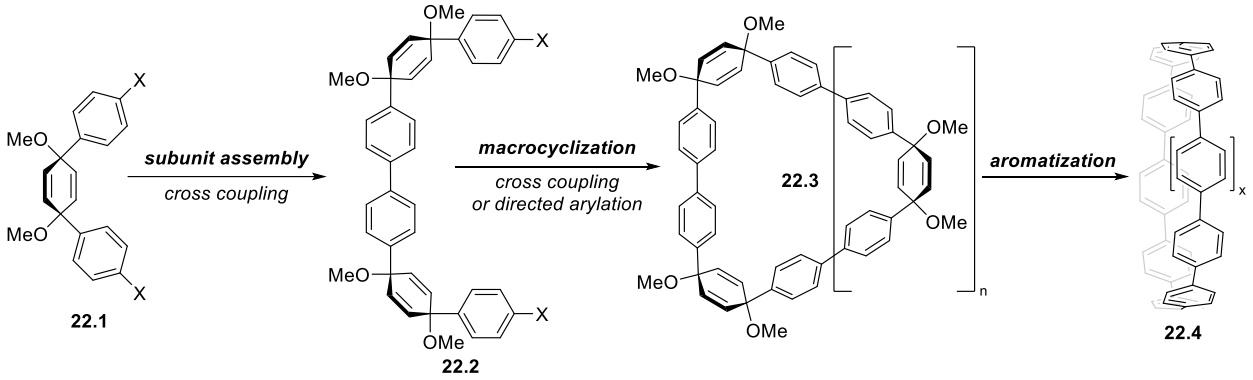

***Figure 22A**: Jasti's general strategy for synthesizing [n]CPPs*

After decades of interest in the synthesis of cycloparaphenylenes, the breakthrough paper was published by Jasti and Bertozzi in 2008. In their paper, the synthesis of [9], [12], and [18]cycloparaphenylenes were reported as the product of a shotgun-type strategy, using the cyclohexadiene moiety as a rigid pre-aromatic ring to build up strain in sequentially, up to 69, 50, and 33 kcal/mol, respectively (**Figure 23**).[20] Beginning from 1,4-diiodobenzene (**23.1**), a monolithiation of the starting material followed by twofold addition to benzoquinone (**23.2**) gives a *syn*-1,4-diol, which was quickly protected as a methyl iodide (**23.3**) before purification.

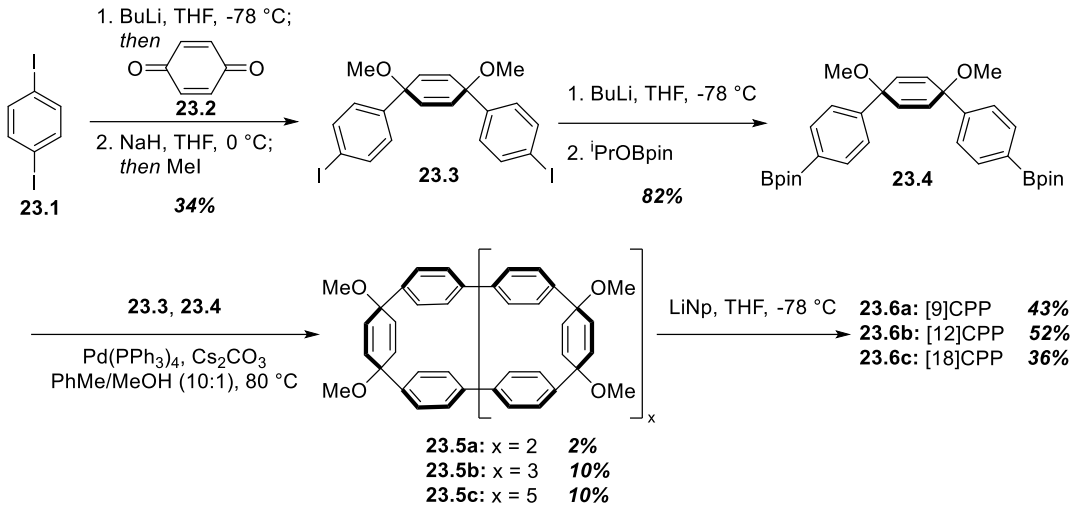

***Figure 23**: Jasti/Bertozzi seminal synthesis of [9], [12], and [18]CPPs*

Diiodide **23.3** was converted to bisboronate **23.4** by treatment with *n*-butyllithium followed by isopropoxyBpin to give **23.4** in 82% yield. Next, typical Suzuki reaction conditions afforded [9], [12], and [18] macrocycles in 2%, 10%, and 10% yield, respectively, all of which were separable by flash chromatography. Finally, they reported a new method for converting 1,4-dimethoxy-2,5-cyclohexadienes directly to the relevant *para*-substituted benzene rings via a radical mechanism by treating them with lithium naphthalide at -78 °C. This aromatization step marked the first successful synthesis of any of the [*n*]CPPs since the beginning of the quest in the 1930s.

As an independent investigator, Jasti continued to develop the field of [*n*]CPP synthesis. In 2011, his group published the selective synthesis of [7]CPP following the report of [8]CPP by Yamago and coworkers the previous year (see section 2.2.3 for details) (**Figure 24**).[22] From precursor **24.1**, which is produced in 68% yield over a single step by hypervalent iodine oxidation of 4-bromophenyl-4'-trimethylsilylphenol in water, treatment with sodium hydride and then 1,2-addition of 4-chlorophenyllithium affords a diol, which is protected as dimethyl ether **24.3** in 49% overall yield. The diastereoselectivity of the addition reaction was roughly 19:1 in favor of the *syn* isomer. It is hypothesized that this selectivity was due to the electrostatic effect of the sodium-oxygen bond after the treatment with sodium hydride, which prevents attack from that side of the molecule, along with the increased steric repulsion from the larger sodium as opposed to a hydrogen.

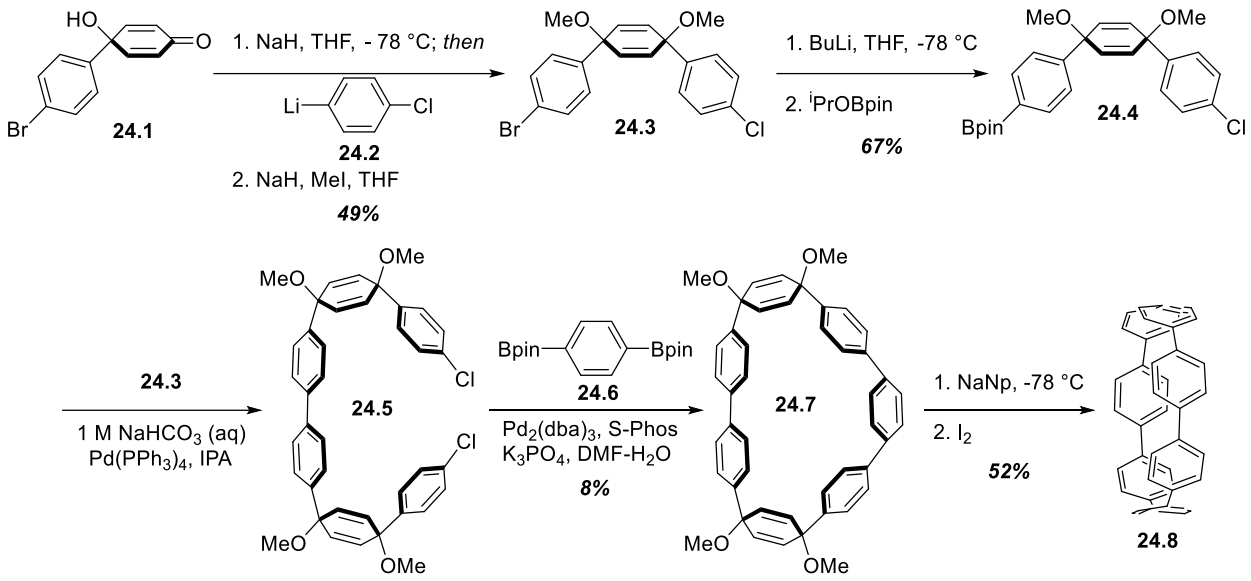

***Figure 24**: Jasti synthesis of [7]CPP*

Next, aryl bromide **24.3** was converted to boronate ester **24.4** through the same method used in the previous synthesis. The two coupling partners were then combined in a Suzuki reaction, carefully leaving the chloride functional groups untouched to afford **24.5**. The following step utilized the S-Phos ligand and $Pd_2(dba)_3$, which are stated to be a more reactive catalytic system, allowing the aryl chloride groups to undergo coupling with 1,4-bis(Bpin)benzene, resulting in macrocycle **24.7** in 8% yield. Subjecting this macrocycle to reductive aromatization, then quenching the resulting radical with iodine crystals, gives [7]CPP in 52% yield.

One year later, Jasti reported the selective synthesis of [6]CPP after a similar fashion (**Figure 25**).[23] Beginning from the same starting material (**24.1**) as [7]CPP, treatment with sodium hydride followed by *tert*-butyldimethylsilyl-protected biphenyllithium **25.1**, then protection with methyl iodide afforded L-shaped precursor **25.2a** with an overall yield of 62%. After deprotection of the TBS group using tetrabutylammonium fluoride to give **25.2b** in 95% yield, the resultant phenol was treated with hypervalent iodine in water to obtain dienone **25.3** in 71% yield. A second sequence of sodium hydride/aryllithium addition/methylation gives U-shaped intermediate **25.4** in 51% yield. Macrocyclization was achieved by Suzuki coupling of dibromide precursor **25.4** with 1,4-bis(Bpin)benzene **24.6**, affording macrocyclic precursor **25.5** in 12% yield. The previous aromatization strategy of sequential treatment with sodium naphthalide, then iodine gives [6]CPP (**25.6**) in a yield of 48%. This was, once again, the smallest CPP to date at the time, with a strain energy of 96 kcal/mol.

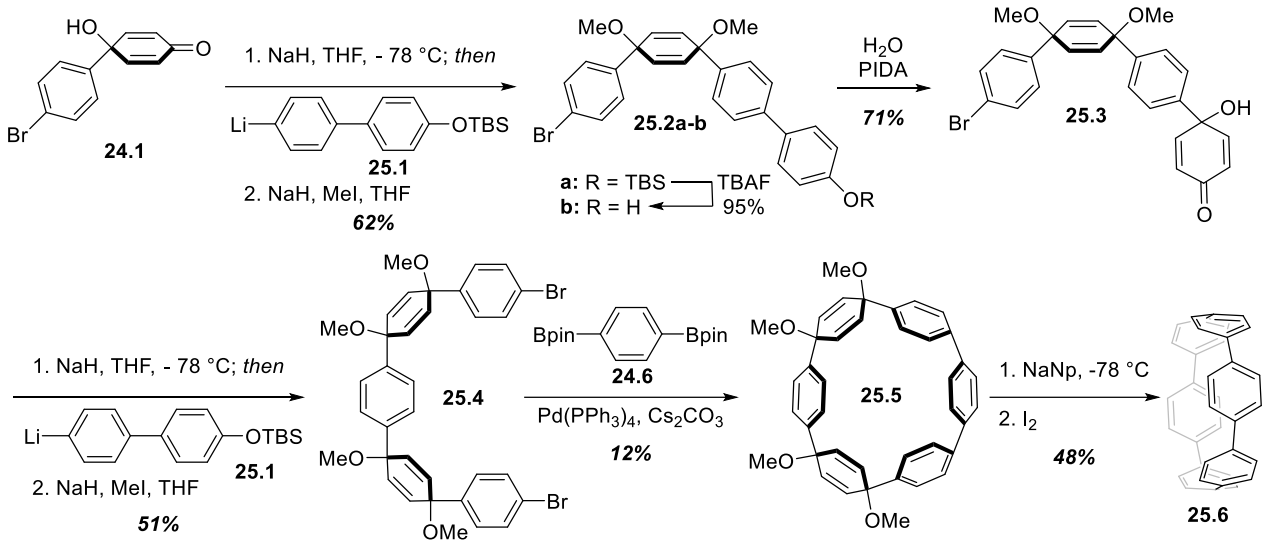

***Figure 25**: Jasti synthesis of [6]CPP*

The Jasti strategy has thus far been the most prolific in the synthesis of smaller and smaller CPPs, along with producing derivatives as well. However, it has not been the only method for creating these strained molecules. Several other groups continue vying for the next advancement in the "nanotube precursor" subgenre of total synthesis-type chemistry, including two groups hailing from Japan: those of Shigeru Yamago and Kenichiro Itami. The next two sections will discuss some of these other reports for the synthesis of CPPs.

2.2.2 Itami method for the size-selective synthesis of CPPs

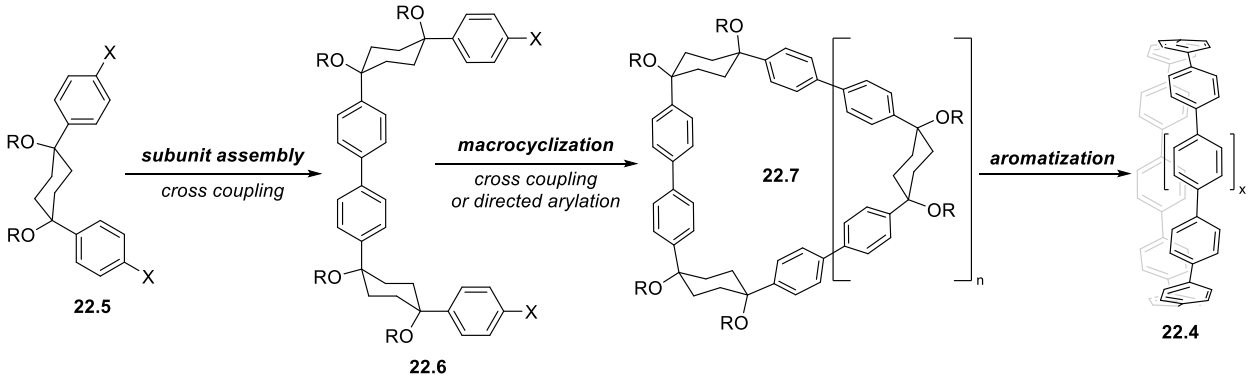

***Figure 22B**: Itami's general strategy for the synthesis of [n]CPPs*

The method used by Itami in his continued work on the CPPs employs a similar general strategy to the Jasti work by deriving the macrocyclic systems from an L-shaped precursor molecule. However, the difference, as seen in **Figure 22B**, is that rather than a 2,5-cyclohexadiene-1,4-diol core structure, the pre-bent ring consists of a 1,4-cyclohexanediol ring with no double bonds.

This decreases the rigidity of the L-shaped precursor, which allows for facile ring flipping of the cyclohexane groups even after macrocyclization. The macrocyclization yield also tends to be higher in Itami's Yamamoto coupling conditions than for Suzuki macrocyclization as seen in the Jasti synthesis. However, the other difference is the aromatization step, which requires a more strenuous set of conditions since all three of the double bonds in the benzene ring must be introduced during the same sequence, which also has the unfortunate side effect of limiting this strategy to the synthesis of the less-strained [*n*]CPPs.

In 2011, Itami and coworkers reported the synthesis of [9]cycloparaphenylene based on a nickel-mediated macrocyclization (Yamamoto reaction).[24] From **26.1**, which can be traced back to 1,4-cyclohexadione, an optimized Yamamoto reaction allowed the chemists to form trimer **26.2a** in 32% yield, alongside square-shaped tetramer **26.2b** in 23% yield (**Figure 26**). At lower concentrations trimer was preferred over tetramer, along with a higher overall yield at lower concentrations as well. Interestingly, it was confirmed by variable-temperature NMR that the cyclohexane rings in the oligomeric macrocycles are capable of undergoing chair flipping, which indicates an unexpected level of flexibility in the molecule. Notably, this is likely a factor in the simplicity of the macrocyclization, though the yield is not fantastic. Trimer was then treated with sodium bisulfate monohydrate in refluxing *m*-xylene/DMSO to grant [9]CPP in 24% yield.

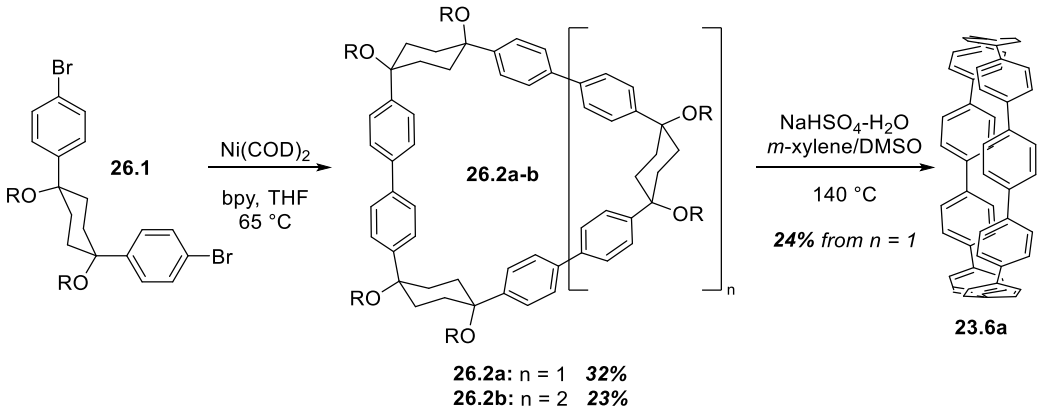

***Figure 26**: Itami synthesis of [9]CPP*

2.2.3 Yamago method for the size-selective synthesis of CPPs

The third and final general strategy has been developed by Yamago and coworkers. The broad technique involves the use of a 4,4'-bis(trimethylstannyl)biphenyl starting material (and/or a triphenyl analog), which undergoes oxidative addition in the presence of stoichiometric amounts of $Pt(cod)Cl_2$ to generate the "platinum square" complex, as shown in **Figure 22C** below. Following this step (sometimes) is a ligand exchange, proceeding then to the reductive elimination to form the macrocycle and generate the CPP in a single smooth step. This strategy helps to solve some of the struggles found in the other two; for example, the step economy is much more desirable in the Yamago sequence. However, there are also some drawbacks: stoichiometric use of platinum catalyst can be cost-prohibitive for large scale productions, and the "platinum square" strategy only works well with even numbered [*n*]CPPs and requires careful development to use for any CPP targets that fall outside the [4*n*]CPP category, as the shotgun approach makes selective synthesis impossible.

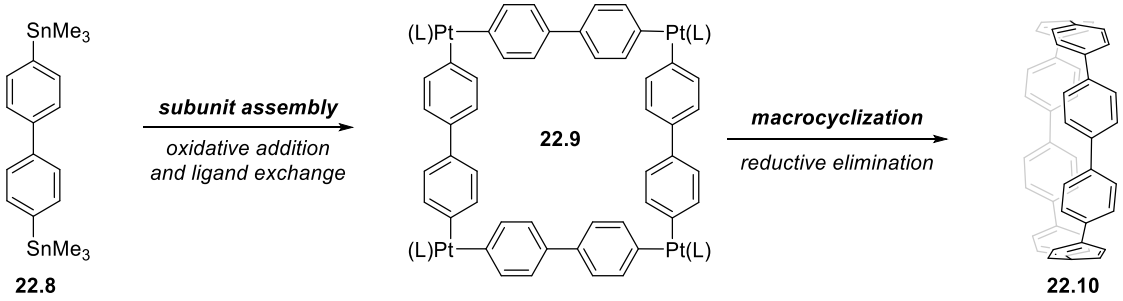

***Figure 22C**: Yamago's general strategy for the synthesis of [n]CPPs*

Yamago's original publication for the synthesis of [8]cycloparaphenylene outlined a simple three-step sequence to obtain the nanohoop from 4,4'-bis(trimethylstannyl)biphenyl **22.8.**[21] Beginning with this starting material, treatment with one equivalent of $Pt(cod)Cl_2$ in refluxing tetrahydrofuran for about a day and a half gives square-shaped tetraplatinum complex **27.1a** in 57% yield (**Figure 27**). After isolation of this material by filtration, it was suspended in dichloromethane and treated with dppf (1,1'-bis(diphenylphosphino)ferrocene) in a ligand exchange reaction to afford **27.1b** in 91% yield. Finally, the complex was converted into the desired [8]CPP by reductive elimination using molecular bromine in toluene at 95 °C, obtaining [8]CPP in 49% yield. The product was purified via gel permeation chromatography followed by a standard flash column with silica gel to afford [8]CPP in a 25% yield over 3 steps with mild, neutral conditions, generating a total of 74 kcal/mol of strain energy in the process.

This method allows for the quick assembly of the [8]CPP framework, as well as providing an opening for functional group introduction, since most groups should survive the gentle reaction conditions applied in the above synthesis. As time went on, Yamago would continue to improve on this strategy and report several modifications for the synthesis of other [*n*]CPPs and [*n*]CPP derivatives, some of which are discussed in the following paragraphs.

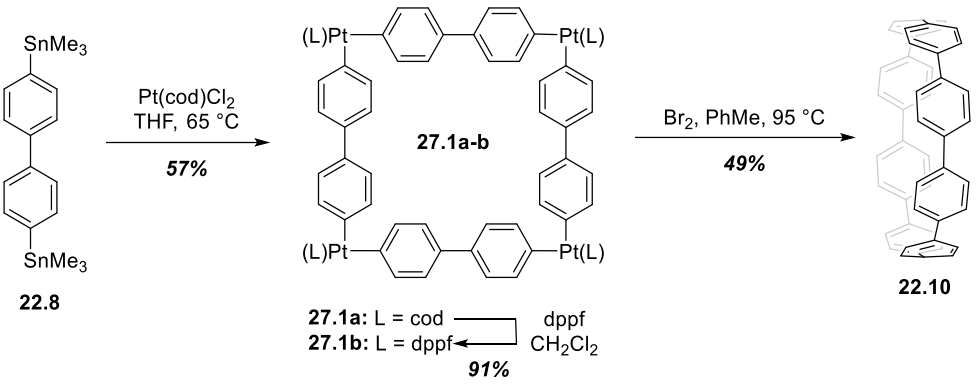

***Figure 27**: Yamago synthesis of [8]CPP*

In 2013, Yamago reported a synthesis of [6]CPP using a modified "platinum square/rectangle" approach.[25] Beginning from 1,4-dibromobenzene, generation of the Grignard reagent followed by treatment with trimethyltin chloride yielded 1,4-bis(trimethylstannyl)benzene **28.2** in 94% yield (**Figure 28**). By the same two step sequence as in the 2010 paper, intermediate **28.3** was afforded in 84% overall yield. Reaction with *in situ* generated aryllithium produced complex **28.5** in 45% yield. Two equivalents of this material formed rectangular complex **28.6** in 63% yield under Yamamoto coupling conditions. Finishing the sequence with bromine was unsuccessful in the case of [6]CPP, which was determined to be due to an undesired C-Br reductive elimination competing with the C-C bond formation. Therefore, an alternative oxidant was needed, and the halogen should be fluorine rather than bromine. After optimizing the reductive elimination step, it was determined that using xenon difluoride was the best choice, affording [6]CPP in 40% isolation yield. [8] and [10]CPP were also synthesized through this homodimerization strategy and reported in the same publication.

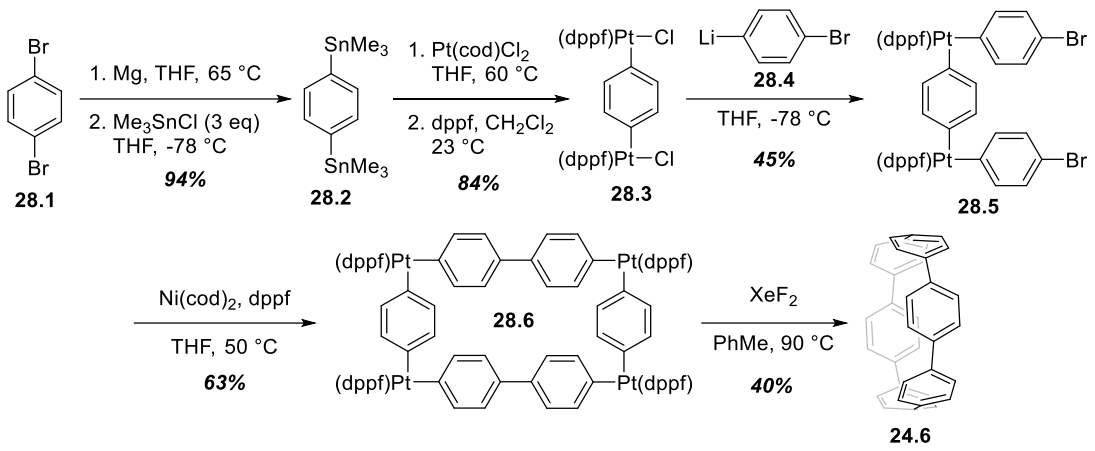

***Figure 28**: Yamago synthesis of [6]CPP*

An additional report of a related synthesis of [10]CPP and several tetraalkoxy derivatives thereof was published by Yamago in 2017.[26] In this paper, [10]CPP is synthesized through a modified "platinum square" type process inspired by Yamago's previous work, as well as Jasti's L-shaped subunits. Starting from benzoquinone (or a functionalized version) **29.1**, twofold addition with lithiated biphenyl **29.2** (derived from 4-iodo-4'-biphenyl) followed by protection as a triethylsilyl ether gives **29.3a** in 42% yield for the undecorated material (**Figure 29**). The terminal bromines are converted to boronate esters by the same method as before (*n*-BuLi and isopropoxyBpin) to afford **29.3b** in 91% yield, and the Bpin groups undergo oxidative addition with $Pt(cod)Cl_2$ to form platinum homodimer complex **29.4** in 68% yield. This complex is treated straightforwardly with triphenylphosphine in near-refluxing toluene to achieve the desired reductive elimination, forming macrocyclic product **29.5a** in 73% yield, then with tetrabutylammonium fluoride to reveal the two cyclohexa-2,5-diene-1,4-diol units (**29.5b**, 96% yield). Reductive aromatization was achieved by treatment of the macrocyclic tetraol with *in situ* generated H_2SnCl_4, giving [10]CPP (**29.6**) in 92% yield. Overall yield of [10]CPP was 17% over 7 steps, which is higher than the previously reported syntheses at the same scale.

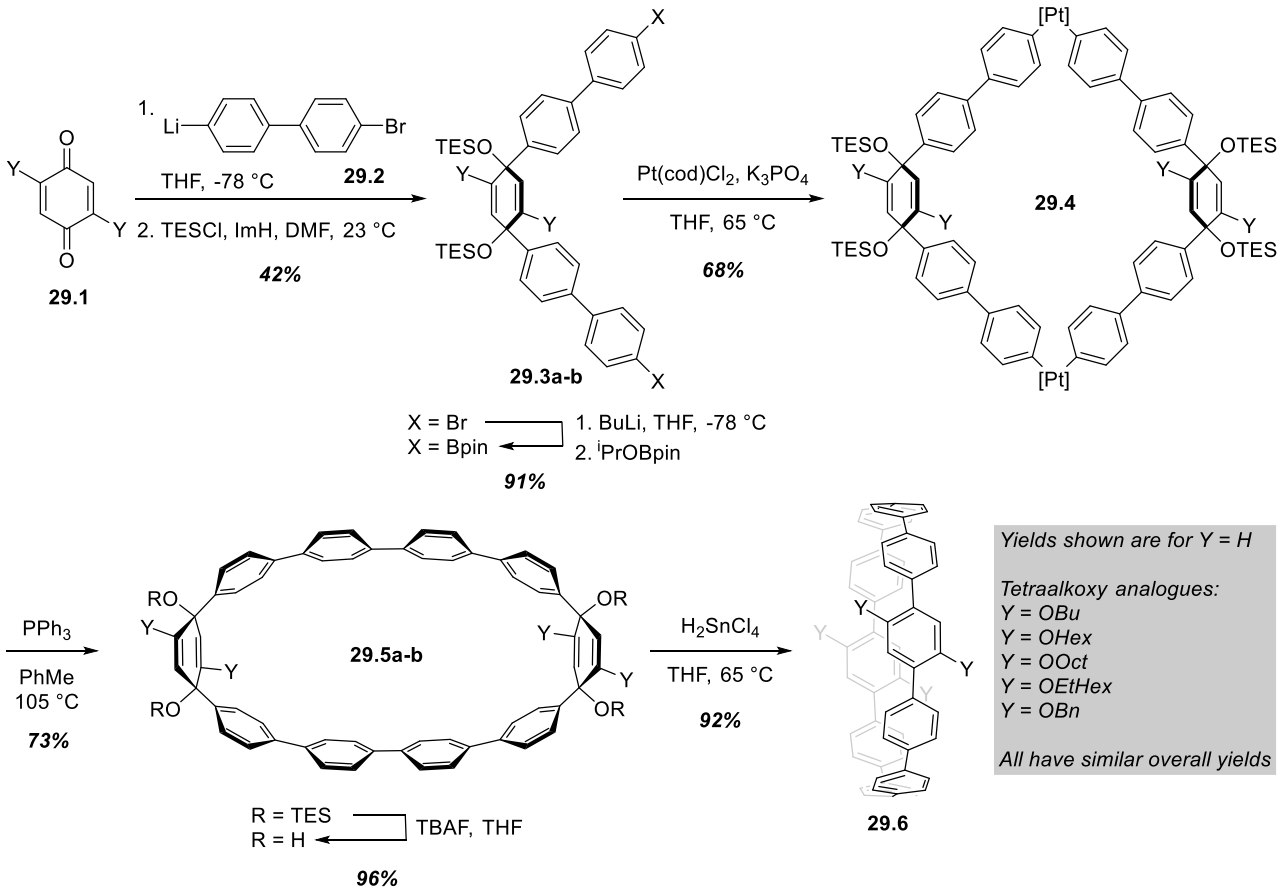

***Figure 29**: Yamago synthesis of [10]CPP and its tetraalkoxy analogues*

2.2.4 Synthesis of [5]CPP by Yamago and Jasti groups

Probably the most noteworthy reported syntheses of cycloparaphenylenes were published only a few weeks apart in 2014. Yamago and coworkers first reported the completed synthesis of [5]CPP, which follows the outline below (**Figure 30A**).[6] Starting from intermediate **30.1** (obtained from addition of a TBS protected biphenyl unit to Jasti's established dienone starting material **24.1**, then desilylation of the protecting group), a hypervalent iodine oxidation in water reveals cyclohexadienone **30.2** in 71% yield. Using Jasti's conditions, Yamago and coworkers treated tertiary alcohol with sodium hydride followed by aryllithium **28.4** to give **30.3** in a high diastereomeric ratio. The two resultant hydroxyl groups were then protected as triethylsilyl ethers, providing U-shaped precursor **30.4** in 53% yield over two steps. Yamamoto coupling of the terminal halogens closed the macrocycle in a yield of 63% for product **30.5**. Near quantitative deprotection of all four TES groups was accomplished by treatment with TBAF, then tetraol **30.6** was aromatized with mild tin(II) chloride in 58% yield to obtain [5]CPP (**30.7**).

Shortly afterward, the Jasti research group published their findings on the synthesis of [5]CPP (**Figure 30B**).[7] From the U-shaped precursor **30.8** (obtained from borylation of intermediate **25.4** in the synthesis of [6]CPP), an unexpected oxidative boronate coupling reaction in the presence of trace oxygen resulted in macrocycle **30.9a** in a low yield when attempting to form the homodimer of **30.8** as a precursor for [10]CPP. Following optimization of the concentration along with the other conditions, the former side product was obtained in a yield of 52%. Tetramethoxy macrocycle **30.9a** was treated with the usual dissolving metal conditions (sodium naphthalenide in tetrahydrofuran), but this reaction was not powerful enough to induce the necessary strain energy in the [5]CPP system, instead resulting in a stable dianion on two of the four positions, which could be quenched with methanol to give dimethoxy macrocycle **30.9b**. This in turn was subjected to LDA reduction, which successfully eliminated two equivalents of methanol to afford [5]CPP (**30.7**) in 69% yield. Jasti's approach, though it was published slightly later and with a lower overall yield, took place on a larger scale and employs a key macrocyclization step that proceeds at room temperature without stringent air-free conditions.

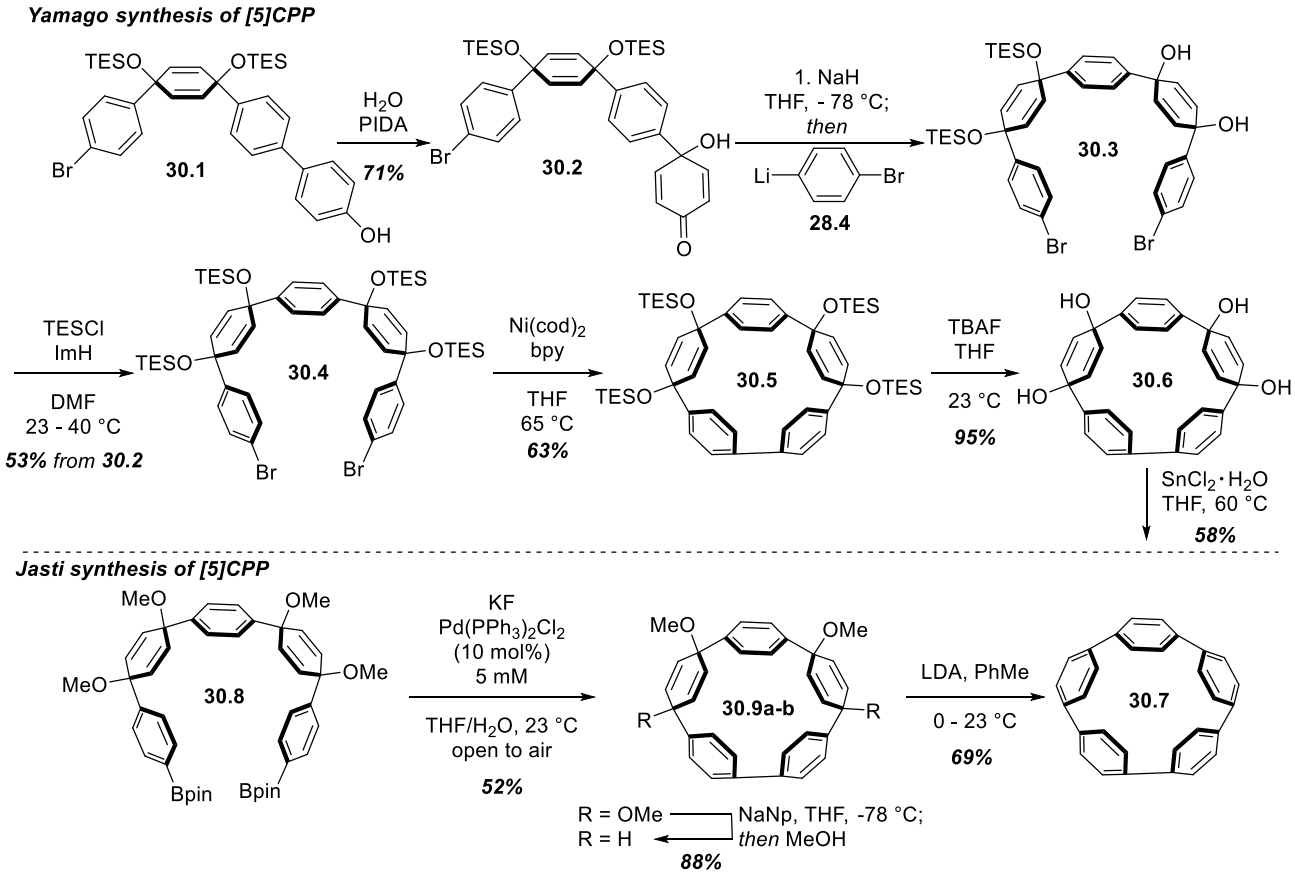

***Figure 30**: Yamago and Jasti syntheses of [5]CPP*

2.3 Selective Synthesis of [6], [8], and [10]CPPs through a cyclohex-2-ene-1,4-diol intermediate

A novel strategy for the synthesis of strained benzenoid macrocyclic systems aimed at the development of new synthetic tools and strategies for a bottom-up approach to carbon nanohoops and nanobelts has been developed in our laboratory over the past 9 years. This approach begins with an efficient and rapid 4-step sequence to generate macrocyclic 1,4-diketones on gram-scale. The resulting 1,4-diketones can then undergo diastereoselective Grignard addition followed by a RCM reaction, and mild dehydrative aromatization (TsOH or Burgess reagent) to yield highly strained benzenoid macrocycles (**Figure 31**) see Chapter 1).

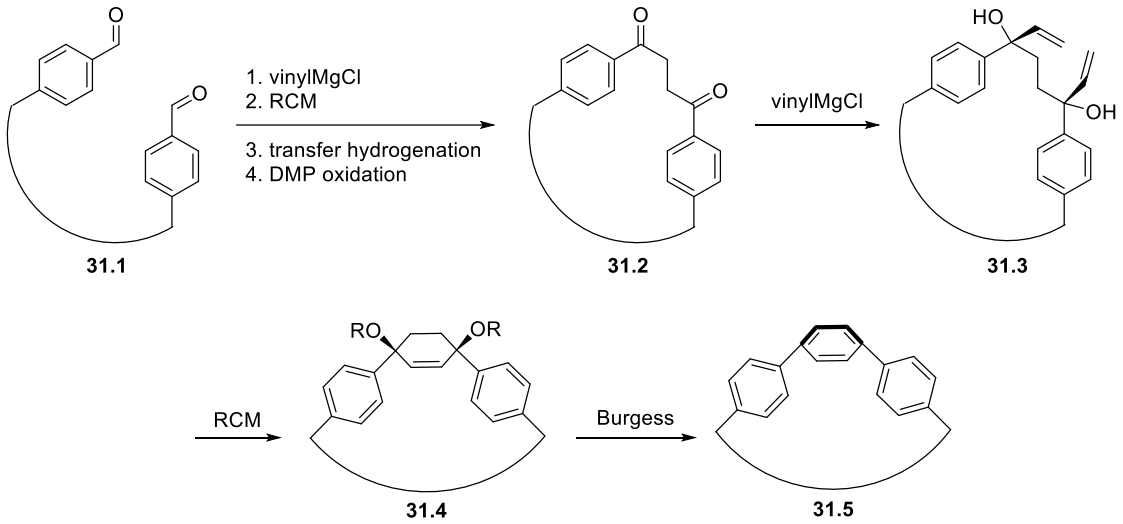

***Figure 31**: General sequence for the cross coupling-free synthesis of strained benzenoid rings*

Given the usefulness of these building blocks in synthesizing highly strained benzenoid systems, it was desired to develop a method for embedding them within [*n*]CPP precursors as a replacement for the L-shaped subunits of Jasti or Itami. Therefore, we sought to investigate the synthesis of [6], [8], and [10]CPP precursors with cyclohex-2-ene-1,4-diol rings included in the macrocyclic framework. Drawing inspiration from previously reported [*n*]CPP syntheses, we envisioned that the subunit assembly could be performed via cross-coupling of two simple blocks, both of which would be derived from a 1,4-diol precursor as shown in Section 2.3.1.

2.3.1 First-generation strategy toward cyclohex-2-ene-1,4-diol building blocks

Our original plan traced the desired L-shaped cyclohexene building block back to the requisite 1,4-diketone precursor via the well-established double Grignard/ring-closing metathesis sequence used in the synthesis of [*n*]PTPPs and [*n*]PQPPs, as detailed in the previous chapter. The 1,4-diketone, in turn, would also be elaborated from a 4-halobenzaldehyde precursor (**32.1** or **32.4**) through the routine four-step protocol (vinyl Grignard addition, ring-closing metathesis, transfer hydrogenation, and Dess-Martin oxidation) commonly used in our lab (**Figure 32**). The four-step protocol proceeded in an overall yield of <20% for the iodide variant, while the dibromo-diketone was obtained in 76% overall yield. We soon discovered, however, that the efficiency of that process was highly dependent on the diastereoselectivity in the second Grignard reaction, which was produced exclusively by the conformation of the macrocyclic system in our lab's previous work, meaning that the non-macrocyclic version had no factors which would promote diastereoselectivity. In the non-macrocyclic case, the diiodide was obtained in 71% yield (35% yield of *syn*) and the dibromide was afforded in 74% yield (37% yield of *syn*) over two steps.

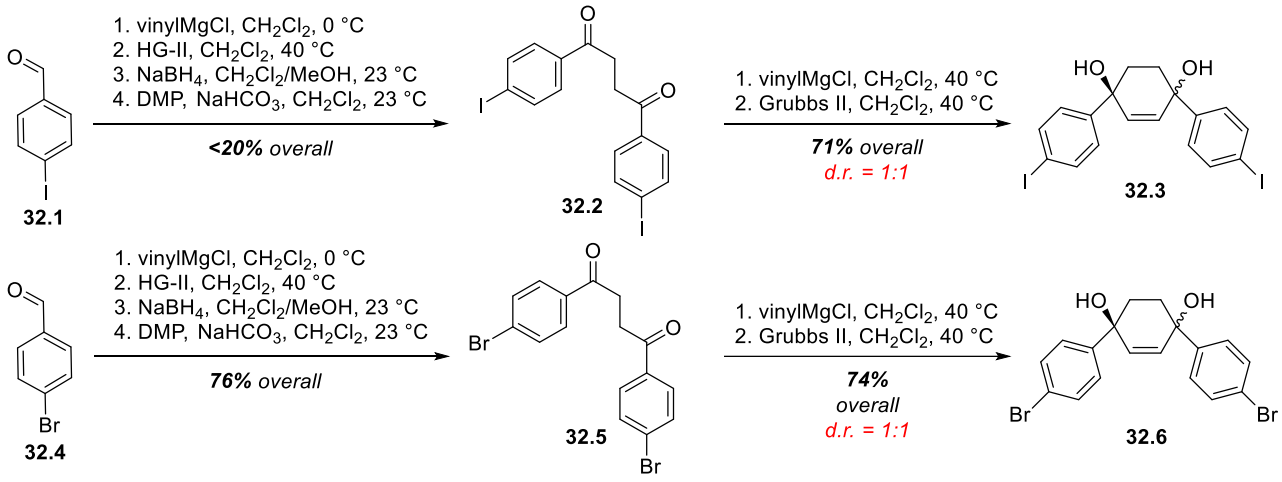

***Figure 32**: First-generation approach toward L-shaped cyclohexene-1,4-diol precursors*

Unfortunately, we observed an entirely unselective addition of vinyl groups in that reaction, meaning only half of the material at most would be suitable for the next step in the sequence. Additionally, we encountered significant solubility issues with some of the intermediates in the non-macrocyclic synthesis (specifically **32.2** and—to a lesser extent—**32.5**), which were likely not seen in the previous work due to a solubility increase from the flexible and non-polar alkoxy chain, while the non-macrocyclic intermediates all have high symmetry and lots of double bonds. With this information, we embarked on another attempt to obtain the desired intermediate.

2.3.2 Second-generation strategy toward cyclohex-2-ene-1,4-diol building blocks

When investigating the potential retrosynthesis of the target cyclohexene-1,4-diol L-shaped material, we observed that it could likely be elaborated from a similar technique to the one used by Jasti and coworkers to convert their cyclohexadienone precursor into the dimethoxycyclohexadiene building block. It was envisioned that enone **33.5** would undergo a similar 1,2-addition to form **33.6a** when treated with sodium hydride followed by 4-iodophenyllithium (**Figure 33**). **33.5** could be traced back to unconjugated enone **33.4** through a recently reported copper triflate-mediated aerobic oxidative rearrangement reaction using tetramethylguanidine as a ligand and triphenylphosphine as a reducing agent. Simple 1,2-addition of 4-iodophenyllithium (**33.2**) to ketone followed by dehydration/ketal deprotection using trifluoroacetic acid in dichloromethane reveals simple monoketal **33.1** as the starting point for our synthesis.

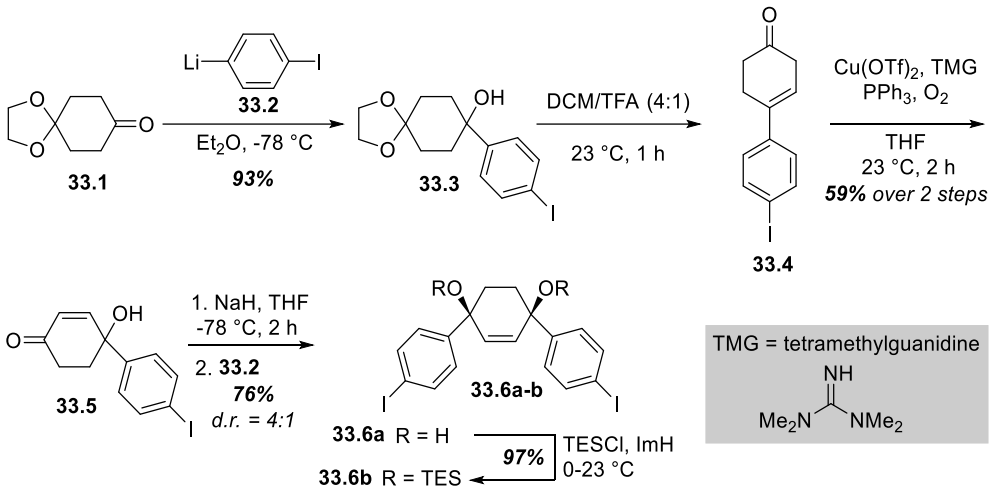

***Figure 33**: Second-generation approach to L-shaped cyclohexene-1,4-diol precursors*

Beginning from this commercially available compound, a 1,2-addition of 4-iodophenyllithium (generated *in situ* by treating 1,4-diiodobenzene with *n*-butyllithium) to monoethyleneketal **33.1** gives tertiary alcohol **33.3** in 93% yield with diethyl ether as the solvent. Treatment with trifluoroacetic acid, then basic workup and subjection of the crude residue to the copper oxidation conditions affords hydroxyenone in 59% yield over the two steps.[27] After a somewhat tedious purification, enone **33.5** is added to a flask containing a slurry of sodium hydride in dry tetrahydrofuran, followed by cannula transfer of aryllithium from another vessel to give diol **33.6a** in 76% overall yield as a 4:1 mixture of *syn* to *anti* diastereomers. This selectivity was expected based on the Jasti results, but was markedly less pronounced than in those reports. We attributed this to the decrease in rigidity from the removal of one of the olefins in our material,

which lowers the selectivity caused by the repulsion of the aryl anion by sodium alkoxide on the top face. Interestingly, the *syn* selectivity of the 1,2-addition was only mildly hampered by the omission of the sodium hydride step (d.r. = 3.3:1 without additive *vs* d.r. = 4:1 with sodium hydride). Since this decreases the complexity of the setup and allows for more consistently high yields without much loss of selectivity, we most often used the second set of conditions. After generation of the diol, simple protection of the diol as a triethylsilyl ether proceeds smoothly in 97% yield to afford **33.6b**. The second-generation strategy allows for the synthesis of the required TES-protected diol in a favorable 34% total yield over 5 steps, as opposed to a meager 17% yield for the first-generation method in 6 steps, along with greater atom economy through a diastereoselective addition of the second aryl unit.

2.3.3 Synthesis of coupling partners and optimization of macrocyclization

After obtaining the necessary L-shaped intermediate block in gram-scale quantities, the next step was to forge our desired coupling partner(s) for the macrocyclization step. Since we had not yet reported a complete synthesis of any cycloparaphenylene target, we thought it best to begin with a target that offered more promise of success. [10]CPP is a relatively unstrained nanohoop compared to the smaller ones that mark the scramble of roughly one decade ago. To our end, we decided to begin by attempting a synthesis of [10]CPP before moving to smaller nanorings.

From diiodide **33.6b**, our original attempt involved a conversion of the starting material to bis(biphenyl) building block **34.3** via a Suzuki coupling reaction with 1,4-bis(pinacolatoboron)benzene to achieve the bis-borylated intermediate, followed by a homocoupling reaction similar to the boric acid-mediated macrocyclization reported by Jasti.[7] Unfortunately, while the initial Suzuki reaction apparently proceeded in moderate yield, the conditions required an excess of 1,4-bis(pinacolatoboron)benzene, which happened to be inseparable from the desired product in column chromatography and was incompatible with the next step in the sequence, as it could also act as a coupling partner, which disrupted the desired macrocyclization.

Instead, we opted for a two-step approach to the borylated intermediate (**Figure 34**). Starting from **33.6b**, twofold Suzuki-Miyaura cross coupling with 4-bromophenylboronic acid **34.1** produced dibromine **34.2** in a promising 79% yield. Great care had to be taken with this step, as the starting material and product had similar R_f values on TLC and column separation. However, after painstaking purification, compound **34.1** was obtained in pure form. Miyaura borylation conditions proved incapable of rendering product **34.3** in sufficient quantities for our needs, so *n*-butyllithium and isopropoxyBpin were utilized instead, mirroring once again the established literature for [*n*]CPPs and resulting in a good yield of 80%. This set of conditions was also used later to synthesize **34.4** as a coupling partner in the synthesis of [6]CPP, smoothly affording **34.4** from diiodide **33.6b** in 71% yield.

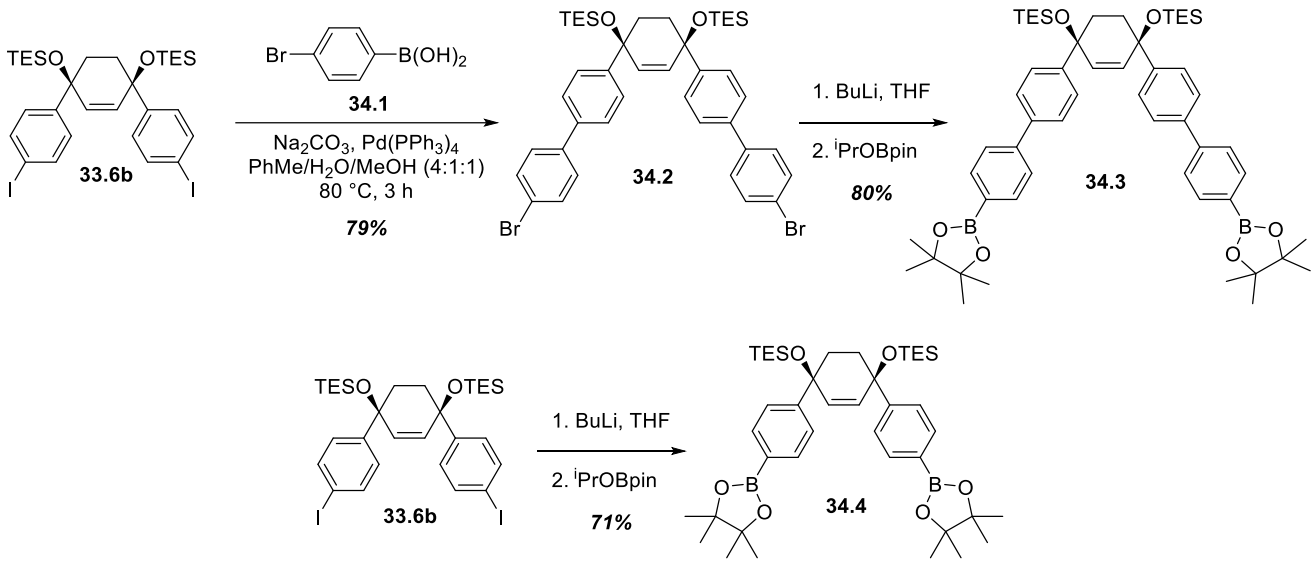

***Figure 34**: Synthesis of bisboronate coupling partners*

After synthesizing each of the L-shaped coupling partners in at least half-gram scale, we sought to find a suitably efficient set of conditions for the macrocycle formation step. Our first attempt was reminiscent of the Yamago synthesis of [10]CPP, in which a modified version of his "platinum square" type chemistry was utilized to form the macrocycle from L-shaped diboronate precursors. However, we encountered multiple problems when applying this technique to our synthesis: the macrocyclization yield tended to be quite low, and some unidentified and inseparable side products were formed (possibly "linear" oligomers) after the reductive elimination step. This may be attributable to the lower rigidity in the cyclohexene versus Yamago's cyclohexadiene, as was proposed in a similar comparison to the Jasti system earlier in this section. We also observed a struggle with reproducibility in this reaction condition. Because of these struggles, we decided to search for other potential options. After some testing, we discovered a set of Suzuki conditions (also reported, as it happens, by Yamago, *et al*) that could achieve the desired macrocyclization, albeit in modest yield.[28]

Several sets of standard Suzuki cross-coupling reactions conditions with diiodide **33.6** and bis-boronate **34.3** were screened for the synthesis of macrocycle **35.1** (**Figure 35**). Optimization of this substrate was selected as we believed its formation would be more challenging than the [10]CPP precursor, due to the more strained geometry the intermediate macrocycle. Treating **33.6** and **34.3** with $Pd(OAc)_2$ (20 mol%) and S-Phos (**35.2**, 20 mol%) in 1,4-dioxane at 80 °C led to the formation of the desired macrocycle **35.1** in 25% yield (**entry 1, Figure 35**). Increasing both the catalysts and ligand loading (30 mol% and 60 mol%, respectively) led to an improved yield of 35% (**entry 2**). Though increasing the catalyst and ligand loading even more (50 mol% and 1 eq, respectively) resulted in a yield of 39% (**entry 3**), we judged that the slight increase in yield was not worth the additional catalyst spent to achieve it on larger scale, and thus proceeded with the loadings from entry 2. A brief catalyst screening (**entries 4-6**) showed

that $PdCl_2$ could produce a similar result as $Pd(OAc)_2$, though $Pd(dppf)_2Cl_2$ and $Pd(PPh_3)_4$ resulted in decreased yield. We decided to use $PdCl_2$ as it was slightly cheaper at the time, and our supply of this catalyst was larger**.**

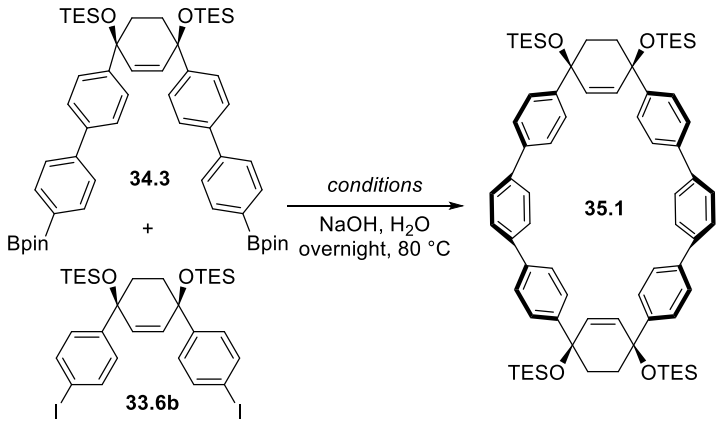

entry	catalyst	ligand	solvent	yield (%)
1[b]	$Pd(OAc)_2$	S-Phos	1,4-dioxane	25
2	$Pd(OAc)_2$	S-Phos	1,4-dioxane	35
3[c]	$Pd(OAc)_2$	S-Phos	1,4-dioxane	39
4	$PdCl_2$	S-Phos	1,4-dioxane	36
5	$Pd(dppf)_2Cl_2$	S-Phos	1,4-dioxane	30
6	$Pd(PPh_3)_4$	S-Phos	1,4-dioxane	19
7	$PdCl_2$	X-Phos	1,4-dioxane	29
8	$PdCl_2$	CyJohnPhos	1,4-dioxane	41
9	$PdCl_2$	PPh_3	1,4-dioxane	28
10	$PdCl_2$	bis(diethylamino-chlorophosphine	1,4-dioxane	trace
11	**$PdCl_2$**	**CyJohnPhos**	**PhMe/MeOH/H_2O[d]**	**47**
12	$PdCl_2$	CyJohnPhos	THF	0
13	$PdCl_2$	CyJohnPhos	DMF	14
14	$PdCl_2$	CyJohnPhos	DMSO	0

Standard conditions: **6b** (1.0 eq), **8** (1.4 eq), catalyst (30 mol%), ligand (60 mol%), NaOH (5.0 eq), H_2O (26 eq), solvent (2 mM);
b: $Pd(OAc)_2$ (20 mol%), S-Phos (20 mol%); *c*: $Pd(OAc)_2$ (50%), S-Phos (1 eq); *d*: PhMe/MeOH/H_2O (4:1:1 ratio)

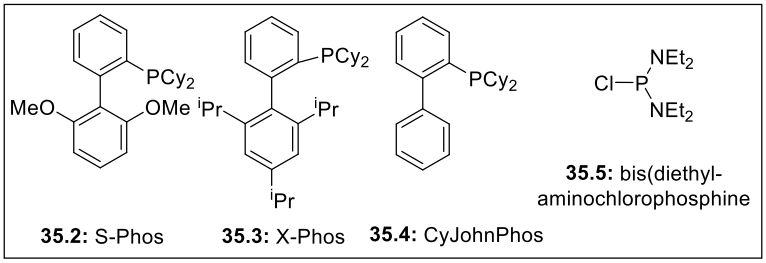

***Figure 35**: Optimization of Suzuki macrocyclization conditions*

Next, we tested several ligands (**entries 7-10**) and found that CyJohnPhos (**35.4**) was suitable for another increase in yield to 41%. Finally, a solvent screening (**entries 11-14**) showed a preference for a 4:1:1 ratio of toluene/water/methanol, giving a yield of 47%. No further improvement was obtained in future screenings, where the proportion of water was increased or removed entirely. Satisfied with the optimized yield, we moved forward with the synthesis.

2.3.4 Completion of the selective syntheses of [n]CPPs (n = 6, 8, 10)

The final few steps for the synthesis of [10]CPP are shown below (**Figure 36**). Starting from coupling partners dibromide **34.2** and diboronate **34.3** (each made up of five 6-membered rings in total), application of the optimized conditions on 70 milligram scale afforded macrocycle **36.1** in 37% yield. This macrocycle is thought to be relatively unstrained compared to the smaller examples (precursors of [6] and [8]CPP) that will be seen later. After macrocyclization, the first attempt toward completion of the CPP target involved deprotection of all four silyl ethers using TBAF, then dehydration with TsOH or Burgess reagent to finish the synthesis. To our disappointment, the tetraol intermediate formed from the deprotection reaction is almost entirely insoluble in any common solvents we tried to use, making it impossible to obtain NMR confirmation of the structure or to continue with the final aromatization step. To work around this problem, we determined that treating the protected TES diols with TsOH directly could conveniently accomplish deprotection and aromatization in one pot, likely performing the dehydration of each individual alcohol immediately following its deprotection, which avoids the solubility problems faced in the stepwise method, since the intermediates would not be as symmetrical or as polar as the tetraol. As it happens, this worked marvelously well, affording [10]CPP (**29.6**) in a strong 81% yield.

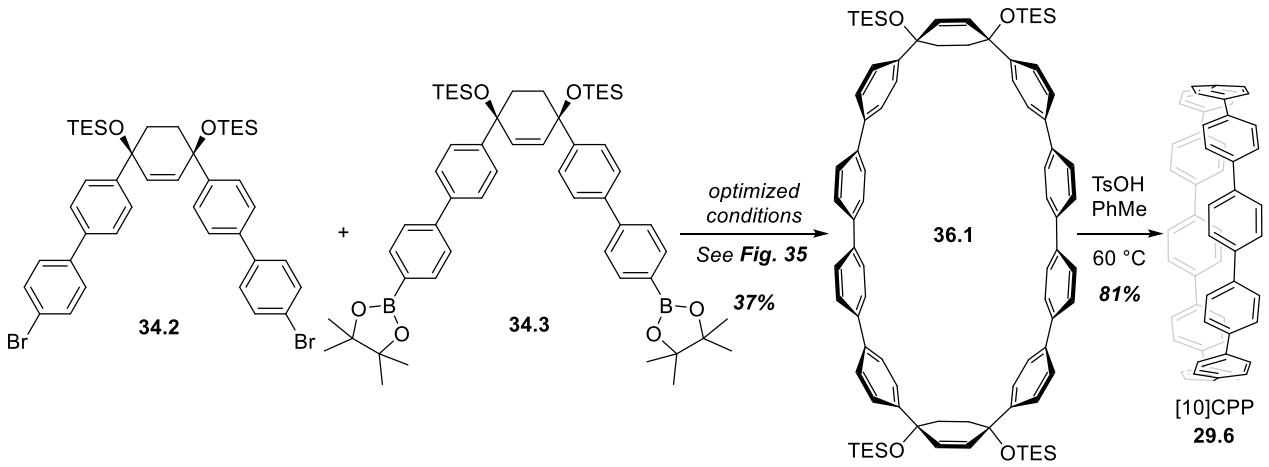

***Figure 36**: Macrocyclization and aromatization to form [10]CPP*

Shortly thereafter, we continued our work by synthesizing [8]CPP (**Figure 37**). Once again using the same optimized reaction setup, a Suzuki coupling/macrocyclization reaction between coupling partners **33.6b** and **34.3** produced macrocycle **35.1** in 39% yield when done on 87 milligram scale—roughly an order of magnitude larger than the test reactions for the optimization, which may account for the slight decrease in isolated yield for this step. Once the macrocyclic material was obtained, a quick treatment with TsOH smoothly afforded [8]CPP (**22.10**) in 66% yield.

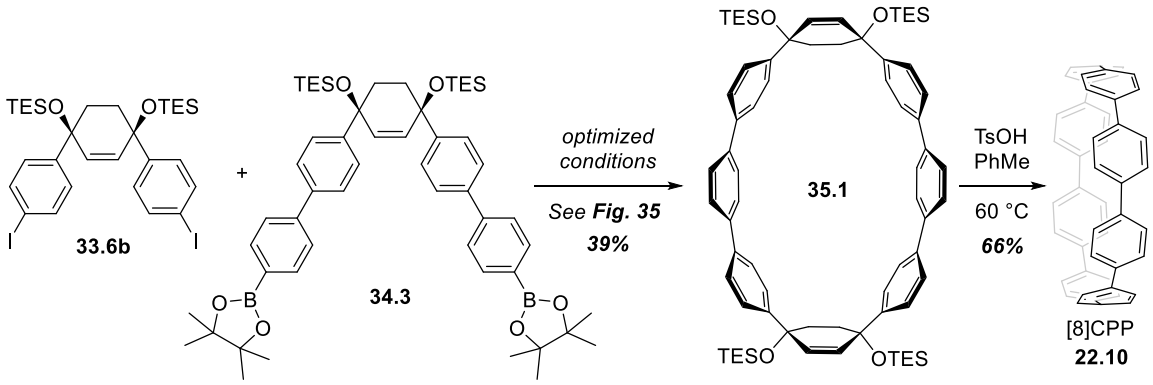

***Figure 37**: Macrocyclization and aromatization to form [8]CPP*

Using the same procedural steps, we decided to make [6]CPP as well (**Figure 38**). As the second-smallest CPP to date and the smallest example with an even-number of phenylene units, we envisioned this target to be a strong indication of the usefulness of our strategy. As a reminder, starting from intermediate **33.6b** and using the same borylation conditions as the earlier synthesis gave **34.4** in 71% yield. Suzuki-based macrocyclization of the two 3-ring building blocks (**33.6b** and **34.4**) using the optimized conditions from before gave macrocycle **38.1** in 35% yield. Lastly, aromatization with TsOH produced [6]CPP (**24.6**) in 21% yield. While this is a lower yield than would be desirable (likely due to strain-induced rearrangement and/or decomposition in the acidic medium), our strategy was sufficient for the synthesis of the highly strained target.

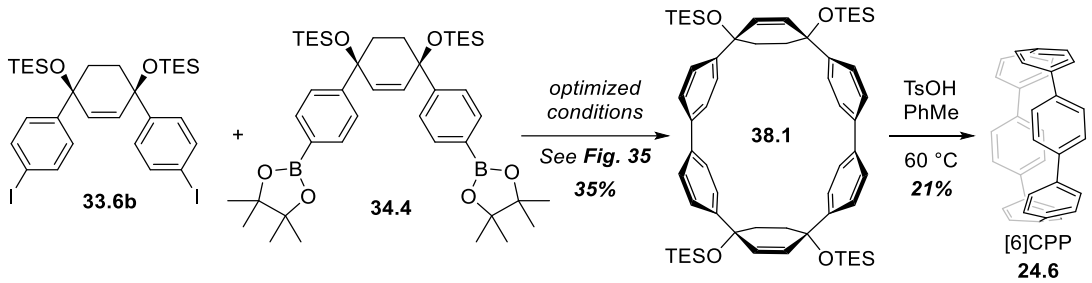

***Figure 38**: Macrocyclization and aromatization to form [6]CPP*

To emphasize the impact of strain energy on the aromatization reaction, it can be helpful to look back over the yields of each aromatization step. The completion of [10]CPP (57.7 kcal/mol, 5.77 per phenylene) proceeded in 81% yield, while the somewhat more strained [8]CPP (74.0 kcal/mol, 9.25 per phenylene) was obtained in 66% yield. A steep drop in yield is observed for [6]CPP (96.0 kcal/mol, 16.0 per phenylene) at 21% yield. It is projected that a neutral dehydration reaction such as the use of Burgess reagent would be higher-yielding for more strained systems, as it would avoid the risk of strain-induced rearrangement with smaller CPPs, but due to the insolubility of the tetraol intermediate, this is not a viable course of action. Regardless, these results show that our key intermediate, the cyclohex-2-ene-1,4-diol, has a place as a strong contender in the field of cycloparaphenylene synthesis moving forward.

2.3.5 Attempted selective synthesis of [5]CPP

To showcase the strength of our intermediate, above and beyond the synthesis of [6]CPP, we desired to accomplish a selective synthesis of [5]CPP, the smallest [*n*]CPP to be synthesized to date, which only two groups have reported to this point. In order to reach this goal, we presumed that a strategy involving a similar sequence of intermediates compared to the Yamago/Jasti publications would be the most suitable for our chemistry as well. In order to fashion a suitable substrate for the oxidative boronate coupling/macrocyclization step used by Jasti and coworkers, we envisaged a bis(enone) intermediate as one of the key steps in the synthesis. We assumed that the sequence used in the formation of **33.6b** would also be applicable in this case; therefore, a substrate was prepared via those steps.

Starting from tertiary alcohol material **33.3**, a second 1,2-addition of the aryllithium formed when **33.3** is treated with an excess of *n*-BuLi to another equivalent of ketone **33.1** produces diketal-protected substrate **39.1** (**Figure 39**). This material was partially purified by trituration in ice-cold hexanes/ethyl acetate (1:1 ratio) to remove the majority of the leftover starting materials, then treated with trifluoroacetic acid in dichloromethane in a dehydration/deprotection step to afford crude **39.2**. After basic workup to neutralize the acid, crude **39.2** was subjected to copper triflate-mediated aerobic oxidation conditions, giving

crude product **39.3** as a mixture with triphenylphosphine oxide and some other minor products. We first attempted purification at this stage, but the polarity of the desired product was quite high. This meant that we could not prevent triphenylphosphine oxide from corrupting the sample by using less polar solvent systems, thus we were unable to get pure material at this stage. Because of this issue, we continued with crude material to the next step, converting both tertiary alcohols to TES ethers and drastically lowering the overall polarity of the molecule. This change allowed us to easily isolate **39.4** from all impurities as an inseparable mixture of diastereomers (1:1 *syn*/*anti*) in 16% overall yield from **33.3**. We decided to carry both stereoisomers forward in the synthesis in order to avoid throwing out useful material, since we could not be certain which, if either, would turn out to be the functional intermediate for macrocyclization, given the increase in flexibility of the cyclohexene rings compared to the Jasti/Yamago cyclohexadiene intermediates.

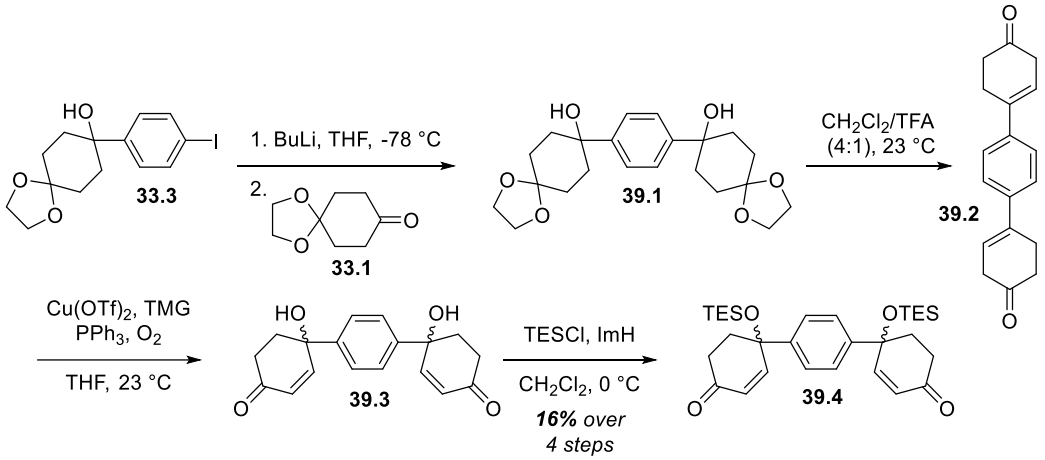

***Figure 39**: Formation of a bis(enone) precursor toward the synthesis of [5]CPP*

After obtaining **39.4** on a multi-100 milligram scale, we continued pushing toward the macrocyclization of our desired [5]CPP precursor (**Figure 40**). **39.4** was treated with excess 4-iodophenyllithium (**33.2**) in tetrahydrofuran to afford diiodide **40.1** in 47% total yield, as an inseparable mixture of isomers. Based on previous results in similar reactions, our best estimation is that the major product exhibits *syn* orientation for each pair of tertiary alcohol substituents. Whether these two pairs are *syn* or *anti* to each other is uncertain at this time. In any case, all **40.1** material is collected together and subjected to borylation via lithiation and treatment with isopropoxyBpin to produce **40.2** in 54% yield. Once again, all diastereomers were combined, because we believed it was possible that more than one would be properly oriented for macrocyclization in the next step (*i.e.* the Bpin groups would be close enough to interact with one another). **40.2** was subjected to oxidative boronate coupling conditions reported by Jasti, et al. (potassium fluoride, boric acid, tetrahydrofuran/water, open to air, very low concentration) to afford

macrocycle **40.3** in 31% yield as the all-*syn* diastereomer. No other diastereomer was observed at this stage, leading us to the conclusion that only one of the isomers that was carried through the synthesis is properly oriented for macrocyclization. However, since the other diastereomers did not seem to be detrimental to the desired reaction, and because they were apparently quite difficult to separate from the active isomer, we concluded that it would be best not to try to separate them and potentially lose valuable material in the process. Finally, with the macrocycle forged, we attempted to complete the aromatization of [5]CPP. Unfortunately, though not unexpectedly, treatment with TsOH did not result in the desired nanohoop, but a messy mixture of aromatic byproducts. Instead, we decided to work with a stepwise deprotection-dehydration sequence to form the CPP. Promisingly, the deprotection of all four silyl groups with TBAF proceeded smoothly, and a crude NMR scan confirmed the presence of the desired tetraol macrocycle. Sadly, treatment of this crude material with Burgess reagent did not result in observable [5]CPP product, but in another messy mixture of dehydration/aromatic side products that were not characterized due to the small scale of the experiment. Some potential avenues for completing the synthesis of [5]CPP will be discussed in the "Future Work" section at the conclusion of this chapter.

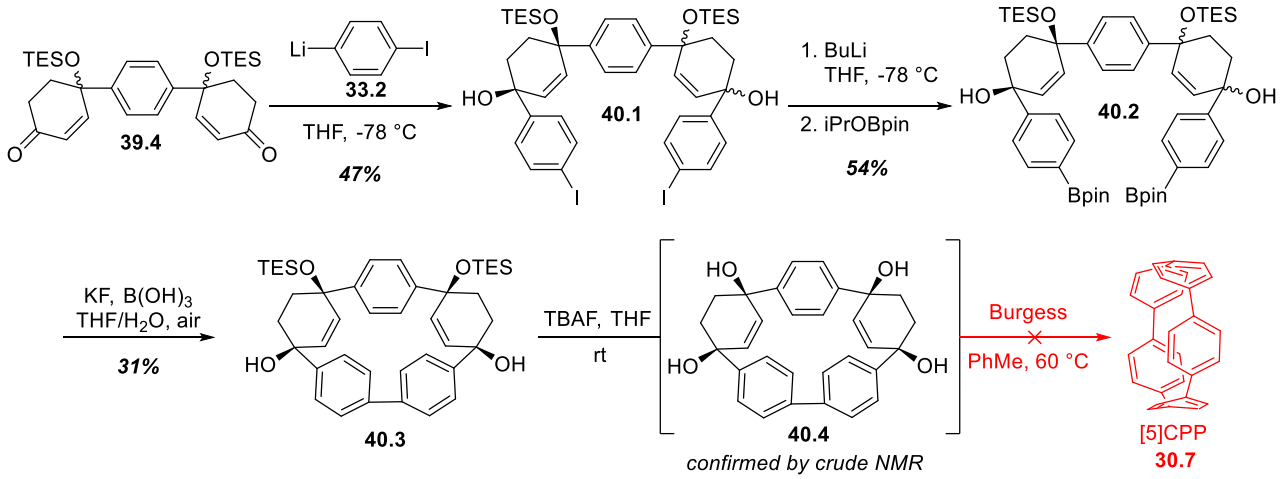

***Figure 40**: Conversion of bis(enone) intermediate to [5]CPP precursor macrocycle and attempted synthesis of [5]CPP*

2.4 Future work

2.4.1 Completion of [5]CPP synthesis

While I was unable to complete the new synthesis of [5]cycloparaphenylene during my time in the Merner group, the advanced intermediate I was able to obtain represents a great opportunity for striking toward the highly strained benzenoid target, as it includes all of the necessary carbon atoms in a macrocyclic structure that is primed for aromatization. While desilylation of **40.3** followed by treatment of the crude tetraol with

Burgess reagent was unsuccessful due to the high strain energy required by the [5]CPP product, another method used in the Merner lab might yield better results (**Figure F3**).

The lofty goal of reporting a new synthesis of [5]CPP could theoretically be accomplished by adapting the technique used for the synthesis of [4]PTPP[3]. Namely, first dehydration of the unprotected alcohols on each cyclohex-2-ene ring with Burgess reagent, then conversion of the silyl ethers to acetate groups by treatment with TBAF, then acetic anhydride, a precursor to the nanohoop (**F3.3**) could be produced. By using LDA as the base for a formal elimination of acetic acid from the relevant rings, a large amount of strain energy can be imparted on the system without risk of acid-catalyzed strain-induced rearrangement (as seen in similar dehydration reactions with tosic acid or cyclodehydrogenation with iron(III) chloride). As a reminder, the strain energy induced by this LDA-mediated elimination in the synthesis of [4]PTPP was 51.3 kcal/mol, which is far above the strain per phenylene unit in [5]CPP (43.7 kcal/mol), so the strategy is powerful enough, assuming the final intermediate can be reached. Conversion of the bis(acetate) intermediate **F3.3** is expected to proceed smoothly and in decent yield when the time comes.

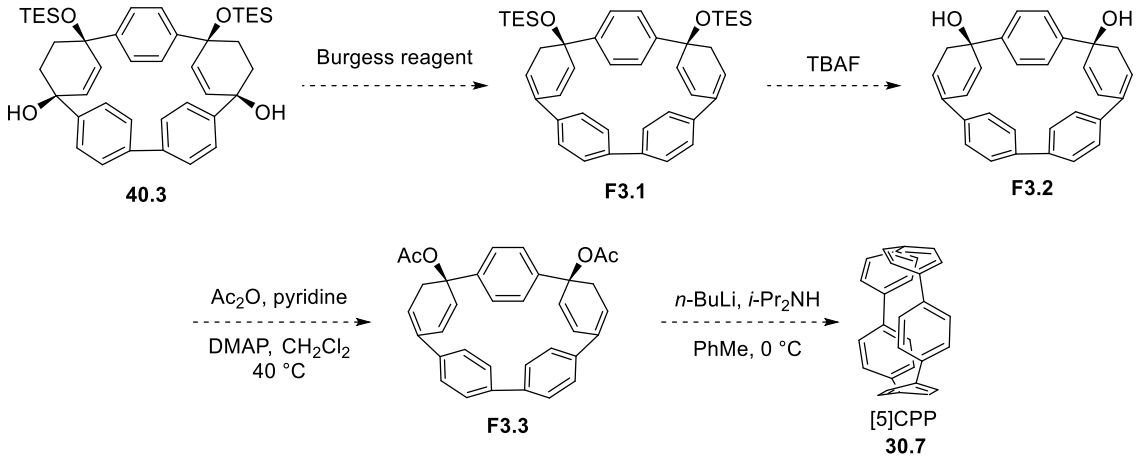

***Figure F3**: Potential path to [5]CPP from obtained late-stage intermediate*

2.4.2 Possible utility of the cyclohex-2-ene-1,4-diol precursor for π-extension of [n]CPP core structures

Finally, another future project to expand on the reported work would involve development of a strategy for the elaboration of the cyclohex-2-ene-1,4-diol moiety into suitable functional group(s) for the *π*-extension of [*n*]CPP-based benzenoid macrocycles. As discussed earlier in this thesis (see **Figure F1**), the cyclohex-2-ene-1,4-diol can be converted to an *α*-ketol functionality by the action of the boron tetrafluoride salt of TEMPO, which can potentially be used for addition of a multitude of useful functional groups. In this way,

the Merner strategy is poised to overcome the weaknesses of the existing methods for synthesis of [*n*]CPPs, which all find themselves severely limited in the *π*-extension field once the aromatization step to achieve the desired CPP is completed. Since our strategy allows for the late-stage inclusion of multiple functional groups, thereby avoiding reduced yields or reagent incompatibility issues, it also stands out from the small crowd of syntheses of functionalized [*n*]CPPs, which generally only include monofunctionalized variants[15b] or very limited *π*-extension potential[13].

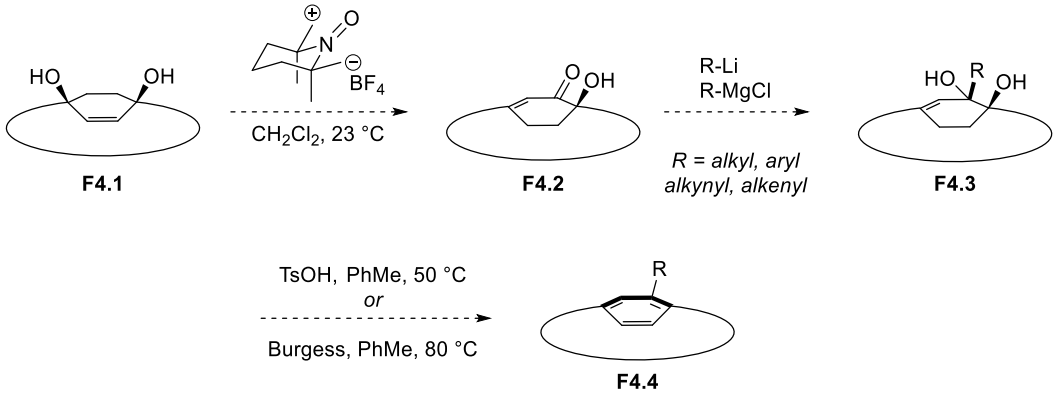

***Figure F4**: Synthesis of functionalized [n]CPPs via cyclohex-2-ene-1,4-diol intermediates*

2.5 REFERENCES

20. “Synthesis, characterization, and theory of [9]-, [12]-, and [18]cycloparaphenylene: carbon nanohoop structures.” Jasti, R. *et al*. *Journal of the American Chemical Society* **2008**, *130*, 17646.

21. “Synthesis of [8]Cycloparaphenylene from a Square-Shaped Tetranuclear Platinum Complex.” Yamago, S. *et al*. *Angewandte Chemie International Edition* **2010**, *49*, 757.

22. “Selective Synthesis of Strained [7]Cycloparaphenylene: An Orange-Emitting Fluorophore.” Sisto, T.J. *et al*. *Journal of the American Chemical Society*, **2011**, *133*, 15800.

23. “Synthesis, Characterization, and Crystal Structure of [6]Cycloparaphenylene.” Xia, J. and Jasti, R. *Angewandte Chemie International Edition* **2012**, *51*, 2474.

24. “[9]Cycloparaphenylene: Nickel-mediated Synthesis and Crystal Structure.” Yasutomo, S. *et al*. *Chemistry Letters* **2011**, *40*, 423.

25. “Selective synthesis of [6]-, [8]-, and [10]cycloparaphenylenes.” Kayahara, E. *et al*. *Chemistry Letters* **2013**, *42*, 621.

26. “Gram-Scale Syntheses and Conductivities of [10]Cycloparaphenylene and Its Tetraalkoxy Derivatives.” Kayahara, E. *et al*. *Journal of the American Chemical Society* **2017**, *139*, 18480.

27. “Copper-Catalyzed Vinylogous Aerobic Oxidation of Unsaturated Compounds with Air.” Zhang, H.J. *et al*. *Journal of the American Chemical Society* **2018**, *140*, 5300.

28. “Selective Synthesis of [12]Cycloparaphenylene.” Takaba, H. *et al*. *Angewandte Chemie International Edition* **2009**, *48*, 6112.

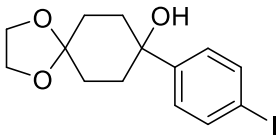

Ethyleneketal (33.3): 1,4-cyclohexadione monoethyleneketal (4.00 g, 25.6 mmol) was dissolved in anhydrous diethyl ether (120 mL) in a flame-dried round bottom flask and transferred via cannula into a vessel containing 4-iodophenyllithium, generated by addition of *n*-butyllithium (25.6 mmol) to a solution of 1,4-diiodobenzene (9.29 g, 28.2 mmol) in anhydrous diethyl ether (50 mL) under argon atmosphere at -78 °C. Solution warmed to 23 °C and quenched by addition of DI water, then extracted with dichloromethane (3 x 50 mL). Combined organics were dried over $MgSO_4$, filtered, and concentrated under reduced pressure. Residue was purified by flash chromatography (15 x 5 cm, 2–10% acetone/dichloromethane) to yield white solid (8.49 g, 92%). R_f = 0.20 (5% acetone/dichloromethane). ^{1}H NMR (500 MHz, $CDCl_3$) δ 7.67 (d, *J* = 8.6 Hz, 2H), 7.28 (d, *J* = 8.6 Hz, 2H), 4.06 – 3.93 (m, 4H), 2.18 – 2.04 (m, 4H), 1.82 – 1.75 (m, 2H), 1.73 – 1.66 (m, 2H), 1.51 (s, 1H). ^{13}C NMR (126 MHz, $CDCl_3$) δ 148.58, 137.56, 127.00, 108.47, 92.65, 72.63, 64.65, 64.52, 36.79, 30.90; HRMS (ESI) $[C_{14}H_{17}O_3INa]^+$: *m/z* = 383.0115, calcd. 383.0015

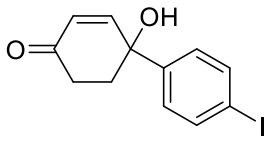

Hydroxyenone (33.5): Compound **33.3** (4.370 g, 12.13 mmol) was dissolved in a 4:1 solution of dichloromethane/trifluoroacetic acid (0.1 M) and stirred for 1 hour at 23 °C. Saturated aq. $NaHCO_3$ was added to the reaction mixture, and the aqueous phase was extracted with dichloromethane (3 x 50 mL), then dried over $MgSO_4$, filtered, and concentrated under reduced pressure. Crude residue was dissolved in tetrahydrofuran and saturated with O_2 by bubbling with a balloon for 30 minutes (and continuing to bubble while reaction begins). Copper(II) triflate (219 mg, 0.607 mmol), tetramethylguanidine (559 mg, 4.85 mmol), and triphenylphosphine (4.77 g, 18.2 mmol) were added, and reaction stirred at 23 °C for 2-20 hours. After completion, solution was concentrated under reduced pressure, and residue preabsorbed onto SiO_2 and purified by flash chromatography (16 x 4 cm, 20–40% ethyl acetate/hexanes) to yield orange solid (2.23 g, 59%). R_f = 0.30 (40% ethyl acetate/hexanes). ^{1}H NMR (500 MHz, $CDCl_3$) δ 7.74 (d, *J* = 8.5 Hz, 2H), 7.24 (d, *J* = 8.5 Hz, 2H), 6.85 (dd, *J* = 10.1, 1.0 Hz, 1H), 6.18 (d, *J* = 10.1 Hz, 1H), 2.64 (ddd, *J* = 15.5, 6.8, 4.3 Hz, 1H), 2.43 – 2.23 (m, 4H). ^{13}C NMR (126 MHz, $CDCl_3$) δ 198.87, 151.45, 143.64, 138.05, 130.27, 127.62, 94.17, 72.65, 39.12, 34.58; HRMS (ESI) $[C_{12}H_{12}O_2I]^+$: *m/z* = 314.9878, calcd. 314.9677

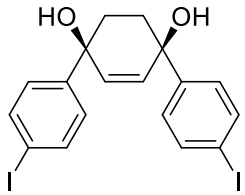

Diol (33.6a): Compound **33.5** (1.57 g, 5.00 mmol) was azeotroped to dryness using PhMe and dissolved in anhydrous tetrahydrofuran under argon atmosphere in a flame-dried round bottom flask, then added via cannula to a slurry of NaH (260 mg, 6.50 mmol, 60% w/w) in anhydrous tetrahydrofuran at -78 °C. This combined solution was stirred for 2 hours at -78 °C. Concurrently, aryllithium reagent was generated by addition of *n*-butyllithium (11.50 mmol) to a -78 °C solution of 1,4-diiodobenzene (3.96 g, 12.0 mmol) in anhydrous tetrahydrofuran under argon atmosphere in a flame-dried round bottom flask. The aryllithium solution was transferred via cannula (or needle and syringe) into the flask containing ketone 3. Solution warmed to rt and quenched by addition of DI water, then extracted with dichloromethane (3 x 30 mL). Combined organics were dried over $MgSO_4$, filtered, and concentrated under reduced pressure. Residue was purified by flash chromatography (15 x 4 cm, 0–20% acetone/dichloromethane) to yield flaky brown solid (1.99 g, 76% overall yield; 4:1 d.r.). R_f = 0.19 (30% ethyl acetate/dichloromethane). ^{1}H NMR (500 MHz, $CDCl_3$) δ 7.70 (d, *J* = 8.5 Hz, 4H), 7.24 (d, *J* = 8.5 Hz, 4H), 6.03 (s, 2H), 2.24 (s, 2H), 2.21 – 2.06 (m, 2H), 1.97 – 1.78 (m, 2H). ^{13}C NMR (126 MHz, $CDCl_3$) δ 145.84, 137.76, 134.65, 127.75, 93.47, 72.37, 36.38; HRMS (ESI) $[C_{18}H_{16}O_2I_2Cl]^-$: *m/z* = 552.8932, calcd. 552.8923.

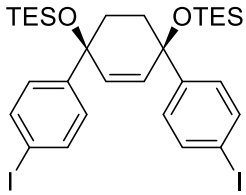

Diiodide (33.6b): Compound **33.6a** (870 mg, 1.17 mmol) and imidazole (318 mg, 4.67 mmol) were dissolved in anhydrous dichloromethane under argon atmosphere in a flame dried flask and cooled to 0 °C. Triethylsilylchloride (703 mg, 4.67 mmol) was added dropwise to the reaction, which was allowed to slowly warm to room temperature. After 3 h, reaction was quenched by addition of DI water, then extracted with ethyl acetate (3 x 15 mL). Combined organics were dried over $MgSO_4$, filtered, and concentrated under reduced pressure. Residue was purified by flash chromatography (12 x 2.5 cm, 5% dichloromethane/hexanes) to yield clear oil (1.21 g, 97%), which crystallized into a white solid upon standing several hours in the freezer. R_f = 0.40 (10% dichloromethane/hexanes). ^{1}H NMR (600 MHz, $CDCl_3$) δ 7.62 (dd, *J* = 8.5, 2.1 Hz, 4H), 7.16 (dd, *J* = 8.4, 2.0 Hz, 4H), 6.12 (d, *J* = 2.0 Hz, 2H), 2.16 (dd, *J* = 13.7, 9.4 Hz, 2H), 1.63 (dt, *J* = 14.4, 6.3 Hz, 2H), 0.89 (td, *J* = 7.9, 2.0 Hz, 18H), 0.52 (tdd, *J* = 15.1, 10.9, 6.9 Hz, 12H). ^{13}C NMR (151 MHz, $CDCl_3$) δ 147.57, 137.33, 134.55, 128.07, 92.87, 74.47, 38.11, 7.29, 6.89; HRMS (ESI) $[C_{30}H_{44}O_2I_2Si_2Na]^+$: *m/z* = 769.0859, calcd. 769.0861

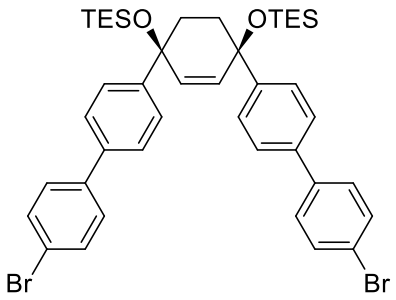

Dibromide (34.2): Compound **33.6b** (750 mg, 1.01 mmol), 4-bromophenylboronic acid (605 mg, 3.02 mmol), Na_2CO_3 (2 M in water), and $Pd(PPh_3)_4$ (350 mg, 0.302 mmol) were dissolved in a toluene/methanol/water solution (4:1:1, 10 mL) under a nitrogen atmosphere (after purging all solvents with N_2 for at least 30 minutes) and heated to 80 °C for 3 hours. At this time, the reaction was cooled to room temperature and water was added. Reaction was extracted with ethyl acetate (3 x 25 mL), then combined organics were dried over $MgSO_4$, filtered, and concentrated under reduced pressure. Residue was purified by flash chromatography (15 x 2.5 cm, 1-2% ethyl acetate/hexanes) to yield clear oil (640 mg, 79%). R_f = 0.36 (2% ethyl acetate/hexanes). ^{1}H NMR (500 MHz, $CDCl_3$) δ 7.61 – 7.40 (m, 16H), 6.21 (s, 2H), 2.28 – 2.20 (m, 2H), 1.77 (dd, *J* = 13.4, 9.1 Hz, 2H), 0.92 (t, *J* = 7.9 Hz, 18H), 0.75 – 0.40 (m, *J* = 7.7 Hz, 12H). ^{13}C NMR (126 MHz, $CDCl_3$) δ 147.39, 139.97, 138.76, 134.70, 132.07, 128.84, 126.68, 126.62, 121.68, 74.67, 38.23, 7.36, 6.92. HRMS (ESI): $[C_{43}H_{52}O_2Br_2Si_2$+formate$]^-$: *m/z* = 847.1852, calcd. 847.1844.

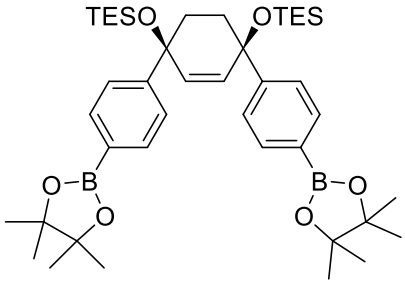

Diboronate (3-ring) (34.4): Compound **33.6b** (150 mg, 0.199 mmol) was dissolved in anhydrous tetrahydrofuran (4 mL) under an argon atmosphere and cooled to -78 °C. Next, *n*-butyllithium (0.597 mmol) was added dropwise via syringe, followed immediately by ^{i}PrOBpin (185 mg, 0.995 mmol). Reaction was allowed to slowly warm to room temperature before quenching with water, then extraction with ethyl acetate (3 x 5 mL). Combined organics were dried over $MgSO_4$, filtered, and concentrated under reduced pressure. Residue was purified by flash chromatography (14 x 1.5 cm, 2-20% ethyl acetate/hexanes) to yield pale yellow oil, which solidifies after standing several hours in freezer (106 mg, 71%). R_f = 0.24 (5% ethyl acetate/hexanes). ^{1}H NMR (600 MHz, $CDCl_3$) δ 7.71 (d, *J* = 7.9 Hz, 4H), 7.43 (d, *J* = 7.9 Hz, 4H), 6.16 (s, 2H), 2.24 – 2.06 (m, 2H), 1.82 – 1.59 (m, 2H), 1.33 (s, 24H), 0.89 (t, *J* = 7.9 Hz, 18H), 0.74 – 0.33 (m, 12H). ^{13}C NMR (126 MHz, $CDCl_3$) δ 150.97, 134.68, 125.38, 83.95, 74.91, 38.22, 25.15, 25.13, 7.34, 6.87.

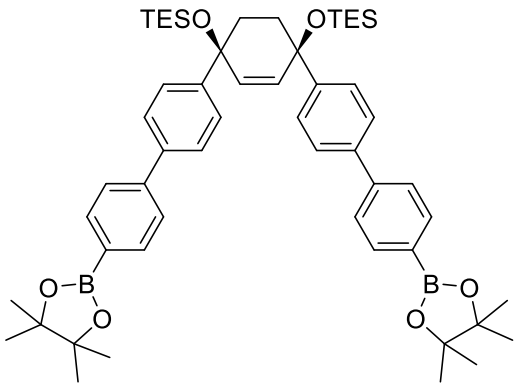

Diboronate (5-ring) (34.3): Compound **34.2** (500 mg, 0.623 mmol) was dissolved in anhydrous tetrahydrofuran (10 mL) under an argon atmosphere and cooled to -78 °C. Next, *n*-butyllithium (1.87 mmol) was added dropwise via syringe, followed immediately by ^{i}PrOBpin (1.08 g, 5.83 mmol). Reaction was allowed to slowly warm to room temperature before quenching with water, then extraction with ethyl acetate (3 x 10 mL). Combined organics were dried over $MgSO_4$, filtered, and concentrated under reduced pressure. Residue was purified by flash chromatography (15 x 2.5 cm, 5-20% ethyl acetate/hexanes) to yield pale yellow oil, which solidifies after standing several hours in freezer (448 mg, 80%). R_f = 0.24 (5% ethyl acetate/hexanes). ^{1}H NMR (500 MHz, $CDCl_3$) δ 7.86 (d, *J* = 8.1 Hz, 2H), 7.60 (d, *J* = 8.1 Hz, 2H), 7.56 (d, *J* = 8.4 Hz, 2H), 7.51 (d, *J* = 8.5 Hz, 2H), 6.21 (s, 2H), 2.24 (td, *J* = 9.6, 2.6 Hz, 2H), 1.82 – 1.73 (m, 2H), 1.36 (s, 24H), 0.92 (t, *J* = 7.9 Hz, 18H), 0.72 – 0.40 (m, 12H). ^{13}C NMR (126 MHz, $CDCl_3$) δ 147.28, 143.75, 139.74, 135.47, 134.71, 126.97, 126.56, 126.49, 84.05, 74.75, 38.25, 25.14, 7.37, 6.93.

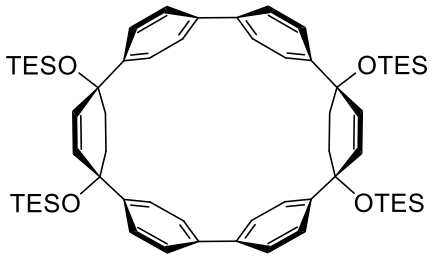

[6] macrocycle (38.1): Compound **33.6b** (44.3 mg, 0.059 mmol), compound **34.4** (62.2 mg, .0834 mmol), $PdCl_2$ (3.3 mg, 0.019 mmol), CyJohnPhos (12.5 mg, 0.036 mmol), and NaOH (14.9 mg, 0.373 mmol) were dissolved in a toluene/methanol/water solution (4:1:1 ratio, 30 mL) after purging all solvents with N_2 for at least 30 minutes. Reaction was heated to 80 °C overnight, then cooled to room temperature and water was added. Reaction was extracted with ethyl acetate (3 x 15 mL), then combined organics were dried over $MgSO_4$, filtered, and concentrated under reduced pressure. Residue was purified by flash chromatography (14 x 1.5 cm, 5-25% dichloromethane/hexanes) to yield clear oil (20.6 mg, 35%). R_f = 0.58 (50% dichloromethane/hexanes). ^{1}H NMR (500 MHz, $CDCl_3$) δ 7.63 – 7.39 (m, 15H), 7.35 – 7.26 (m, 1H), 6.27 – 6.09 (m, 4H), 2.21 (q, *J* = 12.7 Hz, 4H), 1.91 – 1.63 (m, 4H), 0.91 (tdd, *J* = 9.9, 6.2, 3.9 Hz, 36H), 0.77 – 0.42 (m, 24H). ^{13}C NMR (126 MHz, $CDCl_3$) δ 145.54, 138.24, 133.41, 126.86, 125.88, 125.39, 125.17, 124.74, 73.51, 73.45, 36.93, 23.82, 6.11, 6.08, 6.05, 5.65, 5.63, 5.60.

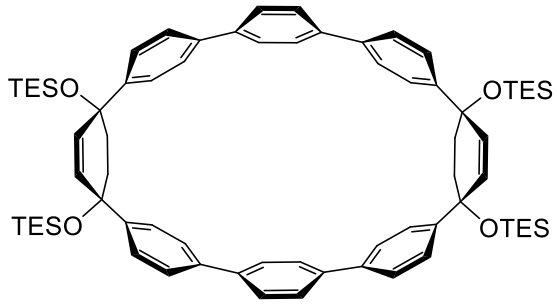

[8] macrocycle (35.1): Compound **33.6b** (52.0 mg, 0.070 mmol), compound **34.3** (87.7 mg, 0.098 mmol), $PdCl_2$ (3.7 mg, 0.021 mmol), CyJohnPhos (14.8 mg, 0.042 mmol), and NaOH (14.0 mg, 0.349 mmol) were dissolved in a toluene/methanol/water solution (4:1:1 ratio, 35 mL) after purging all solvents with N_2 for at least 30 minutes. Reaction was heated to 80 °C overnight, then cooled to room temperature and water was added. Reaction was extracted with ethyl acetate (3 x 15 mL), then combined organics were dried over $MgSO_4$, filtered, and concentrated under reduced pressure. Residue was purified by flash chromatography (15 x 1.5 cm, 5-25% dichloromethane/hexanes) to yield clear oil (31.4 mg, 39%). R_f = 0.58 (50% dichloromethane/hexanes). ^{1}H NMR (500 MHz, $CDCl_3$) δ 7.88 – 7.45 (m, 24H), 6.21 (d, *J* = 10.0 Hz, 4H), 2.25 (s, 4H), 1.81 (s, 4H), 1.05 – 0.74 (m, 36H), 0.58 (ddt, *J* = 17.6, 13.2, 7.0 Hz, 24H). ^{13}C NMR (126 MHz, $CDCl_3$) δ 127.64, 127.54, 126.72, 126.55, 74.73, 38.23, 7.38, 6.93.

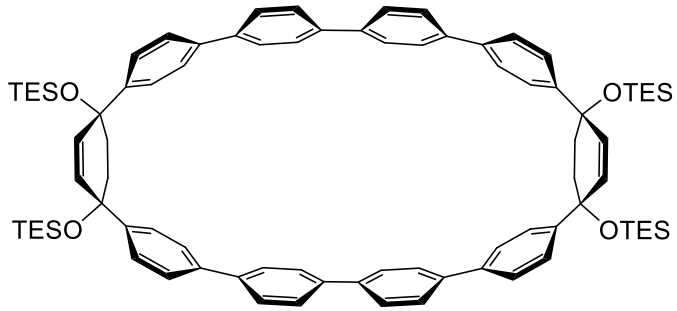

[10] macrocycle (36.1): Compound **34.2** (70 mg, 0.087 mmol), compound **34.3** (109 mg, 0.122 mmol), $PdCl_2$ (4.7 mg, 0.026 mmol), CyJohnPhos (18.5 mg, 0.052 mmol), and NaOH (17 mg, 0.44 mmol) were dissolved in a toluene/methanol/water solution (4:1:1 ratio, 42 mL) after purging all solvents with N_2 for at least 30 minutes. Reaction was heated to 80 °C overnight, then cooled to room temperature and water was added. Reaction was extracted with ethyl acetate (3 x 20 mL), then combined organics were dried over $MgSO_4$, filtered, and concentrated under reduced pressure. Residue was purified by flash chromatography (15 x 1.5 cm, 5-25% dichloromethane/hexanes) to yield clear oil (41.6 mg, 37%). R_f = 0.58 (50% dichloromethane/hexanes). ^{1}H NMR (500 MHz, $CDCl_3$) δ 7.85 – 7.46 (m, 32H), 6.23 (t, *J* = 4.3 Hz, 4H), 2.26 (q, *J* = 11.8 Hz, 4H), 1.82 (s, 4H), 1.10 – 0.80 (m, 36H), 0.59 (dddd, *J* = 23.1, 10.5, 8.0, 5.0 Hz, 24H). ^{13}C NMR (126 MHz, $CDCl_3$) δ 131.82, 128.73, 128.62, 127.40, 127.31, 127.03, 126.63, 126.50, 126.44, 126.39, 126.33, 126.27, 74.49, 38.00, 7.13, 6.69.

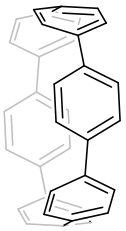

[6]CPP (25.6): Compound **38.1** (1.4 mg, 0.0014 mmol) was dissolved in toluene (0.3 mL) and heated to 60 °C; then, p-toluenesulfonic acid monohydrate (3.9 mg, 0.02 mmol) was added to the stirring reaction. Reaction was cooled to room temperature and water was added, followed by extraction with dichloromethane (3 x 1 mL). Combined organics were dried over $MgSO_4$, filtered, and concentrated under reduced pressure. Residue was purified via flash chromatography (6 x 0.3 cm, 20-40% dichloromethane/hexanes) to yield a highly fluorescent pale yellow solid (0.5 mg, 21%). Spectroscopic data matches previously reported material.

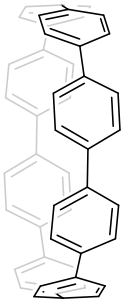

[8]CPP (22.10): Compound **35.1** (4.0 mg, 0.0035 mmol) was dissolved in toluene (0.5 mL) and heated to 60 °C; then, *p*-toluenesulfonic acid monohydrate (7.7 mg, 0.04 mmol) was added to the stirring reaction. Reaction was cooled to room temperature and water was added, followed by extraction with dichloromethane (3 x 1 mL). Combined organics were dried over $MgSO_4$, filtered, and concentrated under reduced pressure. Residue was purified via flash chromatography (6 x 0.3 cm, 30-50% dichloromethane/hexanes) to yield a highly fluorescent pale yellow solid (1.4 mg, 66%). Spectroscopic data matches previously reported material.

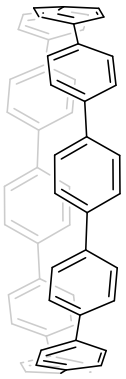

[10]CPP (29.6): Compound **36.1** (11.3 mg, 0.0076 mmol) was dissolved in toluene (1 mL) and heated to 60 °C; then, *p*-toluenesulfonic acid monohydrate (16.5 mg, 0.087 mmol) was added to the stirring reaction. Reaction was cooled to room temperature and water was added, followed by extraction with dichloromethane (3 x 1 mL). Combined organics were dried over $MgSO_4$, filtered, and concentrated under reduced pressure. Residue was purified via flash chromatography (6 x 0.3 cm, 20-50% dichloromethane/hexanes) to yield a highly fluorescent pale yellow solid (4.7 mg, 81%). Spectroscopic data matches previously reported material.

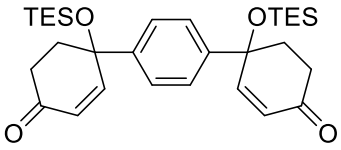

Bis(enone) (39.4): Compound **33.3** (1.50 g, 4.16 mmol) was dissolved in anhydrous tetrahydrofuran (40 mL) in a flame-dried round bottom flask. *n*-butyllithium (9.578 mmol) was added at -78 °C under argon atmosphere. 1,4-cyclohexadione monoethyleneketal (748 g, 4.79 mmol) in anhydrous tetrahydrofuran (20 mL) was then transferred via syringe. Solution warmed to 23 °C and quenched by addition of DI water, then extracted with ethyl acetate (3 x 40 mL). Combined organics were dried over $MgSO_4$, filtered, and concentrated under reduced pressure. Residue was triturated using a cold 1:1 solution of ethyl acetate/hexanes to yield white solid. This material was taken up in dichloromethane and trifluoroacetic acid (4:1, 24 mL) and stirred at 23 °C for 1 h. Saturated sodium bicarbonate solution (25 mL)

was added in order to neutralize the acid, followed by extraction with dichloromethane (3 x 20 mL). Residue dried over $MgSO_4$, filtered, and concentrated under reduced pressure. Crude residue was divided into 3 equal portions, dissolved in tetrahydrofuran (25 mL total) and saturated with O_2 by bubbling with a balloon for 30 minutes (and continuing to bubble while reaction begins). Copper(II) triflate (85.0 mg, 0.235 mmol total), tetramethylguanidine (0.30 mL, 2.44 mmol total), and triphenylphosphine (1.845 g, 7.037 mmol total) were added, and reaction stirred at 23 °C for 20 hours. After completion, solutions were combined and concentrated under reduced pressure. Residue was taken up in dry dichloromethane (48 mL) under N_2 atmosphere at 0 °C along with imidazole (639 mg, 9.383 mmol). After 10 minutes, triethylsilyl chloride (1.57 mL, 9.38 mmol) was added dropwise and reaction stirred at 23 °C for 18 h. Reaction quenched by addition of DI water, then extracted with dichloromethane (3 x 30 mL). Combined organics were dried over $MgSO_4$, filtered, and concentrated under reduced pressure, and residue purified by flash chromatography (17 x 2.5 cm, 5-10% ethyl acetate/hexanes) to yield orange oil comprised of a mixture of inseparable isomers (339 mg, 16% over 4 steps). R_f = 0.30 (15% ethyl acetate/hexanes). ^{1}H NMR (500 MHz, $CDCl_3$) δ 7.42 (d, *J* = 1.0 Hz, 4H), 7.00 (dd, *J* = 10.3, 2.7 Hz, 2H), 6.17 (d, *J* = 10.2 Hz, 2H), 2.82 – 2.54 (m, 2H), 2.40 (ddd, *J* = 13.1, 9.8, 4.5 Hz, 2H), 2.25 (ddt, *J* = 21.5, 13.2, 5.1 Hz, 4H), 0.89 (td, *J* = 8.0, 1.6 Hz, 18H), 0.55 (qdd, *J* = 8.0, 3.6, 2.1 Hz, 12H). ^{13}C NMR (126 MHz, $CDCl_3$) δ 199.53, 152.55, 152.43, 144.60, 144.53, 134.08, 133.93, 130.14, 130.11, 129.05, 128.78, 128.73, 125.75, 125.73, 74.52, 74.48, 40.96, 40.93, 35.05, 7.20, 6.87. (Small triphenylphosphine signal present in NMR sample.)

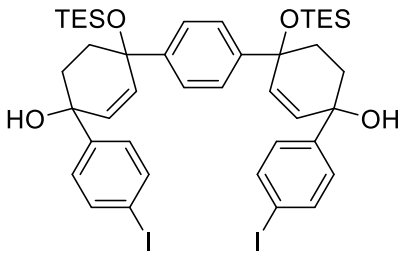

Diiodide (40.1): Compound **39.4** (339.4 mg, 0.6449 mmol) was dissolved in anhydrous tetrahydrofuran (6 mL) in a flame-dried round bottom flask and transferred via cannula into a vessel containing 4-iodophenyllithium, generated by addition of *n*-butyllithium (3.225 mmol) to a solution of 1,4-diiodobenzene (1.170 g, 3.547 mmol) in anhydrous tetrahydrofuran (6 mL) under argon atmosphere at -78 °C. Solution warmed to 23 °C and quenched by addition of DI water, then extracted with ethyl acetate (3 x 10 mL). Combined organics were dried over $MgSO_4$, filtered, and concentrated under reduced pressure. Residue was purified via flash chromatography (16 x 1.5 cm, 30-50% dichloromethane/hexanes) to yield a pale yellow solid comprised of a mixture of inseparable isomers (284.6 mg, 47%). R_f = 0.37 (15% ethyl acetate/hexanes). ^{1}H NMR (500 MHz, $CDCl_3$) δ 7.67 (dd, *J* = 8.4, 2.9 Hz, 4H), 7.51 (d, *J* = 8.7 Hz, 1H), 7.40 (d, *J* = 5.0 Hz, 4H), 7.24 (dd, *J* = 8.3, 5.6 Hz, 4H), 6.62 (d, *J* = 8.7 Hz, 1H), 6.19 (d, *J* = 10.1 Hz, 2H), 5.98 (t, *J* = 9.6 Hz, 2H), 4.83 (s, 0.5H) 2.15 (dddd, *J* = 18.4, 16.0, 9.0, 3.5 Hz, 4H), 1.93 (s, 2H), 1.77 (dtt, *J* = 11.4, 7.4, 3.4 Hz, 4H), 0.90 (td, *J* = 7.9, 3.6 Hz, 18H), 0.68 – 0.44 (m, 12H). ^{13}C NMR (126 MHz, $CDCl_3$) δ 146.44, 146.39, 146.27, 138.70, 137.61, 137.60, 135.74, 135.69, 133.92, 133.88, 127.85, 125.57, 125.52, 118.06, 93.21, 74.42, 74.31, 72.54, 38.20, 38.02, 36.77, 7.34, 7.32, 6.93, 6.90.

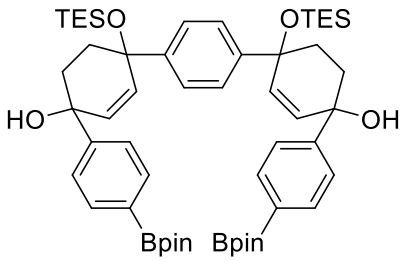

Diboronate (40.2): Compound **40.1** (163.8 mg, 0.1753 mmol) was dissolved in anhydrous tetrahydrofuran (5 mL) under an argon atmosphere and cooled to -78 °C. Next, *n*-butyllithium (.8767 mmol) was added dropwise via syringe, followed immediately by ^{i}PrOBpin (0.19 mL, 0.877 mmol). Reaction was allowed to slowly warm to room temperature before quenching with water, then extraction with ethyl acetate (3 x 10 mL). Combined organics were dried over $MgSO_4$, filtered, and concentrated under reduced pressure. Residue was purified by flash chromatography (14 x 1.5 cm, 8-15% ethyl acetate/hexanes) to yield a pale yellow oil comprised of a mixture of inseparable isomers (88.6 mg, 54%). R_f = 0.23 (15% ethyl acetate/hexanes). ^{1}H NMR (500 MHz, $CDCl_3$) δ 7.84 – 7.76 (m, 2H), 7.51 (dddd, *J* = 9.5, 5.7, 2.4, 1.5 Hz, 4H), 7.45 – 7.39 (m, 4H), 7.36 (td, *J* = 7.7, 2.2 Hz, 2H), 6.31 – 6.12 (m, 2H), 6.11 – 5.96 (m, 2H), 2.31 – 2.05 (m, 4H), 2.01 – 1.93 (m, 2H), 1.90 – 1.66 (m, 4H), 1.33 (d, *J* = 4.8 Hz, 24H), 1.00 – 0.79 (m, 18H), 0.73 – 0.37 (m, 6H). ^{13}C NMR (126 MHz, $CDCl_3$) δ 149.58, 149.49, 146.43, 146.11, 146.06, 136.78, 135.18, 135.10, 134.97, 134.88, 134.86, 134.24, 134.04, 134.00, 128.34, 127.28, 125.45, 125.43, 125.31, 125.26, 124.84, 124.81, 83.80, 83.77, 77.28, 77.23, 77.03, 76.78, 74.40, 74.28, 74.22, 74.13, 72.61, 72.58, 72.53, 72.51, 38.08, 37.91, 37.76, 36.51, 36.45, 36.37, 24.87, 24.86, 7.12, 7.10, 6.71, 6.68.

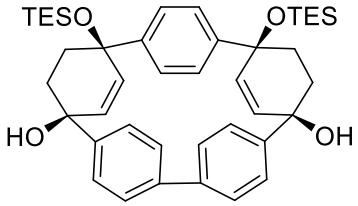

[5] macrocycle (40.3): Compound **40.2** (14.4 mg, 0.015 mmol) was dissolved in a solution of tetrahydrofuran and water (1:1, 10 mL) with potassium fluoride (0.9 mg, 0.015 mmol), $Pd(PPh_3)_2Cl_2$ (2.2 mg, 0.003 mmol), and boric acid (4.8 mg, 0.077 mmol) then stirred in an open flask at 40 °C for 24 h. Reaction quenched with water, then extraction with ethyl acetate (3 x 5 mL). Combined organics were dried over $MgSO_4$, filtered, and concentrated under reduced pressure. Residue was purified by flash chromatography (6 x 0.5 cm, 5-10% ethyl acetate/hexanes) to yield a pale yellow oil (3.3 mg, 31%). R_f = 0.30 (15% ethyl acetate/hexanes). ^{1}H NMR (600 MHz, CDCl3) δ 7.53 – 7.47 (m, 4H), 7.43 (d, *J* = 6.0 Hz, 4H), 7.40 – 7.29 (m, 4H), 6.18 (d, *J* = 10.1 Hz, 2H), 6.03 (dd, *J* = 10.1, 9.1 Hz, 2H), 2.28 – 2.11 (m, 4H), 1.93 (d, *J* = 1.5 Hz, 2H), 1.90 – 1.76 (m, 4H), 0.91 (td, *J* = 7.9, 4.7 Hz, 18H), 0.72 – 0.42 (m, 12H). ^{13}C NMR (126 MHz, $CDCl_3$) δ 146.69, 146.39, 135.21, 134.51, 128.58, 128.55, 127.54, 125.69, 125.57, 125.52, 74.48, 72.75, 36.76, 29.97, 29.69, 22.97, 14.39, 7.36, 7.34, 6.94, 6.92.

CHAPTER 3 SELECTIVE SYNTHESIS OF AN OCTAMETHOXY[12]CYCLOPARAPHENYLENE AND ITS POTENTIAL APPLICATION TOWARD *π*-EXTENSION FROM NANOHOOPS TO NANOTUBES

3 INTRODUCTION

Though by this point in time the selective and efficient gram-scale synthesis of many cycloparaphenylenes has been well-documented, the number of reports of functionalized [*n*]CPPs could be likely be counted on one person's fingers.[14,29-35] This limitation is a severe impediment to the over-arching goal of bottom-up carbon nanotube synthesis and is the next major challenge to be addressed in the field. Regularly functionalized [*n*]CPPs (*e.g.* the functional groups are placed at regular intervals) are desirable in particular due to the simplicity of their eventual *π*-extension into carbon nanobelts. If the groups are set at regular intervals, then the proper conditions, in theory, applied to each group would lead to the bottom-up synthesis of a uniformly-sized single walled carbon nanotube in the least possible number of steps. To this end, we have developed a synthesis of an [12]CPP derivative (**Figure 41**) containing eight methoxy groups at regular intervals (at the 2 and 5 positions on every third phenylene unit) which we propose could act as a template for future *π*-extension utility.

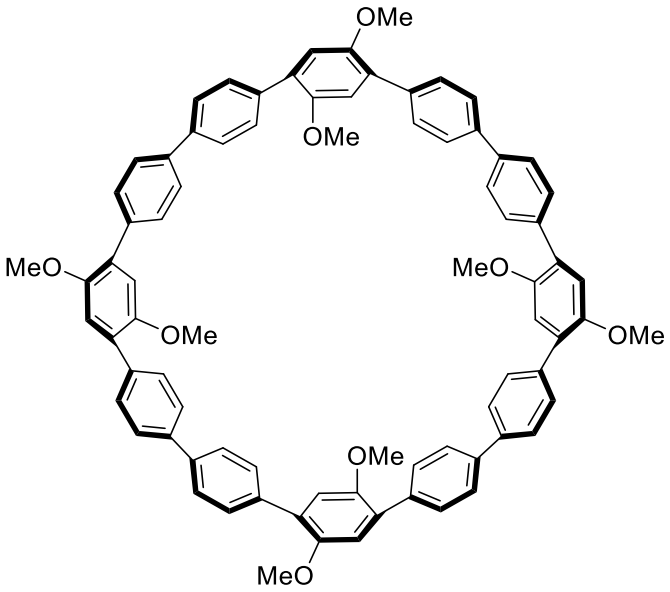

***Figure 41**: Octamethoxy[12]cycloparaphenylene*

3.1 Challenges and approaches to functionalized [*n*]CPPs

As we discussed in the previous chapters, the functionalization of [*n*]CPPs is challenging and rare in the literature. In fact, reported functionalizations of [*n*]CPPs only date back about a decade from the time of this writing, which is unsurprising since the [*n*]CPP field only opened up fifteen years ago in 2008. Of particular note are functional groups which are regularly spaced around the nanohoop (see Sections 3.2 and 3.3), as these theoretically may offer a straightforward path toward the bottom-up synthesis of CNBs. However, this goal has not yet been realized. On the other hand, during that time, several groups (including the significant players from Chapters 1 and 2 along with Wang and coworkers) have reported interesting and potentially useful functionalized [*n*]CPP derivatives. These examples involve both pre-installed functional groups and—less often—late-stage modification of a completed [*n*]CPP.

The first of these functionalizations which we will discuss was reported by the Jasti group in 2012.[29] After the synthesis of [6]CPP via a U-shaped block as a coupling partner, (see **Figure 25**, compound **25.4**), key intermediate **25.4** was converted to the analogous bisboronate derivative **42.1** by simple treatment with *n*-BuLi followed by isopropoxyBpin. **42.1** was coupled with L-shaped block **42.2** (synthesized easily via the typical Jasti sequence starting from a brominated quinone derivative) in a Suzuki reaction to afford macrocycle **42.3** in a modest 30% yield. This set of Suzuki conditions left the vinyl bromide group untouched, allowing it to be carried through to the next step. Two equivalents of **42.3** could then be treated with **24.6** in another Suzuki reaction to forge **42.4**, an interesting bis-macrocyclic dimeric structure bridged by a *para*-phenylene unit, in 66% yield. A 1,5-naphthyl-bridged dimer (not shown) was also obtained in like manner from 1,5-(bisBpin)naphthalene. Reductive aromatization was achieved by subjection of **42.4** to sodium naphthalenide followed by quenching with iodine, giving [8]CPP dimer **42.5** in 75% yield. Two conformational arrangements can be envisioned: the *trans* orientation, in which the two nanohoops point away from one another; and the *cis* configuration (shown in **Figure 42**), in which the [8]CPP units stack directly above one another, which would seem to allow for additional *π*-extension toward CNBs and CNTs. Interestingly, computational studies [B3LYP-D/6-31G(d,p)] found that the *cis* conformer is actually lower in energy than the *trans* conformer by about 7 kcal/mol, due to the van der Waals interactions between monomeric [8]CPP units in the structure. Based on additional calculations, the group determined that directly linked [*n*]CPP oligomers would be highly useful synthetic targets for the synthesis of *π*-extended products due to the apparent ease of performing a cyclodehydrogenation reaction on the oligomers under suitable conditions by exploiting the closeness of each nanohoop unit to the other(s).

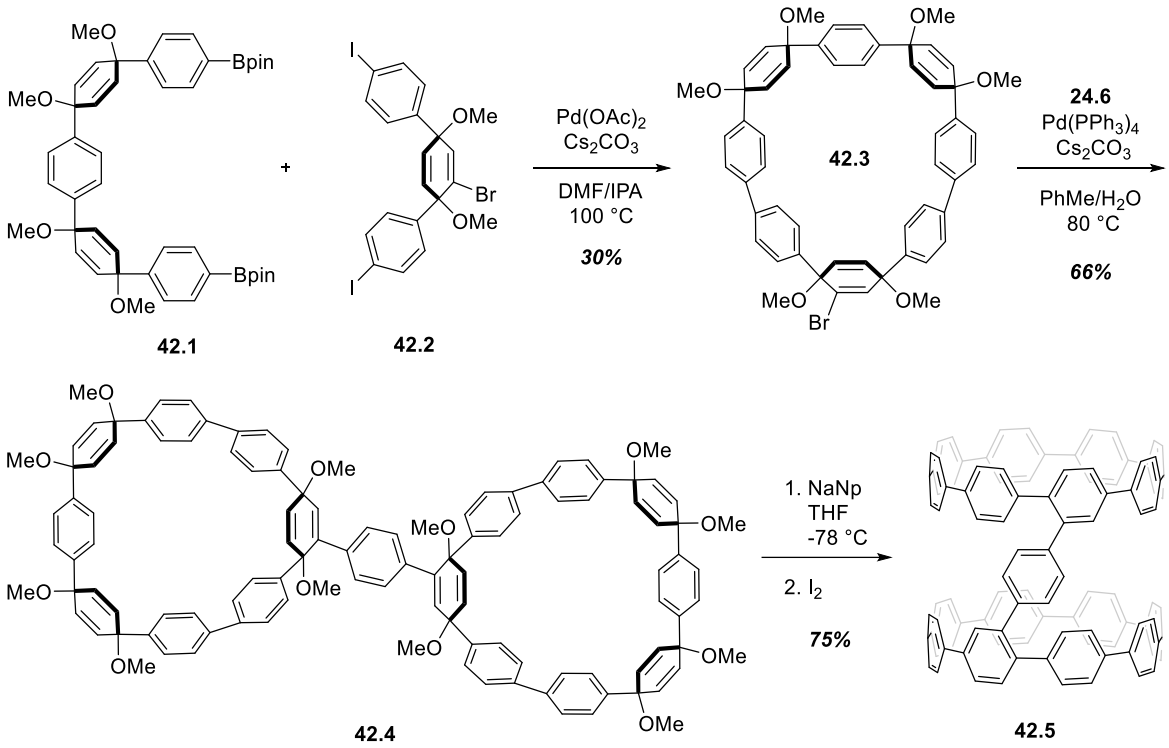

***Figure 42**: Synthesis of an [8]cycloparaphenylene dimer by Jasti*

Two years later, the Itami research group published the synthesis of a directly connected [10]cycloparaphenylene dimer derived from chloro[10]CPP.[30] Potentially inspired by Jasti's proposal that a directly linked [n]CPP dimer would be a highly useful precursor for *π*-extension toward CNTs based on the computational findings, Itami and coworkers adapted their L-shaped cyclohexane-based building block strategy to this synthesis. Beginning from **26.1** and **43.1**, a Suzuki cross coupling reaction constructed C-shaped 9-ring block **43.2** in 65% yield (**Figure 43**). Using the same strategy as their previous selective synthesis of [10]CPP, a [9+1]-type cyclization was performed to combine **43.2** and 2-chloro-1,4-bisBpinbenzene (**43.3**) (derived from 1,4-dibromo-2-chlorobenzene via Miyaura borylation) under a mild Suzuki protocol to avoid reaction of the chloro group, successfully completing the triangular macrocycle **43.4** in 41% yield. Acid-mediated aromatization using sodium hydrogen sulfate in *m*-xylene and DMSO at high temperatures resulted in the synthesis of chloro[10]cycloparaphenylene **43.5** in 31% yield with no undecorated [10]CPP observed (*i.e*. the chlorine was left untouched). After characterization, **43.5** was treated with $Ni(cod)_2$ in a Yamamoto coupling reaction to dimerize, forming compound **43.6** in 37% yield. Based on DFT calculations performed by the Itami group following the synthesis, the lowest energy conformation of **43.6** is seen in the *cis*-type arrangement (where the nanohoops are stacked together, as shown in **Figure 43**) as opposed to the *trans*-type structure, which has an additional 5.1 kcal/mol of energy (ΔG), though the transition state between them only has 8.9 kcal/mol, so the isomerization barrier is not very high and both may be observable with the proper experimental setup. Additionally, a carbon nanobelt

can be envisioned as the product of a manyfold cyclodehydrogenation performed on **43.6** (with 19 bond formations proposed), but this experiment was not attempted for this publication.

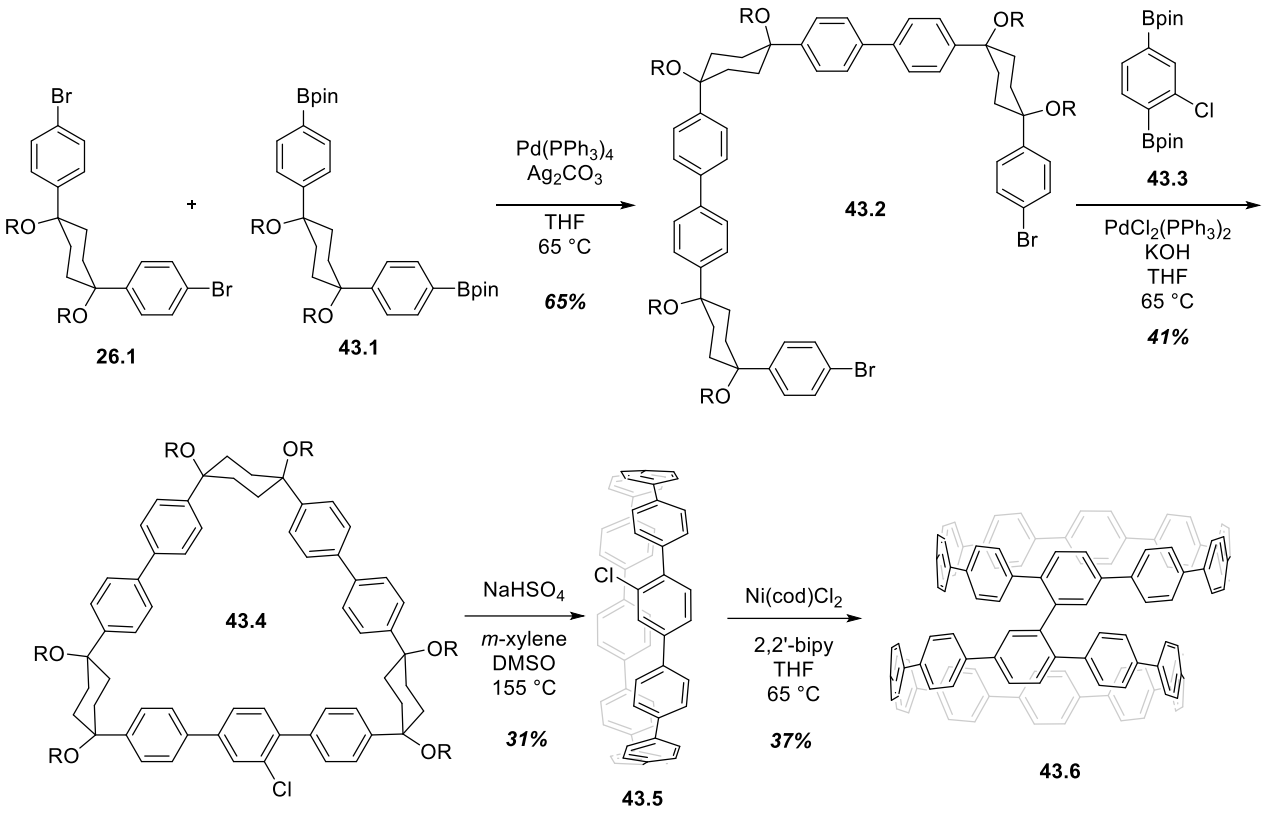

Figure 43*: Synthesis of a directly connected [10]cycloparaphenylene dimer by Itami*

Another monofunctionalization of an [*n*]CPP was accomplished in the Itami lab in 2015.[15b] While investigating the reactions of [9]- or [12]CPP with group 6 transition metal hexacarbonyl complexes, *η*6-coordination to one of the benzene rings in the nanohoop was observed, affording [*n*]CPP-M(CO)$_3$ complexes when heated to 160 °C in the dark (**Figure 44**). One of these complexes, [9]CPP-Cr(CO)$_3$ **44.1**, was isolable even though it was unstable, and confirmation of the structure by X-ray indicated complexation at the outer surface of the CPP. Treating the complex **44.1** with *n*-butyllithium at -78 °C gives intermediate **44.2.** This is followed by treatment with various electrophiles (trimethylsilyl chloride, methoxyBpin, or methyl chloroformate), affording selectively monofunctionalized [9]CPP derivatives after decomplexation by exposure to light. This four step sequence can even be performed in rapid succession in one pot by keeping the reaction vessel in the dark until the final stage of the synthesis. Isolation by preparatory TLC gave clean TMS-[9]CPP **44.3**, methoxycarbonyl-[9]CPP **44.4**, and boryl-[9]CPP **44.5** in moderate absolute yield (40%, 38%, and 21%, respectively). However, based on the recovered unreacted starting material, all of the

monofunctionalized products were obtained in over 70% yield from the reacted [9]CPP. Though no attempts at π-extension were reported for this publication, the groups that were installed are readily converted into other functionalities which may be used in the context of π-extension in future work.

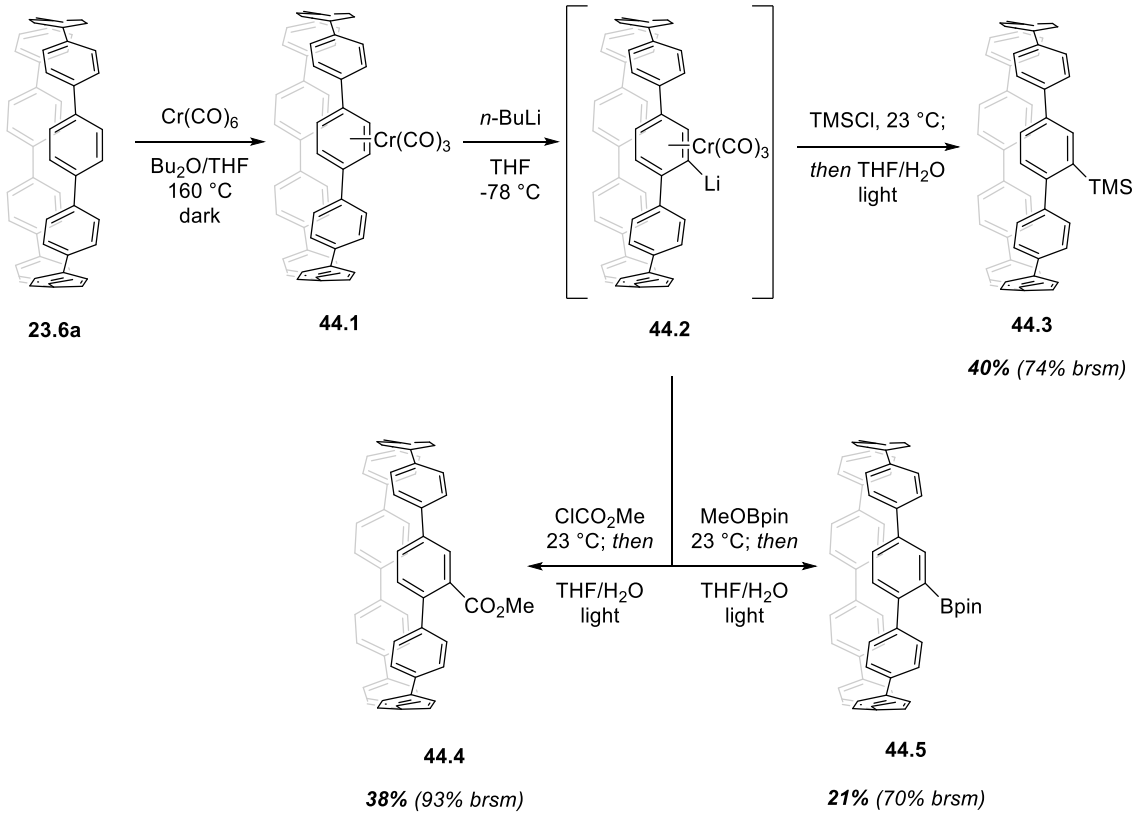

***Figure 44**: Complexation of [9]CPP with chromium and subsequent monofunctionalization*

In 2016, the research group of Kung Wang reported a synthesis of functionalized [9]cycloparaphenylene derivatives (**Figure 45**).[31] Starting from bis(*para*-bromophenyl)diene **45.1**, a Diels-Alder cycloaddition with alkyne **45.2** allows quick construction of the Jasti-type functionalized cyclohexadiene L-shaped unit with complete selectivity for the *cis* configuration of the aryl groups, affording **45.3** in 85% yield. A Yamamoto coupling reaction of this precursor block resulted in 4 products: a dimer (**45.4**, x = 1) in both *syn* and *anti* relative stereochemistry (referring to the vicinal pairs of methyl ester functional groups) and a trimer (**45.4**, x = 2) which was also observed and isolated as *syn* and *anti* relative stereochemistry. The ratio was reported as roughly 1:10 dimers to trimers. All parts of this mixture were treated together with DDQ to afford aromatized [9]CPP derivative **45.5** in 14% overall yield from **45.3**. No [6]CPP derivative was observed, and the relative stereochemistry for the trimer was determined to be irrelevant since the yield for each stereoisomer was about the same and the functionalized phenylene rings are capable of bond rotation to interchange between *syn* and *anti*.

[9]CPP derivative **45.5** can be further functionalized to incorporate *N*-phenylphthalimido groups by condensation of **45.5** with aniline derivatives (not shown), which proceeds smoothly and simply. Additionally, another [9]CPP derivative which harbors a 1,4-naphthylene unit was obtained by the same sequence of reactions from a derivative of **45.1** that contains a cyclohexane ring attached to the diene unit (not shown). However, the most significant continuation of this work came in the following year.[32] Starting from the now-readily available intermediate **45.5**, it was proposed that acid-mediated acylation reactions could form **45.6** based on previous reports of this reaction on non-macrocyclic systems. After several attempts, suitable conditions were found. Partial acylation could be achieved by initially treating with trifluoroacetic acid and trifluoroacetic anhydride in refluxing methanol, followed by completion of the desired **45.6** by acylation with Eaton's reagent (P_2O_5), giving the completed target in 25% yield over two steps.

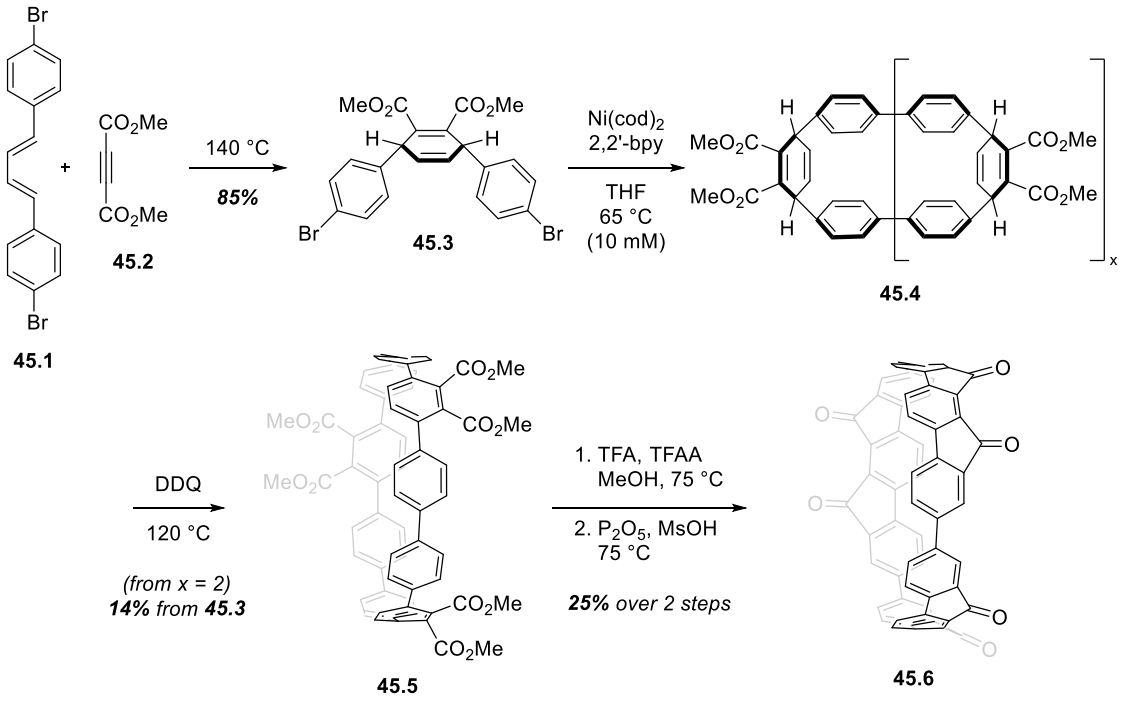

***Figure 45**: Synthesis of hexa(methyl ester)[9]CPP and further annulation by Wang*

In 2017, Yamago and coworkers reported the site-selective bromination of small [*n*]CPPs, in which the reactivity was driven by the release of ring strain in the small nanohoops.[33] As they discussed in the article, the reported bromination reaction was only observed in [*n*]CPPs where n < 9, because in the more strained [*n*]CPPs, the energy benefit of the release of ring strain when performing the bromination is high enough to overcome the energy cost of breaking aromaticity in two of the benzene rings during the reaction. In fact, the reaction was most useful in the case of [5]CPP, the smallest available benzenoid nanohoop available; therefore, this is the example that will be highlighted in our discussion.

Beginning from [5]CPP (**30.7**), 1,4-addition of bromine across two of the strained benzene rings in the nanohoop produced **46.1** in 94% yield when two equivalents of bromine were used (**Figure 46**). Increasing the excess of bromine did not result in additional brominations, reinforcing the assessment that strain release is the driving force of the reaction. DFT calculations are reported which confirm that the bromination of [5]CPP is exothermic with a ΔH of -87 kcal/mol. Further reactions of **46.1** were then screened. A substitution using methanol or water in basic conditions gave **46.2** as the tetraol or tetramethoxy derivative in quantitative yield. Strong bases, such as potassium *tert*-butoxide or LDA, or organometallics such as *n*-butyllithium or lithium dibutylcuprate, all reformed the starting [5]CPP in quantitative yields. Heating the brominated intermediate at 100 °C for three minutes quantitatively formed allylic isomerization product **46.3**, which is slightly more stable according to calculations by the authors. Finally, catalytic bromination with six equivalents of bromine in the presence of iron powder afforded octabromide **46.4** in 94% yield with site-selective addition across the already-brominated rings.

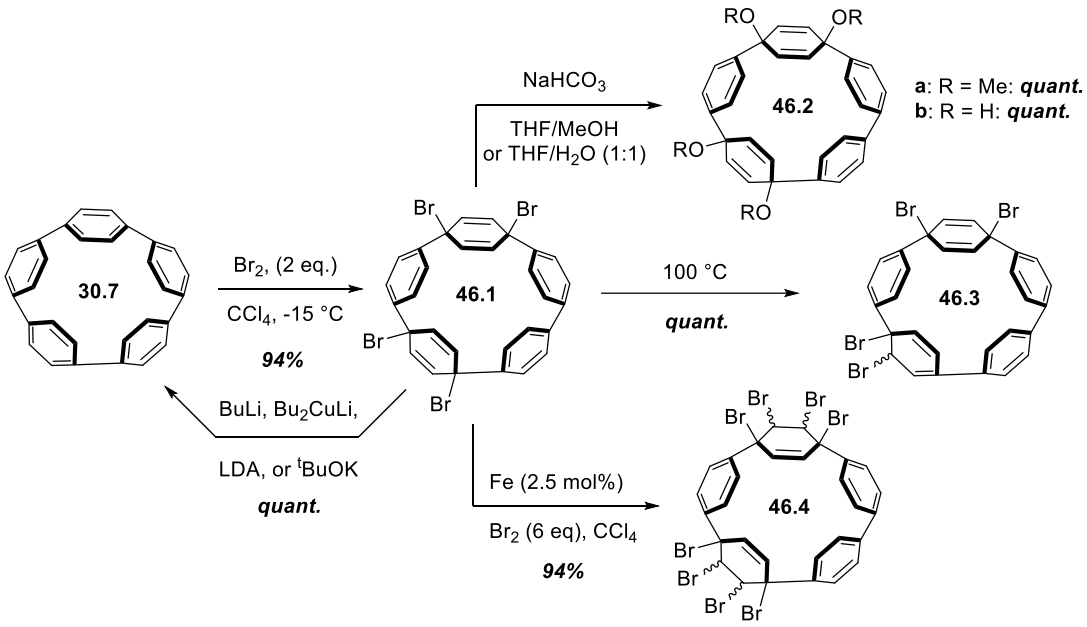

***Figure 46**: Bromination of [5]CPP by Yamago*

46.3 and **46.4** were chosen for further testing and derivatization (**Figure 47**). From **46.3**, aromatization was achieved by treating the tetrabromide with phosphazene superbase P_4-*t*Bu (pK_a = 42 in acetonitrile), converting **46.3** to monobromo[5]CPP (**47.1**) in 56% yield after several unsuccessful aromatization attempts with other bases. Lithium exchange with *n*-BuLi followed by reaction with various electrophiles afforded **47.2a-e**; acyl products **47.2a** (aldehyde), **47.2b** (methyl ketone), and **47.2c** (carboxylic acid) came from reaction of lithiated [5]CPP with DMF, acetic anhydride, and carbon dioxide respectively, while using ^{i}PrOBpin as the electrophile resulted in a borylated [5]CPP (**47.2d**) and treatment

with iodine monochloride yielded iodinated [5]CPP (**47.2e**). **47.2e** could be converted to TMS-protected alkyne in 73% yield by palladium-catalyzed coupling with trimethyltin alkyne **47.3**. In the case of **46.4**, aromatization with P_4-*t*Bu gave a mixture of isomers that were separated by HPLC (**47.4**, **47.5**, and **47.6** in 21%, 38%, and 23% yield, respectively). **47.4** was converted to bisBpin[5]CPP by standard borylation conditions (lithium exchange, then ^{i}PrOBpin) in 70% yield, respresenting the first late-stage multifunctionalization of a cycloparaphenylene. While this is an exceptional step forward in the field, it has yet to be applied to the area of *π*-extension, either in the initial paper or in any report since 2017. In fact, very few successful attempts toward *π*-extension of [*n*]CPPs have been reported in the literature at all, as we will cover in the following section.

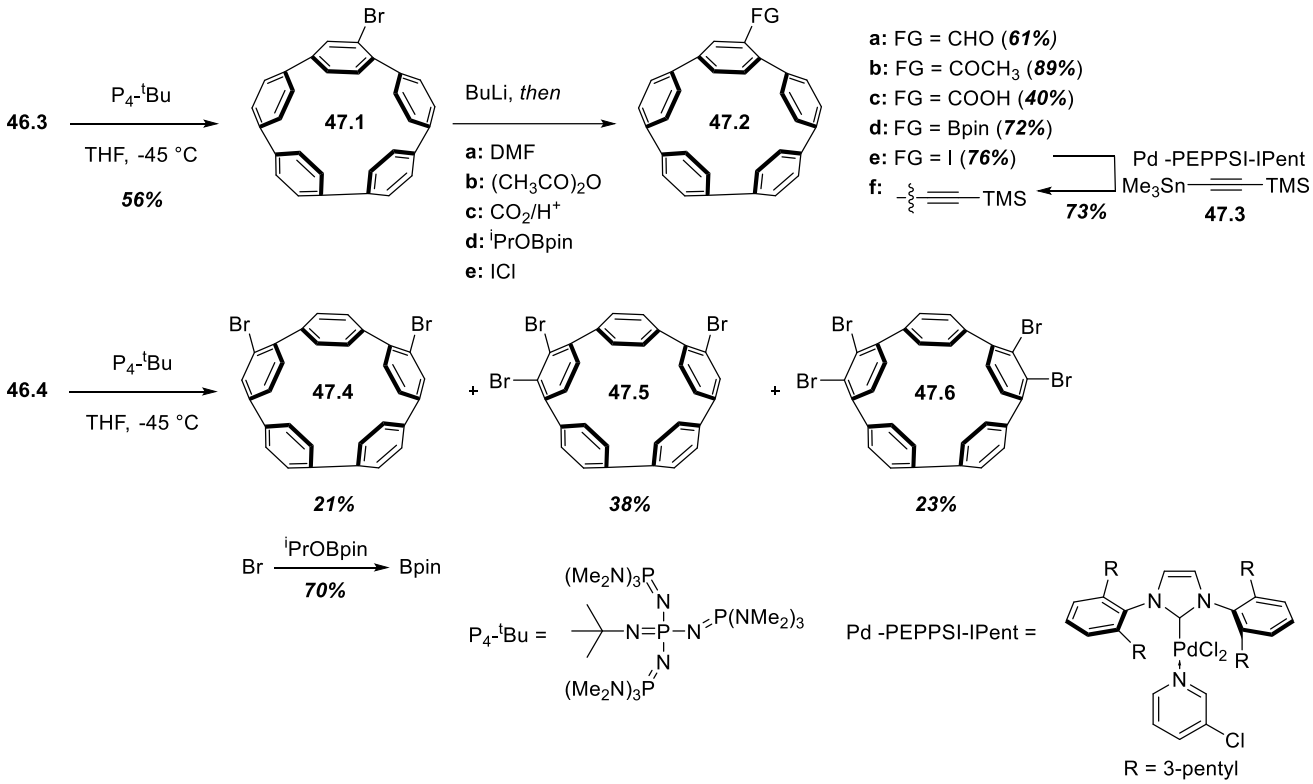

***Figure 47**: Additional functionalizations of brominated [5]CPP derivatives*

3.2 Previously reported attempted Scholl reactions on [*n*]CPP derivatives

3.2.1 Miao synthesis of a carbon nanobelt based on [12]CPP

In Chapter 1, we discussed the report from the group of Qian Miao that outlined the synthesis of two *π*-extended carbon nanobelt targets, one based on a [12]cycloparaphenylene scaffold (which is the focus in this section) and the other derived from a chiral nanohoop.[14] To review, incorporation of benzyl ether functional groups onto the [*n*]CPP backbone allowed *π*-extension to a large carbon nanobelt via functional group manipulation followed by Scholl reaction to facilitate annulation (see **Figure 9**, Chapter 1). Happily, the necessary benzyl ethers were resistant enough to the conditions used by Miao and coworkers that they survived throughout the synthesis until they were needed.

While the reported nanobelt did undergo an increase in strain energy upon cyclization, it was less severe than other annulative *π*-extension reactions, based on DFT calculations, only increasing by 8.4 kcal/mol over the Scholl reaction step. The transition state for this regioisomer of the Scholl reaction was also predicted based on the regioselectivity of the Scholl reaction due to transition state stability in cases where the aromatic ring contains an alkoxy substituent (*i.e.* the alkoxy groups tend to drive annulation in *ortho* and *para* positions).

3.2.2 Müllen's attempted synthesis of a hexabenzocoronene-based CPP derivative

In 2012, the group of Klaus Müllen published a synthesis of [9]CPP derivative **48.5** from another modification of the Bertozzi report.[34] Starting from tetraaryl benzoquinone (**48.1a-b**), addition of aryllithium to obtain **48.2a-b** followed by protection of the resulting diol gives dimethoxylated material **48.3a-b** in greater than 80% yield. Yamamoto coupling conditions lead to trimerization in moderate yield to form **48.4a-b**, which is aromatized by treatment with titanium(IV) chloride and lithium aluminum hydride to afford cyclo-4',4''''-hexa-phenylbenzenes (CHPBs) as a dodecaarylated [9]CPP derivative. Unfortunately, the next step (cyclodehydrogenation via the Scholl reaction) failed to afford any isolable nanobelt product. While the final annulation step was unsuccessful, it offers hope that the precursors are within reach, though the annulation must be achieved by some means other than Scholl chemistry. To further this notion, continued efforts by the Müllen research group in this area in the years since this report have not offered a complete solution for the shortcomings of the Scholl reaction. Larger [*n*]CPP derivatives in future iterations of this research (*e.g.* [15] and [21]CPP-based strategies) still fell victim to strain-induced rearrangement during the annulation step, and attempts to prevent the rearrangement by inclusion of blocking groups were only partially successful.[35]

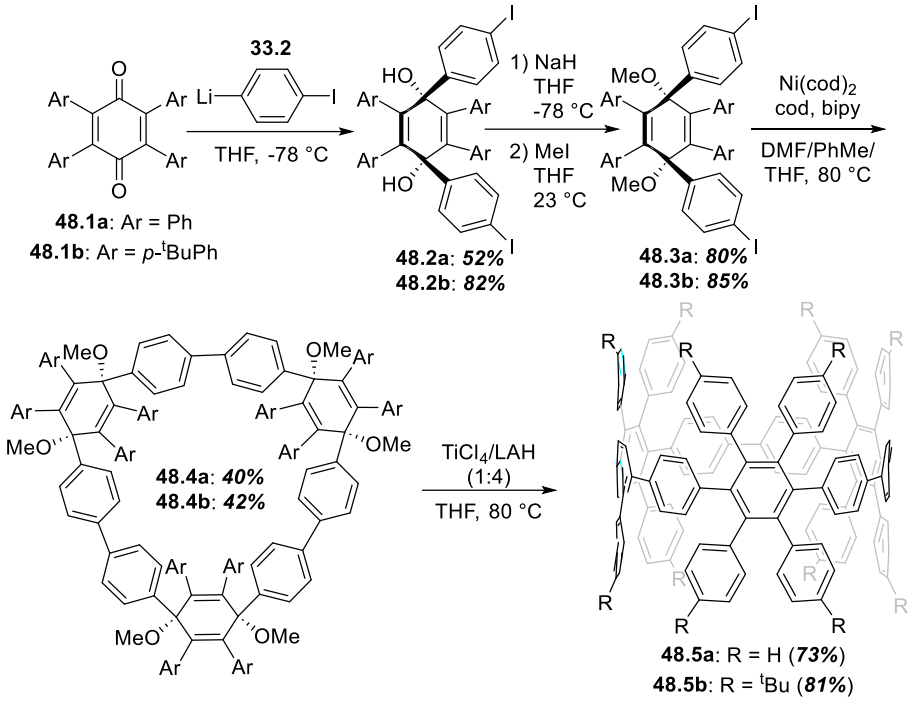

***Figure 48**: Synthesis of dodecaaryl[9]CPP*

3.3 Synthesis of an octamethoxy derivative of [12]CPP

Realizing the dearth of reported progress in this subfield of cycloparaphenylene chemistry, we took it upon ourselves to begin an investigation into using our group's strategies, along with the methods reported by other groups and discussed in more detail in Chapter 2, to achieve the synthesis of uniformly functionalized cycloparaphenylenes as progenitors for *π*-extension products such as carbon nanobelts and short, uniform-diameter CNTs.

For the early stages of this work, we chose to utilize the Yamago "platinum square" approach to the synthesis of our starting [12]CPP derivative, which was chosen based on its low strain energy compared to the smaller [*n*]CPPs that were discussed in Chapter 2 and because it is a member of the class of [3*n*]CPPs (importance of this point discussed in the Future Work section of this chapter). This method has been showcased as the most yield-efficient and step-economic way of making [4n]cycloparaphenylenes, and since our target is based on a [12]CPP backbone, this is the best choice. For alternative sizes of regularly-methoxylated [*n*]CPPs, a sequence based on the Jasti/Itami/Merner L-shaped precursor strategy is under development.

Beginning from 1,4-dimethoxybenzene, a bis(iodination) reaction with sulfuric acid, molecular iodine crystals, and sodium metaperiodate in acetic acid/water affords 2,5-dimethoxy-1,4-diiodobenzene (**49.2**).[36] After quenching with sodium thiosulfate, crude material was filtered and washed with water, then purified by recrystallization in cold ethanol/chloroform (1:1). Suzuki coupling between diiodide **49.2** and two equivalents of 4-bromophenylboronic acid under standard conditions results in a mixture of the desired compound, leftover starting material, and higher-order polymerization products (from overreaction of desired dibromide with additional equivalents of boronic acid). After careful purification, a 68% isolation yield was obtained for product **49.3a**. Borylation of this material uneventfully furnishes the macrocyclization precursor **49.3b** in 53% yield. Treatment of **49.3b** with platinum-cod complex results in intermediate **49.4** (not isolated), which after aqueous workup is subjected to reductive elimination under the guidance of triphenylphosphine. Macrocyclization/aromatization was achieved in a high yield of 79%, affording octamethoxy[12]CPP cleanly and efficiently (23% yield over 5 steps) with only 3 chromatographic operations needed.

This success represents one of only a handful of reports of simple, uniformly-functionalized cycloparaphenylene scaffolds that can be envisioned as a precursor for π-extension toward higher-order nanobelt structures. In Section 3.4, I will discuss some potential future applications of this discovery that are under investigation in our lab, including a modification of the previous synthesis to install alkyne groups in the place of the methoxy groups, potentially providing a handle for the iodine monochloride-mediated annulative π-extension of alkynylated [*n*]CPPs. As we will see, this strategy may hold the key to obtaining π-extended nanotube structures from bottom-up synthesis.

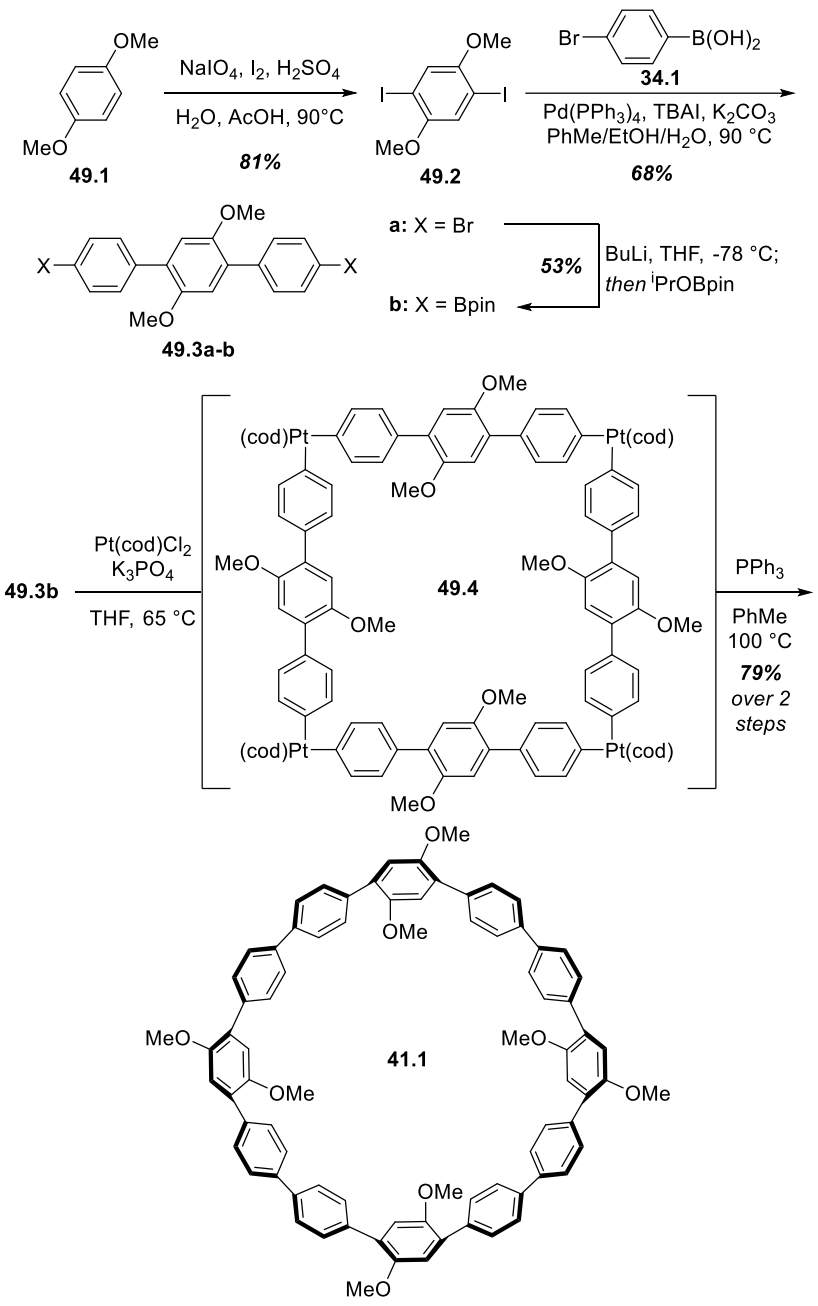

***Figure 49**: Synthesis of octamethoxy[12]CPP*

3.4 Attempts to further functionalize the CPP template

After successfully obtaining the [12]CPP derivative (**Figure 49**), we turned our efforts to the further application of the macrocyclic nanohoop, specifically the inclusion of alkyne groups in the positions bearing methoxy groups. Initially, we applied ceric ammonium nitrate oxidation conditions to intermediate **50.3**,

resulting in an 88% yield of quinone-based product **50.1.** Borylation of this intermediate with *n*-butyllithium-based conditions was not trivial due to the presence of the enone moiety, so Miyaura borylation using B_2pin_2 and a palladium catalyst was attempted in order to generate a material which could be assembled via "platinum square" conditions to form a CPP-adjacent macrocycle (**51.3**), which was envisioned as a suitable material for the installation of alkyne groups (*i.e.* by Grignard reagent). This borylation failed, however. Next, we tried converting the already-obtained [12]CPP derivative into compound **50.3** by treatment with ceric ammonium nitrate (CAN) in acetonitrile/water. All material in this reaction was decomposed after just one hour, with no desired compound observed. As an alternative method, we sought to convert the methoxy groups into triflate handles (**50.4**), presuming that Sonogashira conditions might allow for the incorporation of alkyne units.

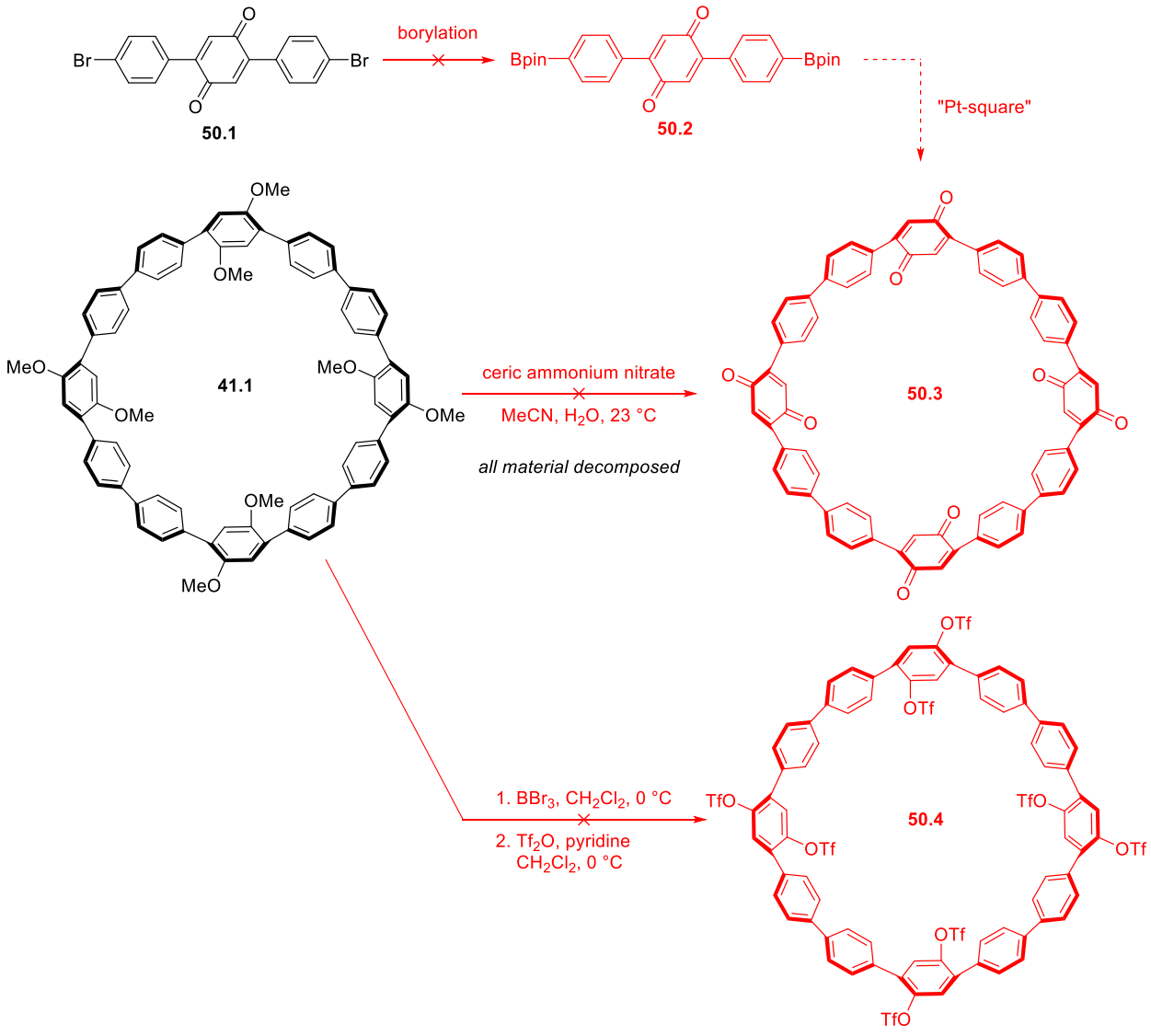

Figure 50: Unsuccessful derivation of *π*-extension precursors

However, all materials decomposed in this reaction sequence as well. A triflate-containing derivative of **49.3a** also failed to provide borylated material upon treatment with BuLi and isopropoxyBpin. Undeterred, we continued to seek a suitable reaction sequence for our desired alkynylated [12]CPP.

At this stage, I was compelled by lack of time to pass the project to another student in the lab, who continues to investigate this direction of research, with promising initial results.

3.5 Future work

3.5.1 Installation of alkyne groups

The next major step in this project is the incorporation of regularly spaced alkyne groups onto the [12]CPP structure. Based on the theoretical design shown in **Figure F5**, a [3*n*]CPP with alkyne handles installed on every third ring in the 2 and 5 positions can be envisioned as a precursor to a highly *π*-extended five-ring-wide CNB **F5.6**. This would represent the longest carbon nanobelt ever generated through bottom-up organic synthesis from a cycloparaphenylene scaffold. Beginning with the terminal alkyne-containing [3*n*]CPP (shown in planar orientation for simplicity of drawing and visualization) **F5.1**, a Sonogashira coupling reaction with 1-naphthaleneboronic acid (**F5.2**) would ideally produce fully arylated structure **F5.3**. Using the iodine monochloride-mediated annulation conditions discussed in Chapter 1, a series of curved phenanthrene units could be constructed at regular intervals along the cycloparaphenylene backbone, with 1-naphthyl groups and iodine handles well-positioned for further reactions (**F5.4**). (Depending on the final step, a preliminary Scholl reaction may be necessary at this stage due to the known issues discussed earlier in this chapter. When attempting a manyfold Scholl reaction on a strained system, a partial cyclodehydrogenation at this stage may be more practical, followed by another one later when the risk of strain-induced rearrangement is mitigated by the highly annulated PAH structure, since all the rings of the initial [3*n*]CPP will be connected by at least two bonds.) Next, a Suzuki reaction with the iodine handles, once again using 1-naphthaleneboronic acid, would likely produce **F5.5**, which contains all the carbon atoms of the desired target carbon nanobelt. The final reaction, a cyclodehydrogenation step, would hopefully be powerful enough to “stitch” all of the arene units together, forming the bonds shown in bold (**F5.6**).

Theoretically, **F5.1** is attainable through a similar sequence of steps to the ones that afforded [12]CPP derivative **41.1**. At this time, the necessary precursor has not been synthesized, but work is in progress by other researchers in the Merner lab based on the established protocol for the synthesis of **41.1** and will hopefully be reported in the near future.

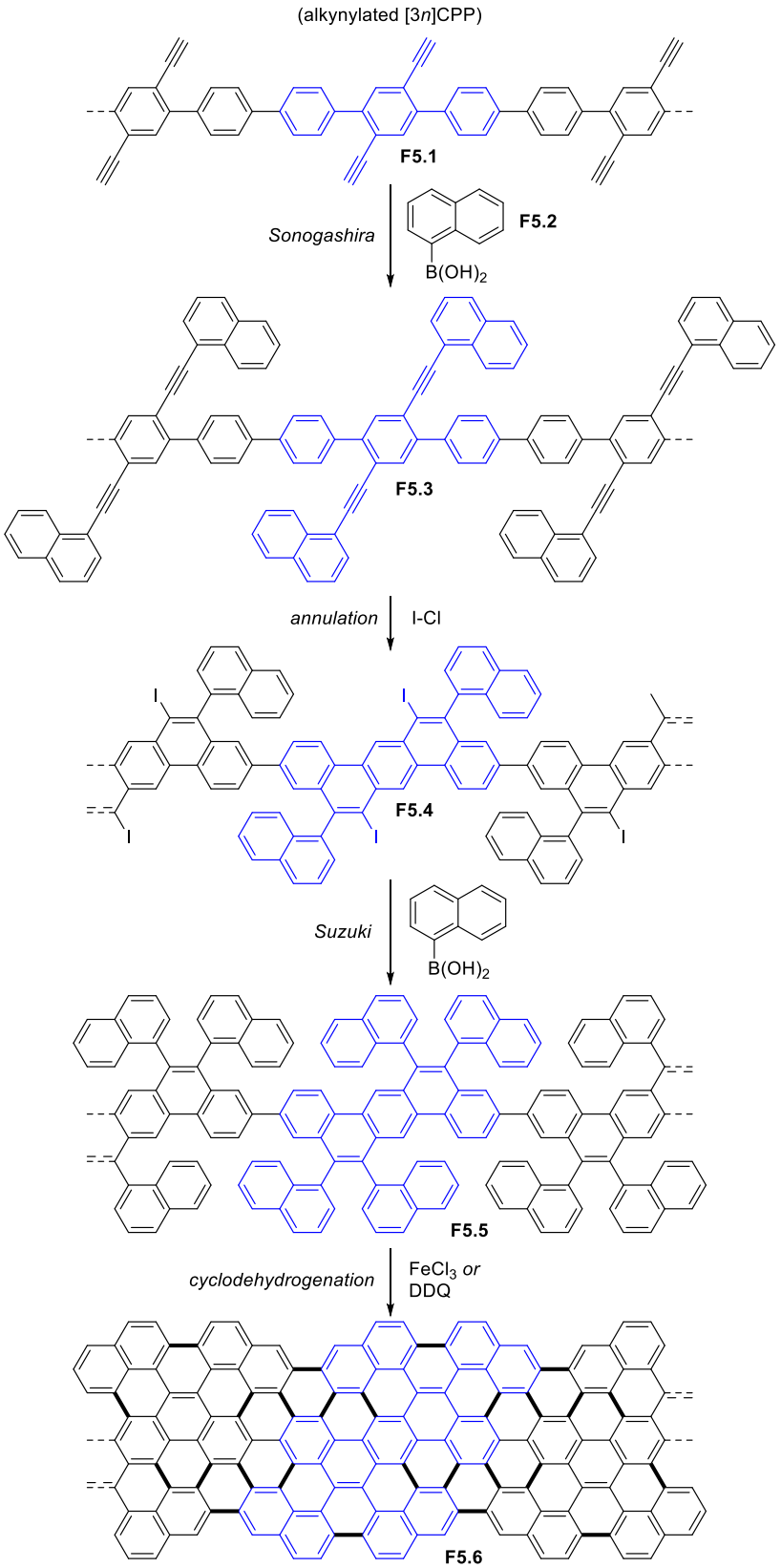

***Figure F5**: Design and construction strategy for a wide carbon nanobelt (CNB) from alkynylated[3n]CPP*

3.5.2 Use of methoxy substituents as directing groups

Another way forward in the further functionalization of our [12]CPP derivative may be found in the electrophilic aromatic substitution of **41.1** with a range of electrophiles. Fortunately, the indicated positions (see **Figure F6**) are highly activated; each of them has strongly activating methoxy groups on both the *ortho* and *para* positions of the benzene ring. It is expected that the electrophilic aromatic substitution of this intermediate would proceed quickly and efficiently due to these factors. Since S_EAr offers a wide range of possible substituents (Friedel-Crafts acylation or alkylation, bromination using Br_2 or NBS, or sulfonylation could all provide useful products), various functional groups could be screened for π-extension utility. This would not only provide a path toward more π-extension products, but also would represent a great step forward in the development of late-stage functionalization of [*n*]CPP materials.

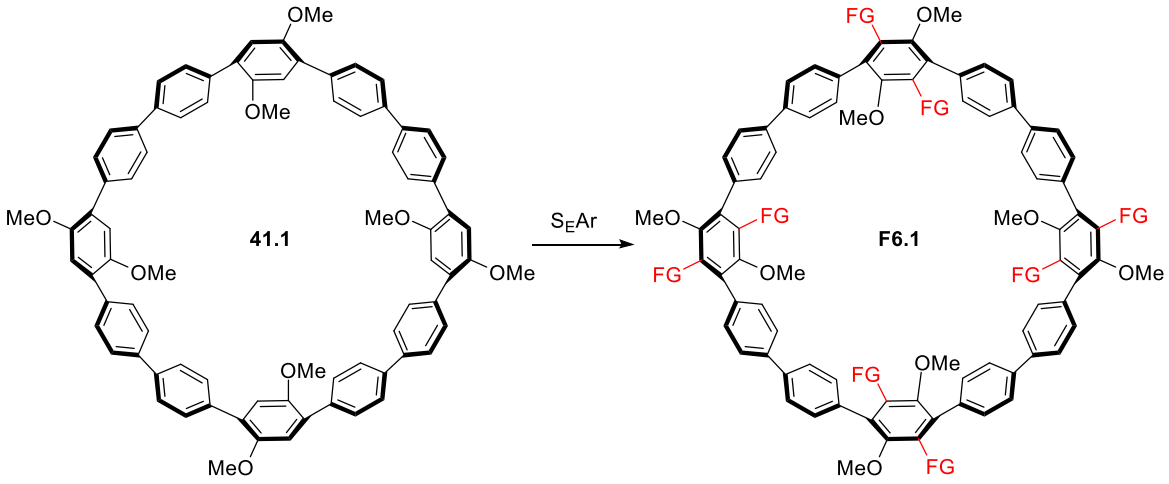

***Figure F6**: Electrophilic aromatic substitution of octamethoxy[12]CPP*

3.6 REFERENCES

29. "Synthesis, Characterization, and Computational Studies of Cycloparaphenylene Dimers." Xia, J. *et al*. *Journal of the American Chemical Society* **2012**, *134*, 19709.
30. "Synthesis and Dimerization of Chloro[10]cycloparaphenylene: A Directly Connected Cycloparaphenylene Dimer." Ishii, Y. *et al*. *Organic Letters* **2014**, *16*, 2174.
31. "Syntheses and Structures of Functionalized [9]Cycloparaphenylenes as Carbon Nanohoops Bearing Carbomethoxy and N-Phenylphthalimido Groups." Li, S. *et al*. *Organic Letters* **2016**, *18*, 2268.
32. "Synthesis and Structure of a Functionalized [9]Cycloparaphenylene Bearing Three Indeno[2,1-a]fluorene-11,12-dione-2,9-diyl Units." Li, S. *et al*. *Organic Letters*, **2017**, *19*, 4078.
33. "Bromination of Cycloparaphenylenes: Strain-Induced Site-Selective Bis-Addition and Its Application for Late-Stage Functionalization." Kayahara, E. *et al*. *Angewandte Chemie International Edition* **2017**, *56*, 10428.
34. "Three-Dimensionally Arranged Cyclic *p*-Hexaphenylbenzene: Toward a Bottom-Up Synthesis of Size-Defined Carbon Nanotubes." Nishiuchi, T. *et al.* *Chemistry: A European Journal* **2012**, *18*, 16621.
35. "The Precise Synthesis of Phenylene-Extended Cyclic Hexa-peri-hexabenzocoronenes from Polyarylated[n] Cycloparaphenylenes by the Scholl Reaction." Quernheim, M. *et al*. *Angewandte Chemie International Edition* **2015**, *54*, 10341.
36. “Nature of Color Diversity in Phenylenevinylene-Based Polymorphs.” Cardenas, J.C. *et al*. *Crystal Growth & Design* **2019**, *19*, 3913

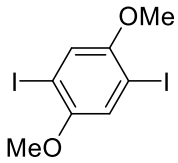

2,5-diiodo-1,4-dimethoxybenzene (49.2): 1,4-dimethoxybenzene (4.00 g, 29.0 mmol), sodium metaperiodate (3.096 g, 14.47 mmol), and iodine crystals (5.878 g, 23.16 mmol) were dissolved in acetic acid (20 mL), followed by addition of sulfuric acid in water (1:3, 4 mL total). Reaction was heated to 90 °C for 18 h, then cooled to 23 °C and quenched by addition of a saturated solution of sodium thiosulfate (50 mL). The mixture was filtered, then washed with DI water. The resulting solid was recrystallized in a cold 1:1 solution of ethanol/chloroform, then vacuum dried to yield a light brown powder (9.11 g, 81%). Melting point and spectroscopic data match previously reported material.

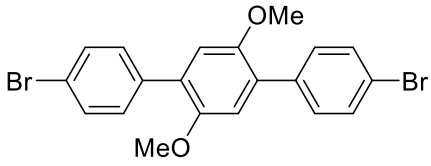

Dibromide (49.3a): Compound **49.2** (499 mg, 1.28 mmol), 4-bromophenylboronic acid (560 mg, 2.82 mmol), tetrakis(triphenylphosphine)palladium(0) (148 mg, 0.128 mmol), tetrabutylammonium iodide (47 mg, 0.128 mmol), and potassium carbonate (884 mg, 6.40 mmol) were flushed with nitrogen for 30 minutes, then dissolved in a toluene/ethanol/water solution (4:1:1, 26 mL) after purging all solvents with N_2 for at least 30 minutes. Reaction was heated to 90 °C with an air-cooled condenser and N_2 balloon for 24 h, then cooled to 23 °C. DI water was added, then reaction was extracted with ethyl acetate (3 x 30 mL). Combined organics were dried over $MgSO_4$, filtered, and concentrated under reduced pressure. Residue was preabsorbed on SiO_2 and purified by flash chromatography (15 x 2.5 cm, 15-30% dichloromethane/hexanes) to yield white solid (386 mg, 68%). R_f = 0.28 (20% dichloromethane/hexanes). ^{1}H NMR (500 MHz, $CDCl_3$) δ 7.60 – 7.54 (m, 4H), 7.48 – 7.43 (m, 4H), 7.20 (s, 2H), 6.93 (s, 2H), 3.83 (s, 6H), 3.78 (s, 6H). ^{13}C NMR (126 MHz, $CDCl_3$) δ 153.62, 150.82, 137.27, 131.53, 131.34, 129.78, 123.18, 121.90, 121.66, 114.69, 113.50, 85.72, 57.46, 56.69, 53.68.

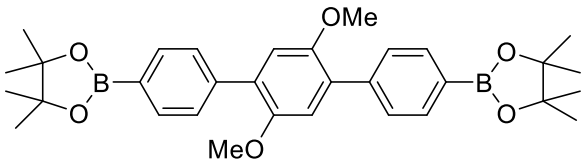

Diboronate (49.3b): Compound **49.3a** (52.3 mg, 0.117 mmol) was dissolved in anhydrous tetrahydrofuran (5 mL) under an argon atmosphere and cooled to -78 °C. Next, *n*-butyllithium (0.352 mmol) was added dropwise via syringe, followed immediately by ^{i}PrOBpin (131 mg, 0.704 mmol). Reaction was allowed to slowly warm to 23 °C before quenching with water, then extraction with ethyl acetate (3 x 5 mL). Combined organics were dried over $MgSO_4$, filtered, and concentrated under reduced pressure. Residue was preabsorbed on SiO_2, then purified by flash chromatography (14 x 1.5 cm, 50-80% dichloromethane/hexanes) to yield clear oil (30.0 mg, 53%). R_f = 0.15 (dichloromethane). ^{1}H NMR (500 MHz, $CDCl_3$) δ 7.88 (d, J = 8.0 Hz, 4H),

7.59 (d, *J* = 8.1 Hz, 4H), 6.97 (s, 2H), 3.77 (s, 6H), 1.36 (s, 24H). ^{13}C NMR (126 MHz, $CDCl_3$) δ 151.01, 141.46, 134.81, 130.86, 129.06, 115.07, 84.02, 56.78, 31.85, 25.12, 22.92, 14.38.

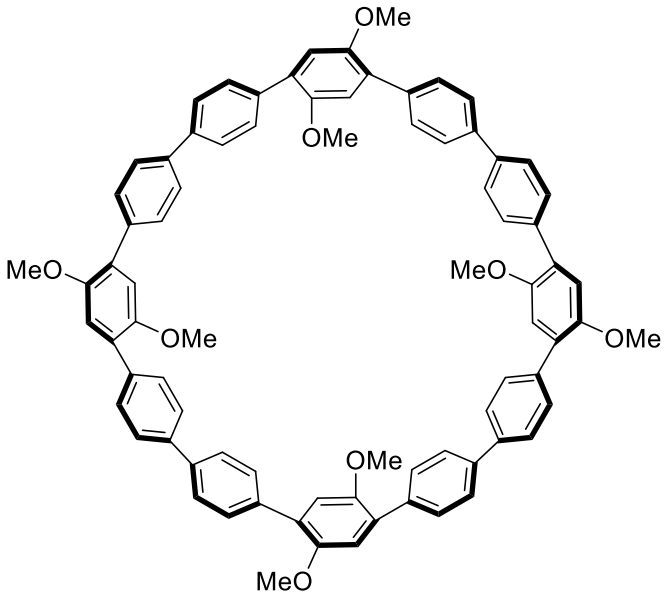

Octamethoxy[12]CPP **(41.1)**: Compound **49.3b** (6.7 mg, 0.014 mmol), dichloro(cyclooctadiene)platinum(II) (5.8 mg, 0.015 mmol), and tribasic potassium phosphate (14.9 mg, 0.070 mmol, crushed and oven-dried) were dissolved in anhydrous tetrahydrofuran (4.7 mL) under an argon atmosphere, sealed with a Teflon-lined cap, and heated to 65 °C for 3.5 h. Reaction was cooled to 23 °C and DI water was added, followed by extraction with ethyl acetate (3 x 3 mL). Combined organics were dried over $MgSO_4$, filtered, and concentrated under reduced pressure. Residue was flushed with argon, then dissolved in anhydrous toluene (0.3 mL) with triphenylphosphine (16.5 mg, 0.063 mmol) and heated to 105 °C for 18 h. Reaction was cooled to 23 °C and concentrated under reduced pressure, then purified by flash chromatography (6 x 0.3 cm, 30-60% dichloromethane/hexanes) to yield fluorescent off-white solid (3.2 mg, 79%). R_f = 0.17 (50% dichloromethane/hexanes). ^{1}H NMR (500 MHz, $CDCl_3$) δ 7.77 – 7.69 (m, 12H), 7.64 – 7.59 (m, 6H), 7.46 (q, *J* = 6.8 Hz, 10H), 7.36 (t, *J* = 7.3 Hz, 3H), 7.05 (d, *J* = 2.3 Hz, 5H), 7.01 (s, 3H), 3.85 (s, 12H), 3.82 (s, 12H). ^{13}C NMR (126 MHz, $CDCl_3$) δ 150.65, 138.34, 130.43, 129.48, 128.12, 127.14, 114.81, 56.47, 29.73.

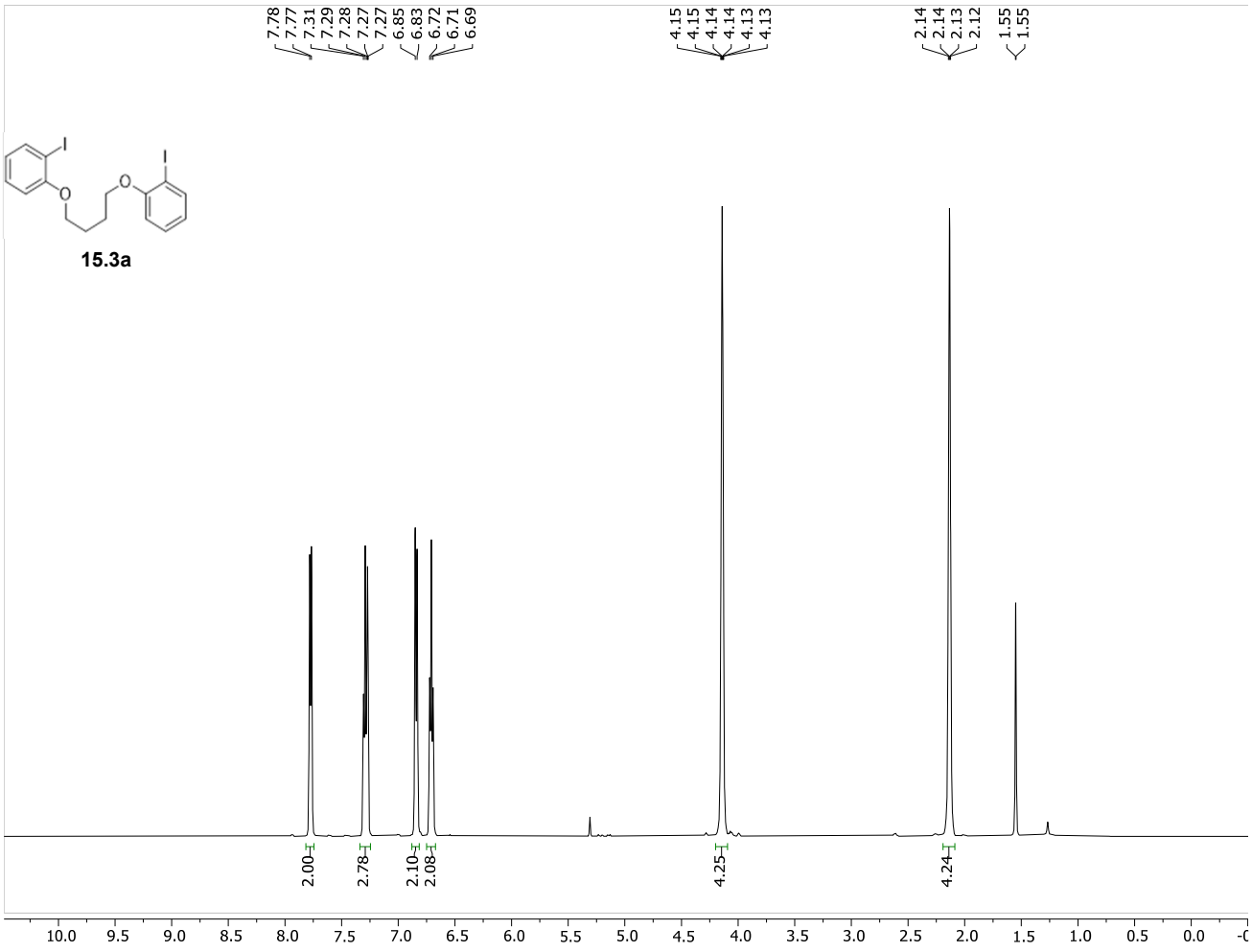
7.78
7.77
7.31
7.29
7.28
7.27
7.27
6.85
6.83
6.72
6.71
6.69
4.15
4.15
4.14
4.14
4.13
4.13
2.14
2.14
2.13
2.12
1.55
1.55
15.3a
2.00
2.78
2.10
2.08
4.25
4.24
10.0
9.5
9.0
8.5
8.0
7.5
7.0
6.5
6.0
5.5
5.0
4.5
4.0
3.5
3.0
2.5
2.0
1.5
1.0
0.5
0.0

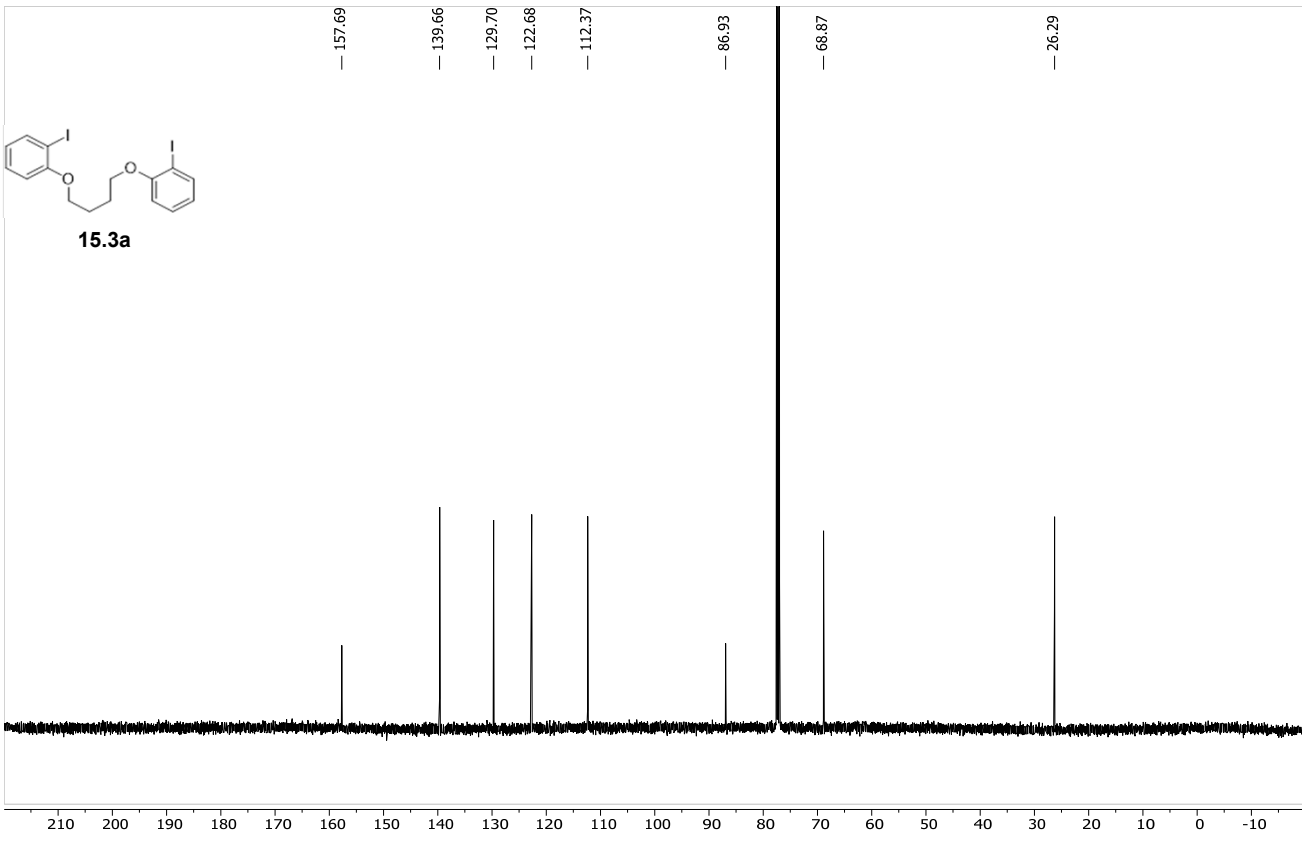
157.69
139.66
129.70
122.68
112.37
86.93
68.87
26.29
15.3a
210
200
190
180
170
160
150
140
130
120
110
100
90
80
70
60
50
40
30
20
10
0
-10

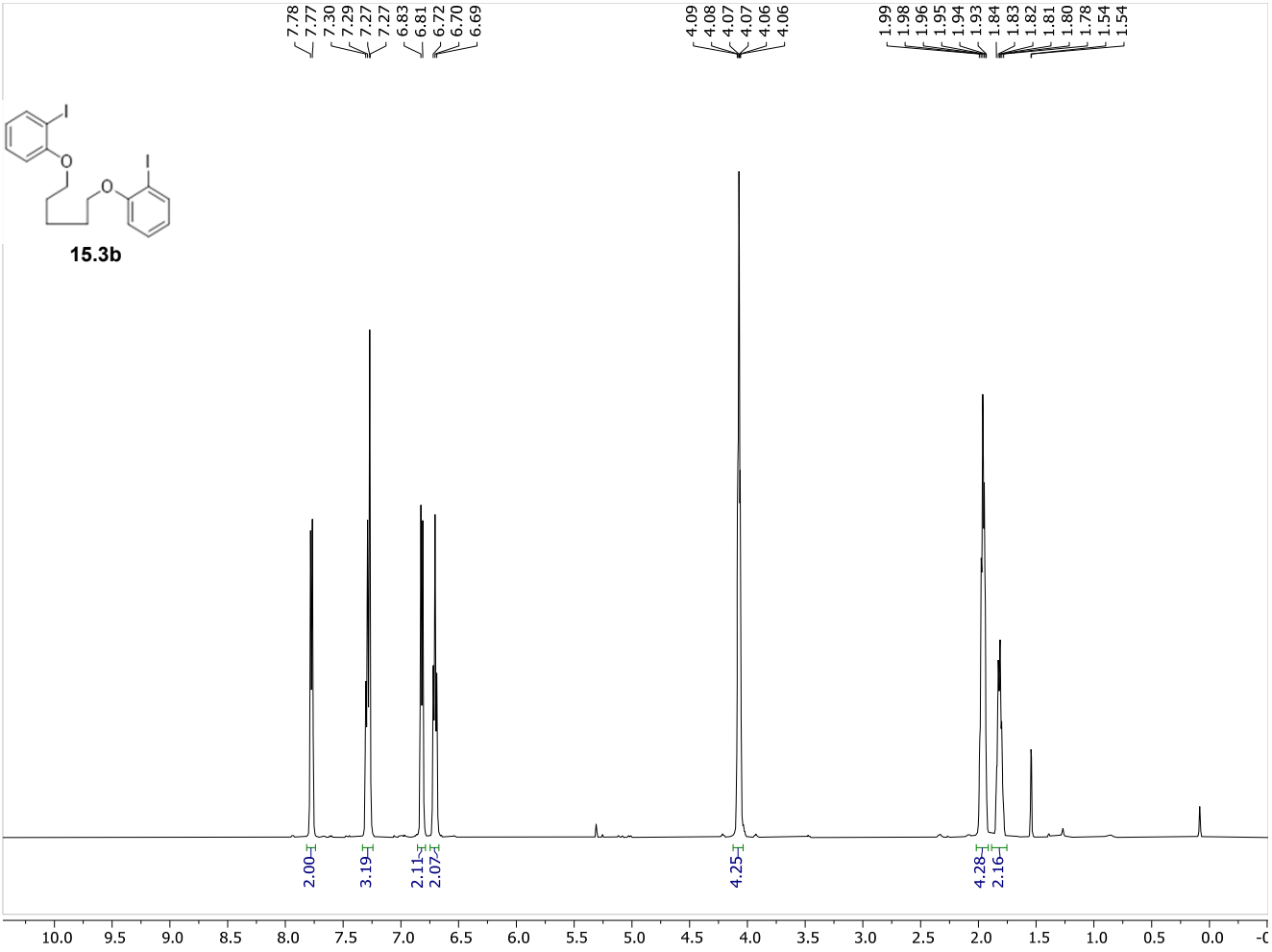
7.78
7.77
7.30
7.29
7.27
7.27
6.83
6.81
6.72
6.70
6.69
4.09
4.08
4.07
4.07
4.06
4.06
1.99
1.98
1.96
1.95
1.94
1.93
1.84
1.83
1.82
1.81
1.80
1.78
1.54
1.54
15.3b
2.00
3.19
2.11
2.07
4.25
4.28
2.16
10.0
9.5
9.0
8.5
8.0
7.5
7.0
6.5
6.0
5.5
5.0
4.5
4.0
3.5
3.0
2.5
2.0
1.5
1.0
0.5
0.0

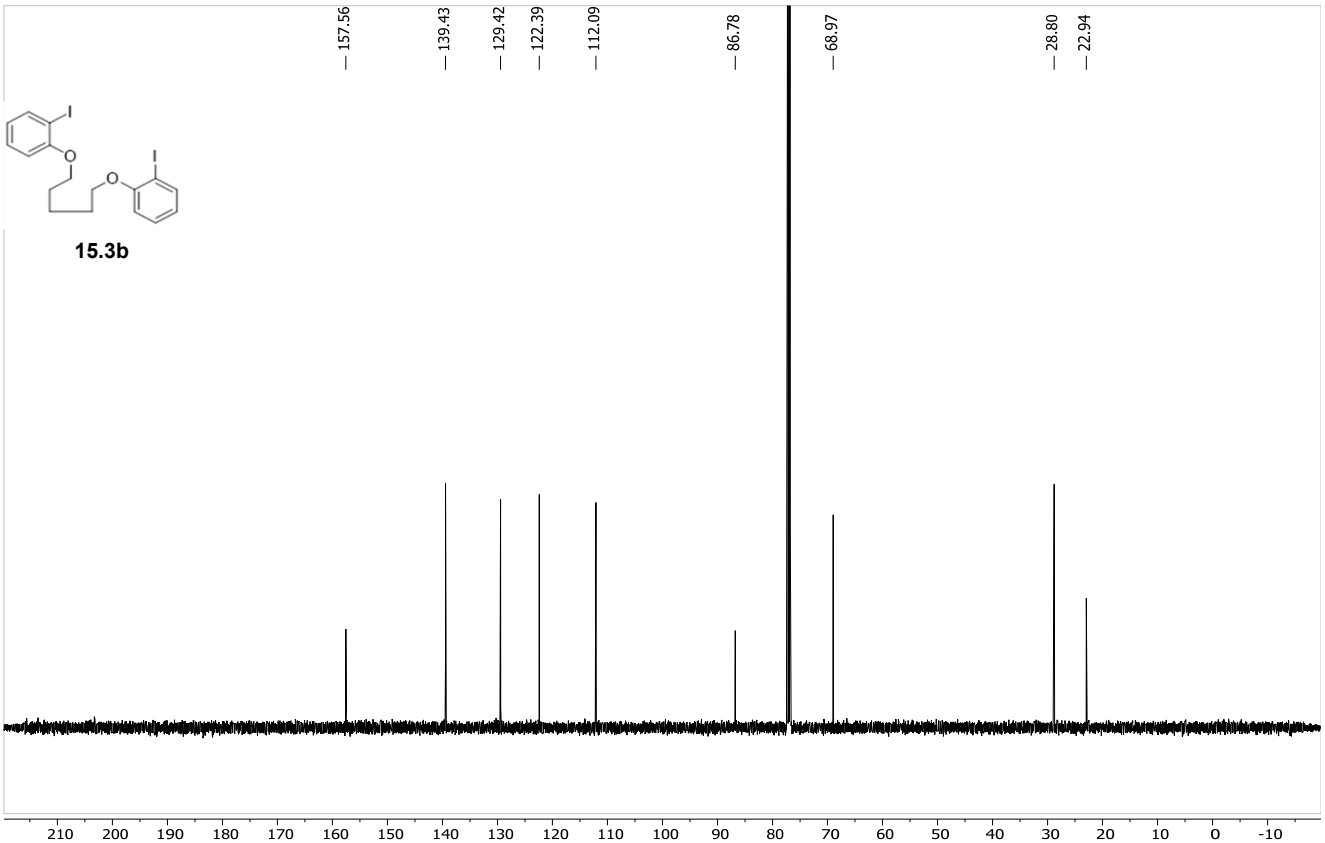
157.56
139.43
129.42
122.39
112.09
86.78
68.97
28.80
22.94
15.3b
210
200
190
180
170
160
150
140
130
120
110
100
90
80
70
60
50
40
30
20
10
0
-10

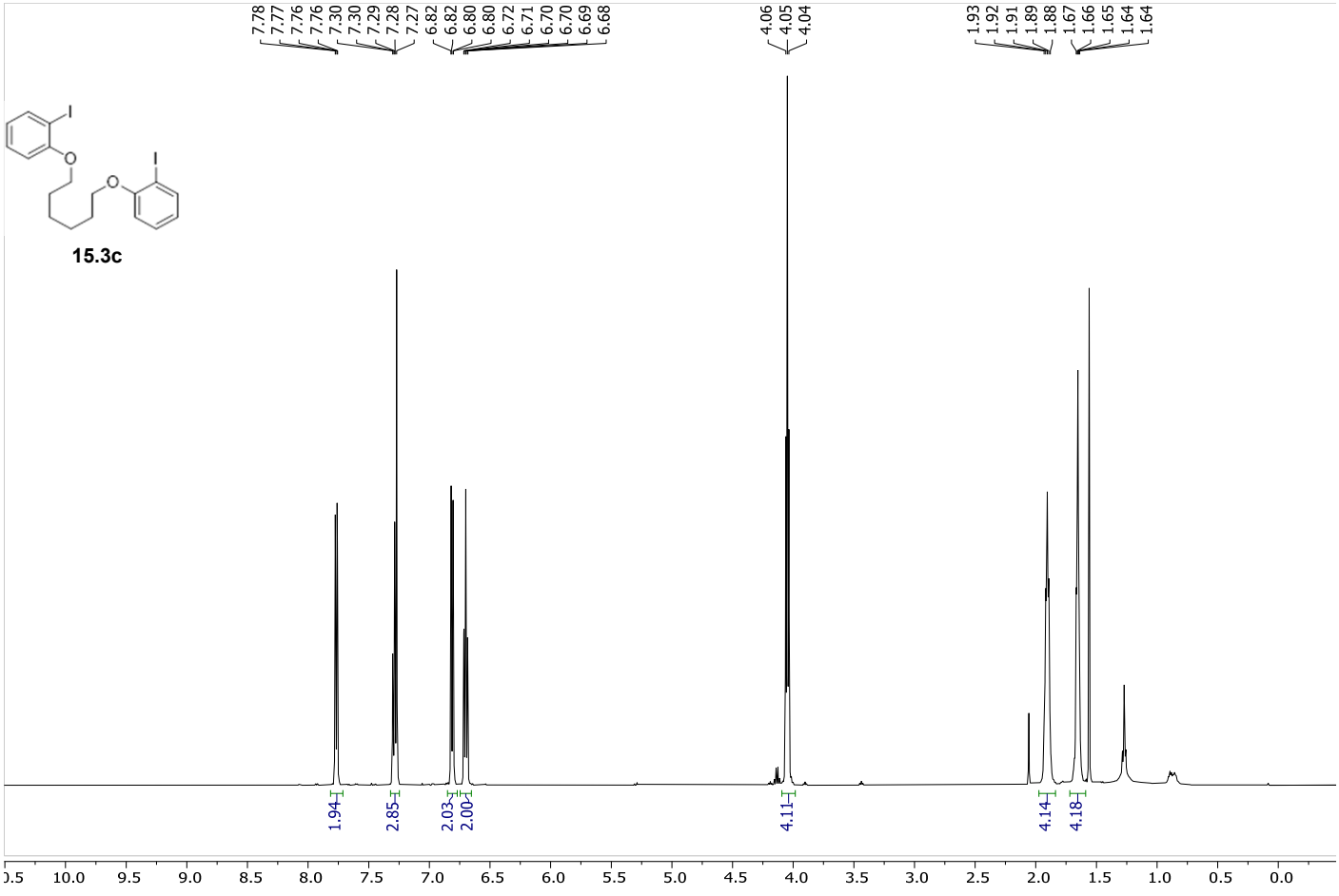
7.78
7.77
7.76
7.76
7.30
7.29
7.28
7.27
6.82
6.82
6.80
6.80
6.72
6.71
6.70
6.70
6.69
6.68
4.06
4.05
4.04
1.93
1.92
1.91
1.89
1.88
1.67
1.66
1.65
1.64
1.64
15.3c
1.94
2.85
2.03
2.00
4.11
4.14
4.18

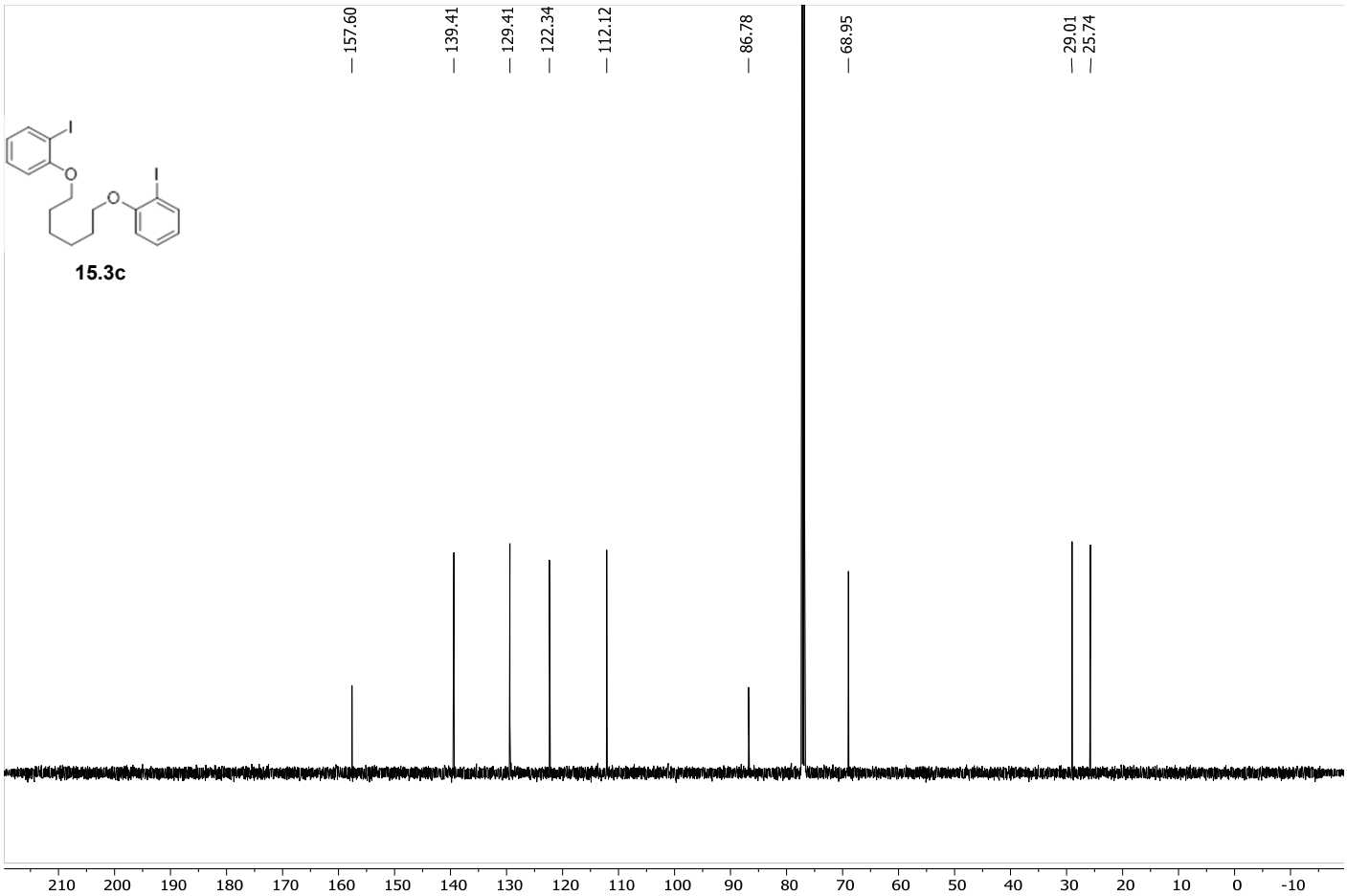
157.60
139.41
129.41
122.34
112.12
86.78
68.95
29.01
25.74
15.3c

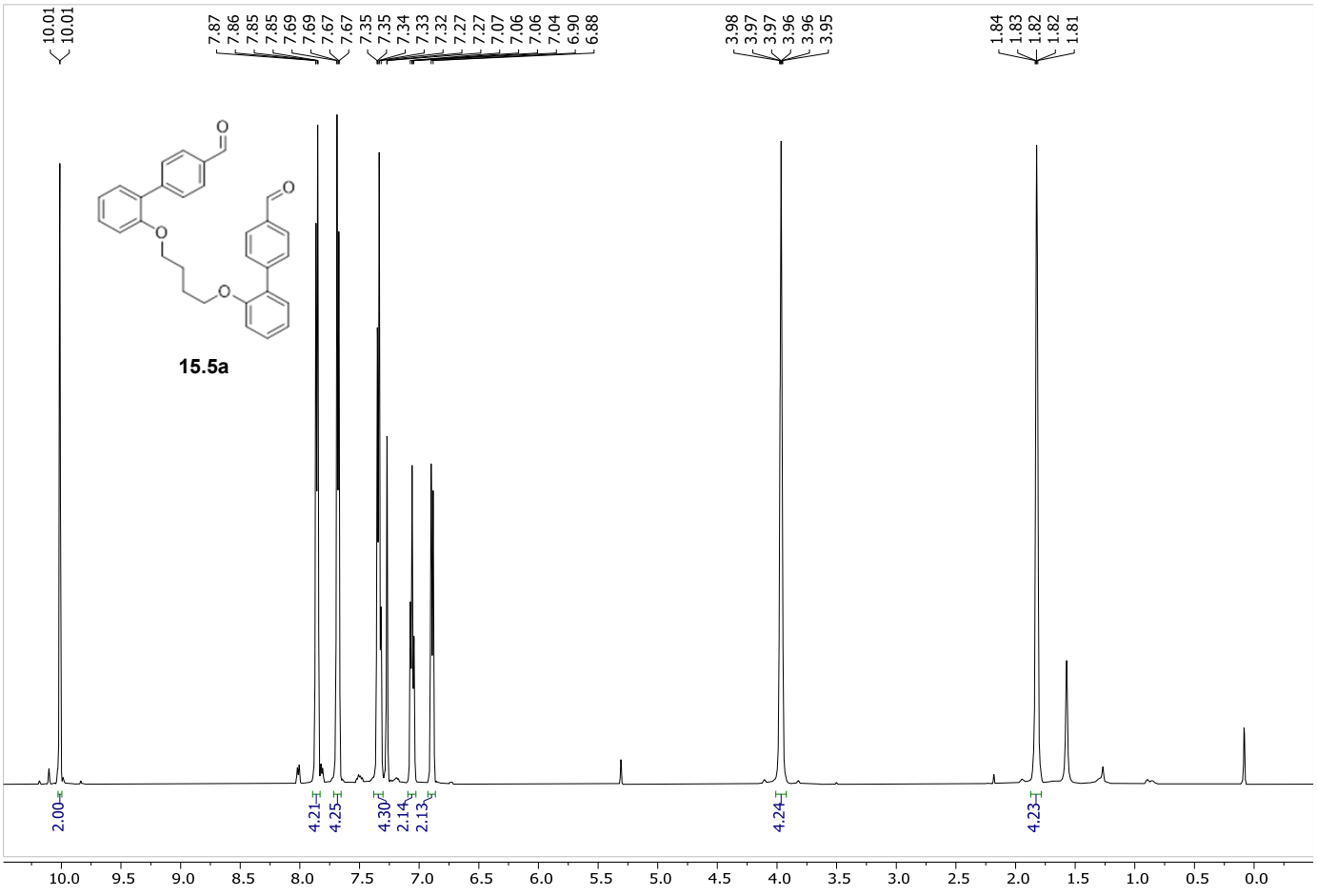
10.01
10.01
7.87
7.86
7.85
7.85
7.69
7.69
7.67
7.67
7.35
7.35
7.34
7.33
7.32
7.27
7.27
7.07
7.06
7.06
7.04
6.90
6.88
3.98
3.97
3.97
3.96
3.96
3.95
1.84
1.83
1.82
1.82
1.81
15.5a
2.00
4.21
4.25
4.30
2.14
2.13
4.24
4.23
10.0
9.5
9.0
8.5
8.0
7.5
7.0
6.5
6.0
5.5
5.0
4.5
4.0
3.5
3.0
2.5
2.0
1.5
1.0
0.5
0.0

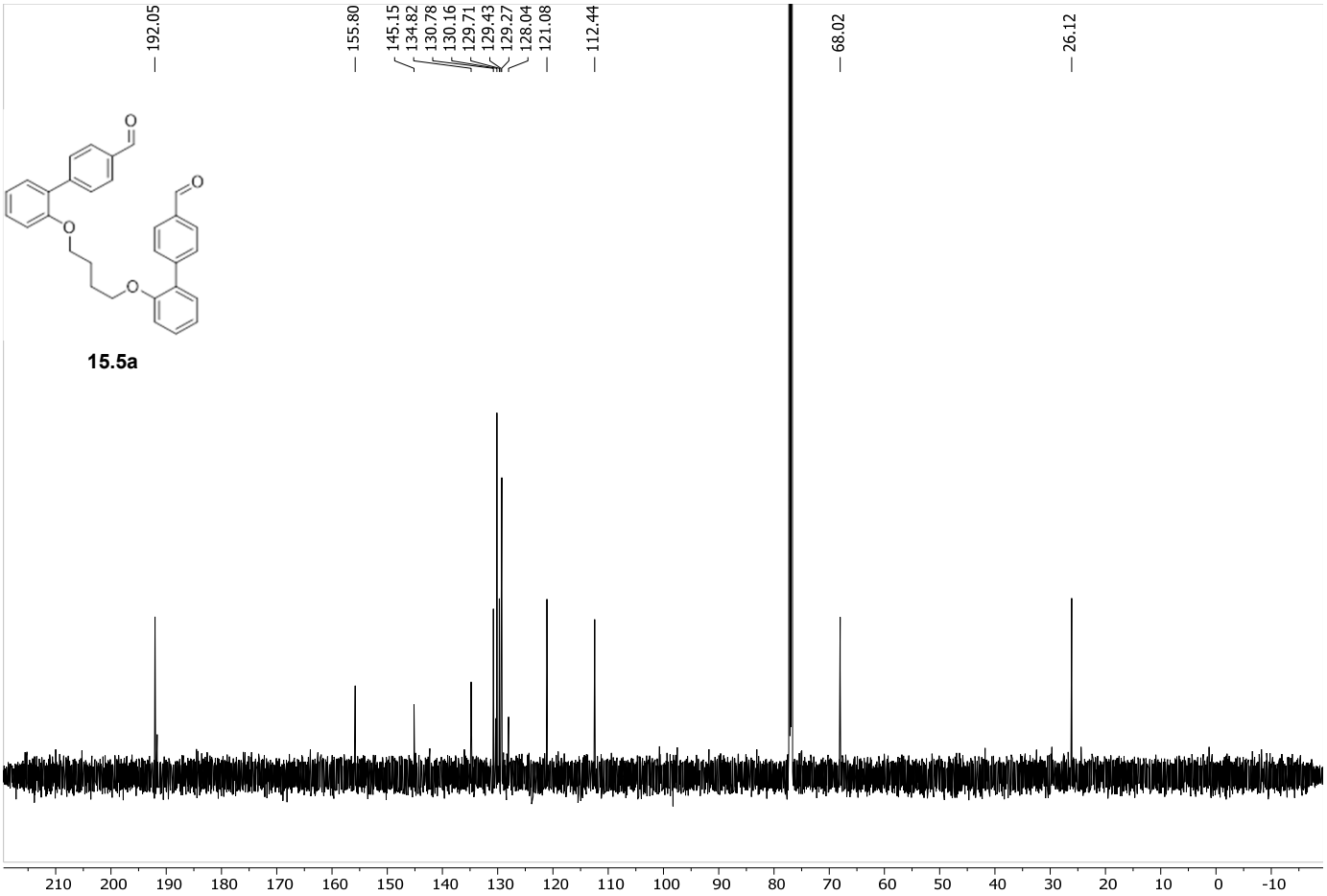
192.05
155.80
145.15
134.82
130.78
130.16
129.71
129.43
129.27
128.04
121.08
112.44
68.02
26.12
15.5a
210
200
190
180
170
160
150
140
130
120
110
100
90
80
70
60
50
40
30
20
10
0
-10

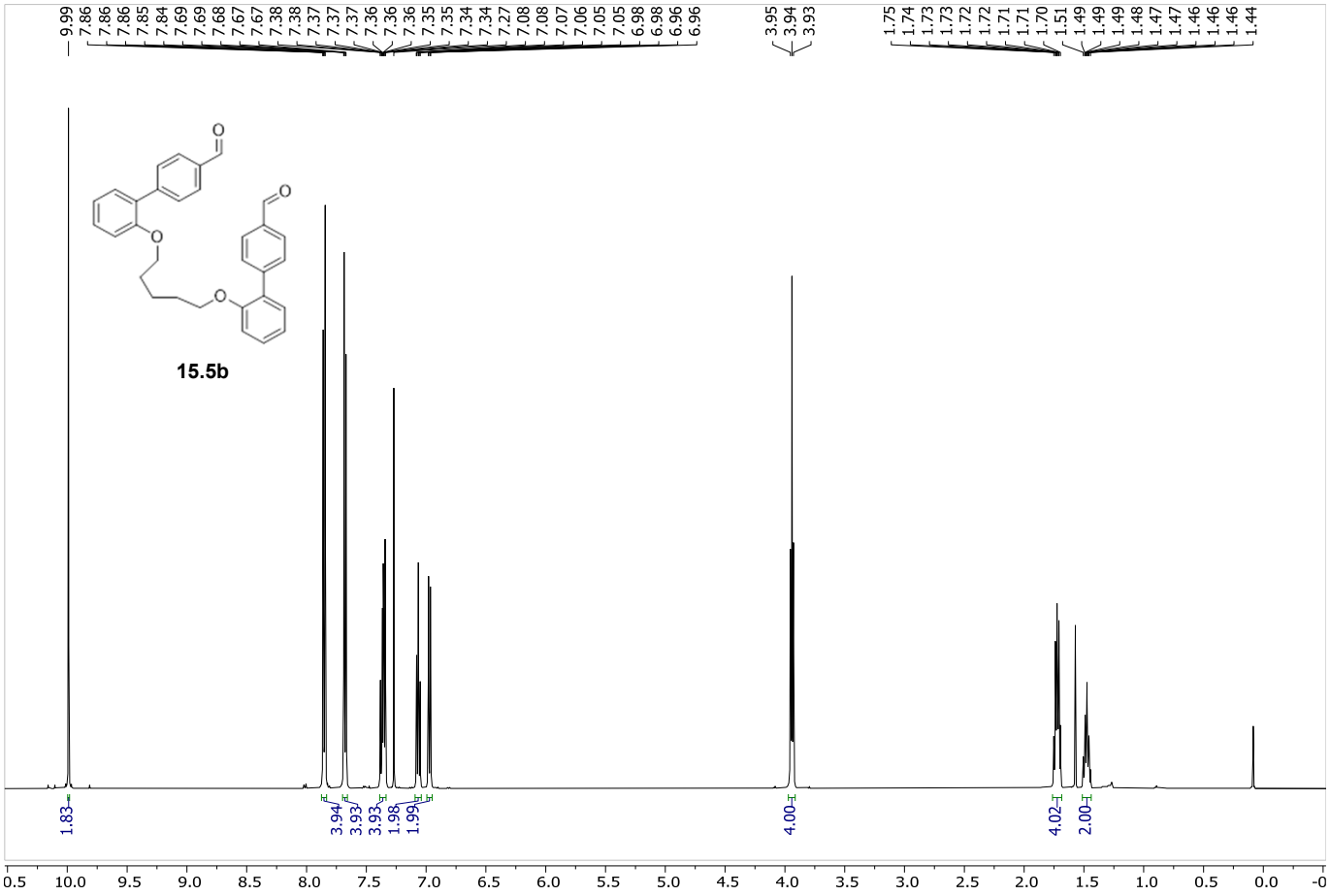
9.99
7.86
7.86
7.86
7.85
7.84
7.69
7.69
7.68
7.67
7.67
7.38
7.38
7.37
7.37
7.37
7.37
7.36
7.36
7.36
7.35
7.35
7.34
7.34
7.34
7.27
7.08
7.08
7.07
7.06
7.05
7.05
6.98
6.98
6.96
6.96
3.95
3.94
3.93
1.75
1.74
1.73
1.73
1.72
1.72
1.71
1.71
1.70
1.51
1.49
1.49
1.49
1.48
1.47
1.47
1.46
1.46
1.46
1.44
15.5b
1.83
3.94
3.93
3.93
1.98
1.99
4.00
4.02
2.00
0.5
10.0
9.5
9.0
8.5
8.0
7.5
7.0
6.5
6.0
5.5
5.0
4.5
4.0
3.5
3.0
2.5
2.0
1.5
1.0
0.5
0.0
-0

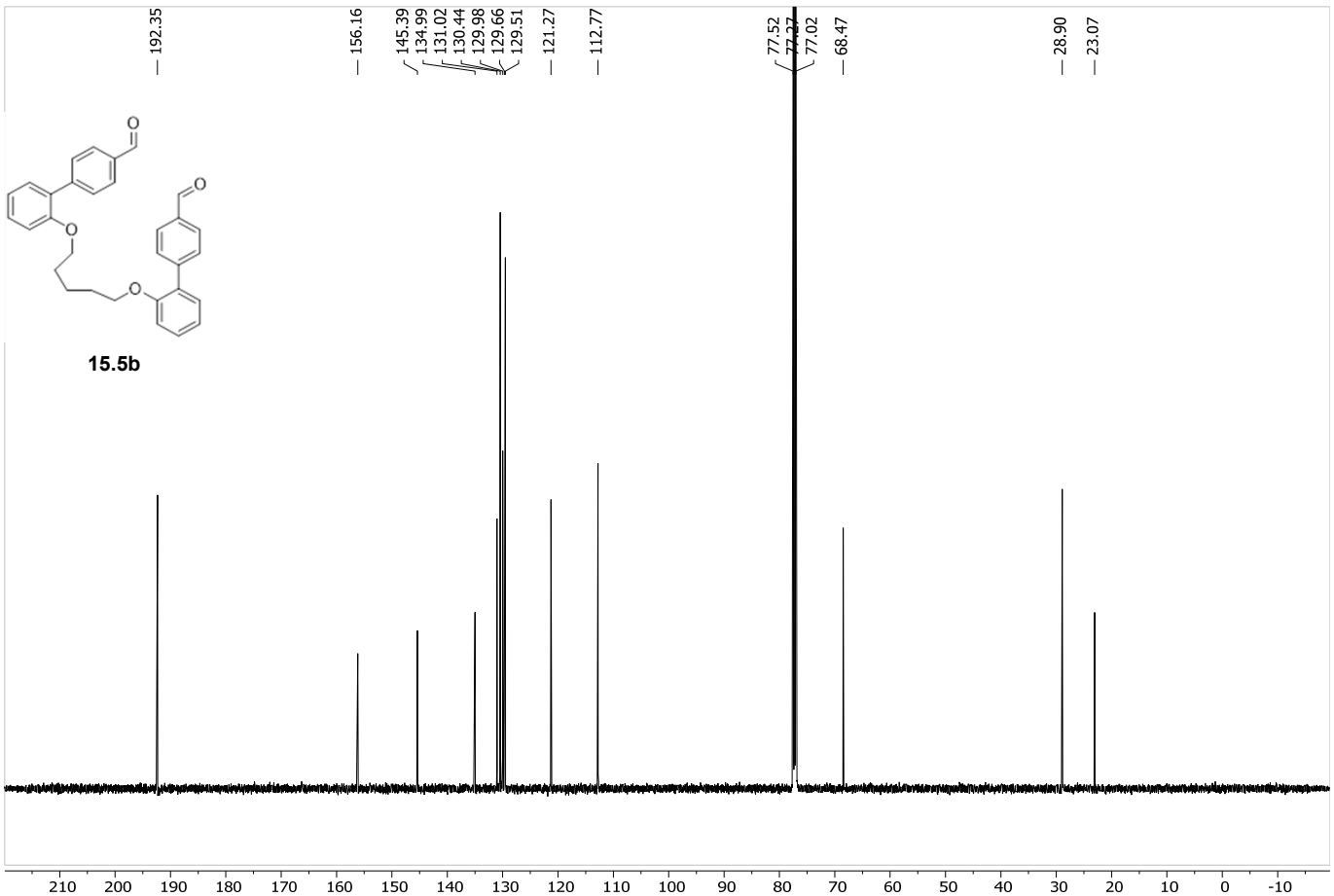
192.35
156.16
145.39
134.99
131.02
130.44
129.98
129.66
129.51
121.27
112.77
77.52
77.27
77.02
68.47
28.90
23.07
15.5b
210
200
190
180
170
160
150
140
130
120
110
100
90
80
70
60
50
40
30
20
10
0
-10

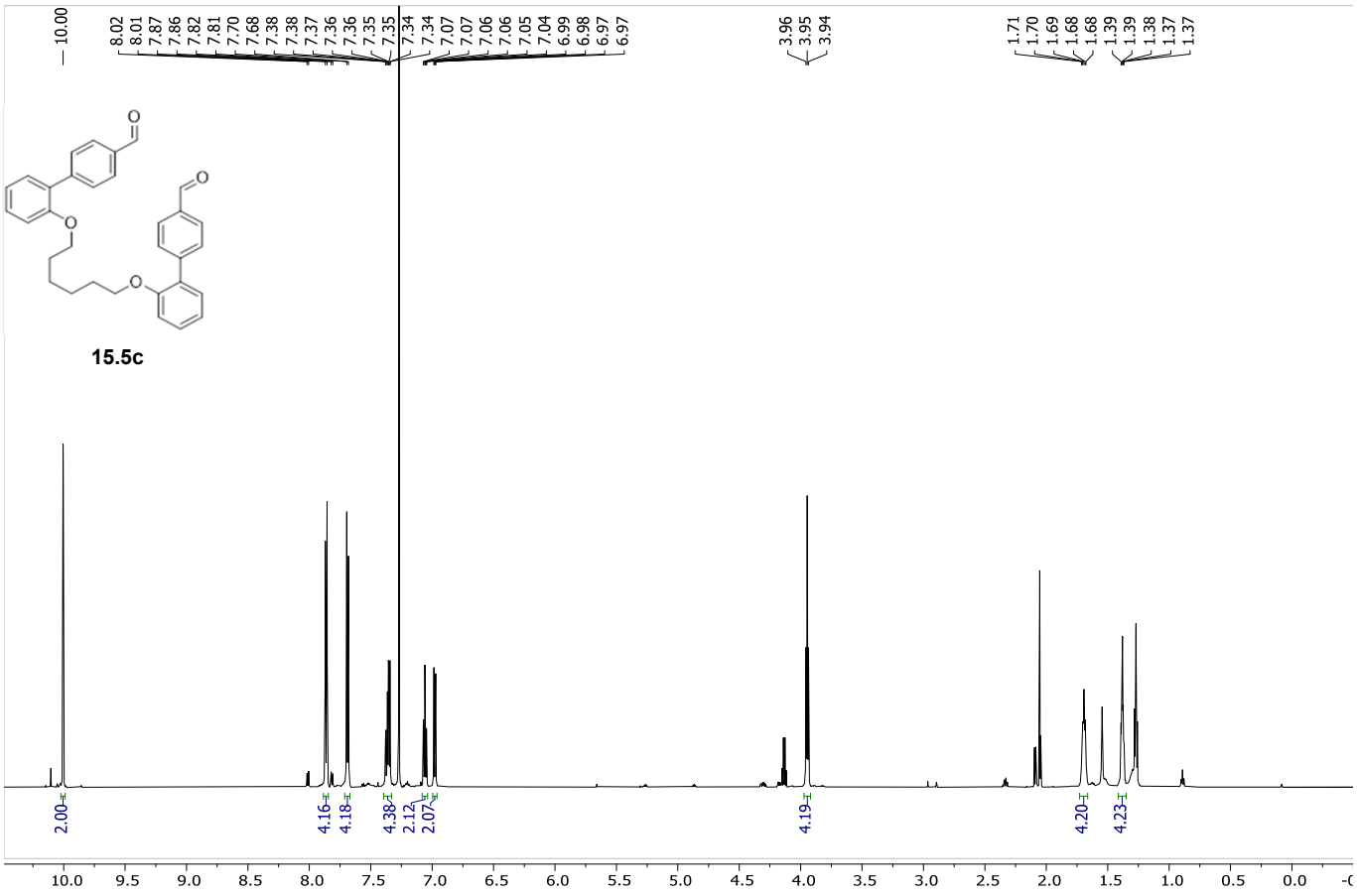
10.00
8.02
8.01
7.87
7.86
7.82
7.81
7.70
7.68
7.38
7.38
7.37
7.36
7.36
7.35
7.35
7.34
7.34
7.07
7.07
7.06
7.06
7.05
7.04
6.99
6.98
6.97
6.97
3.96
3.95
3.94
1.71
1.70
1.69
1.68
1.68
1.39
1.39
1.38
1.37
1.37
15.5c
2.00
4.16
4.18
4.38
2.12
2.07
4.19
4.20
4.23
10.0
9.5
9.0
8.5
8.0
7.5
7.0
6.5
6.0
5.5
5.0
4.5
4.0
3.5
3.0
2.5
2.0
1.5
1.0
0.5
0.0

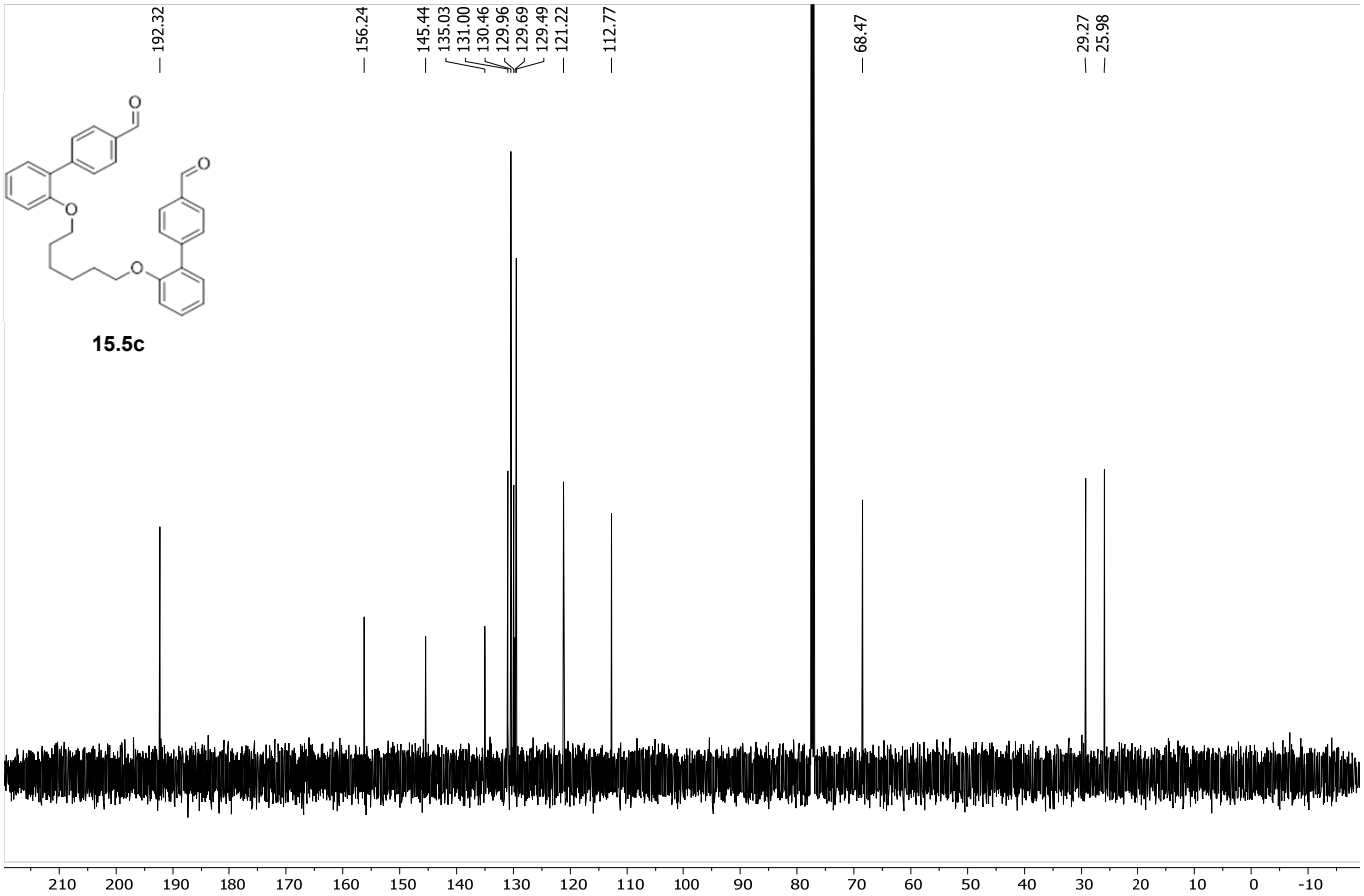
192.32
156.24
145.44
135.03
131.00
130.46
129.96
129.69
129.49
121.22
112.77
68.47
29.27
25.98
15.5c
210
200
190
180
170
160
150
140
130
120
110
100
90
80
70
60
50
40
30
20
10
0
-10

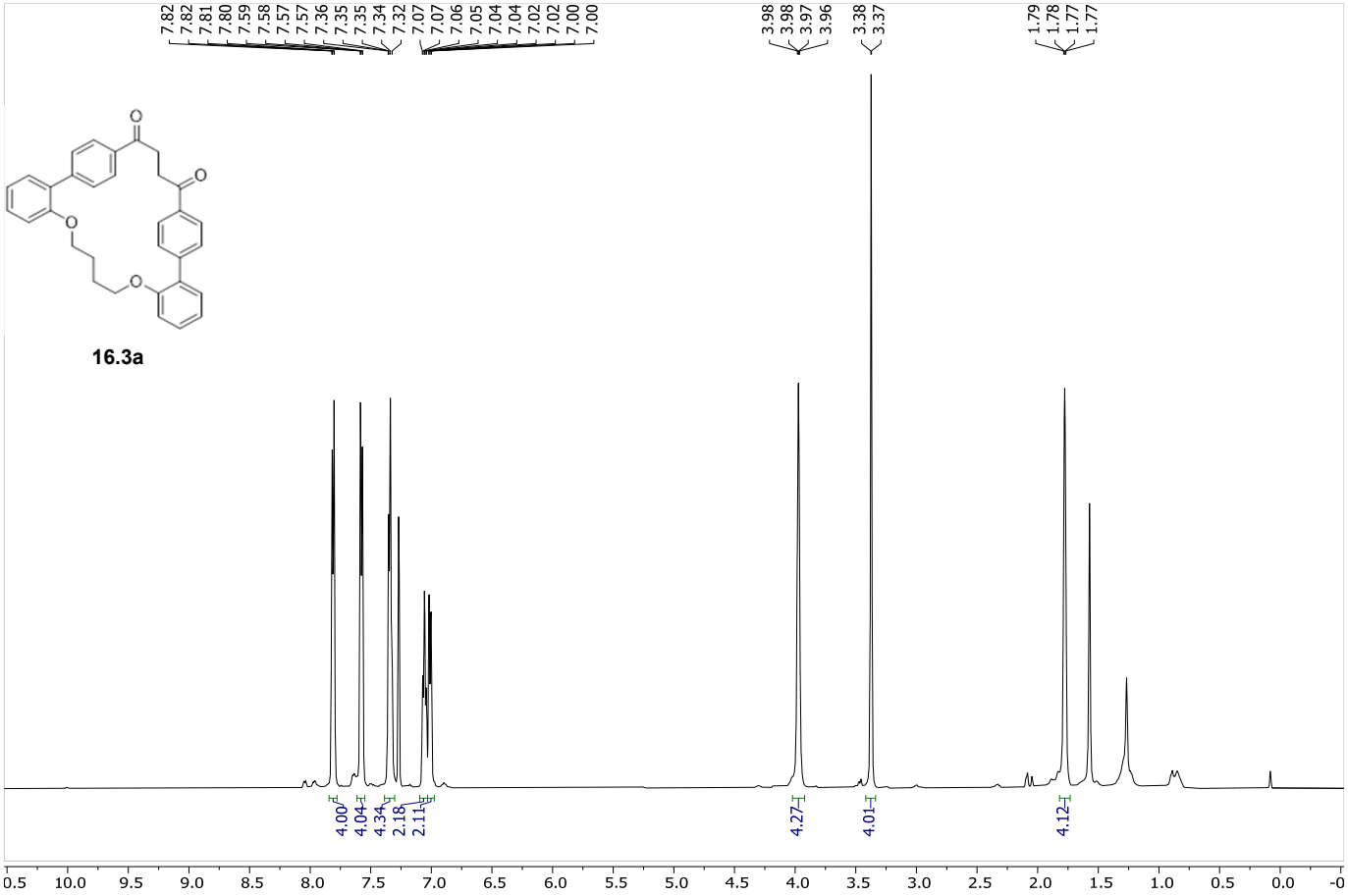
7.82
7.82
7.81
7.80
7.59
7.58
7.57
7.57
7.36
7.35
7.35
7.34
7.32
7.07
7.07
7.06
7.05
7.04
7.04
7.02
7.02
7.00
7.00
3.98
3.98
3.97
3.96
3.38
3.37
1.79
1.78
1.77
1.77
16.3a
4.00
4.04
4.34
2.18
2.11
4.27
4.01
4.12
0.5 10.0 9.5 9.0 8.5 8.0 7.5 7.0 6.5 6.0 5.5 5.0 4.5 4.0 3.5 3.0 2.5 2.0 1.5 1.0 0.5 0.0 -0

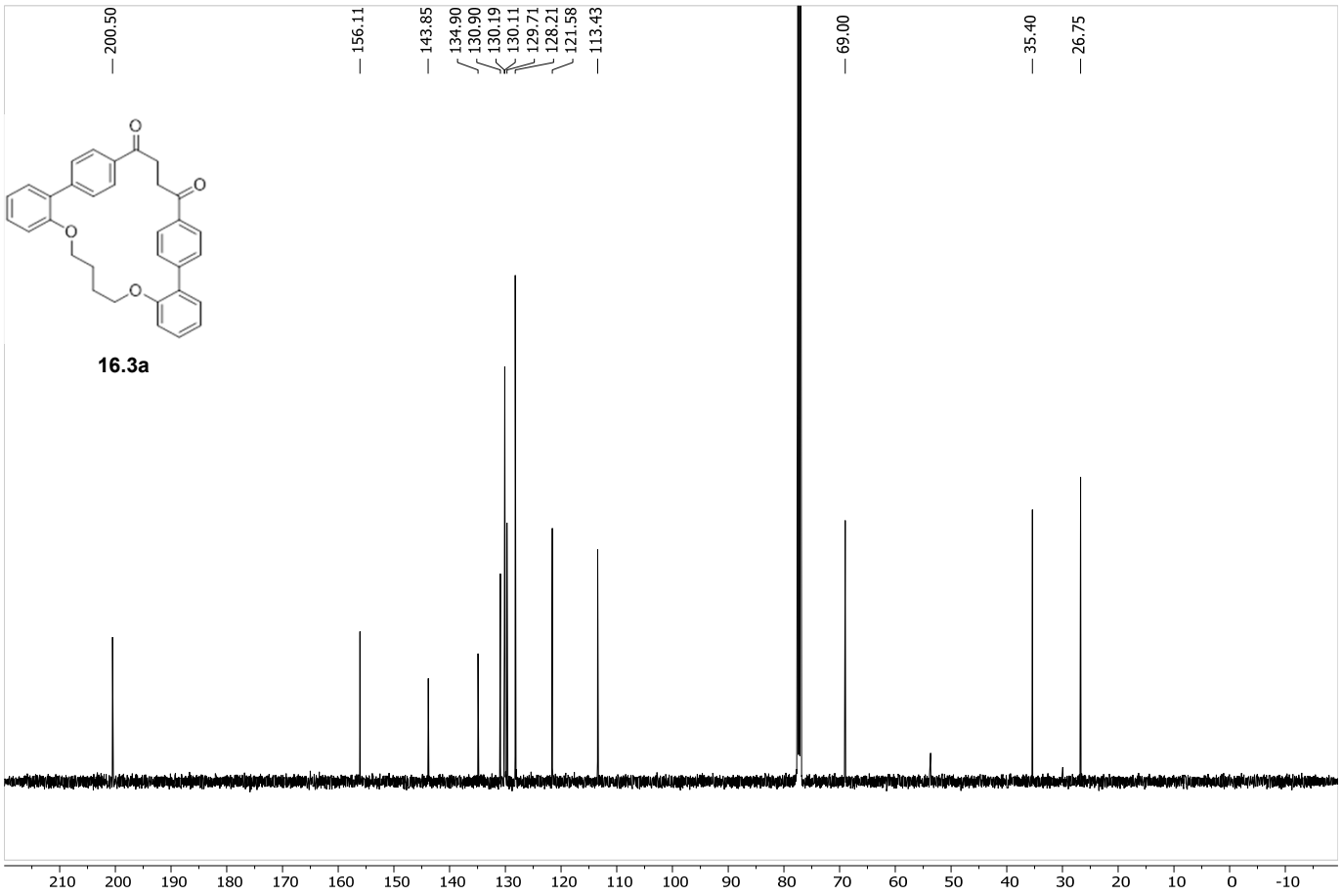
200.50
156.11
143.85
134.90
130.90
130.19
130.11
129.71
128.21
121.58
113.43
69.00
35.40
26.75
16.3a
210 200 190 180 170 160 150 140 130 120 110 100 90 80 70 60 50 40 30 20 10 0 -10

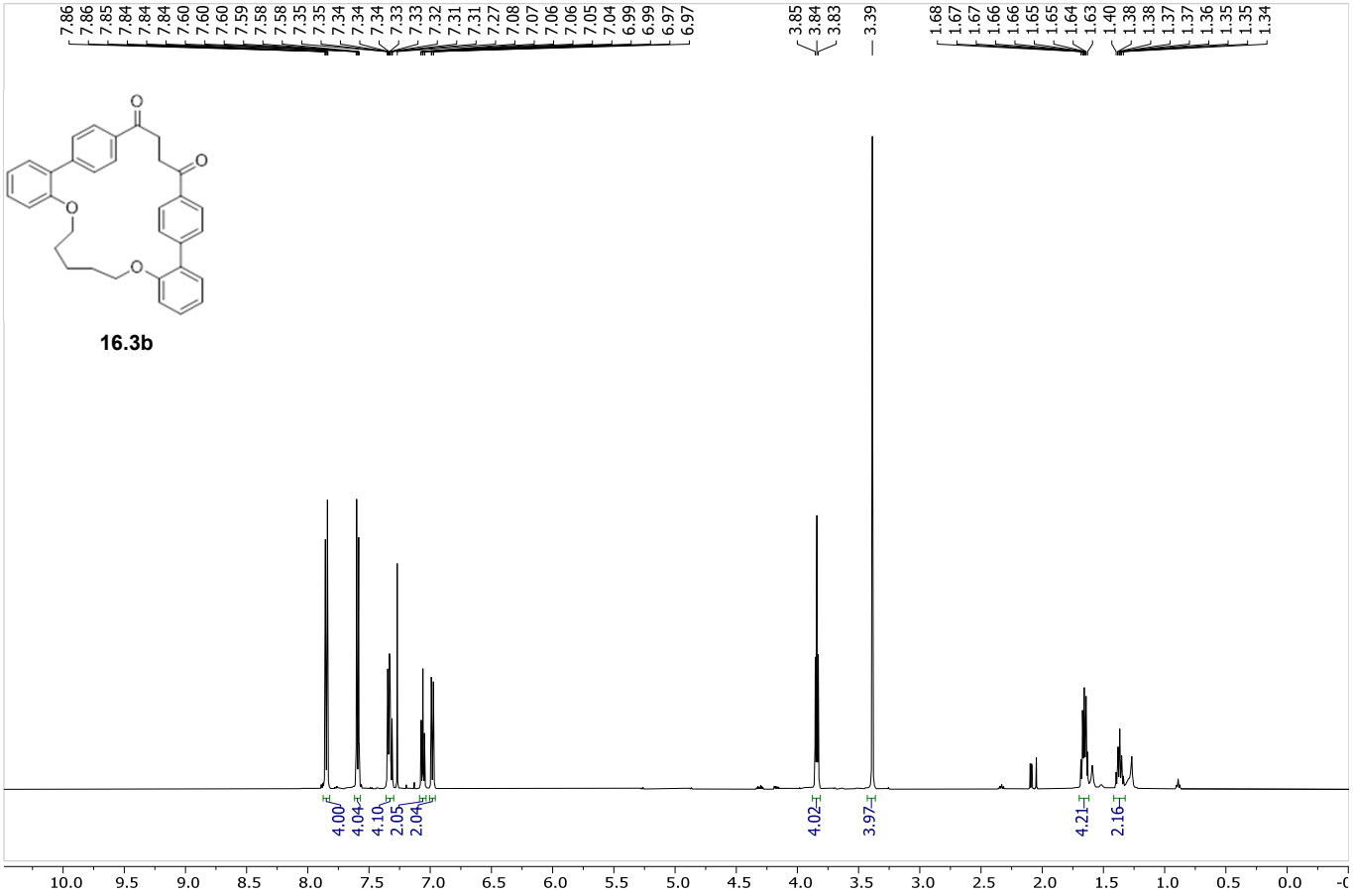
7.86 7.86 7.85 7.84 7.84 7.84 7.60 7.60 7.60 7.59 7.58 7.58 7.35 7.35 7.34 7.34 7.34 7.33 7.33 7.32 7.31 7.31 7.27 7.08 7.07 7.06 7.06 7.05 7.04 6.99 6.97 6.97
3.85 3.84 3.83 3.39
1.68 1.67 1.67 1.66 1.66 1.65 1.65 1.64 1.63 1.40 1.38 1.38 1.37 1.37 1.36 1.35 1.35 1.34
16.3b
4.00 4.04 4.10 2.05 2.04 4.02 3.97 4.21 2.16
10.0 9.5 9.0 8.5 8.0 7.5 7.0 6.5 6.0 5.5 5.0 4.5 4.0 3.5 3.0 2.5 2.0 1.5 1.0 0.5 0.0

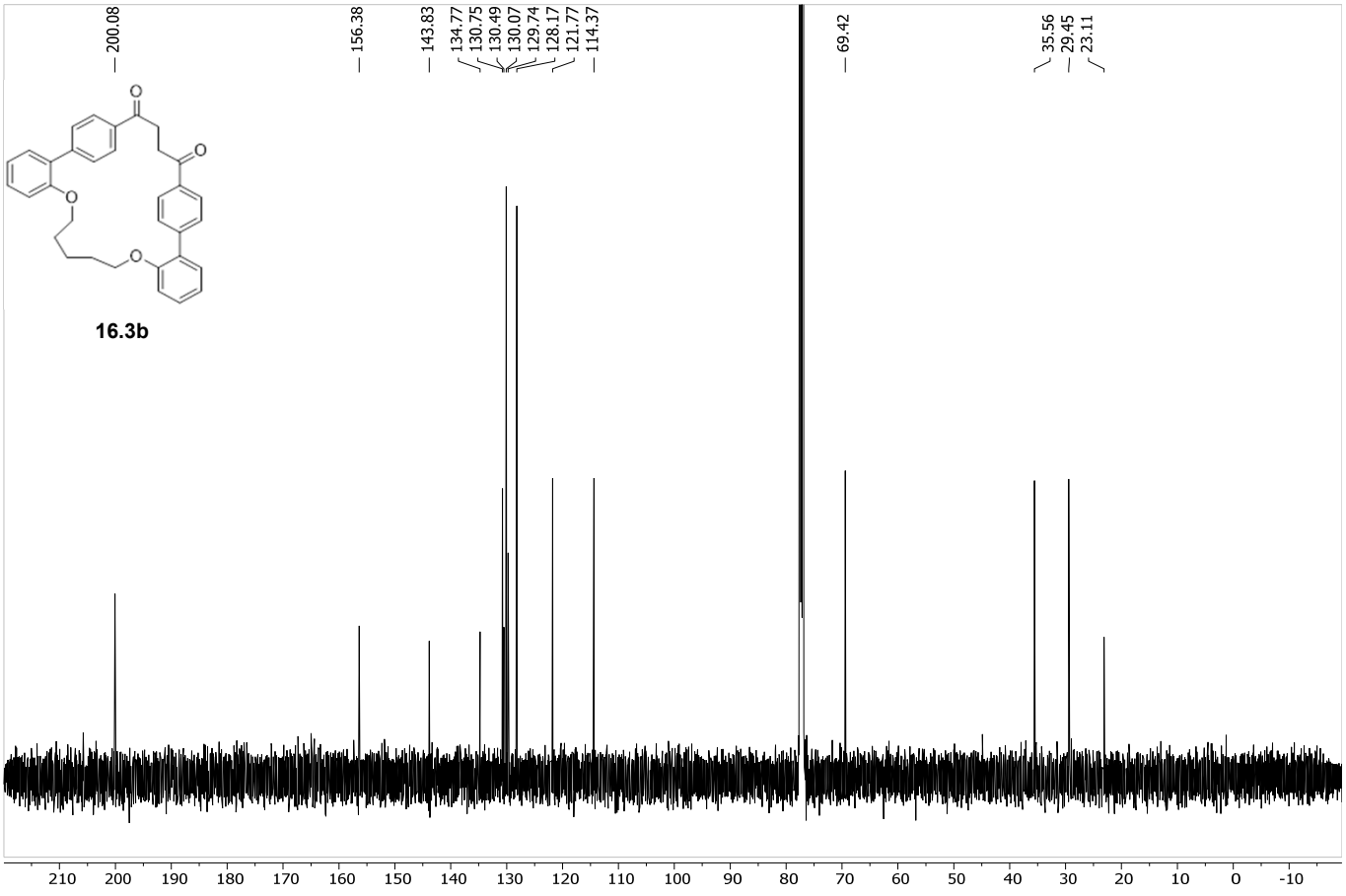
200.08
156.38
143.83
134.77 130.75 130.49 130.07 129.74 128.17 121.77 114.37
69.42
35.56 29.45 23.11
16.3b
210 200 190 180 170 160 150 140 130 120 110 100 90 80 70 60 50 40 30 20 10 0 -10

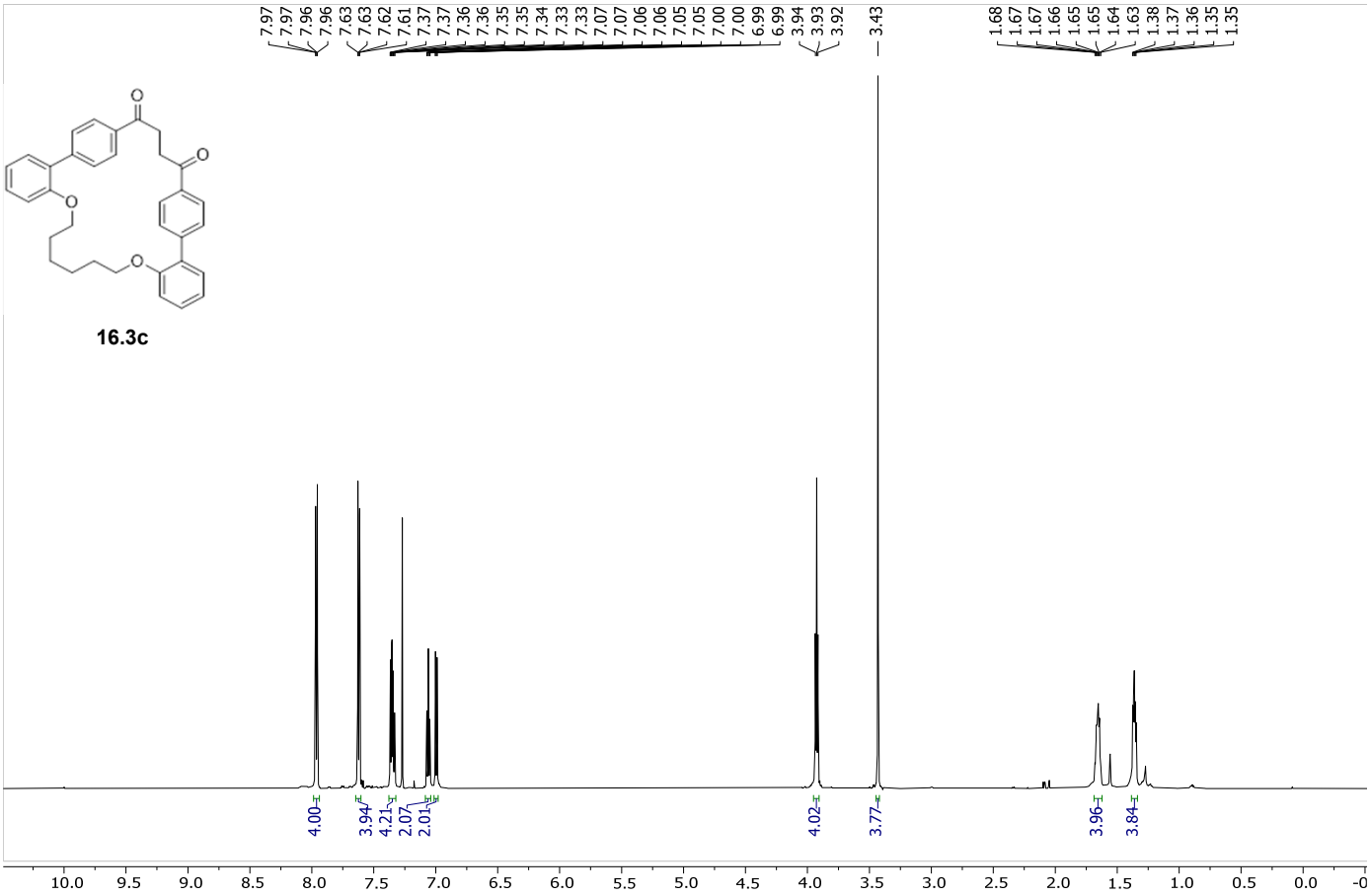
7.97
7.97
7.96
7.96
7.63
7.63
7.62
7.61
7.37
7.37
7.36
7.36
7.35
7.35
7.34
7.33
7.33
7.07
7.07
7.06
7.06
7.05
7.05
7.00
7.00
6.99
6.99
3.94
3.93
3.92
3.43
1.68
1.67
1.67
1.66
1.65
1.65
1.64
1.63
1.38
1.37
1.36
1.35
1.35
16.3c
4.00
3.94
4.21
2.07
2.01
4.02
3.77
3.96
3.84
10.0
9.5
9.0
8.5
8.0
7.5
7.0
6.5
6.0
5.5
5.0
4.5
4.0
3.5
3.0
2.5
2.0
1.5
1.0
0.5
0.0

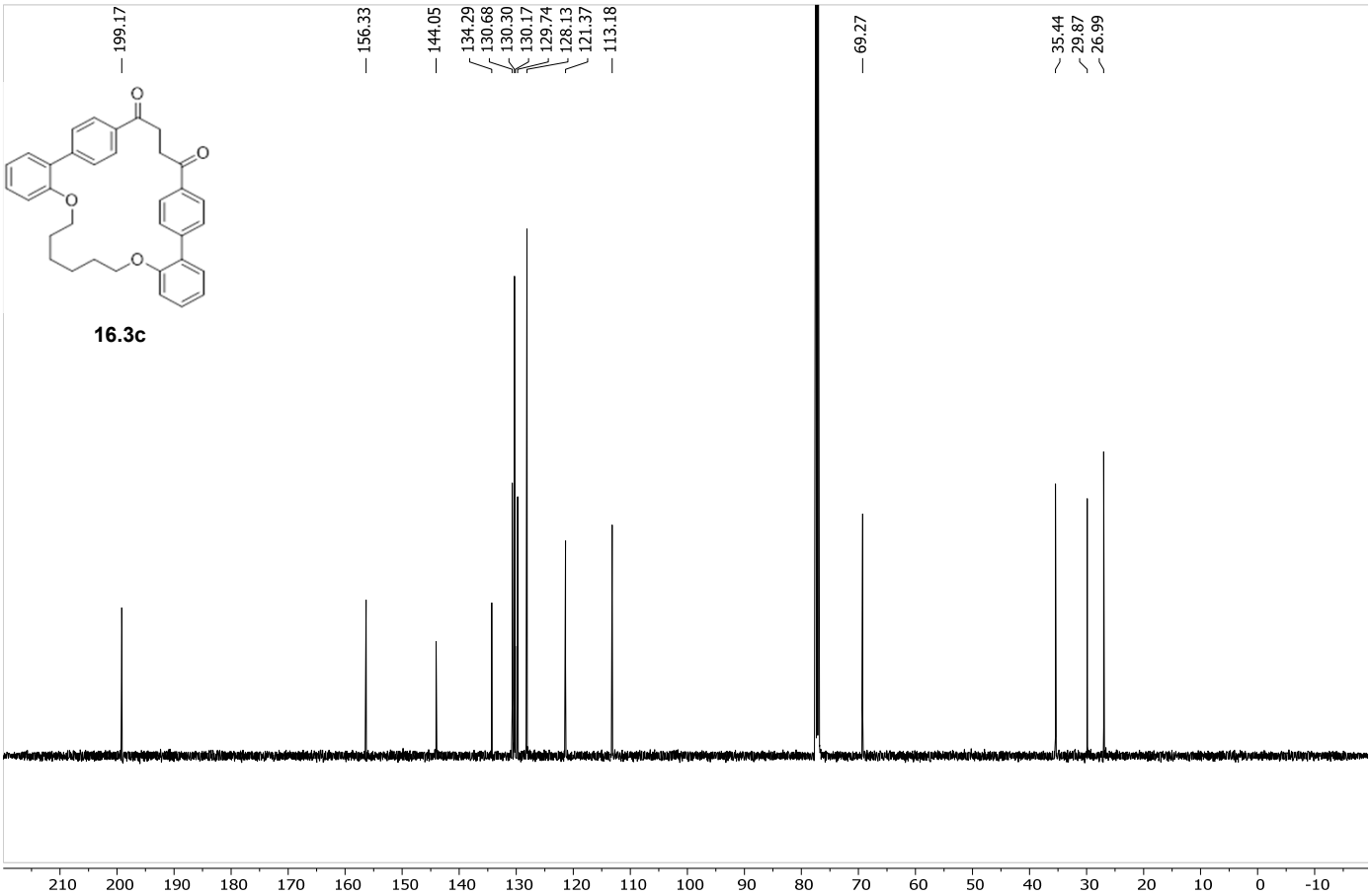
199.17
156.33
144.05
134.29
130.68
130.30
130.17
129.74
128.13
121.37
113.18
69.27
35.44
29.87
26.99
16.3c
210
200
190
180
170
160
150
140
130
120
110
100
90
80
70
60
50
40
30
20
10
0
-10

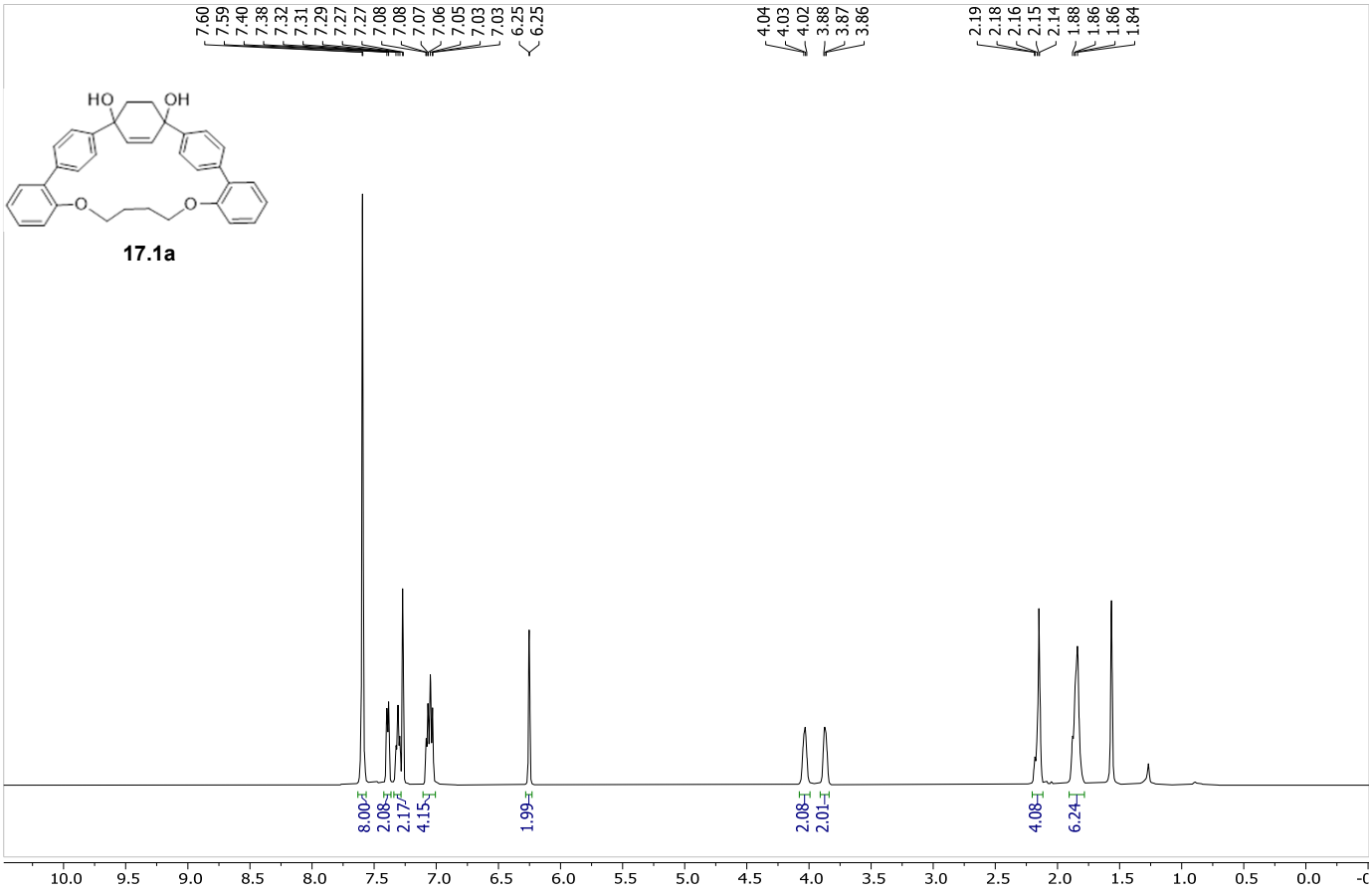
7.60
7.59
7.40
7.38
7.32
7.31
7.29
7.27
7.27
7.08
7.08
7.07
7.06
7.05
7.03
7.03
6.25
6.25
4.04
4.03
4.02
3.88
3.87
3.86
2.19
2.18
2.16
2.15
2.14
1.88
1.86
1.86
1.84
HO
OH
O
O
17.1a
8.00
2.08
2.17
4.15
1.99
2.08
2.01
4.08
6.24
10.0
9.5
9.0
8.5
8.0
7.5
7.0
6.5
6.0
5.5
5.0
4.5
4.0
3.5
3.0
2.5
2.0
1.5
1.0
0.5
0.0

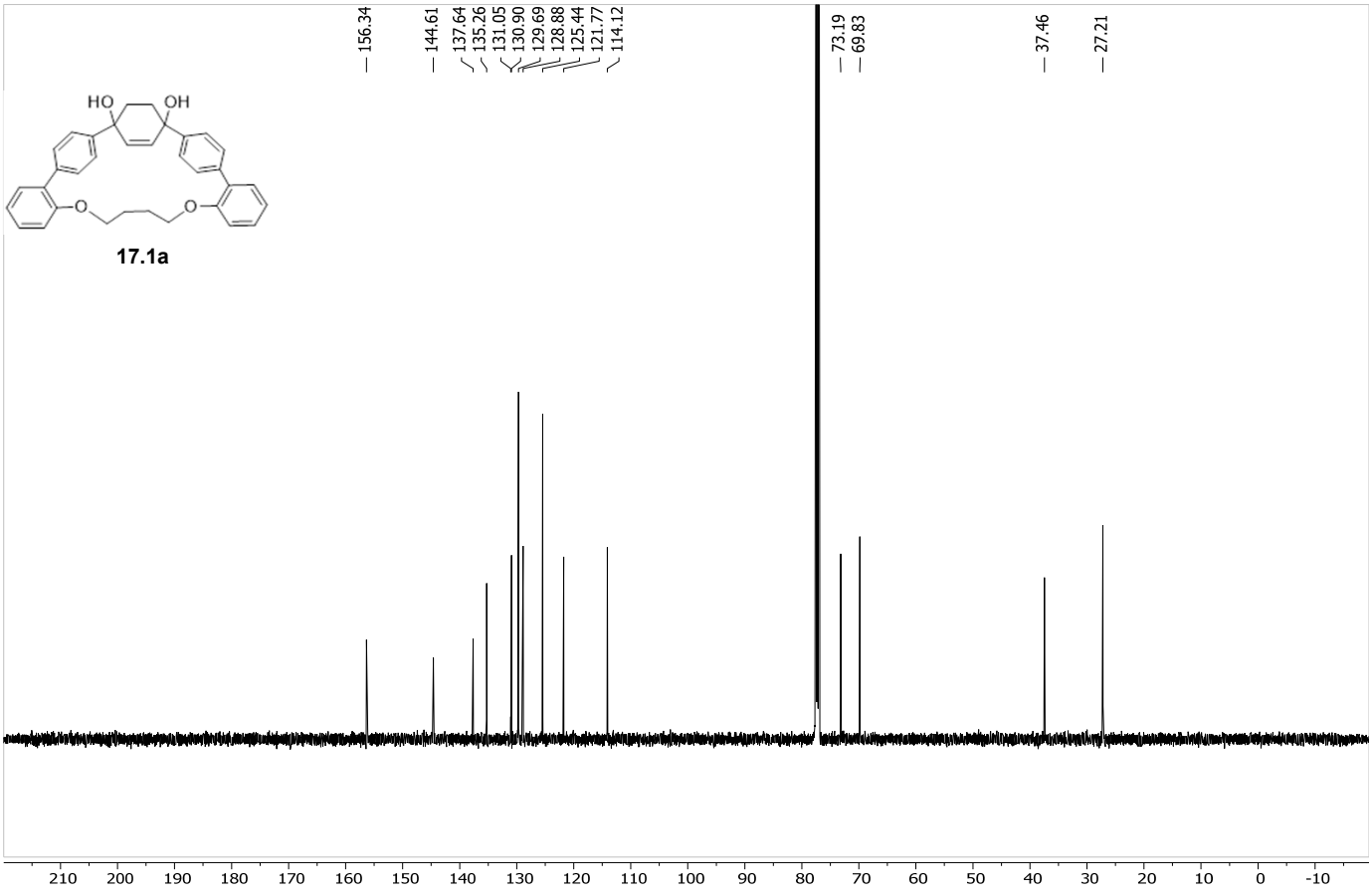
156.34
144.61
137.64
135.26
131.05
130.90
129.69
128.88
125.44
121.77
114.12
73.19
69.83
37.46
27.21
HO
OH
O
O
17.1a
210
200
190
180
170
160
150
140
130
120
110
100
90
80
70
60
50
40
30
20
10
0
-10

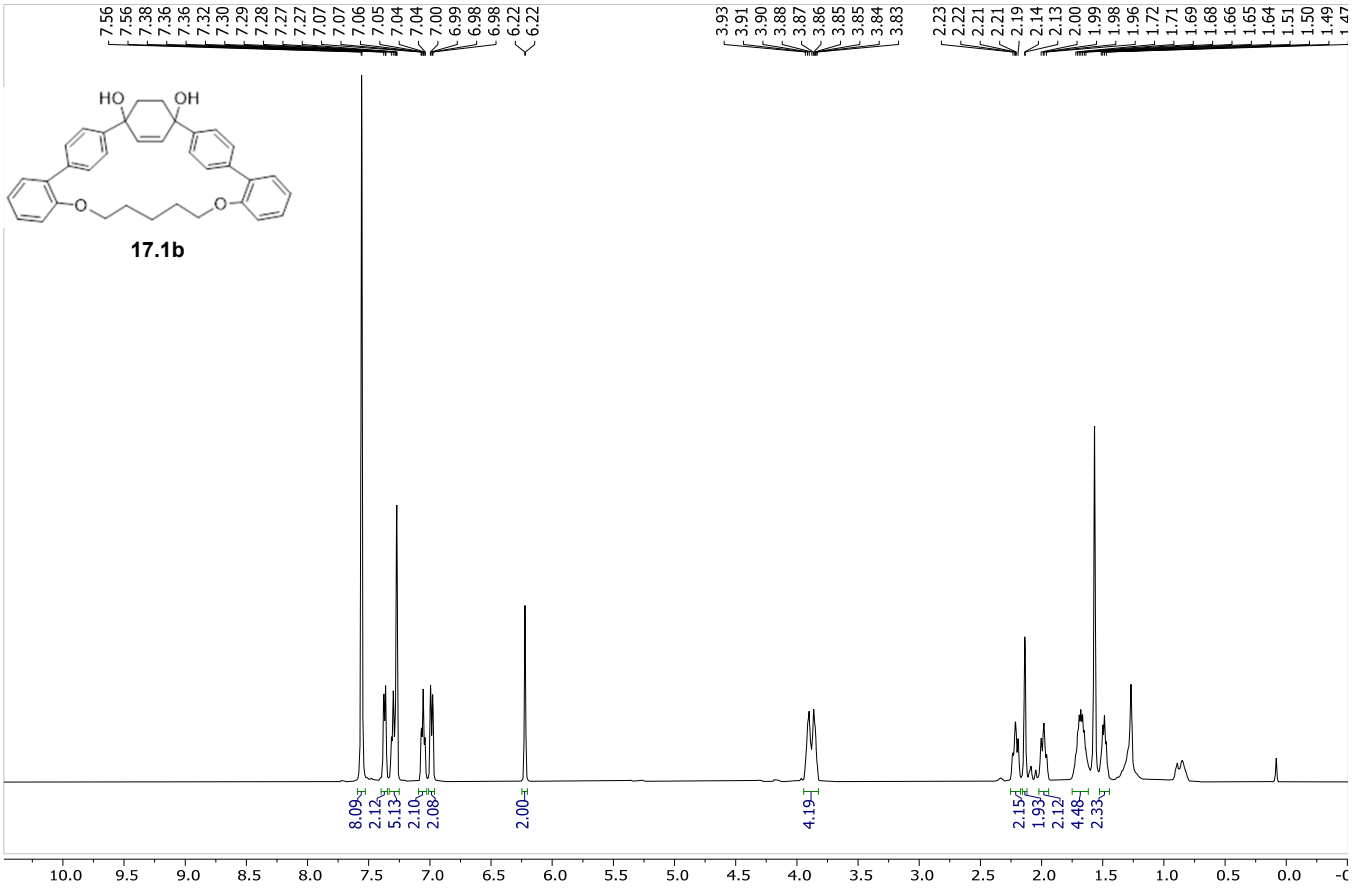
HO
OH
O
O
17.1b
7.56 7.56 7.38 7.36 7.36 7.32 7.30 7.29 7.28 7.27 7.27 7.07 7.07 7.06 7.05 7.04 7.04 7.00 6.99 6.98 6.98 6.22 6.22
3.93 3.91 3.90 3.88 3.87 3.86 3.85 3.85 3.84 3.83
2.23 2.22 2.21 2.21 2.19 2.14 2.13 2.00 1.99 1.98 1.96 1.72 1.71 1.69 1.68 1.66 1.65 1.64 1.51 1.50 1.49
8.09 2.12 5.13 2.10 2.08 2.00 4.19 2.15 1.93 2.12 4.48 2.33
10.0 9.5 9.0 8.5 8.0 7.5 7.0 6.5 6.0 5.5 5.0 4.5 4.0 3.5 3.0 2.5 2.0 1.5 1.0 0.5 0.0

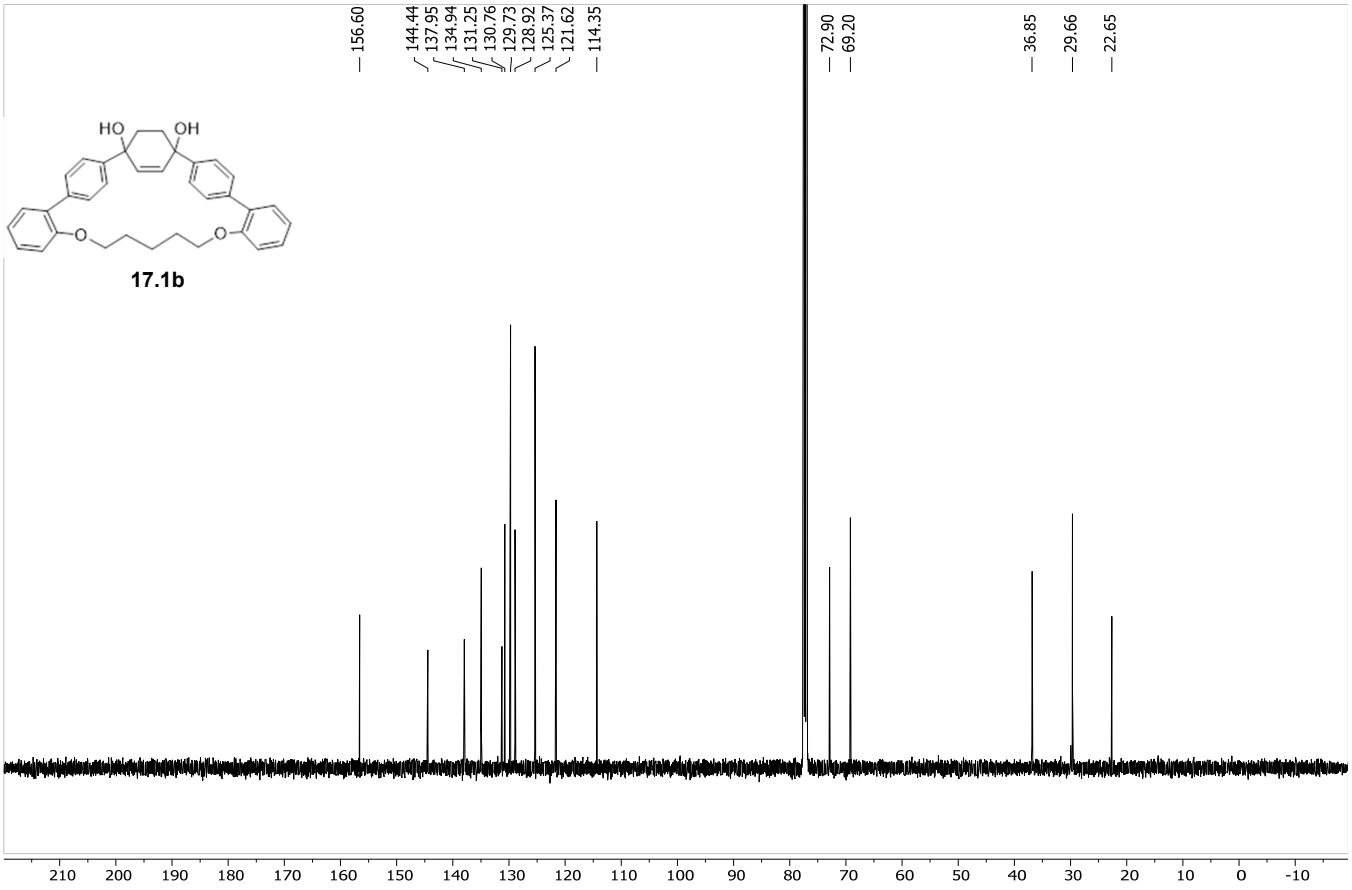
HO
OH
O
O
17.1b
156.60
144.44
137.95
134.94
131.25
130.76
129.73
128.92
125.37
121.62
114.35
72.90
69.20
36.85
29.66
22.65
210 200 190 180 170 160 150 140 130 120 110 100 90 80 70 60 50 40 30 20 10 0 -10

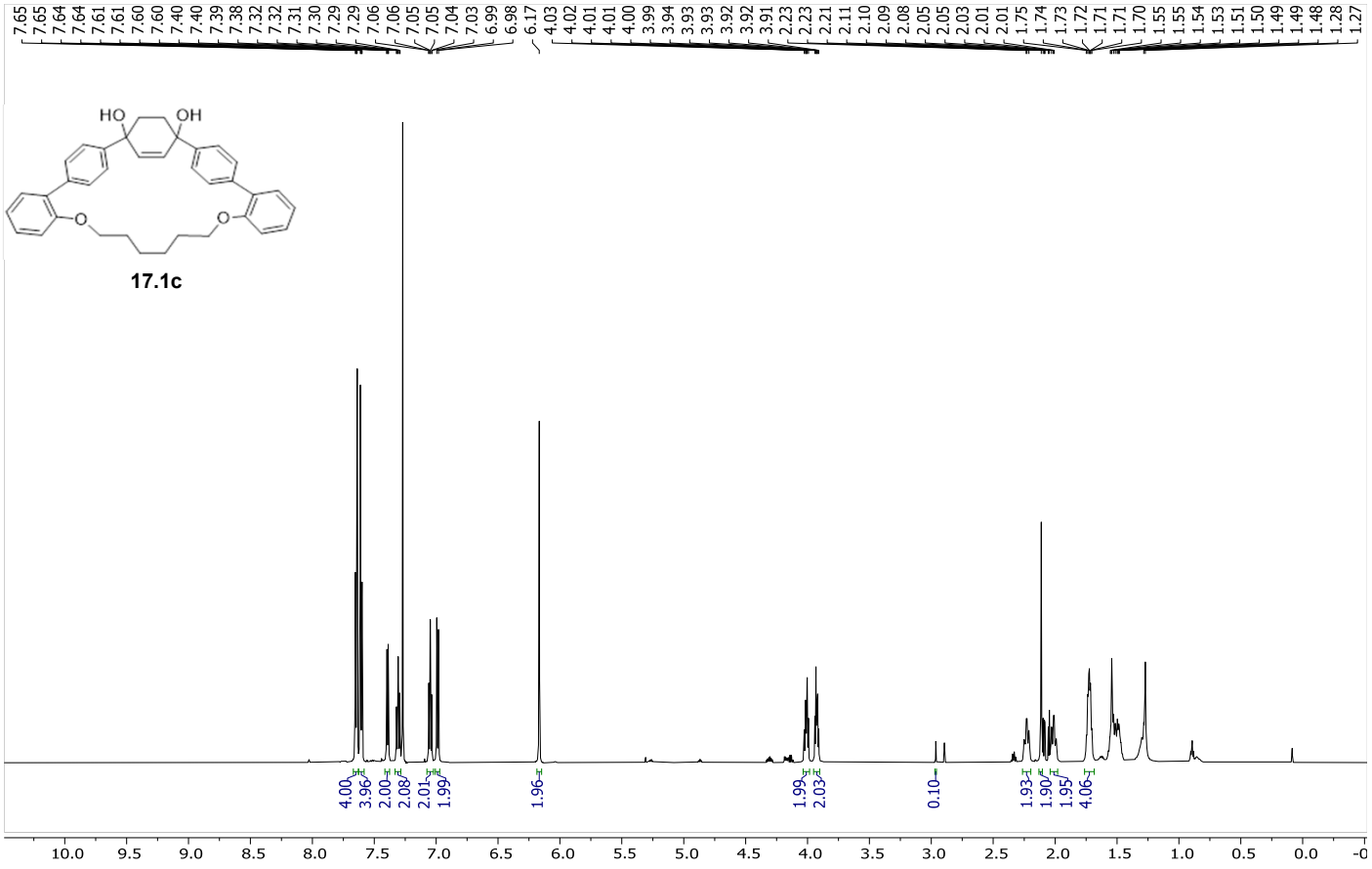
HO
OH
O
O
17.1c

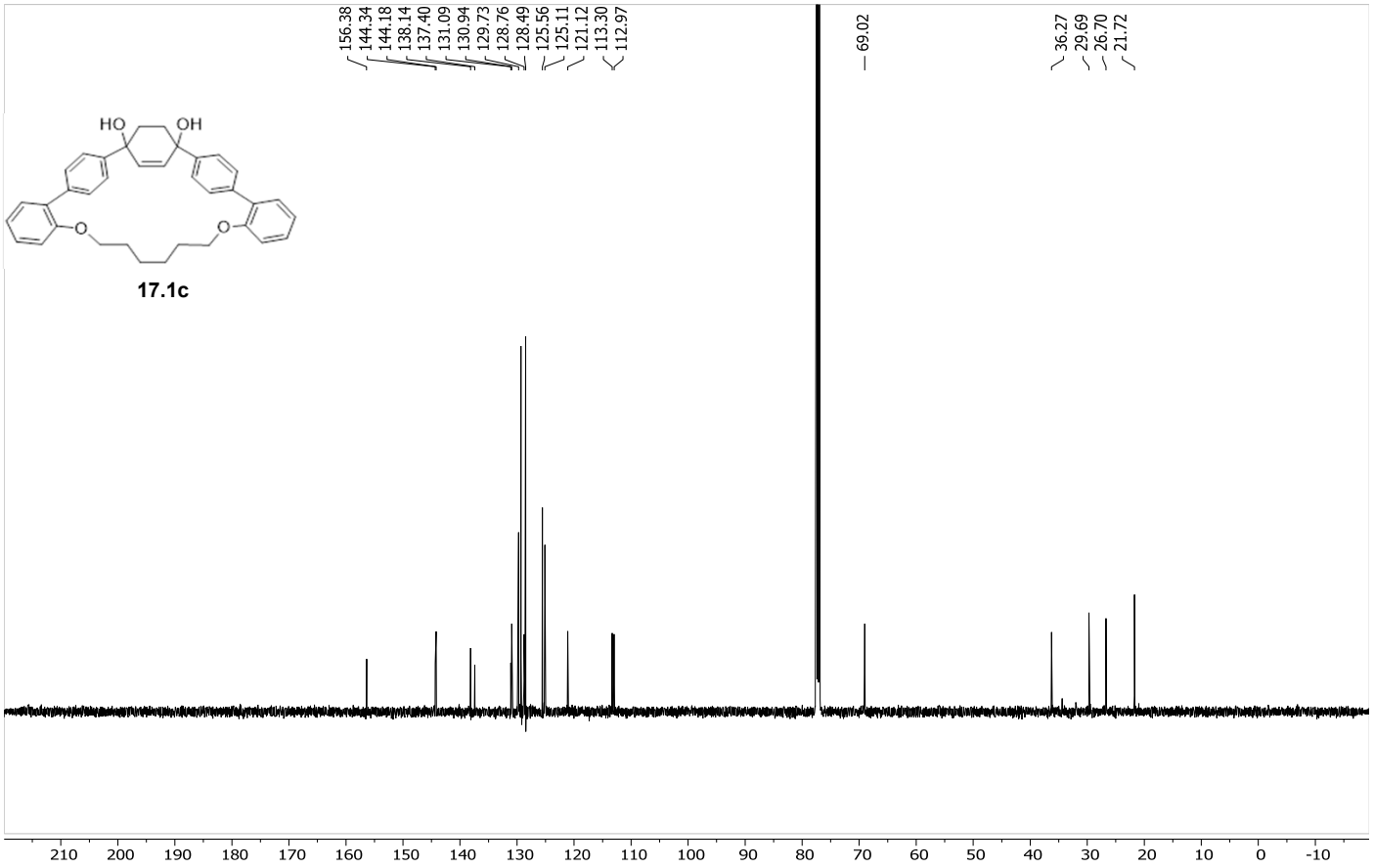
HO
OH
O
O
17.1c

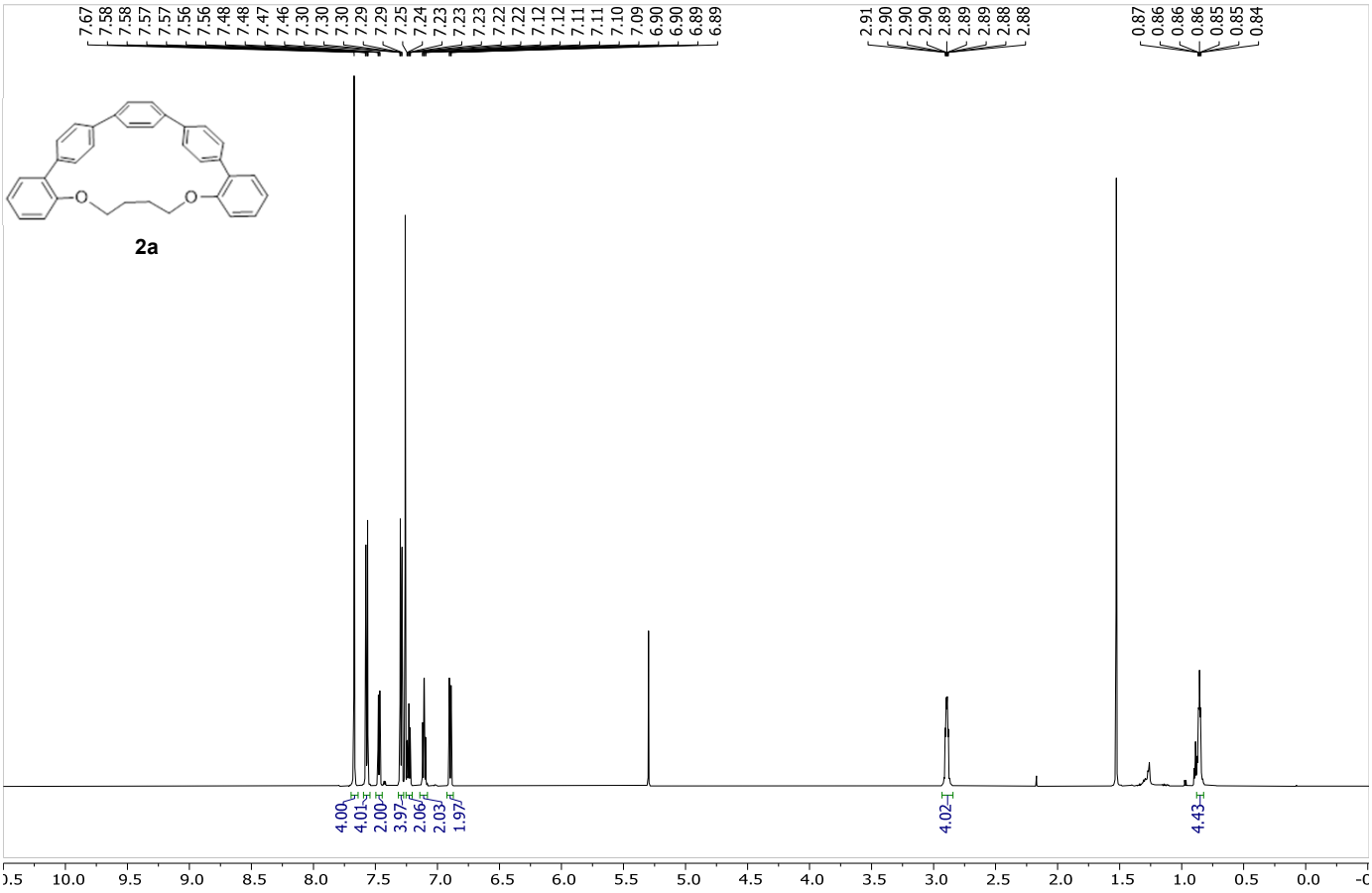
7.67
7.58
7.58
7.57
7.57
7.56
7.56
7.48
7.47
7.46
7.30
7.30
7.29
7.29
7.25
7.24
7.23
7.23
7.23
7.22
7.22
7.12
7.12
7.11
7.11
7.10
7.09
6.90
6.90
6.89
6.89
2.91
2.90
2.90
2.90
2.89
2.89
2.89
2.88
2.88
0.87
0.86
0.86
0.86
0.86
0.85
0.85
0.84
2a
4.00
4.01
2.00
3.97
2.06
2.03
1.97
4.02
4.43
10.5
10.0
9.5
9.0
8.5
8.0
7.5
7.0
6.5
6.0
5.5
5.0
4.5
4.0
3.5
3.0
2.5
2.0
1.5
1.0
0.5
0.0

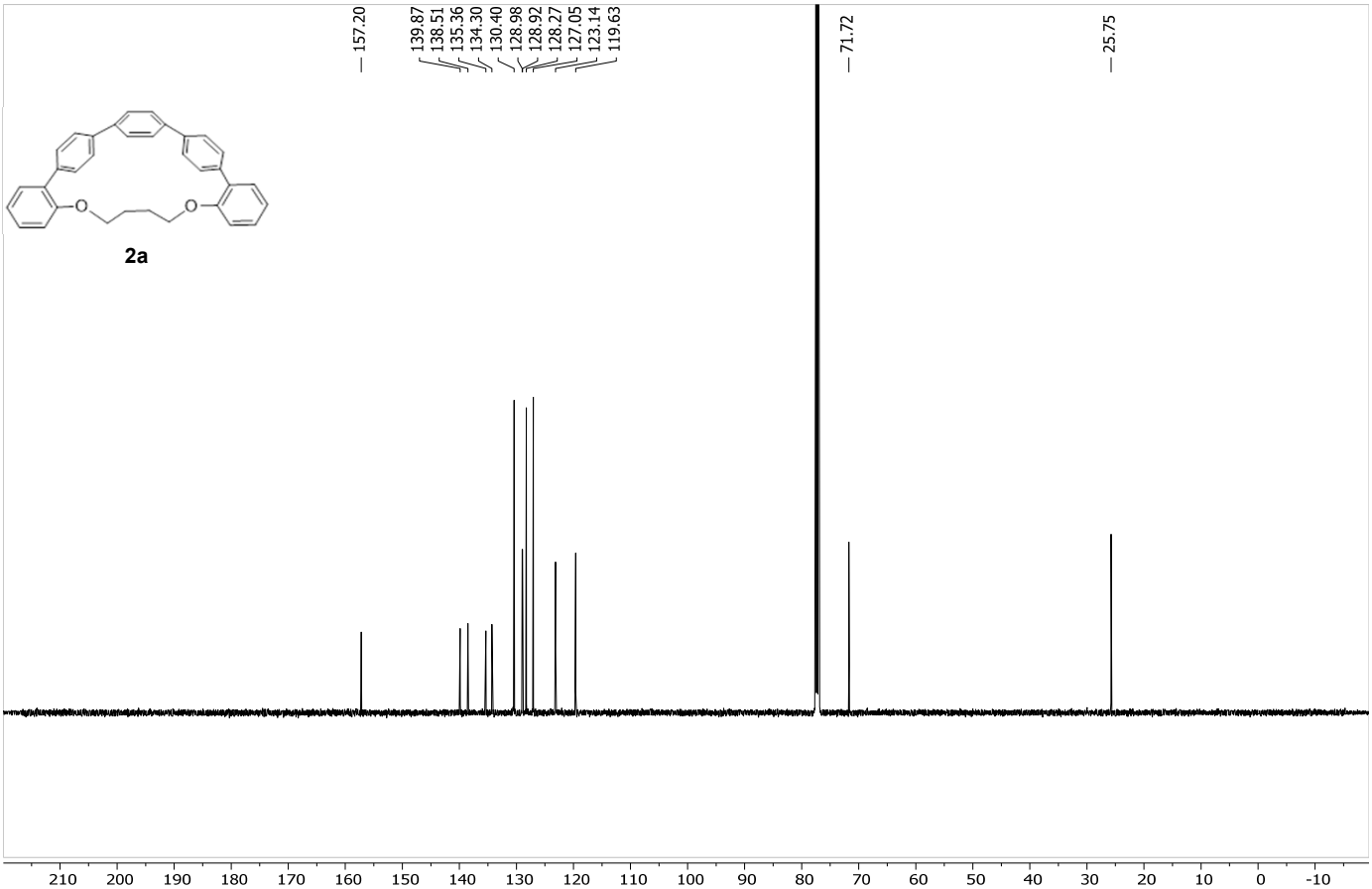
157.20
139.87
138.51
135.36
134.30
130.40
128.98
128.92
128.27
127.05
123.14
119.63
71.72
25.75
2a
210
200
190
180
170
160
150
140
130
120
110
100
90
80
70
60
50
40
30
20
10
0
-10

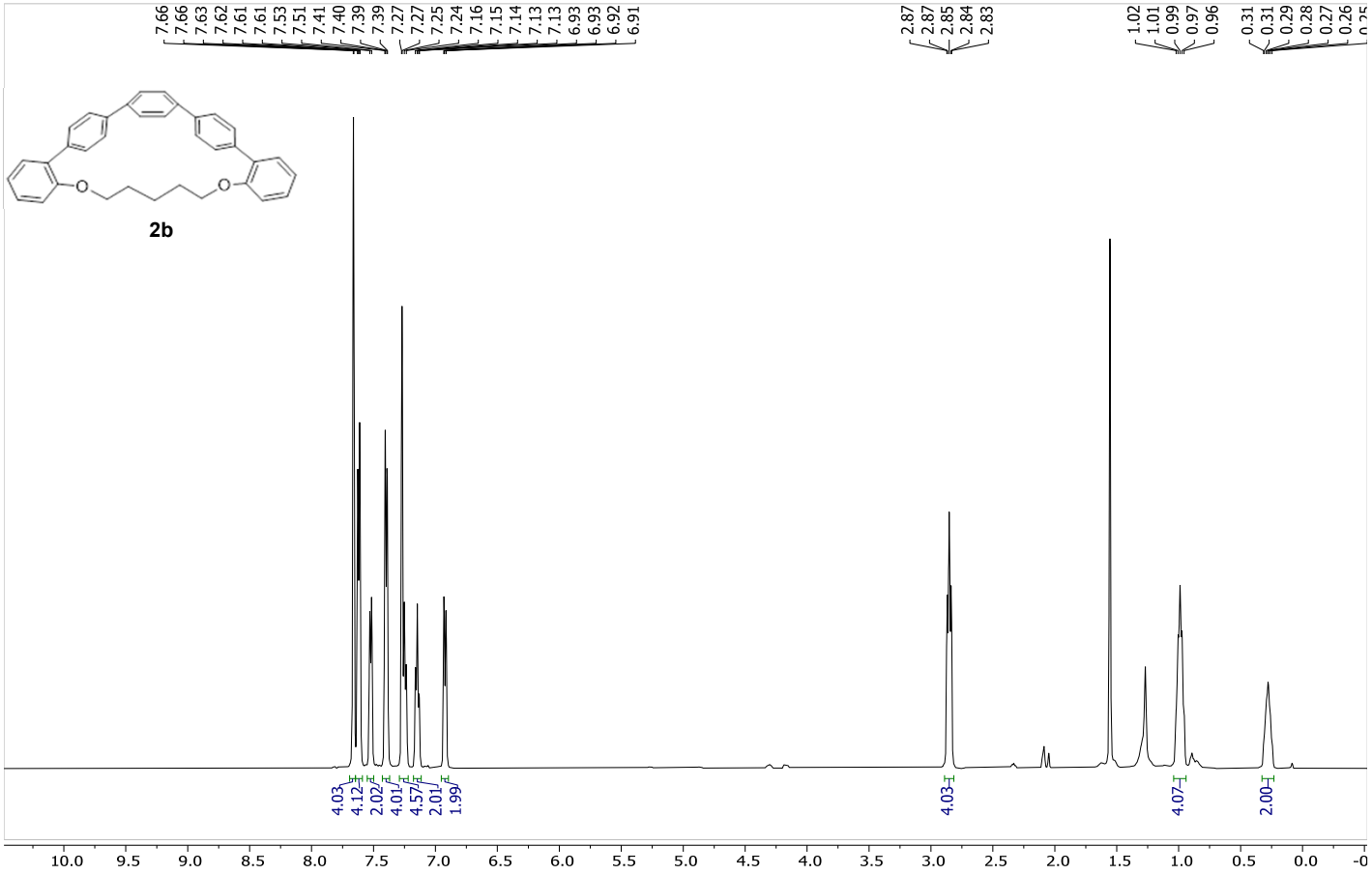
7.66
7.66
7.63
7.62
7.61
7.61
7.53
7.51
7.41
7.40
7.39
7.39
7.27
7.25
7.24
7.16
7.15
7.14
7.13
7.13
6.93
6.93
6.92
6.91
2.87
2.87
2.85
2.84
2.83
1.02
1.01
0.99
0.97
0.96
0.31
0.31
0.29
0.28
0.27
0.26
4.03
4.12
2.02
4.01
4.57
2.01
1.99
4.03
4.07
2.00
10.0
9.5
9.0
8.5
8.0
7.5
7.0
6.5
6.0
5.5
5.0
4.5
4.0
3.5
3.0
2.5
2.0
1.5
1.0
0.5
0.0

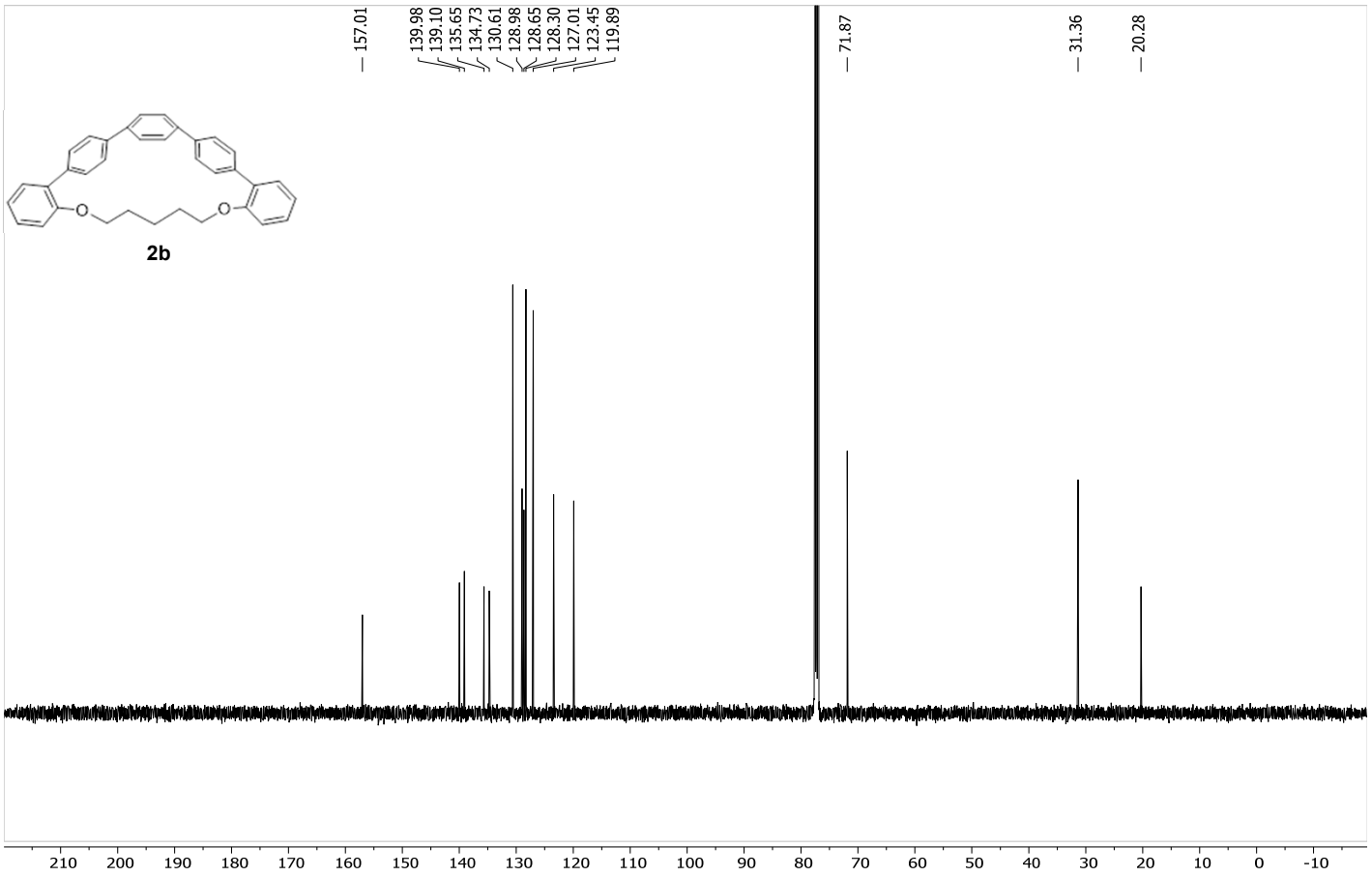
157.01
139.98
139.10
135.65
134.73
130.61
128.98
128.65
128.30
127.01
123.45
119.89
71.87
31.36
20.28
210
200
190
180
170
160
150
140
130
120
110
100
90
80
70
60
50
40
30
20
10
0
-10

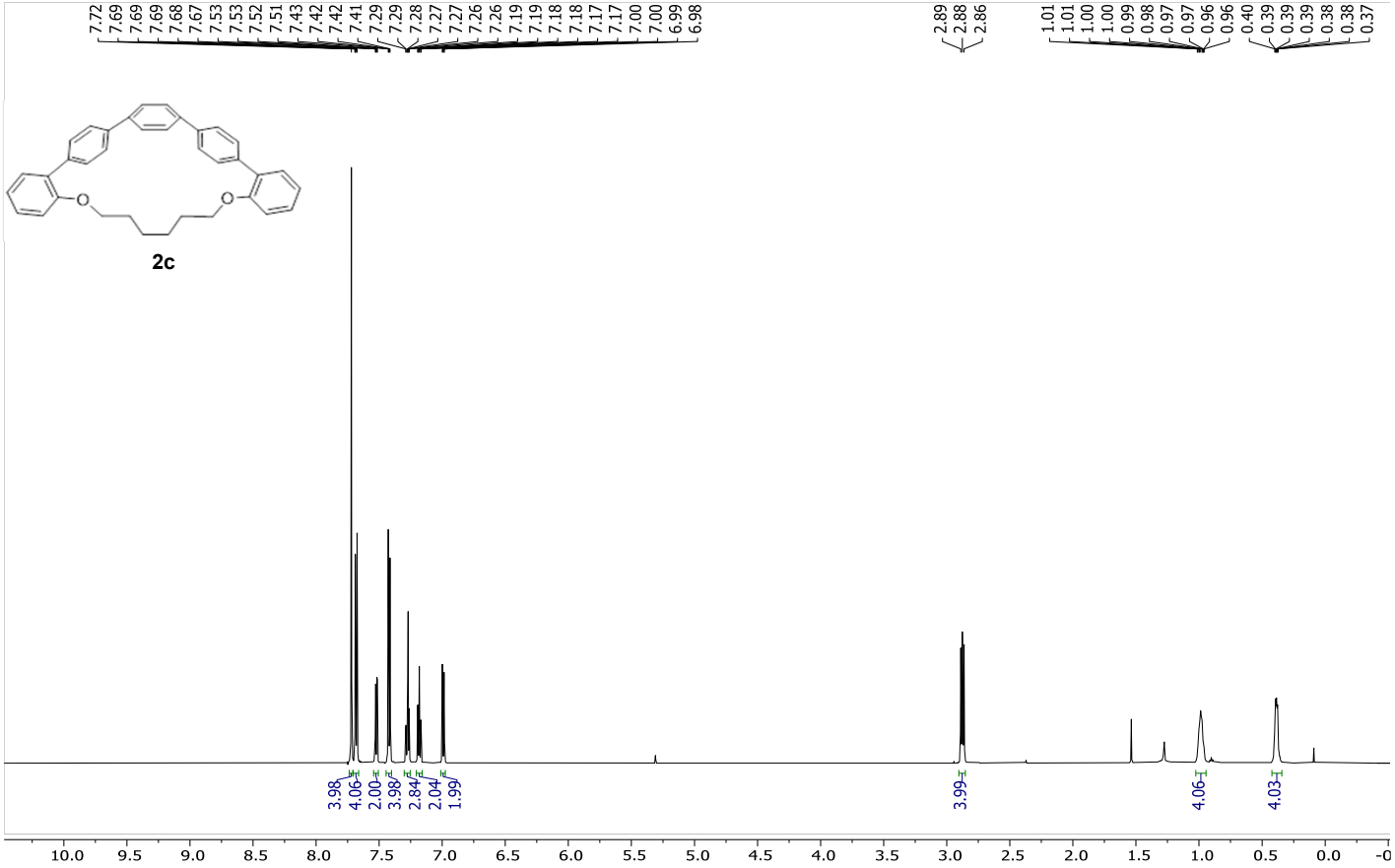
7.72 7.69 7.69 7.69 7.68 7.67 7.53 7.53 7.52 7.51 7.43 7.42 7.42 7.41 7.29 7.29 7.28 7.27 7.27 7.26 7.26 7.19 7.19 7.18 7.18 7.17 7.17 7.00 7.00 6.99 6.98
2.89 2.88 2.86
1.01 1.01 1.00 1.00 0.99 0.98 0.97 0.97 0.96 0.96 0.40 0.39 0.39 0.39 0.38 0.38 0.37
2c
3.98 4.06 2.00 3.98 2.84 2.04 1.99
3.99
4.06
4.03
10.0 9.5 9.0 8.5 8.0 7.5 7.0 6.5 6.0 5.5 5.0 4.5 4.0 3.5 3.0 2.5 2.0 1.5 1.0 0.5 0.0

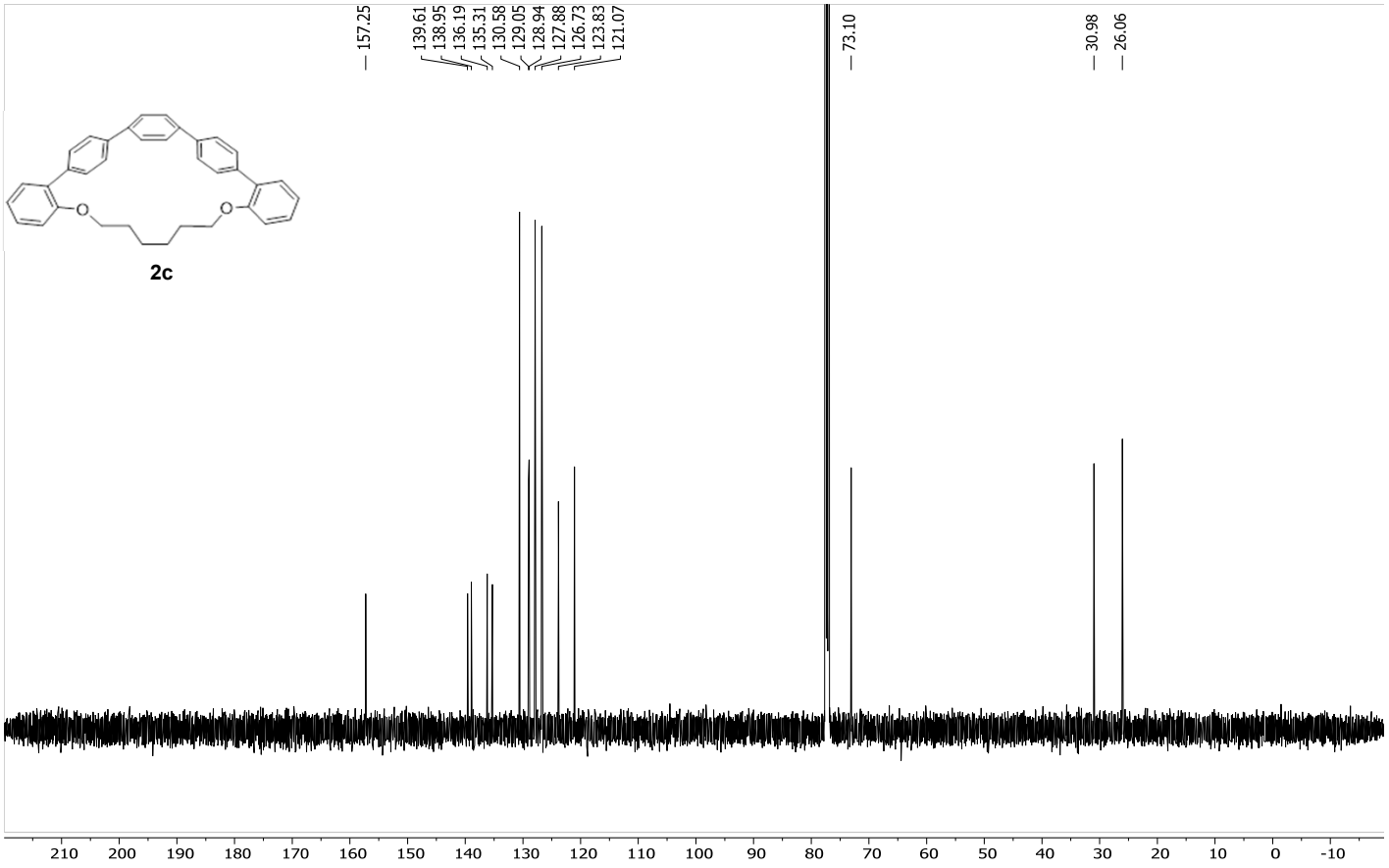
157.25
139.61 138.95 136.19 135.31 130.58 129.05 128.94 127.88 126.73 123.83 121.07
73.10
30.98 26.06
2c
210 200 190 180 170 160 150 140 130 120 110 100 90 80 70 60 50 40 30 20 10 0 -10

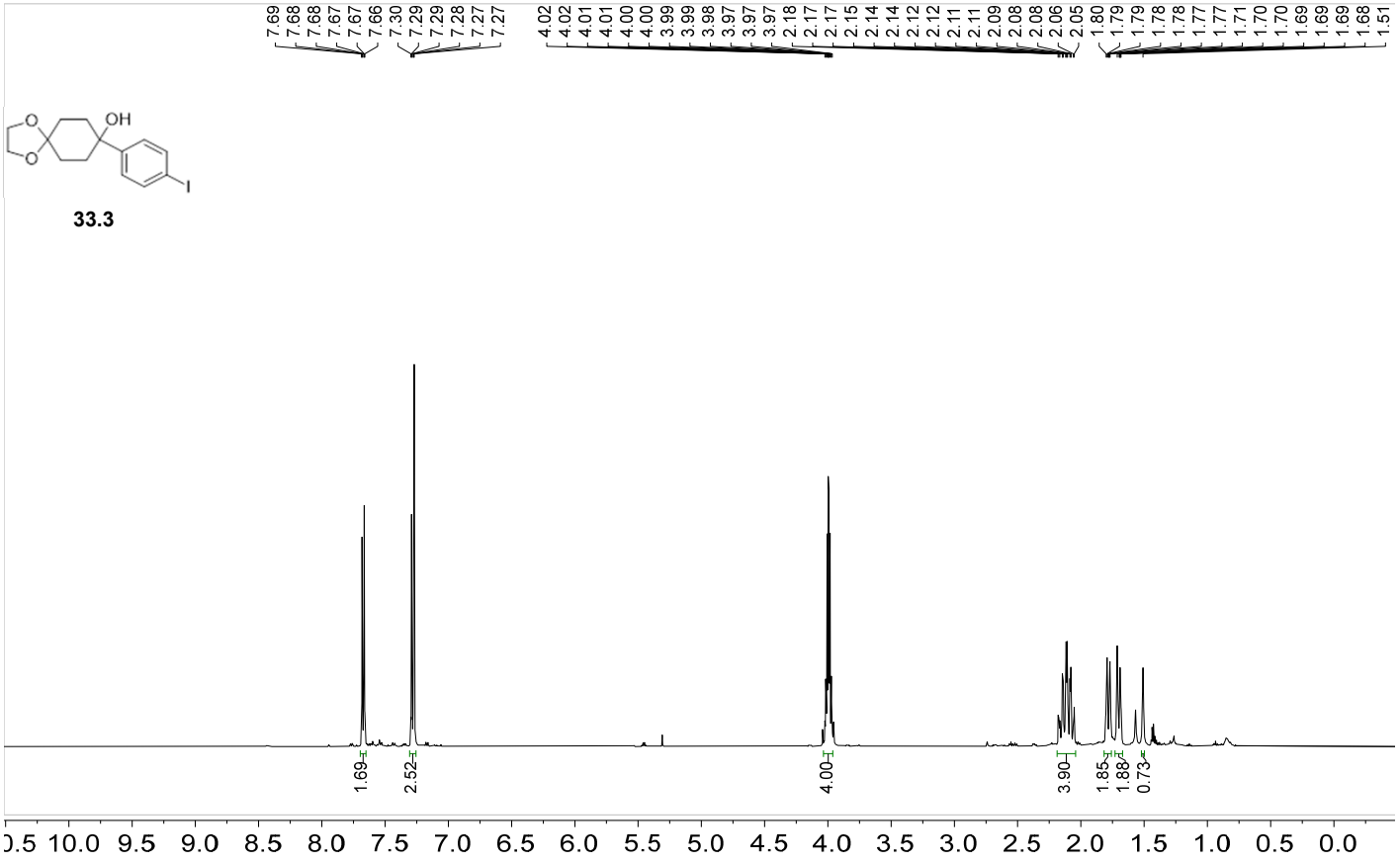
7.69 7.68 7.68 7.67 7.67 7.66 7.30 7.29 7.29 7.28 7.27 7.27
4.02 4.02 4.01 4.01 4.00 4.00 3.99 3.99 3.98 3.97 3.97 3.97 2.18 2.17 2.17 2.15 2.14 2.14 2.12 2.12 2.11 2.11 2.09 2.08 2.08 2.06 2.05 1.80 1.79 1.79 1.78 1.78 1.77 1.77 1.71 1.70 1.70 1.69 1.69 1.69 1.68 1.51
OH
I
1.69
2.52
4.00
3.90
1.85
1.88
0.73
0.5 10.0 9.5 9.0 8.5 8.0 7.5 7.0 6.5 6.0 5.5 5.0 4.5 4.0 3.5 3.0 2.5 2.0 1.5 1.0 0.5 0.0

33.3

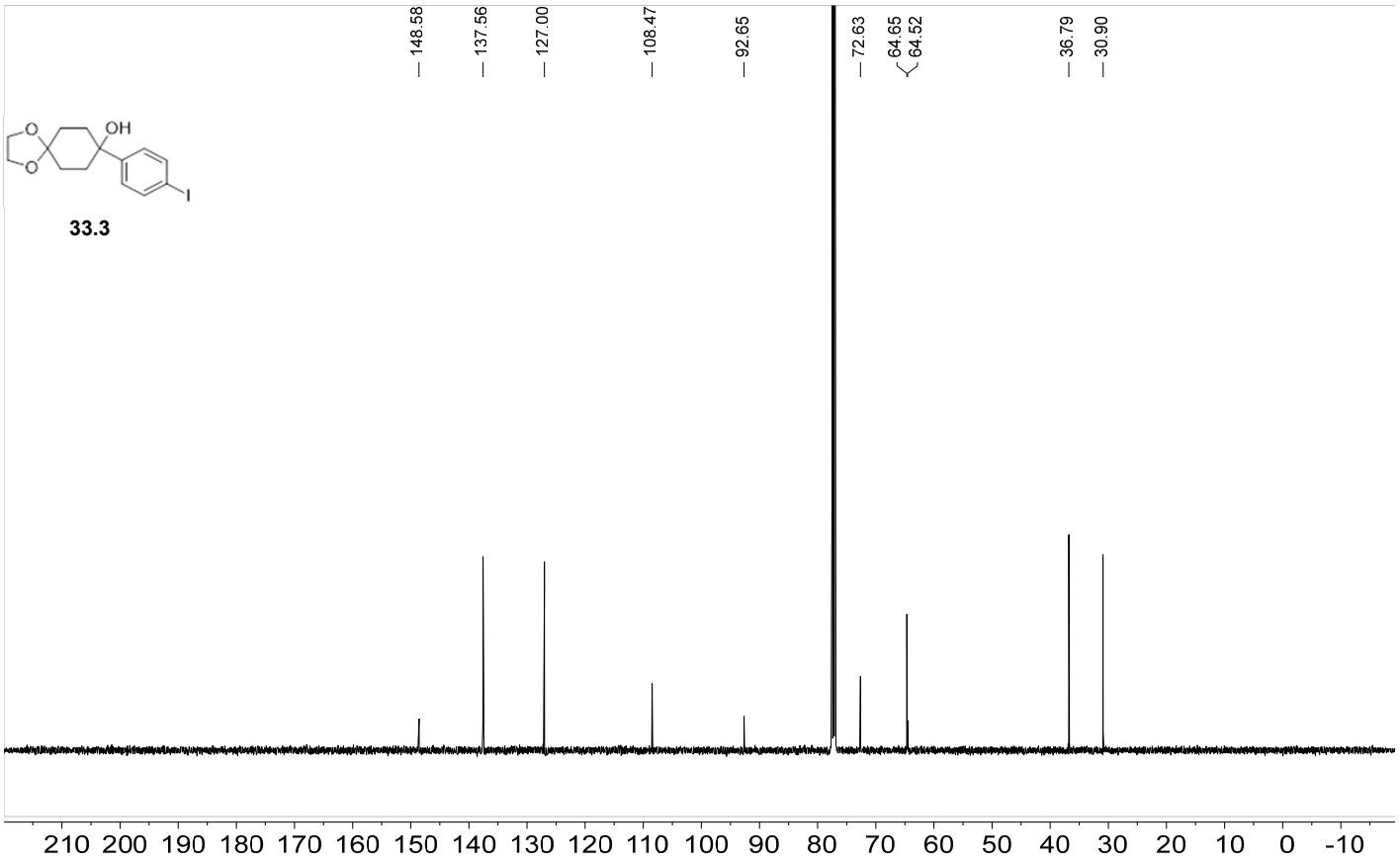
148.58
137.56
127.00
108.47
92.65
72.63
64.65
64.52
36.79
30.90
OH
I
210 200 190 180 170 160 150 140 130 120 110 100 90 80 70 60 50 40 30 20 10 0 -10

33.3

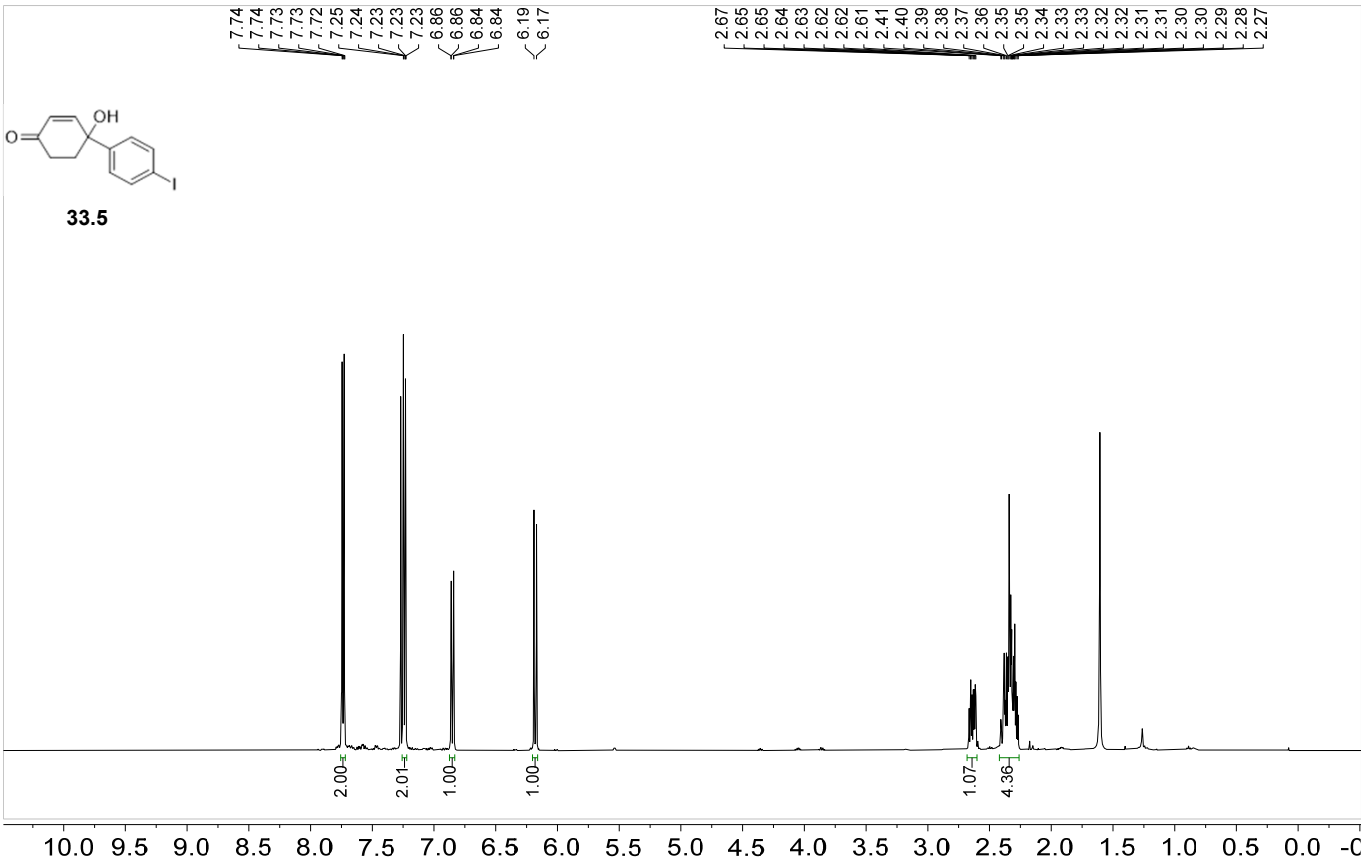
7.74
7.74
7.73
7.73
7.72
7.25
7.24
7.23
7.23
7.23
6.86
6.86
6.84
6.84
6.19
6.17
2.67
2.65
2.65
2.64
2.63
2.62
2.62
2.61
2.41
2.40
2.39
2.38
2.37
2.36
2.35
2.35
2.34
2.33
2.33
2.32
2.32
2.31
2.31
2.30
2.30
2.29
2.28
2.27
OH
O
I
33.5
2.00
2.01
1.00
1.00
1.07
4.36
10.0 9.5 9.0 8.5 8.0 7.5 7.0 6.5 6.0 5.5 5.0 4.5 4.0 3.5 3.0 2.5 2.0 1.5 1.0 0.5 0.0

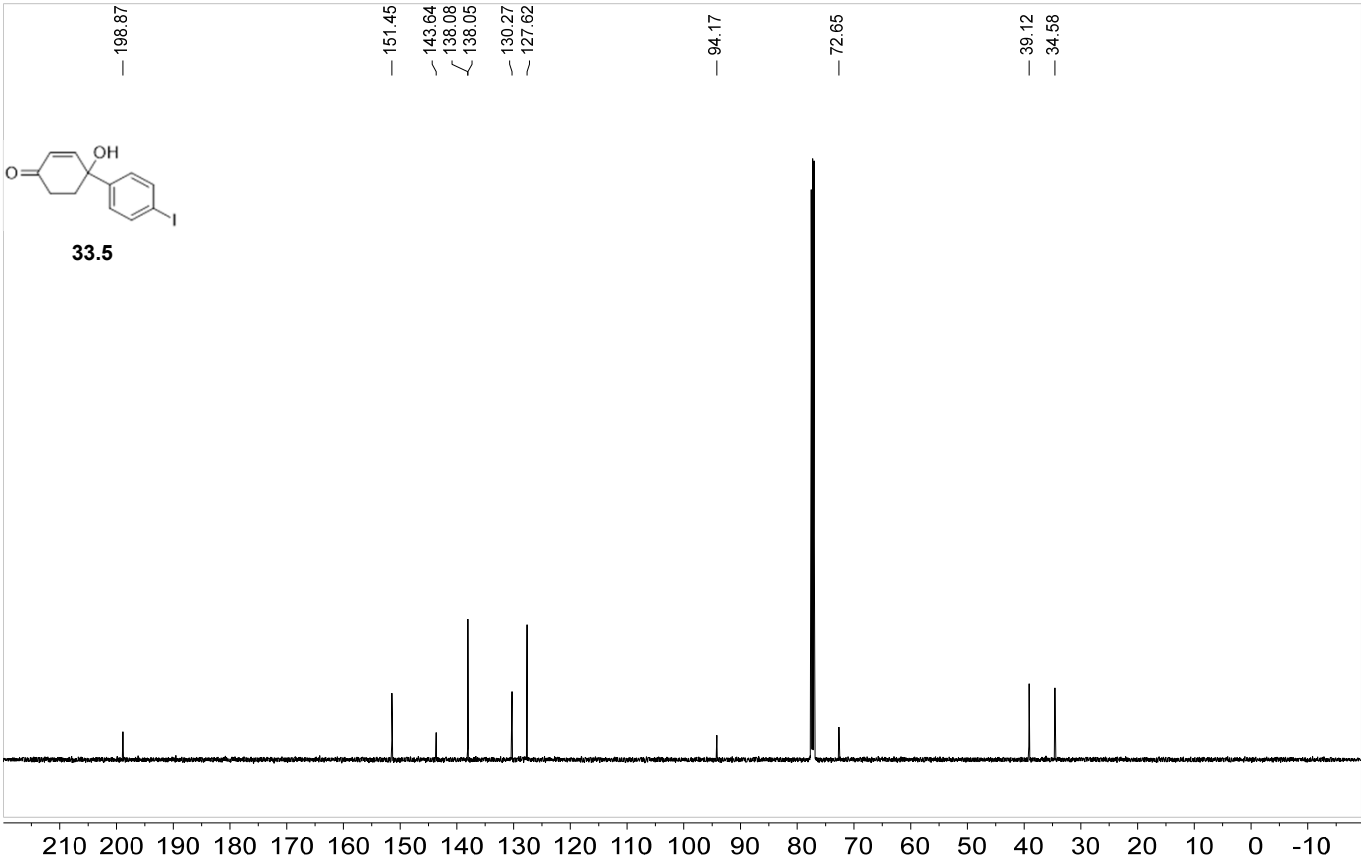
198.87
151.45
143.64
138.08
138.05
130.27
127.62
94.17
72.65
39.12
34.58
OH
O
I
33.5
210 200 190 180 170 160 150 140 130 120 110 100 90 80 70 60 50 40 30 20 10 0 -10

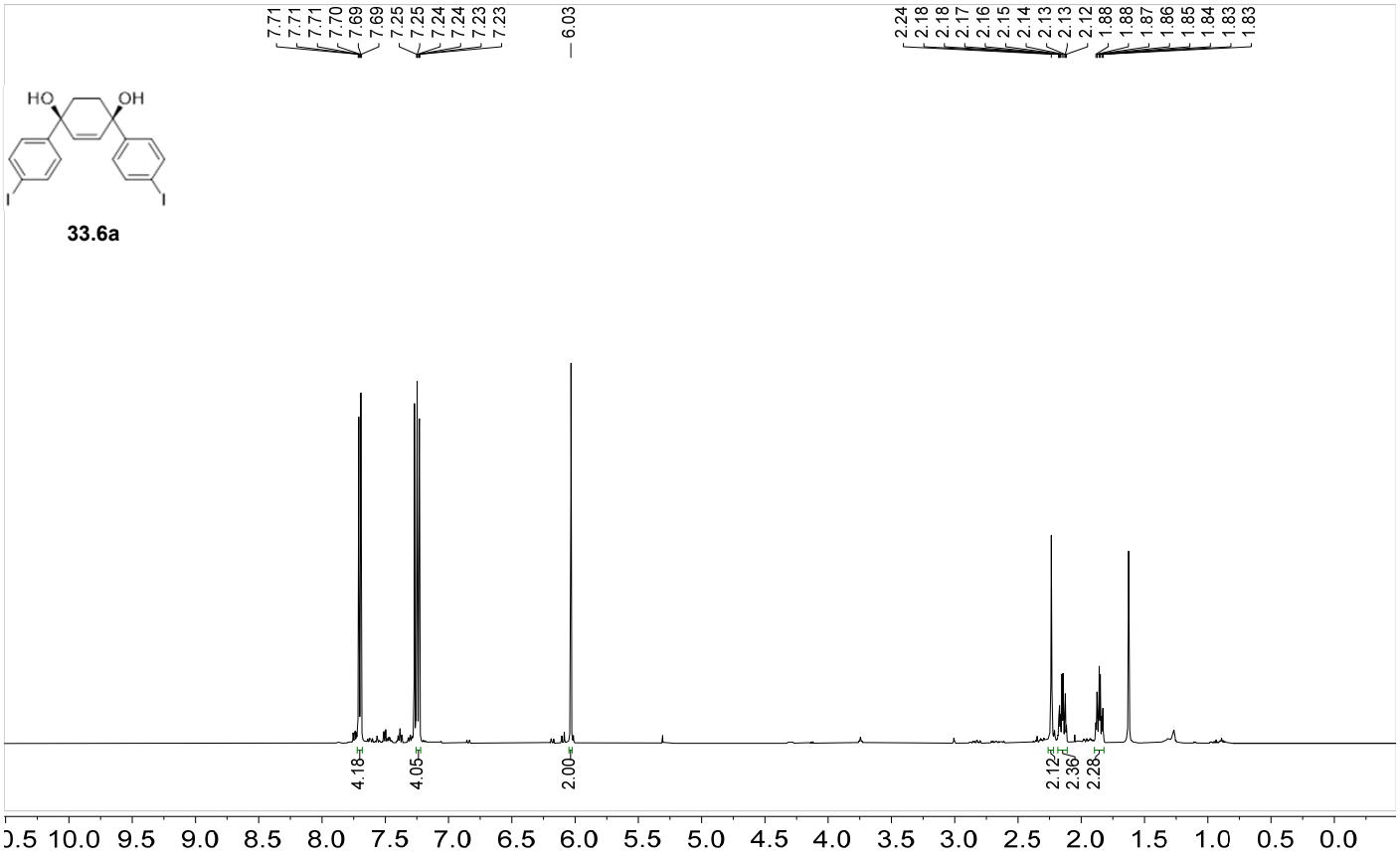
7.71
7.71
7.71
7.70
7.69
7.69
7.25
7.24
7.24
7.23
7.23
6.03
2.24
2.18
2.18
2.17
2.16
2.15
2.14
2.13
2.13
2.12
1.88
1.88
1.87
1.86
1.85
1.84
1.83
1.83
HO
OH
I
I
4.18
4.05
2.00
2.12
2.36
2.28
0.5 10.0 9.5 9.0 8.5 8.0 7.5 7.0 6.5 6.0 5.5 5.0 4.5 4.0 3.5 3.0 2.5 2.0 1.5 1.0 0.5 0.0

33.6a

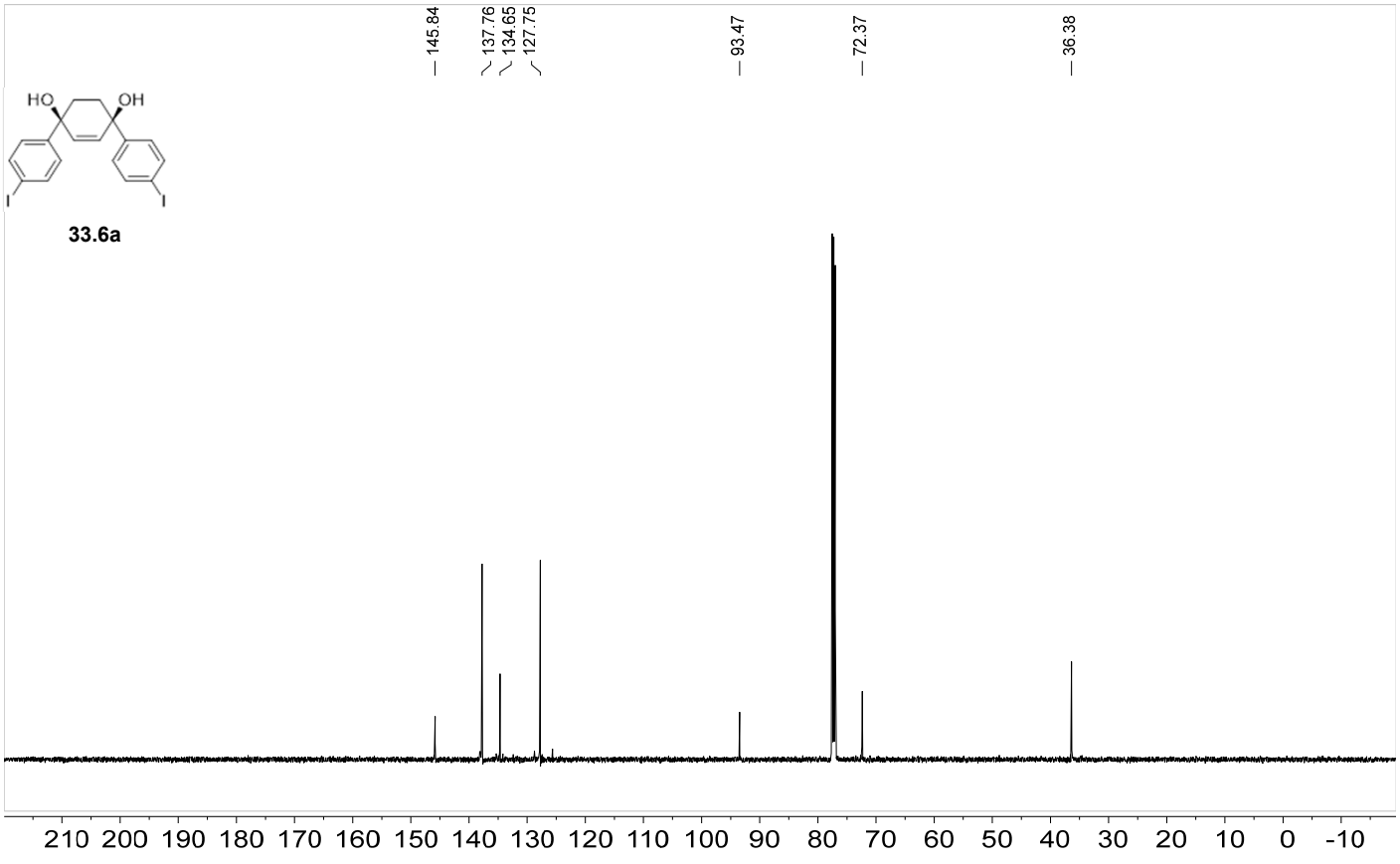
145.84
137.76
134.65
127.75
93.47
72.37
36.38
HO
OH
I
I
210 200 190 180 170 160 150 140 130 120 110 100 90 80 70 60 50 40 30 20 10 0 -10

33.6a

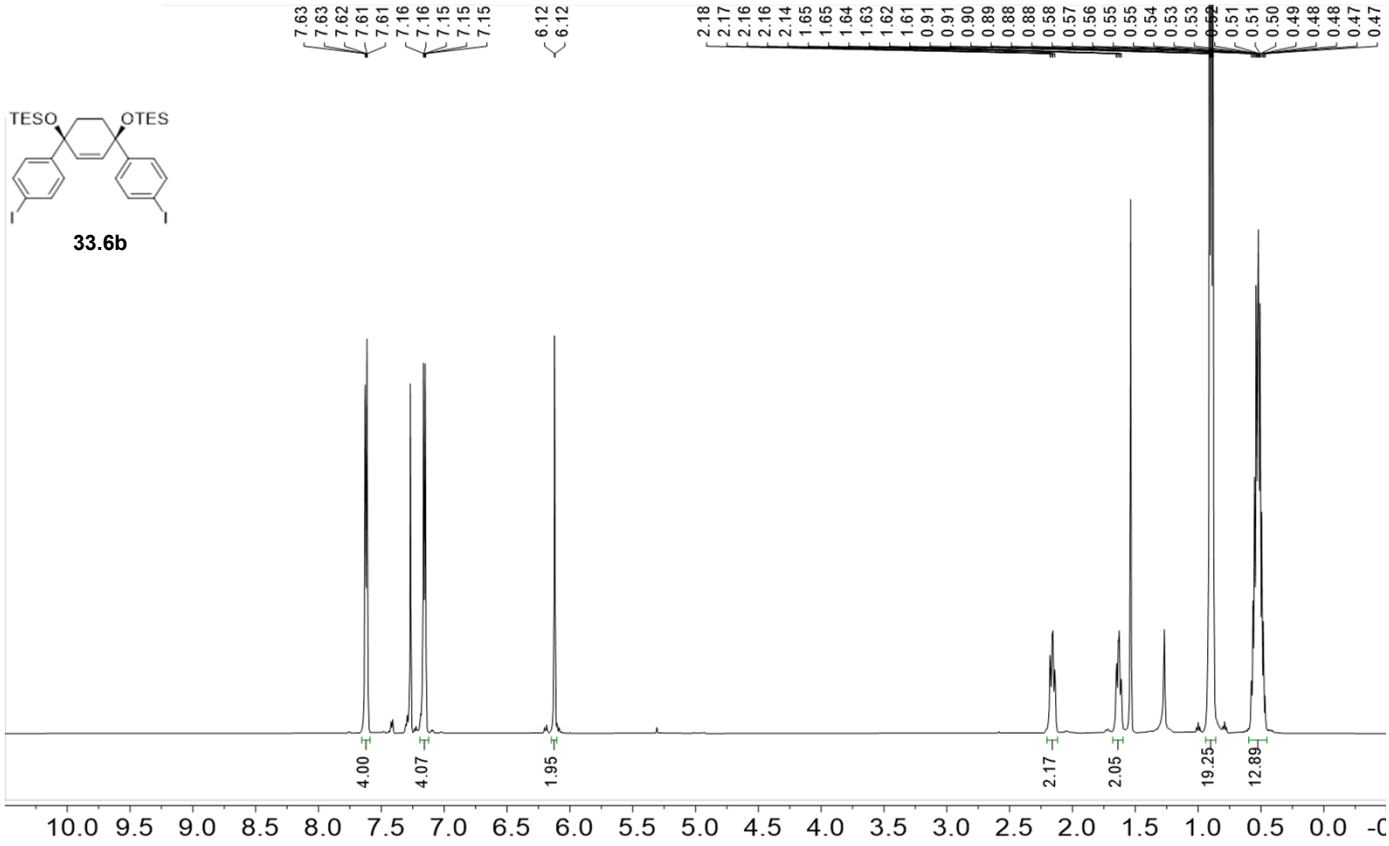
TESO
OTES
I
I
33.6b
7.63 7.63 7.62 7.61 7.61 7.16 7.16 7.15 7.15 7.15 6.12 6.12
2.18 2.17 2.16 2.16 2.14 1.65 1.65 1.64 1.63 1.62 1.61 0.91 0.91 0.90 0.89 0.88 0.88 0.58 0.57 0.56 0.55 0.55 0.54 0.53 0.53 0.52 0.51 0.51 0.50 0.49 0.48 0.48 0.47 0.47
4.00 4.07 1.95 2.17 2.05 19.25 12.89
10.0 9.5 9.0 8.5 8.0 7.5 7.0 6.5 6.0 5.5 5.0 4.5 4.0 3.5 3.0 2.5 2.0 1.5 1.0 0.5 0.0

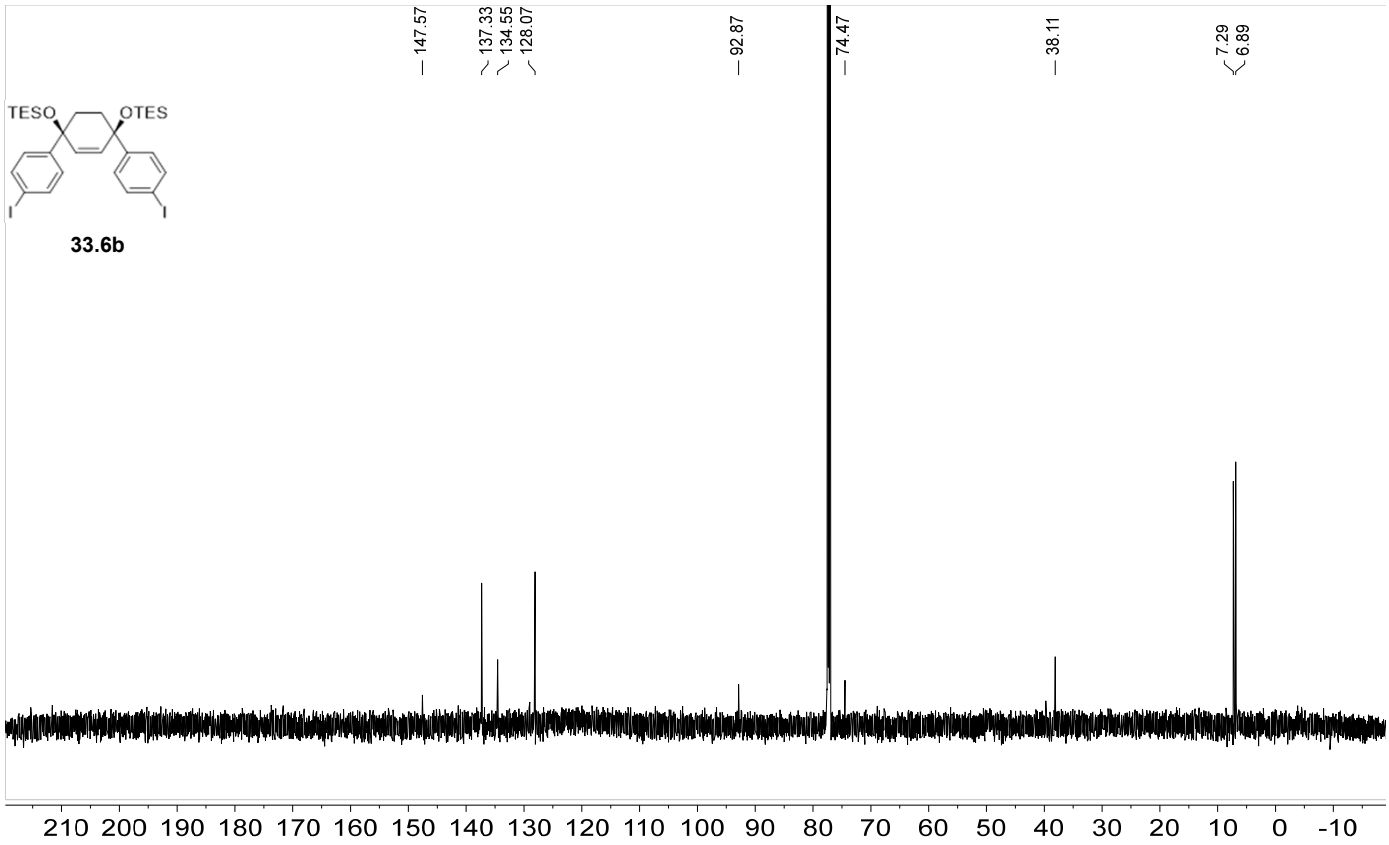
TESO
OTES
I
I
33.6b
147.57
137.33
134.55
128.07
92.87
74.47
38.11
7.29
6.89
210 200 190 180 170 160 150 140 130 120 110 100 90 80 70 60 50 40 30 20 10 0 -10

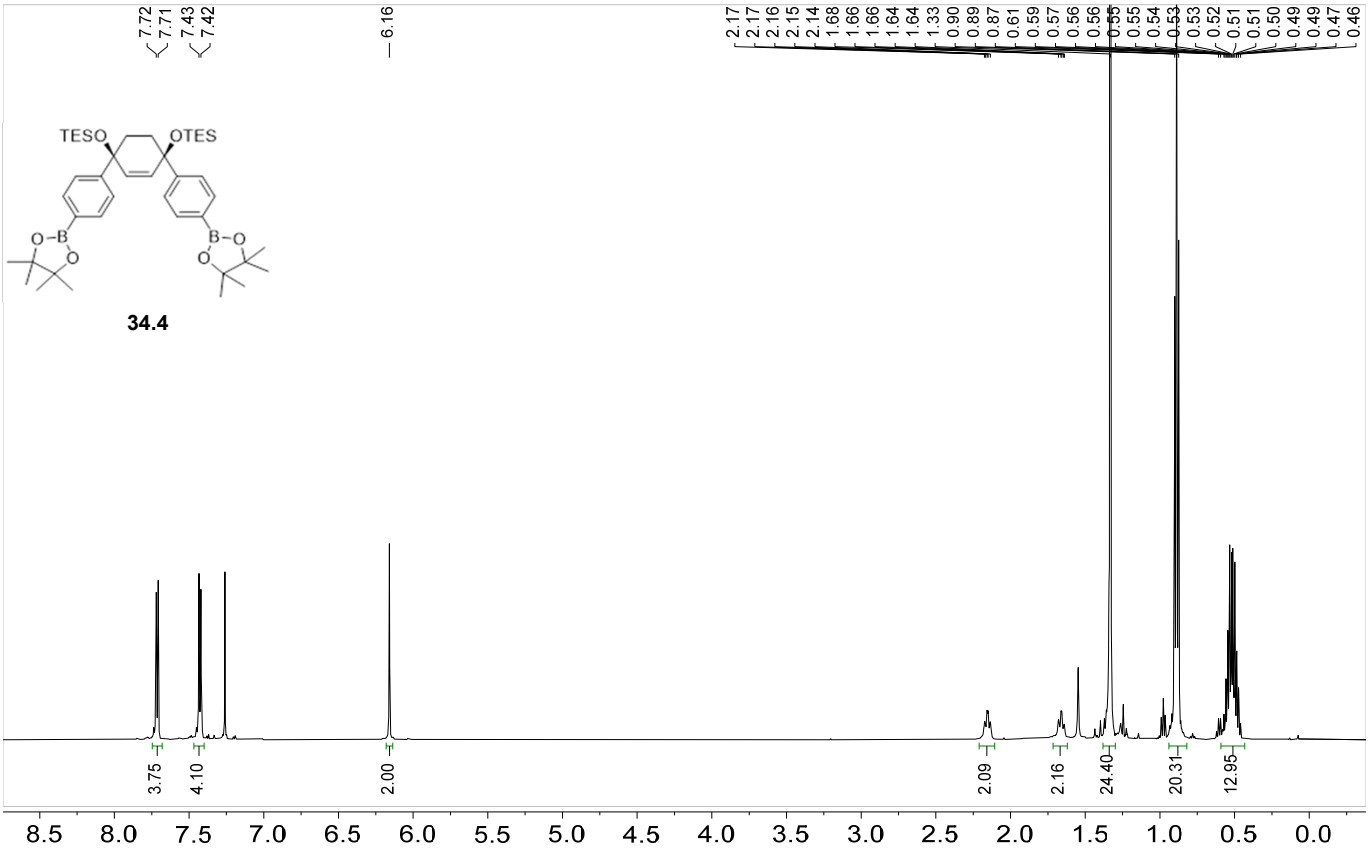
7.72
7.71
7.43
7.42
6.16
2.17
2.17
2.16
2.15
2.14
1.68
1.66
1.66
1.64
1.64
1.33
0.90
0.89
0.87
0.61
0.59
0.57
0.56
0.56
0.55
0.55
0.54
0.53
0.53
0.52
0.51
0.51
0.50
0.49
0.49
0.47
0.46
TESO
OTES
O–B
B–O
3.75
4.10
2.00
2.09
2.16
24.40
20.31
12.95
8.5
8.0
7.5
7.0
6.5
6.0
5.5
5.0
4.5
4.0
3.5
3.0
2.5
2.0
1.5
1.0
0.5
0.0

34.4

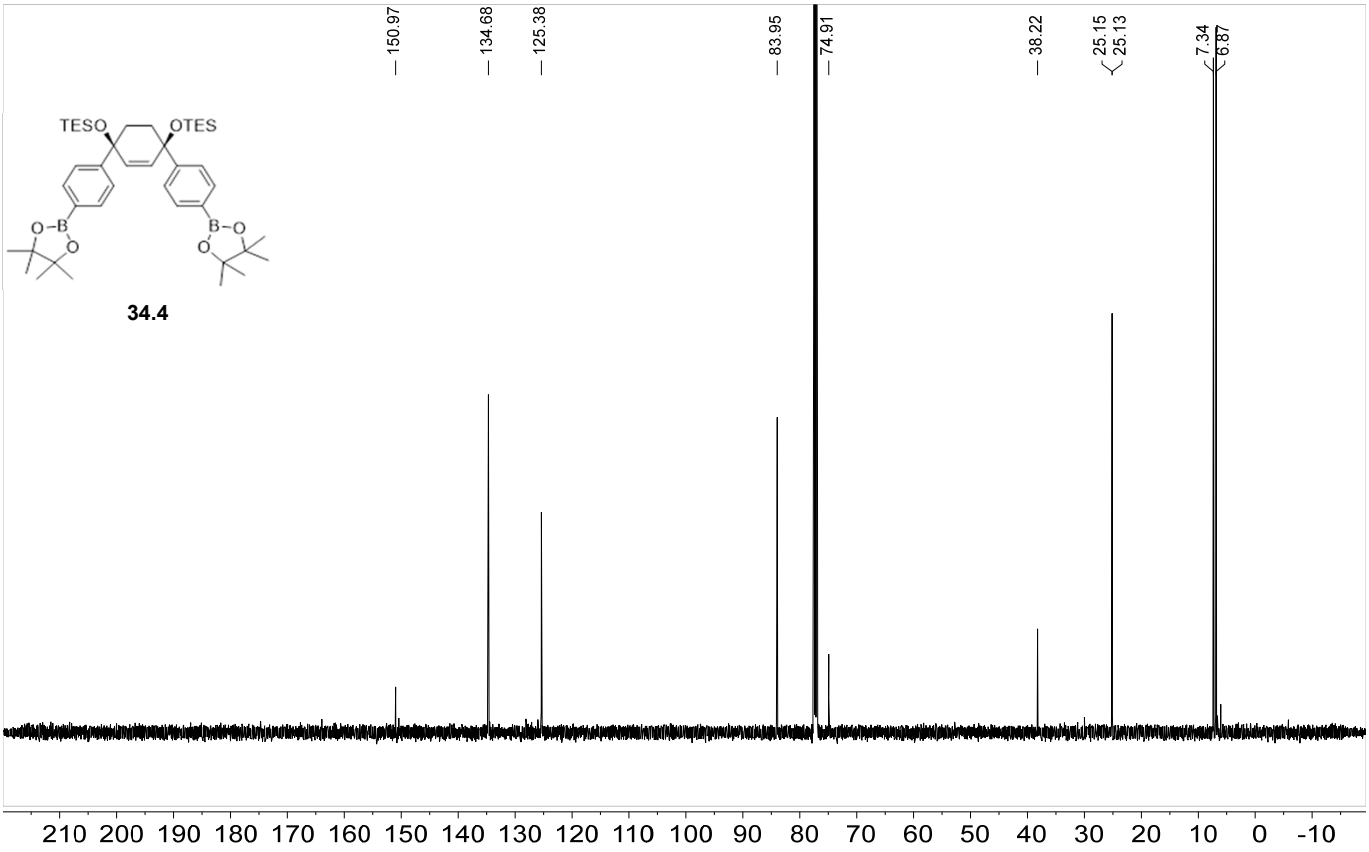
150.97
134.68
125.38
83.95
74.91
38.22
25.15
25.13
7.34
6.87
TESO
OTES
O–B
B–O
210
200
190
180
170
160
150
140
130
120
110
100
90
80
70
60
50
40
30
20
10
0
-10

34.4

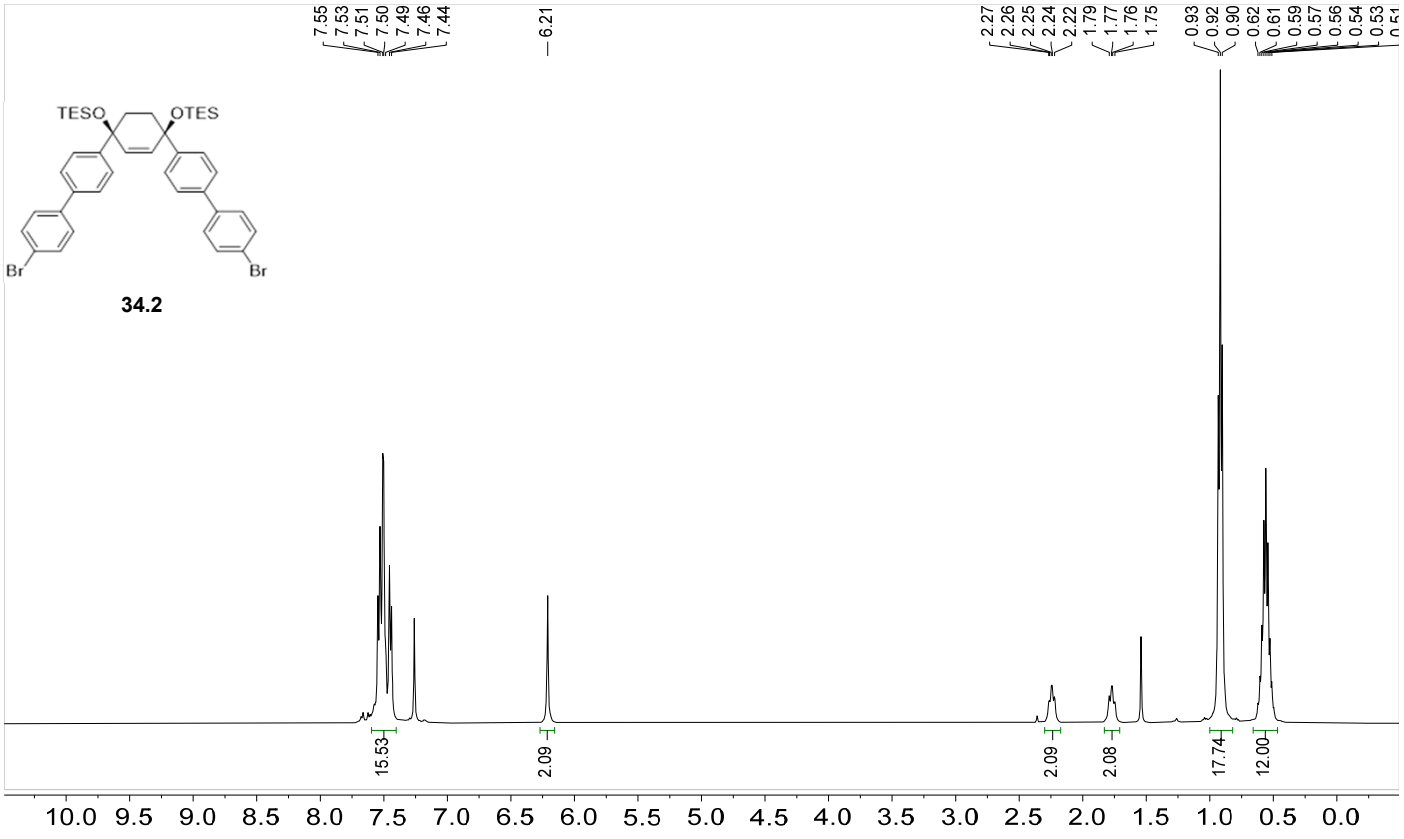
7.55
7.53
7.51
7.50
7.49
7.46
7.44
6.21
2.27
2.26
2.25
2.24
2.22
1.79
1.77
1.76
1.75
0.93
0.92
0.90
0.62
0.61
0.59
0.57
0.56
0.54
0.53
TESO
OTES
Br
Br
15.53
2.09
2.09
2.08
17.74
12.00
10.0 9.5 9.0 8.5 8.0 7.5 7.0 6.5 6.0 5.5 5.0 4.5 4.0 3.5 3.0 2.5 2.0 1.5 1.0 0.5 0.0

34.2

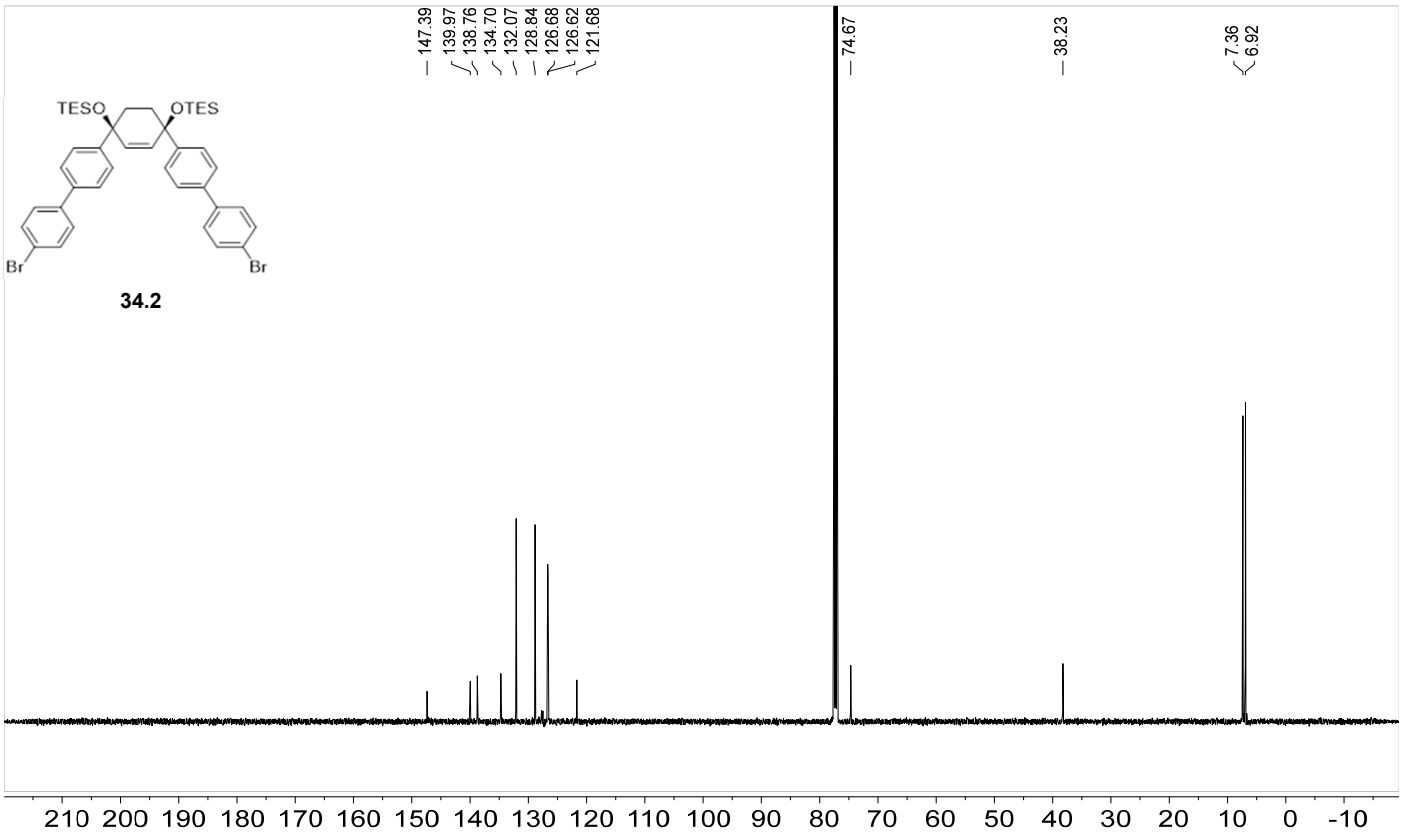
147.39
139.97
138.76
134.70
132.07
128.84
126.68
126.62
121.68
74.67
38.23
7.36
6.92
TESO
OTES
Br
Br
210 200 190 180 170 160 150 140 130 120 110 100 90 80 70 60 50 40 30 20 10 0 -10

34.2

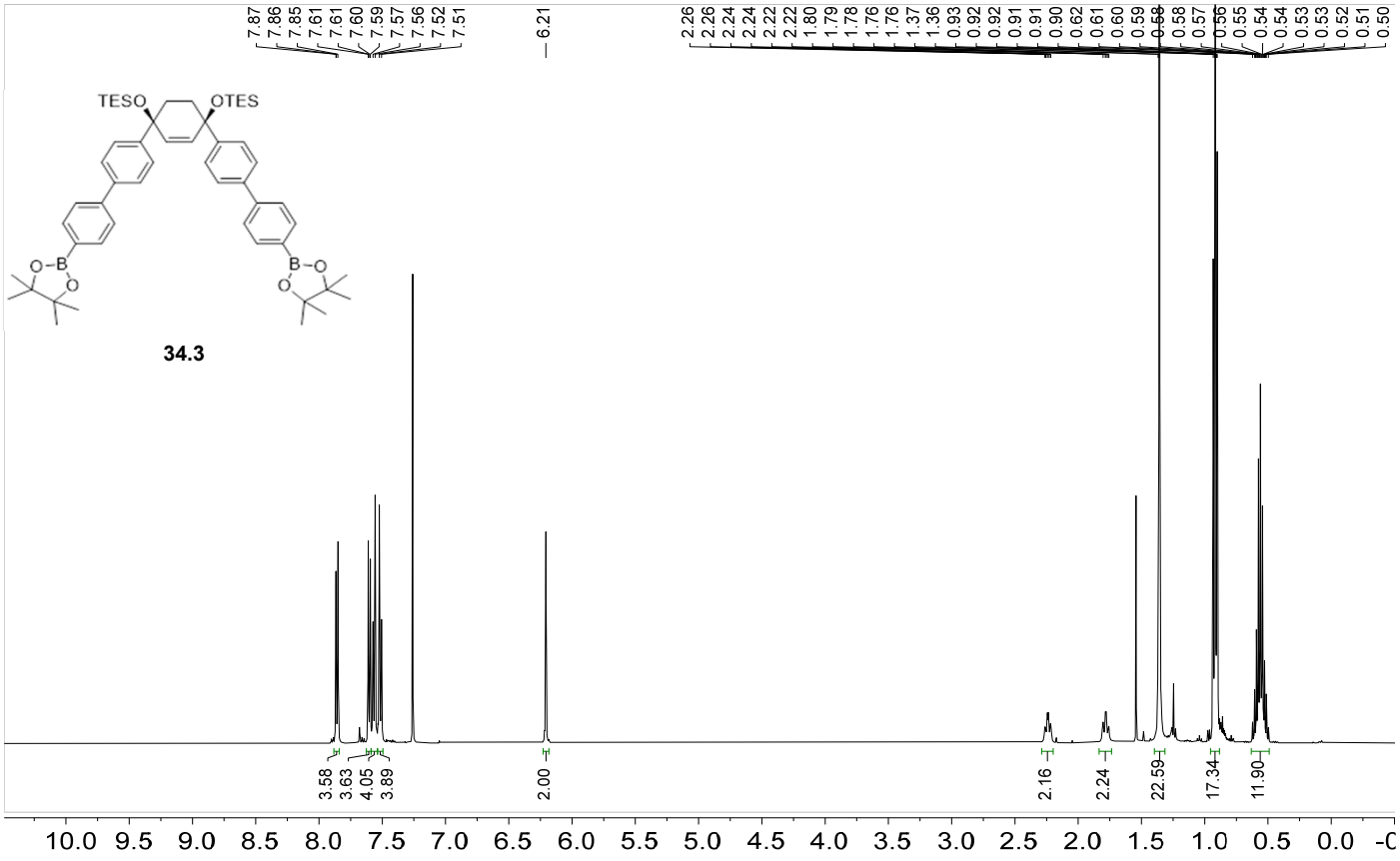
TESO
OTES
O-B
B-O
34.3
7.87
7.86
7.85
7.61
7.61
7.60
7.59
7.57
7.56
7.52
7.51
6.21
2.26
2.26
2.24
2.24
2.22
2.22
1.80
1.79
1.78
1.76
1.76
1.37
1.36
0.93
0.92
0.92
0.91
0.91
0.90
0.62
0.61
0.60
0.59
0.58
0.58
0.57
0.56
0.55
0.54
0.54
0.53
0.53
0.52
0.51
0.50
3.58
3.63
4.05
3.89
2.00
2.16
2.24
22.59
17.34
11.90
10.0 9.5 9.0 8.5 8.0 7.5 7.0 6.5 6.0 5.5 5.0 4.5 4.0 3.5 3.0 2.5 2.0 1.5 1.0 0.5 0.0 -0

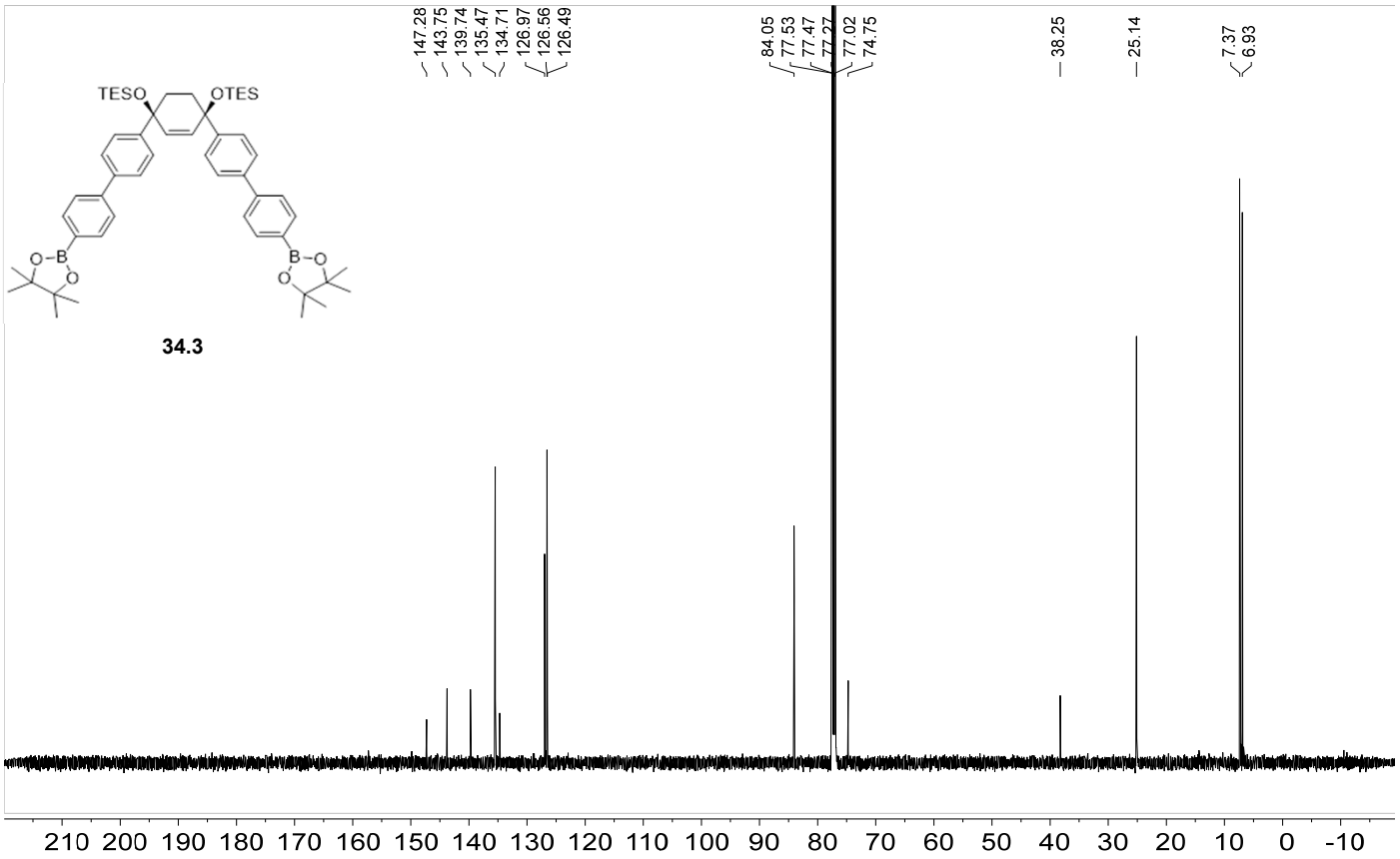
TESO
OTES
O-B
B-O
34.3
147.28
143.75
139.74
135.47
134.71
126.97
126.56
126.49
84.05
77.53
77.47
77.27
77.02
74.75
38.25
25.14
7.37
6.93
210 200 190 180 170 160 150 140 130 120 110 100 90 80 70 60 50 40 30 20 10 0 -10

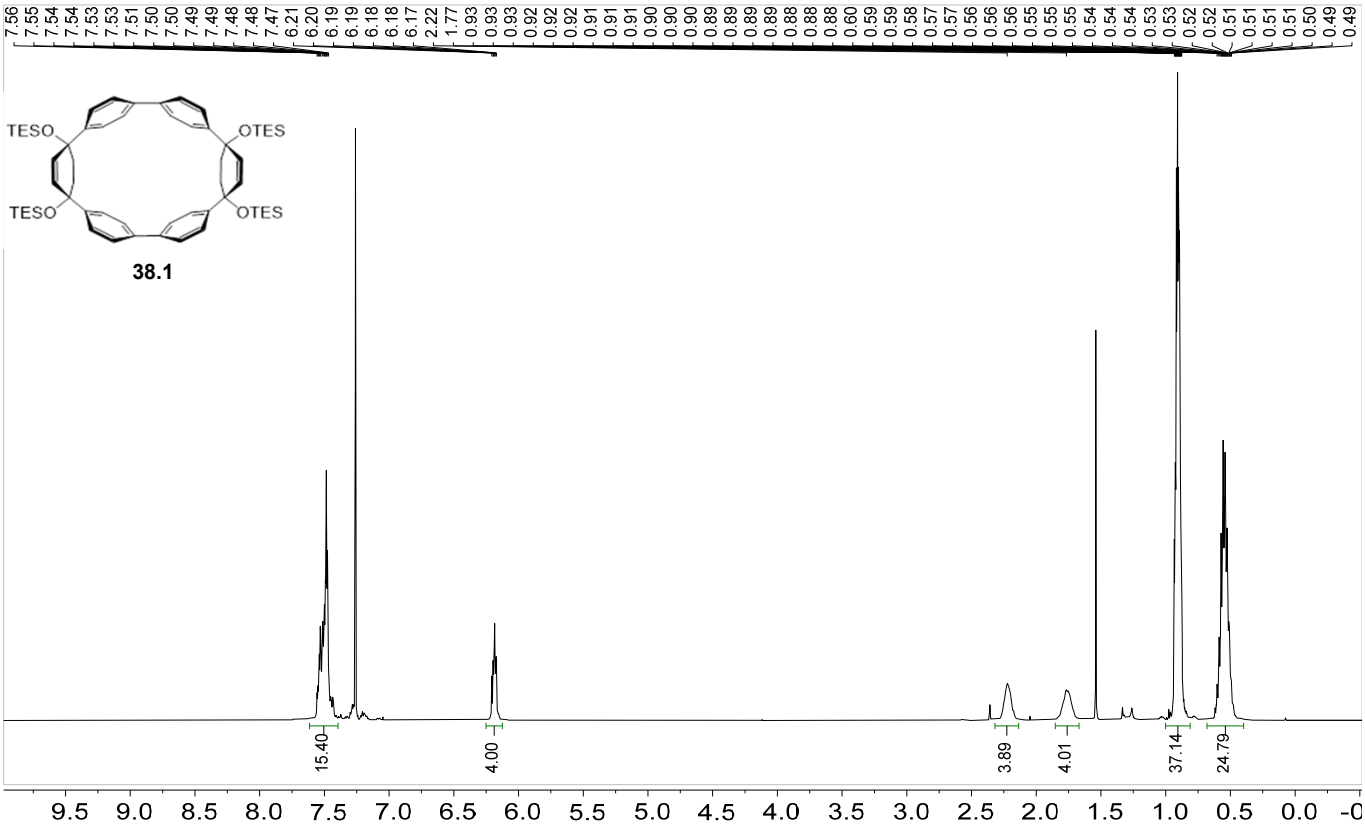
TESO
OTES
TESO
OTES
38.1
15.40
4.00
3.89
4.01
37.14
24.79

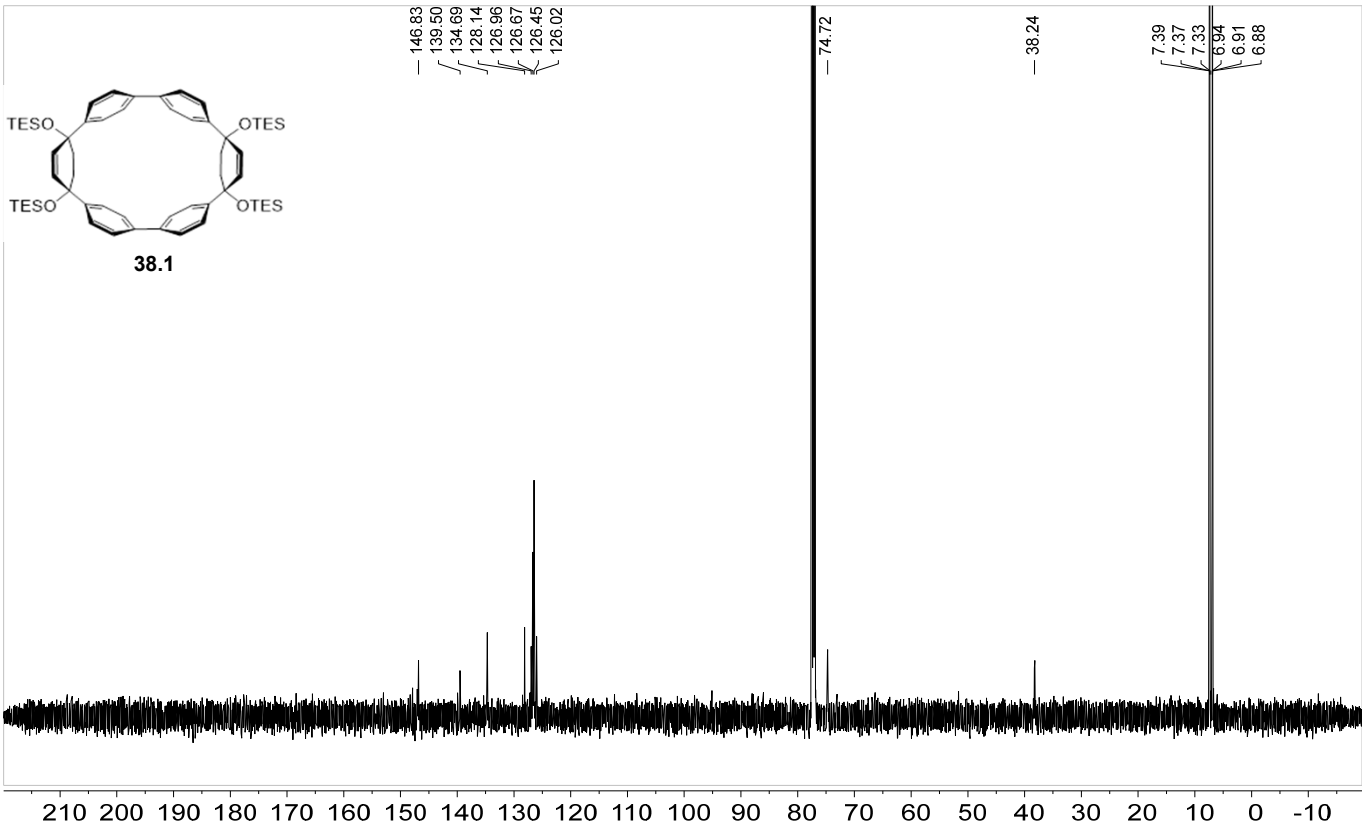
TESO
OTES
TESO
OTES
38.1
146.83
139.50
134.69
128.14
126.96
126.67
126.45
126.02
74.72
38.24
7.39
7.37
7.33
6.94
6.91
6.88

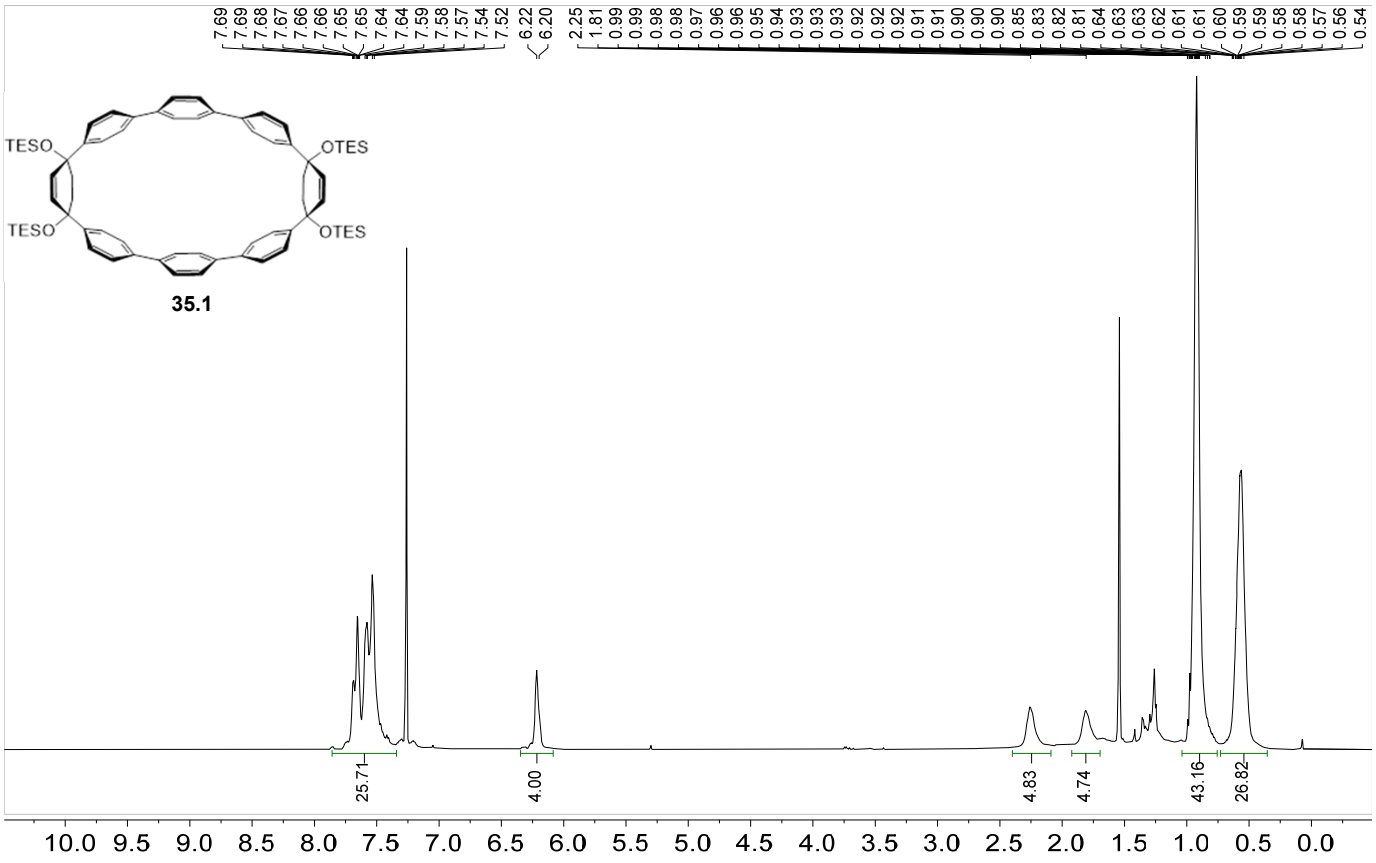
TESO
OTES
TESO
OTES
35.1
7.69 7.69 7.68 7.67 7.66 7.66 7.65 7.65 7.64 7.64 7.59 7.58 7.57 7.54 7.52 6.22 6.20
2.25 1.81 0.99 0.99 0.98 0.98 0.97 0.96 0.96 0.95 0.94 0.93 0.93 0.92 0.92 0.92 0.91 0.91 0.90 0.90 0.90 0.85 0.83 0.82 0.81 0.64 0.63 0.63 0.62 0.61 0.61 0.60 0.59 0.59 0.58 0.58 0.57 0.56 0.54
25.71
4.00
4.83
4.74
43.16
26.82
10.0 9.5 9.0 8.5 8.0 7.5 7.0 6.5 6.0 5.5 5.0 4.5 4.0 3.5 3.0 2.5 2.0 1.5 1.0 0.5 0.0

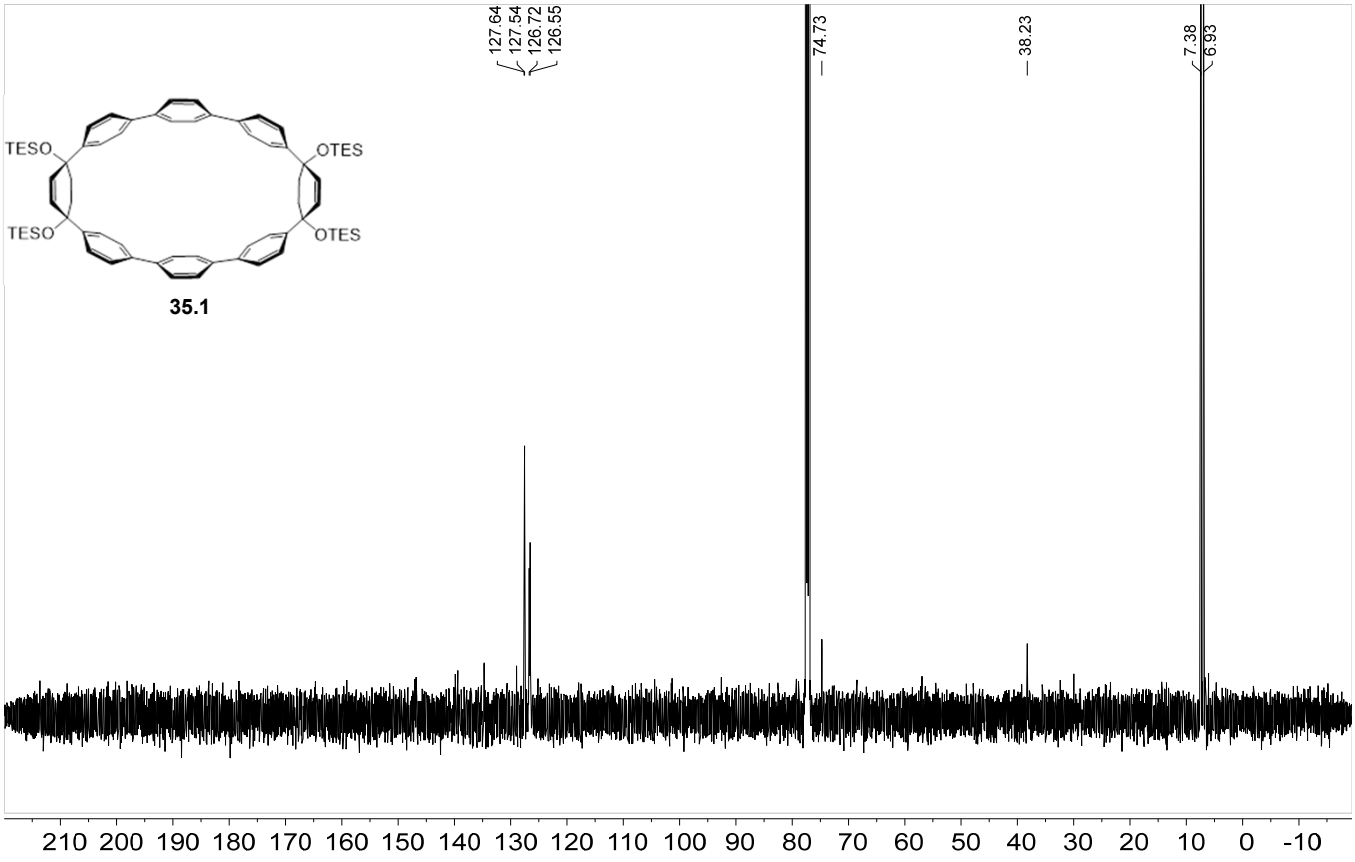
TESO
OTES
TESO
OTES
35.1
127.64
127.54
126.72
126.55
74.73
38.23
7.38
6.93
210 200 190 180 170 160 150 140 130 120 110 100 90 80 70 60 50 40 30 20 10 0 -10

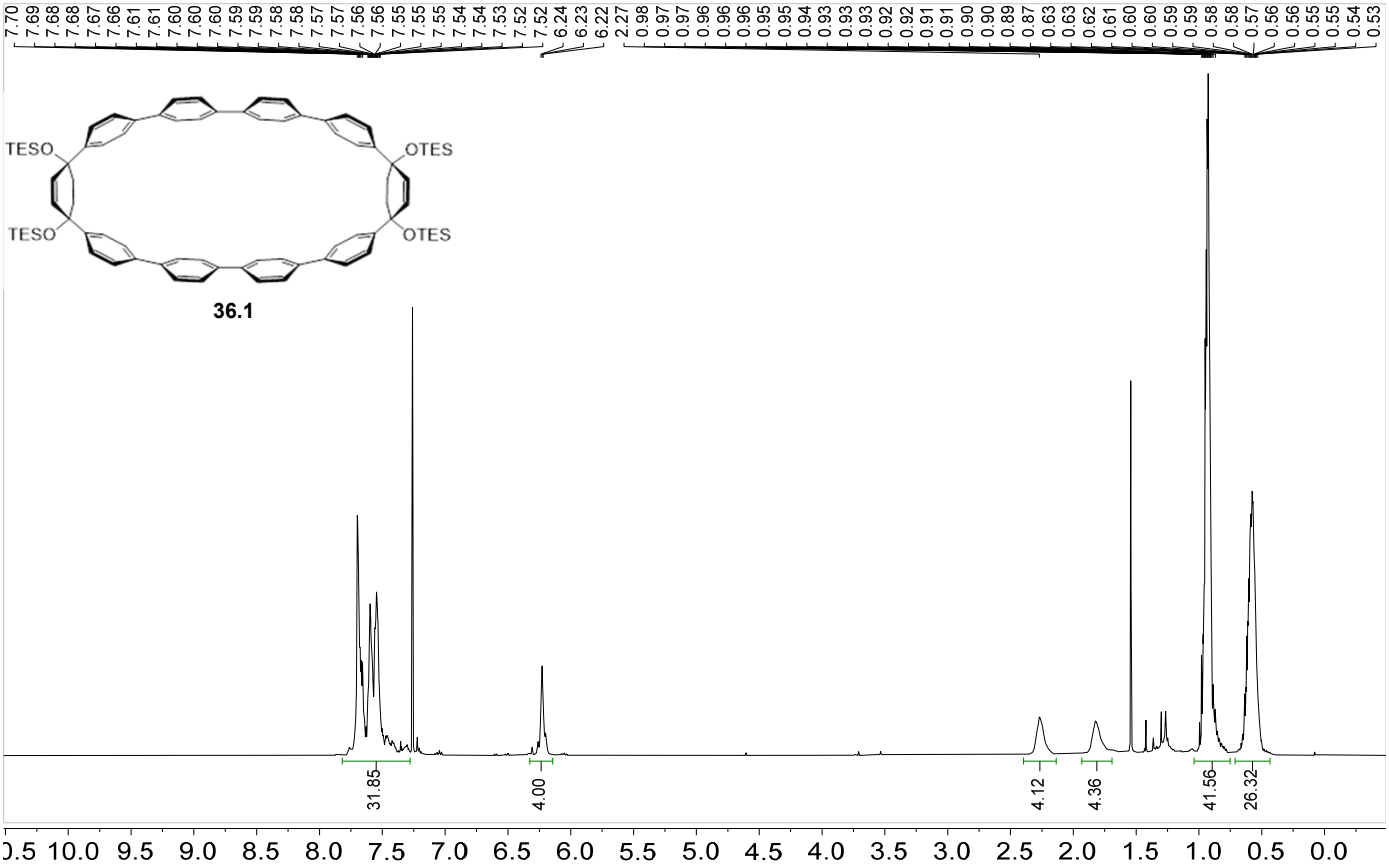
TESO
OTES
TESO
OTES
36.1
31.85
4.00
4.12
4.36
41.56
26.32

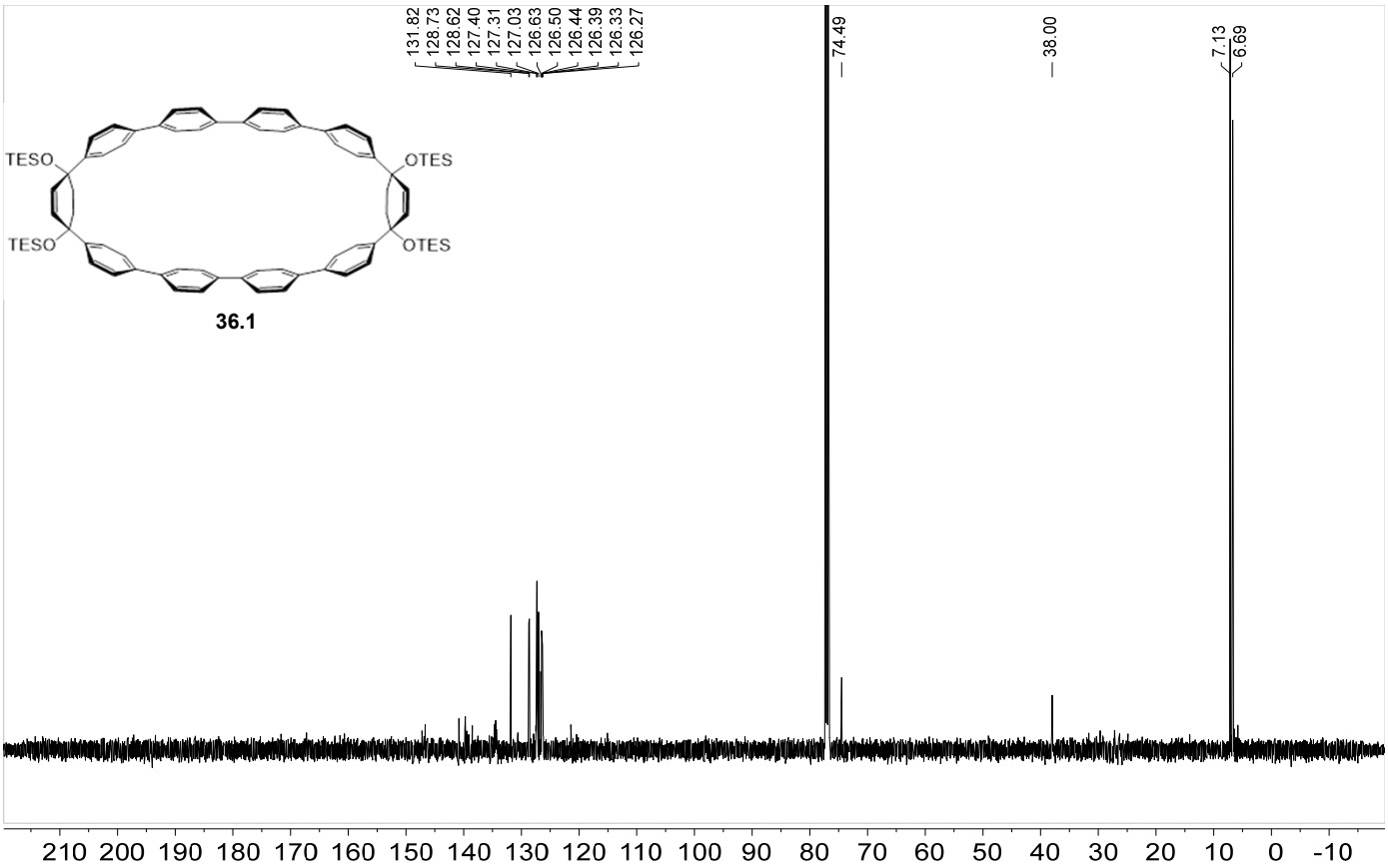
TESO
OTES
TESO
OTES
36.1
74.49
38.00
7.13
6.69

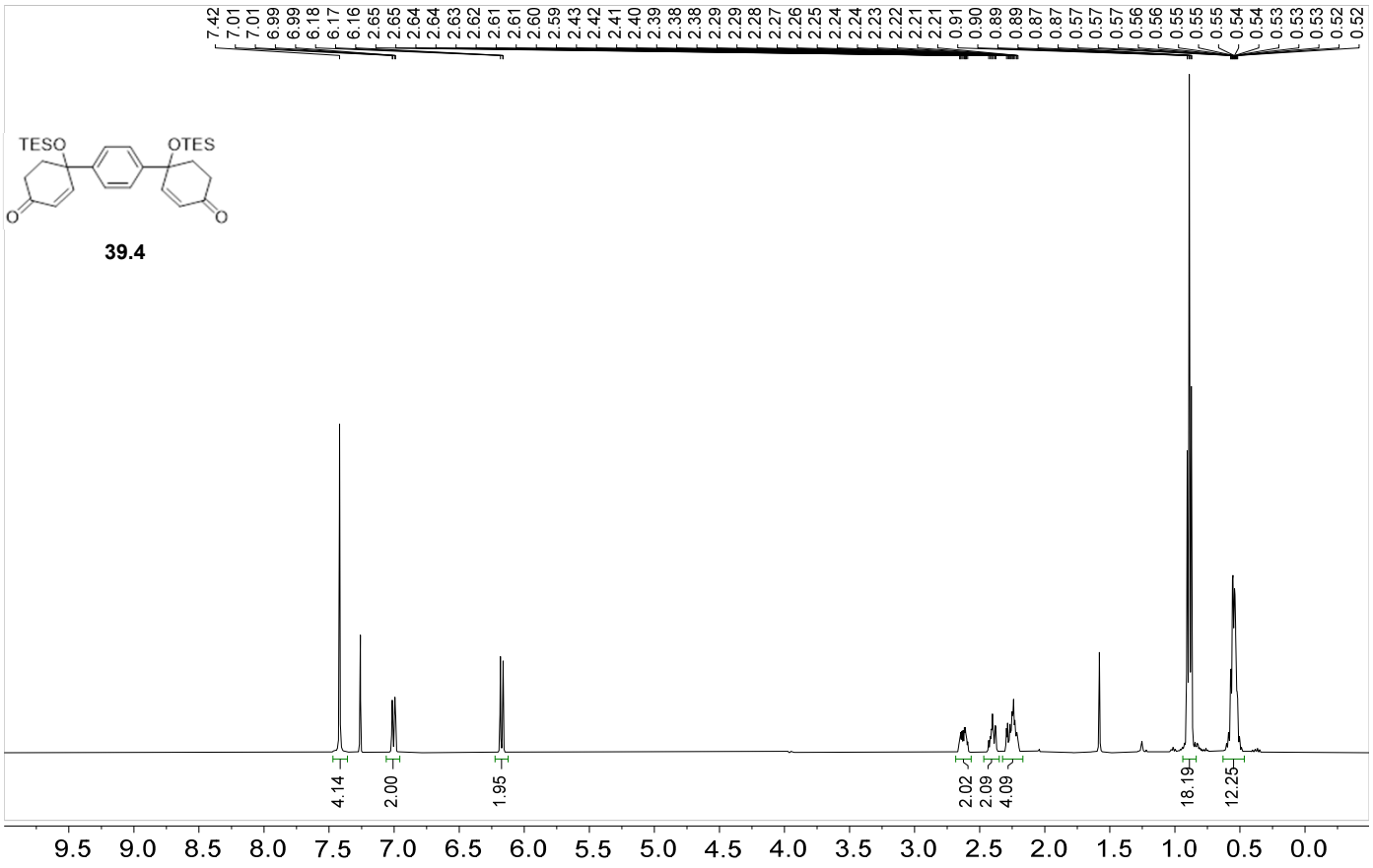
TESO
OTES
O
O
39.4
4.14
2.00
1.95
2.02
2.09
4.09
18.19
12.25

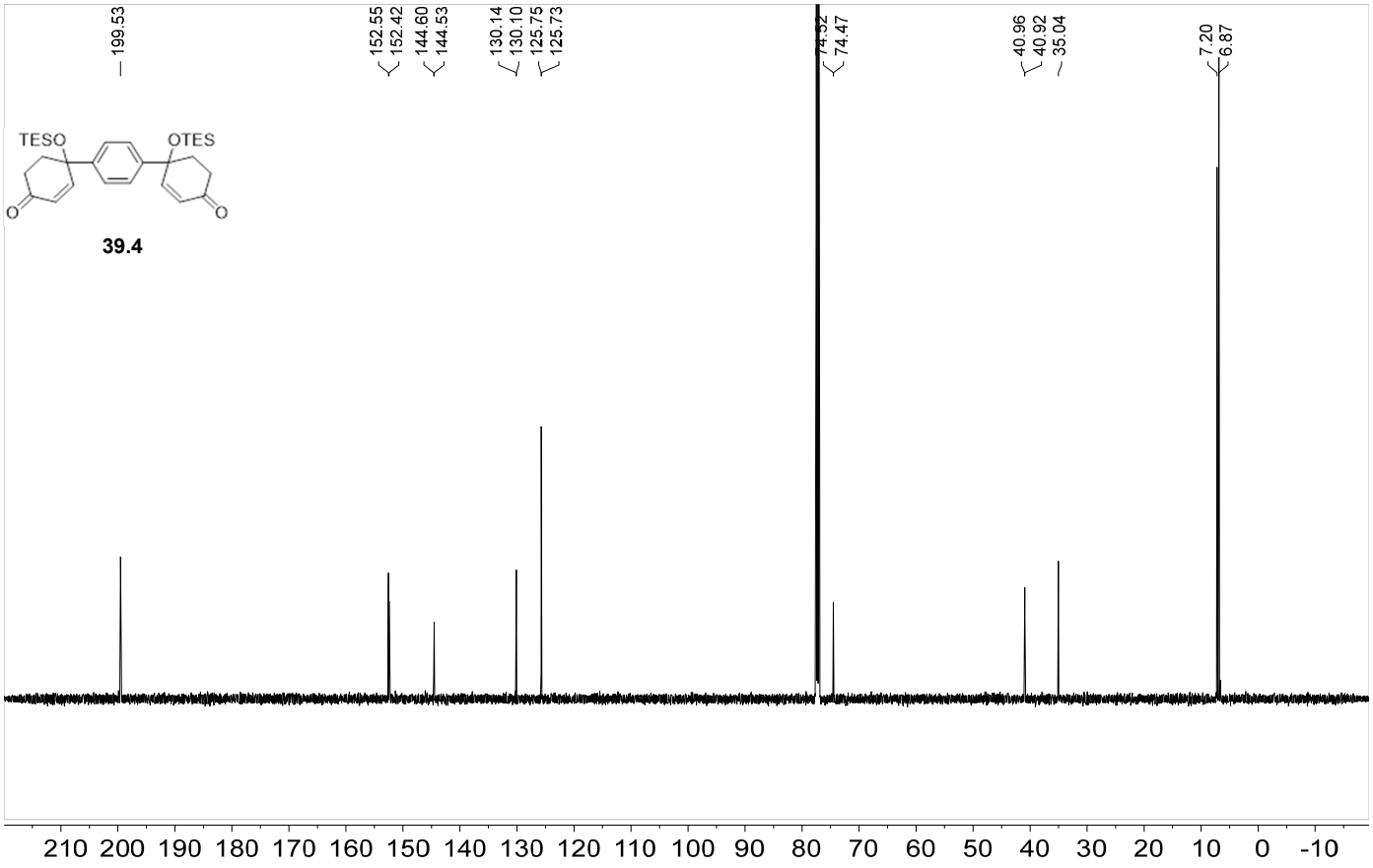
199.53
152.55
152.42
144.60
144.53
130.14
130.10
125.75
125.73
74.52
74.47
40.96
40.92
35.04
7.20
6.87
TESO
OTES
O
O
39.4

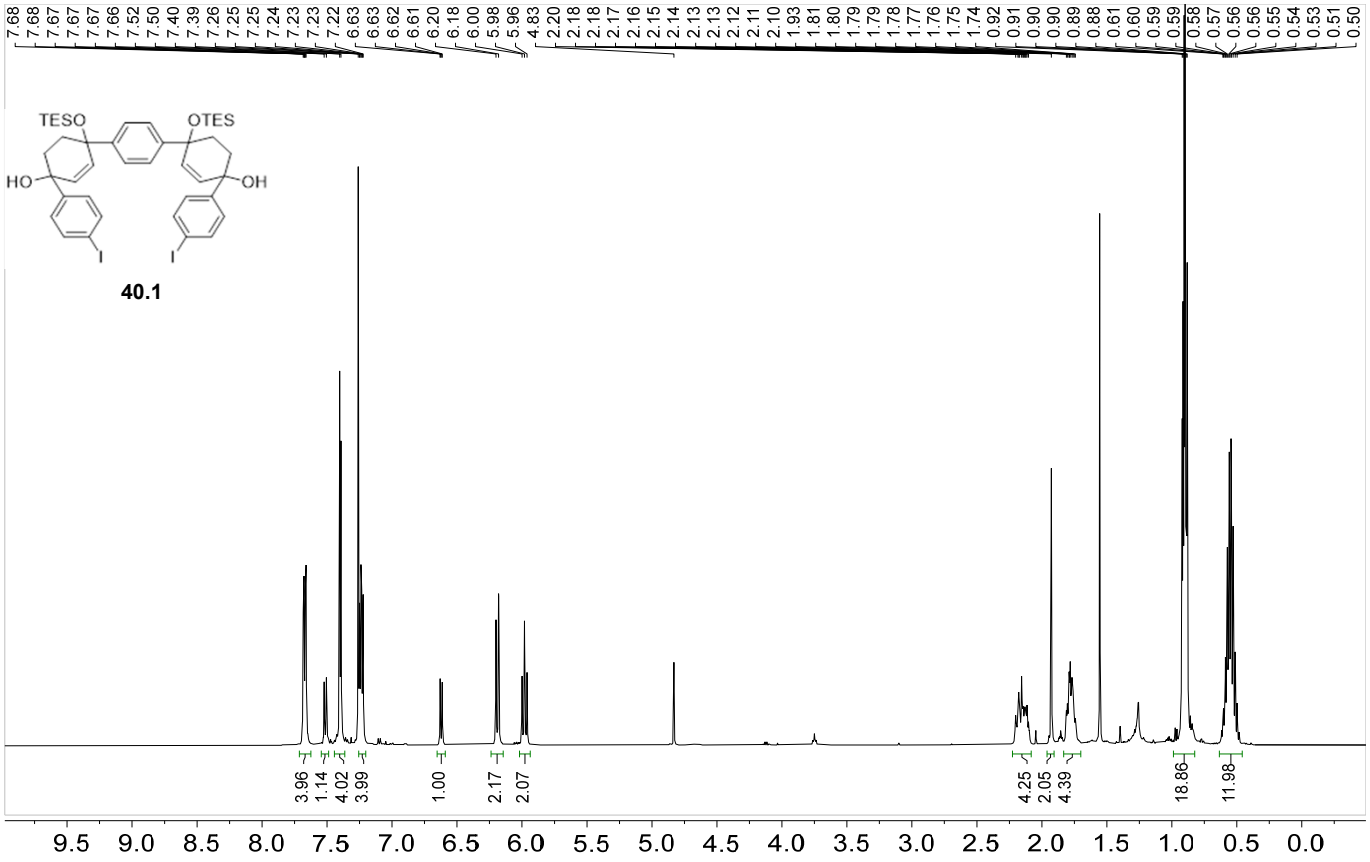
TESO
OTES
HO
OH
I
I
40.1

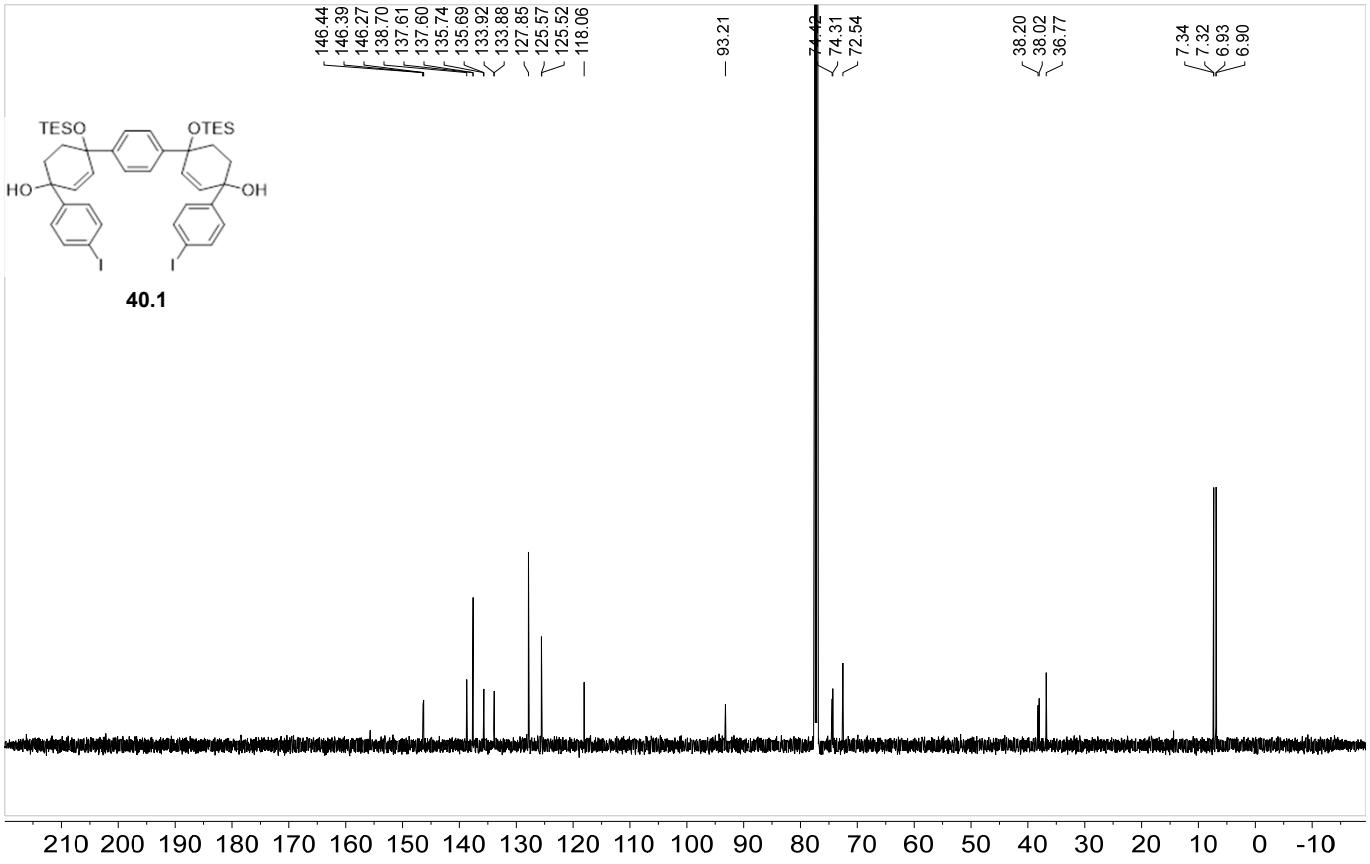
TESO
OTES
HO
OH
I
I
40.1

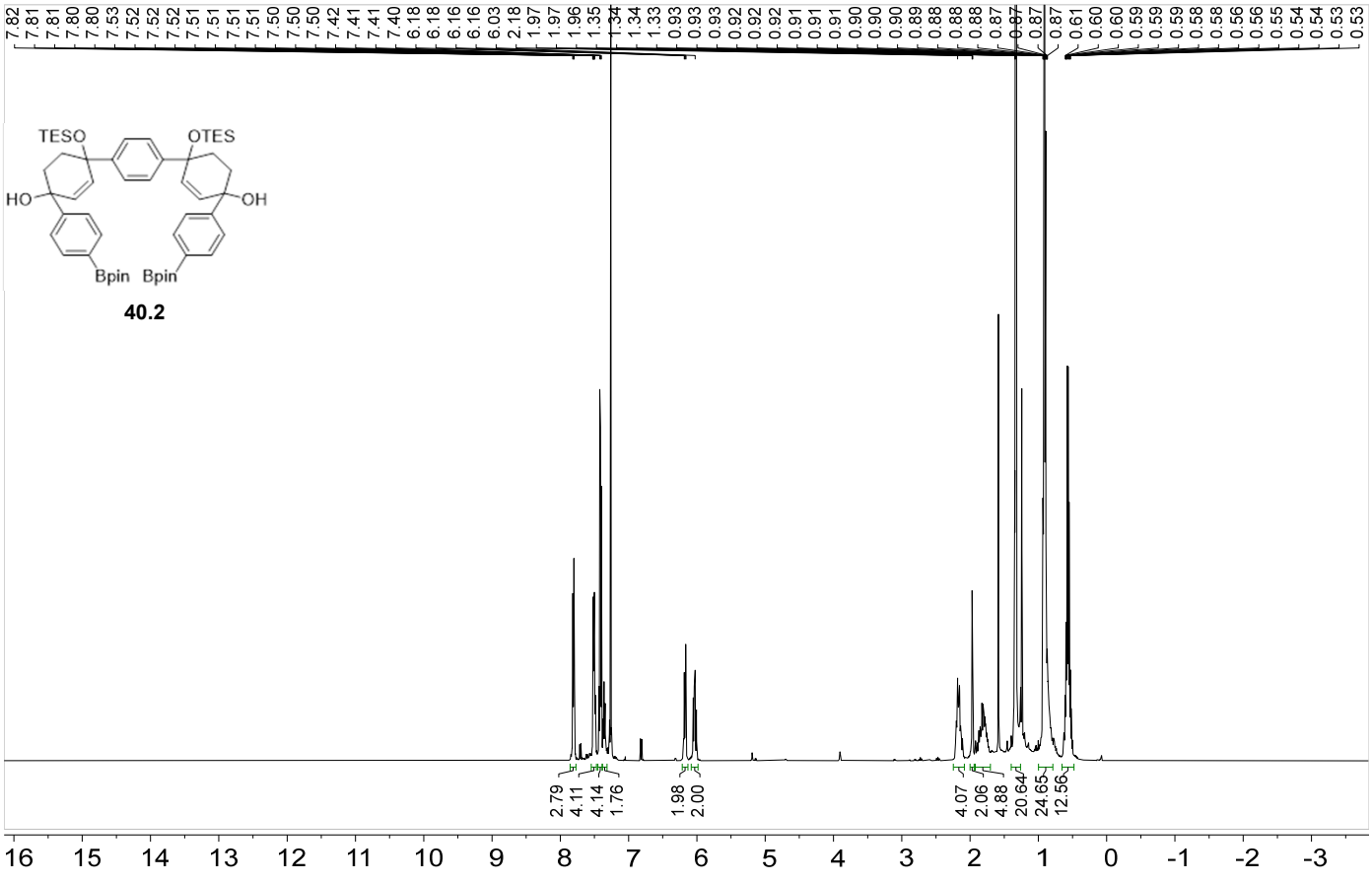

40.2

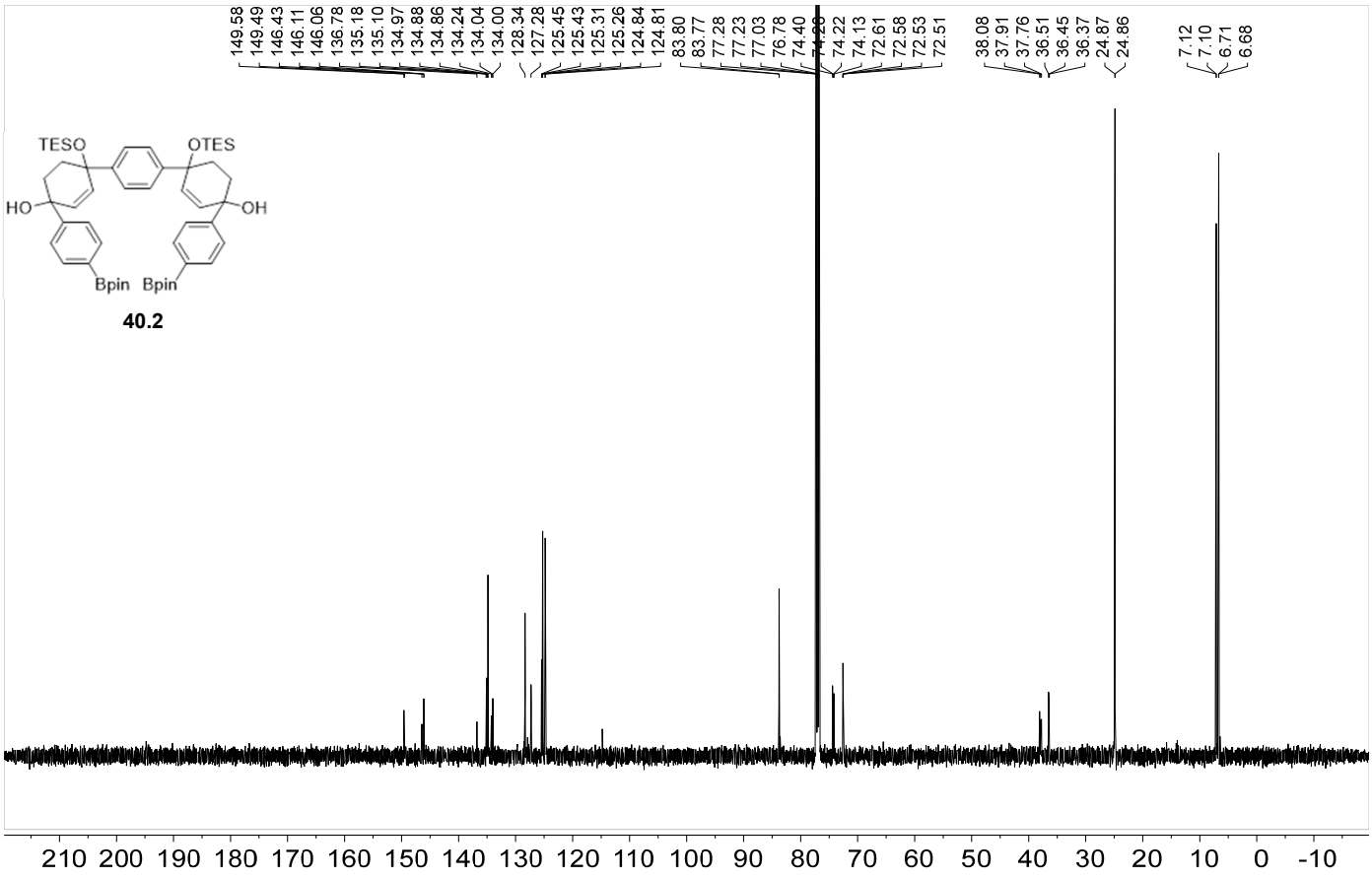

40.2

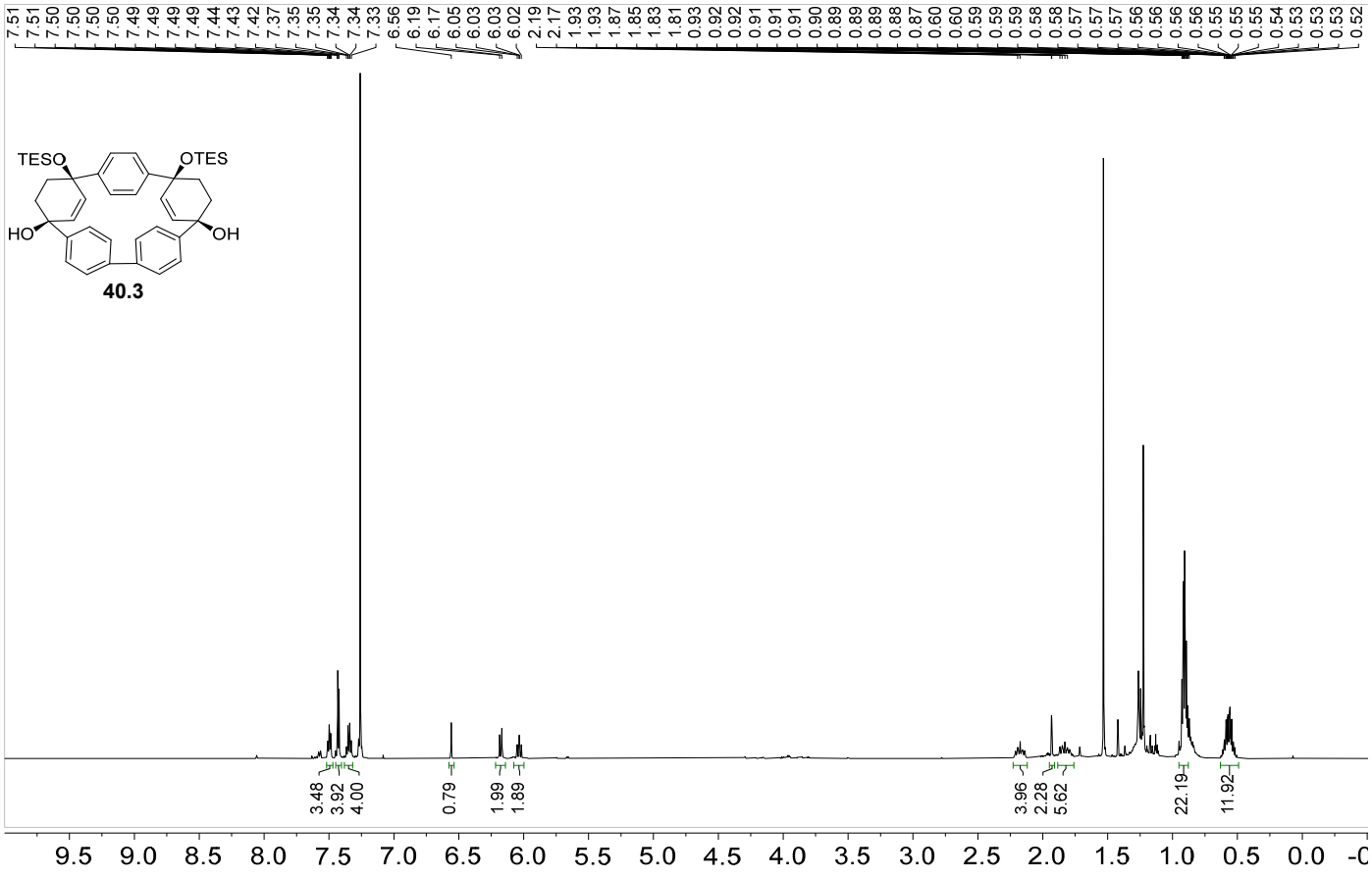
TESO
OTES
HO
OH
40.3

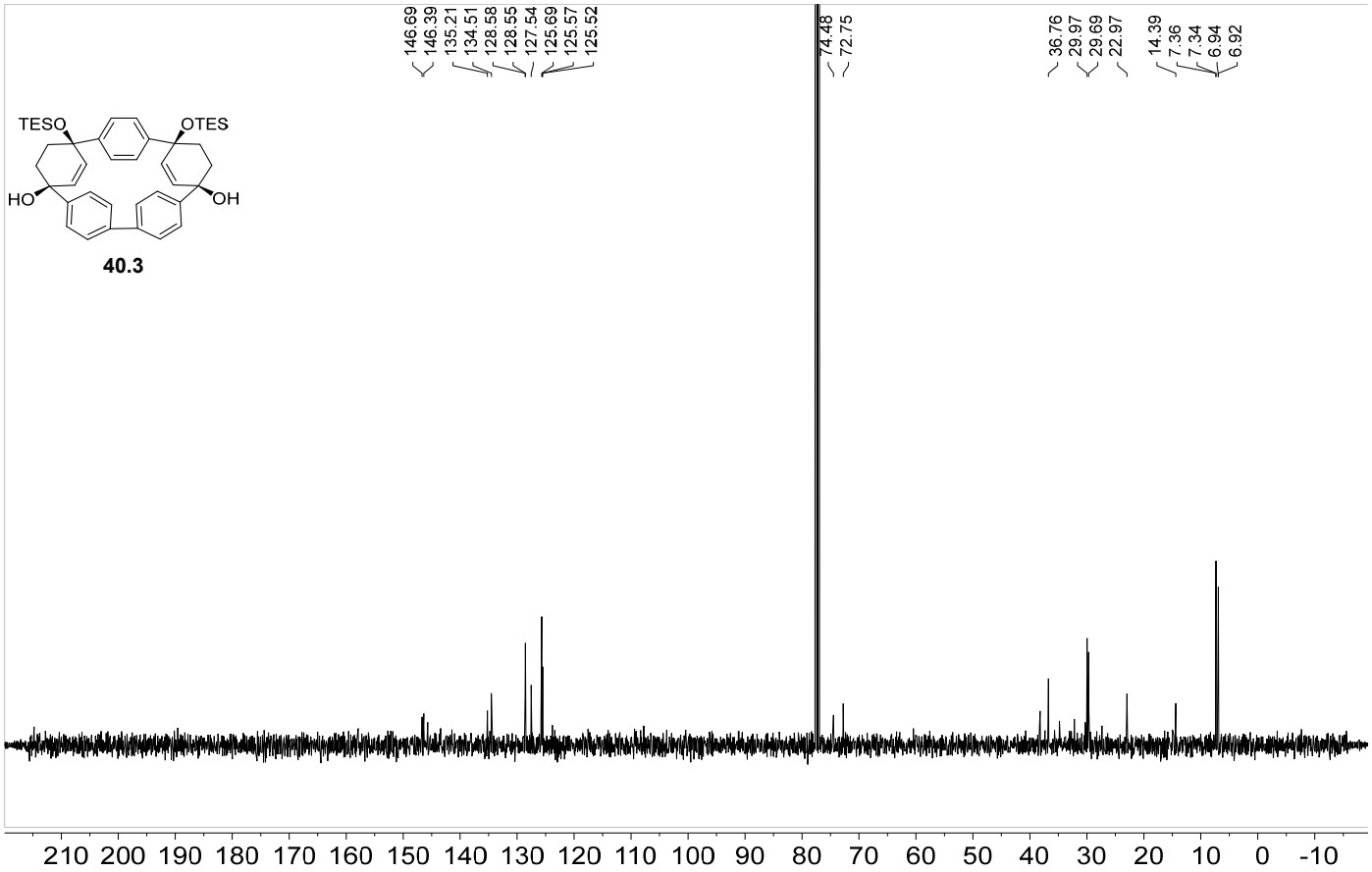
TESO
OTES
HO
OH
40.3

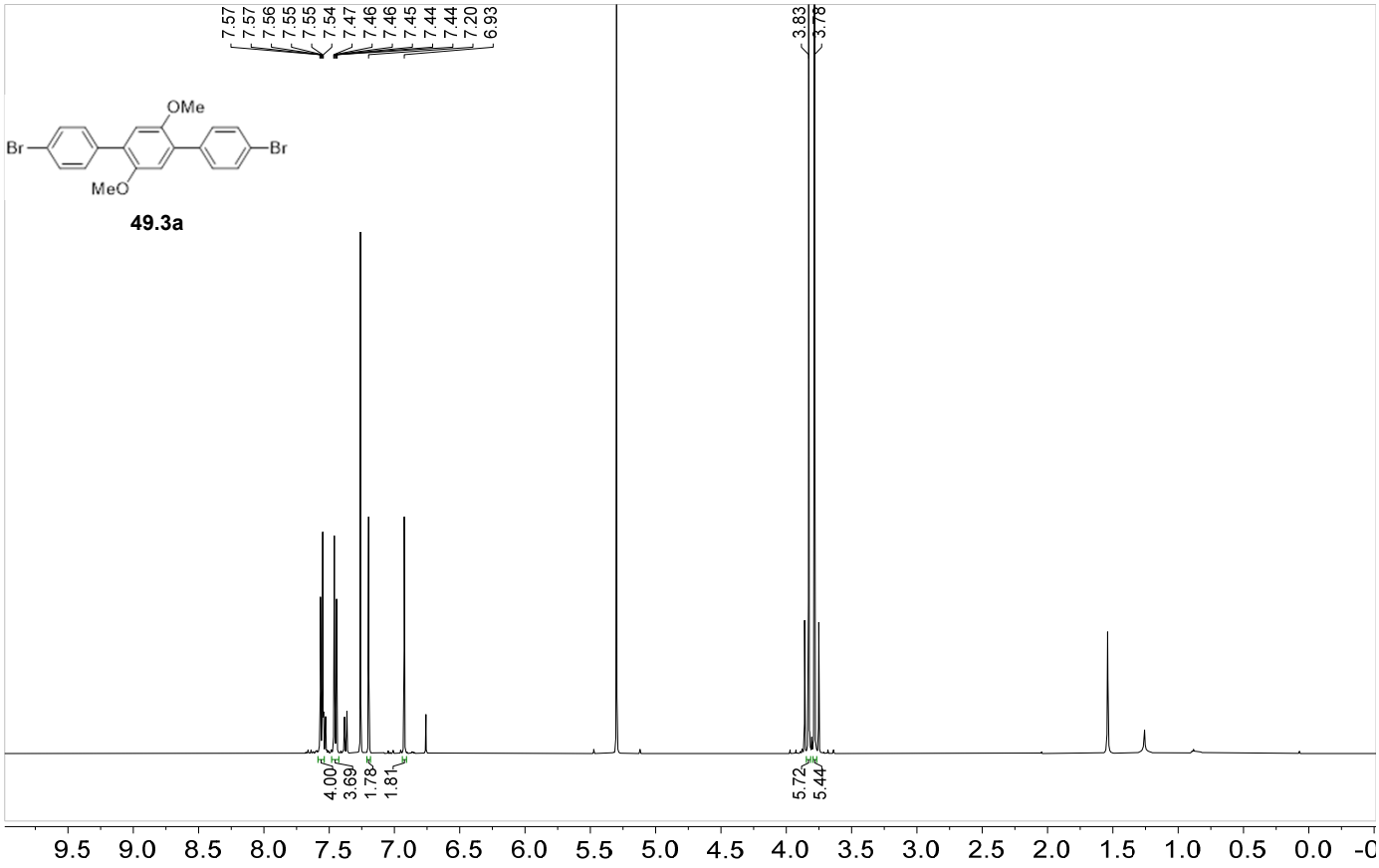
7.57
7.57
7.56
7.55
7.55
7.54
7.47
7.46
7.46
7.45
7.44
7.44
7.20
6.93
3.83
3.78
OMe
Br
Br
MeO
49.3a
4.00
3.69
1.78
1.81
5.72
5.44
9.5 9.0 8.5 8.0 7.5 7.0 6.5 6.0 5.5 5.0 4.5 4.0 3.5 3.0 2.5 2.0 1.5 1.0 0.5 0.0

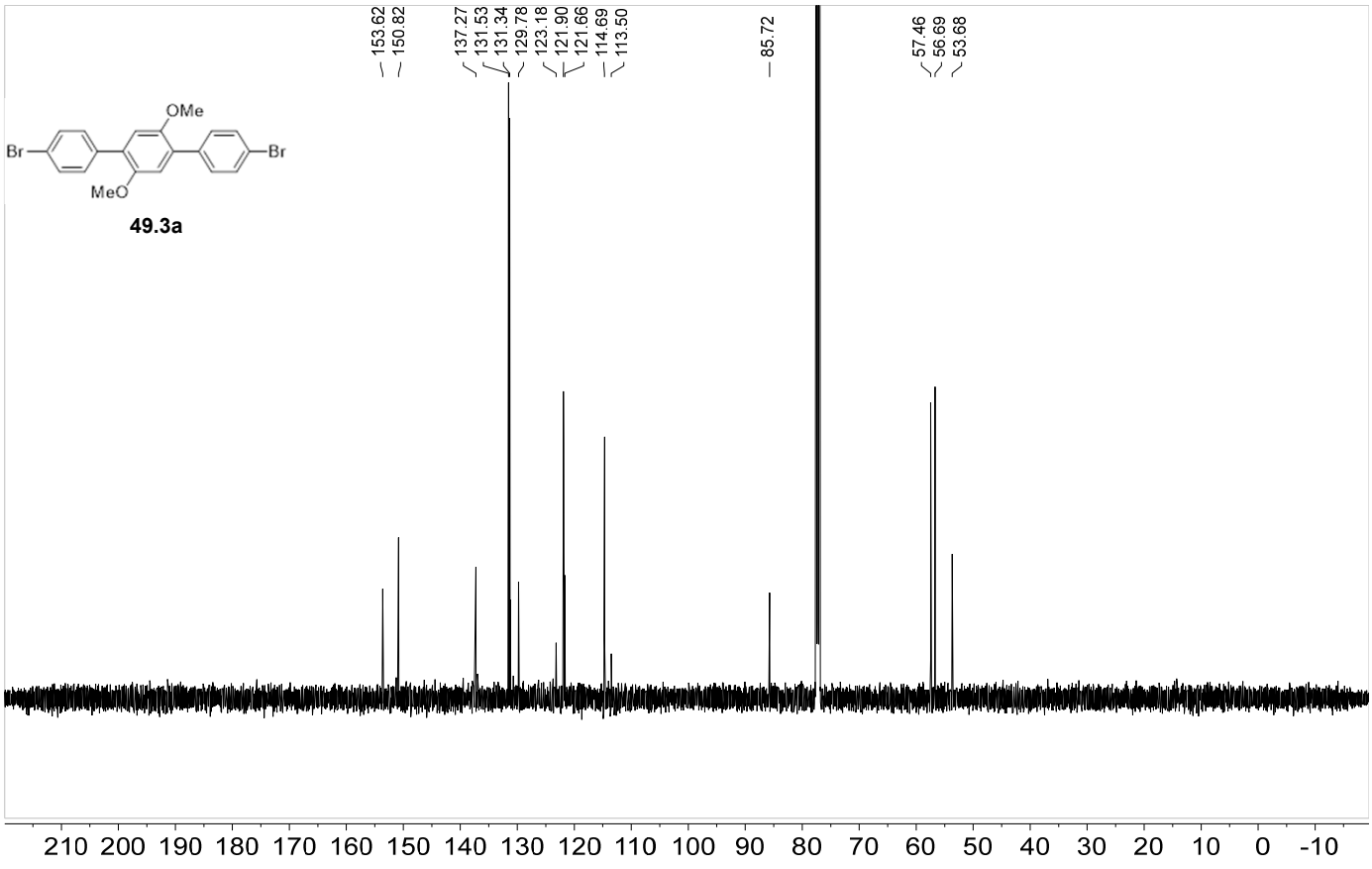
153.62
150.82
137.27
131.53
131.34
129.78
123.18
121.90
121.66
114.69
113.50
85.72
57.46
56.69
53.68
OMe
Br
Br
MeO
49.3a
210 200 190 180 170 160 150 140 130 120 110 100 90 80 70 60 50 40 30 20 10 0 -10

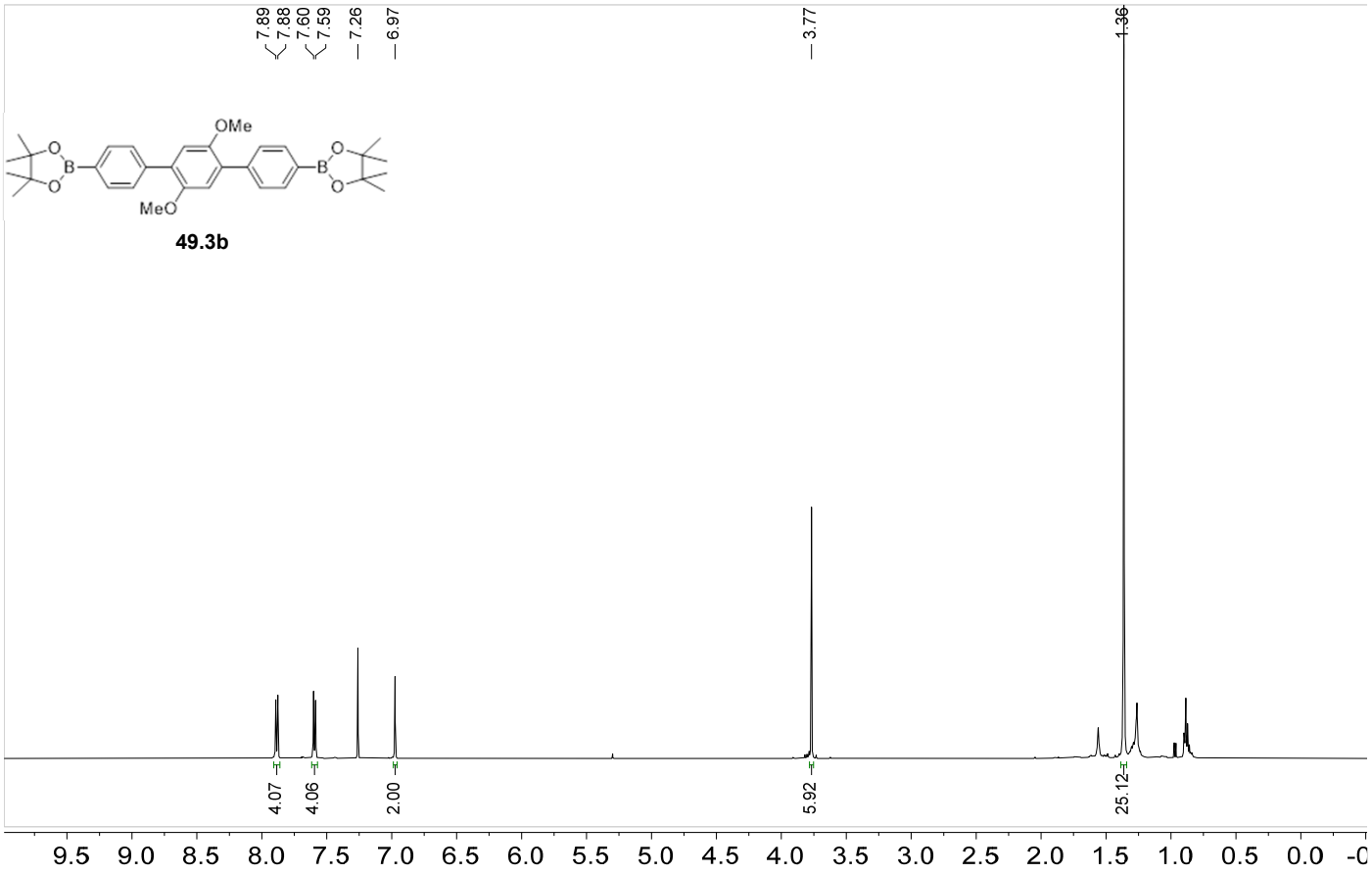
7.89
7.88
7.60
7.59
7.26
6.97
3.77
1.36
OMe
MeO
B
O
4.07
4.06
2.00
5.92
25.12
9.5 9.0 8.5 8.0 7.5 7.0 6.5 6.0 5.5 5.0 4.5 4.0 3.5 3.0 2.5 2.0 1.5 1.0 0.5 0.0

49.3b

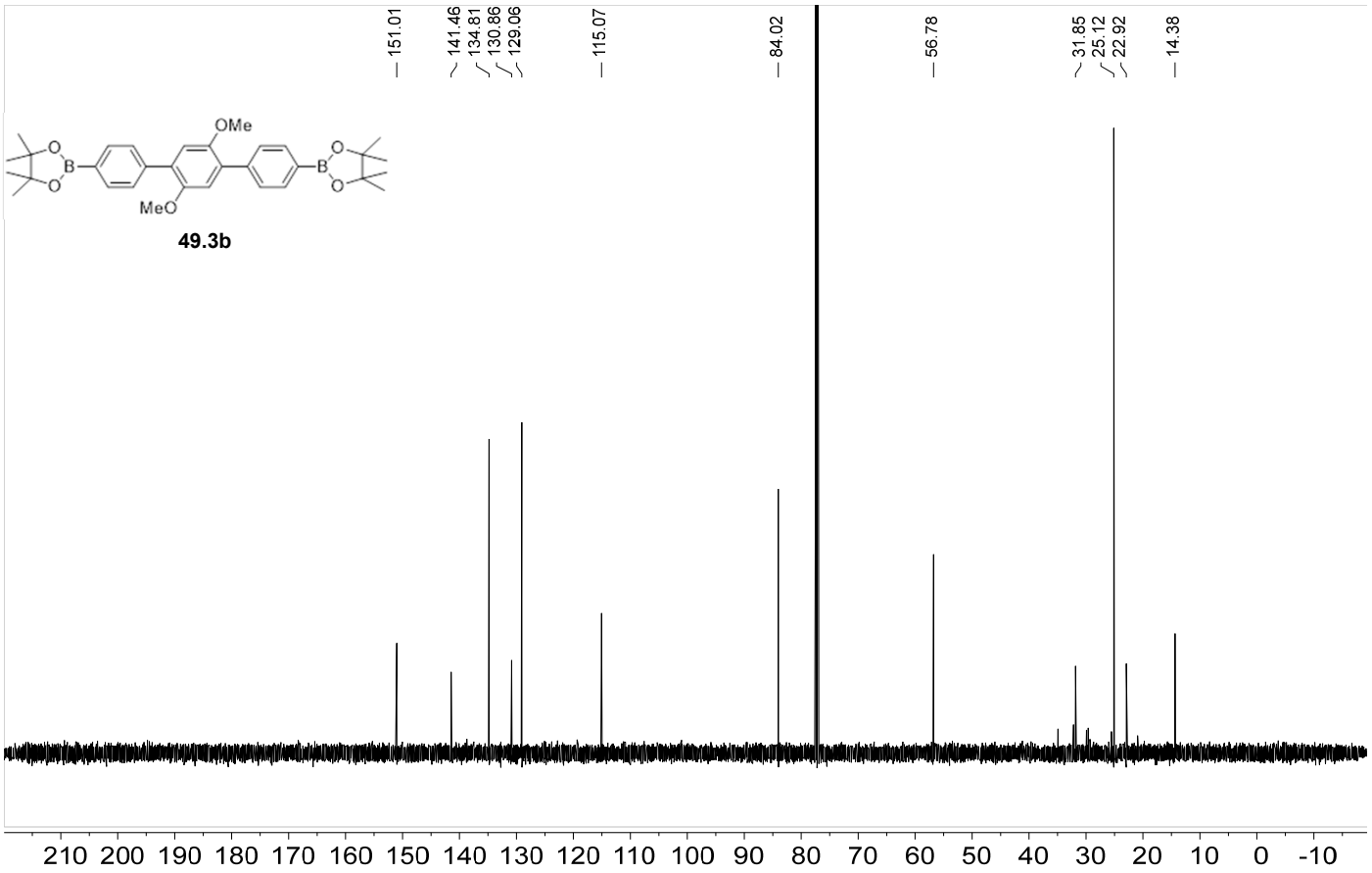
151.01
141.46
134.81
130.86
129.06
115.07
84.02
56.78
31.85
25.12
22.92
14.38
OMe
MeO
B
O
210 200 190 180 170 160 150 140 130 120 110 100 90 80 70 60 50 40 30 20 10 0 -10

49.3b

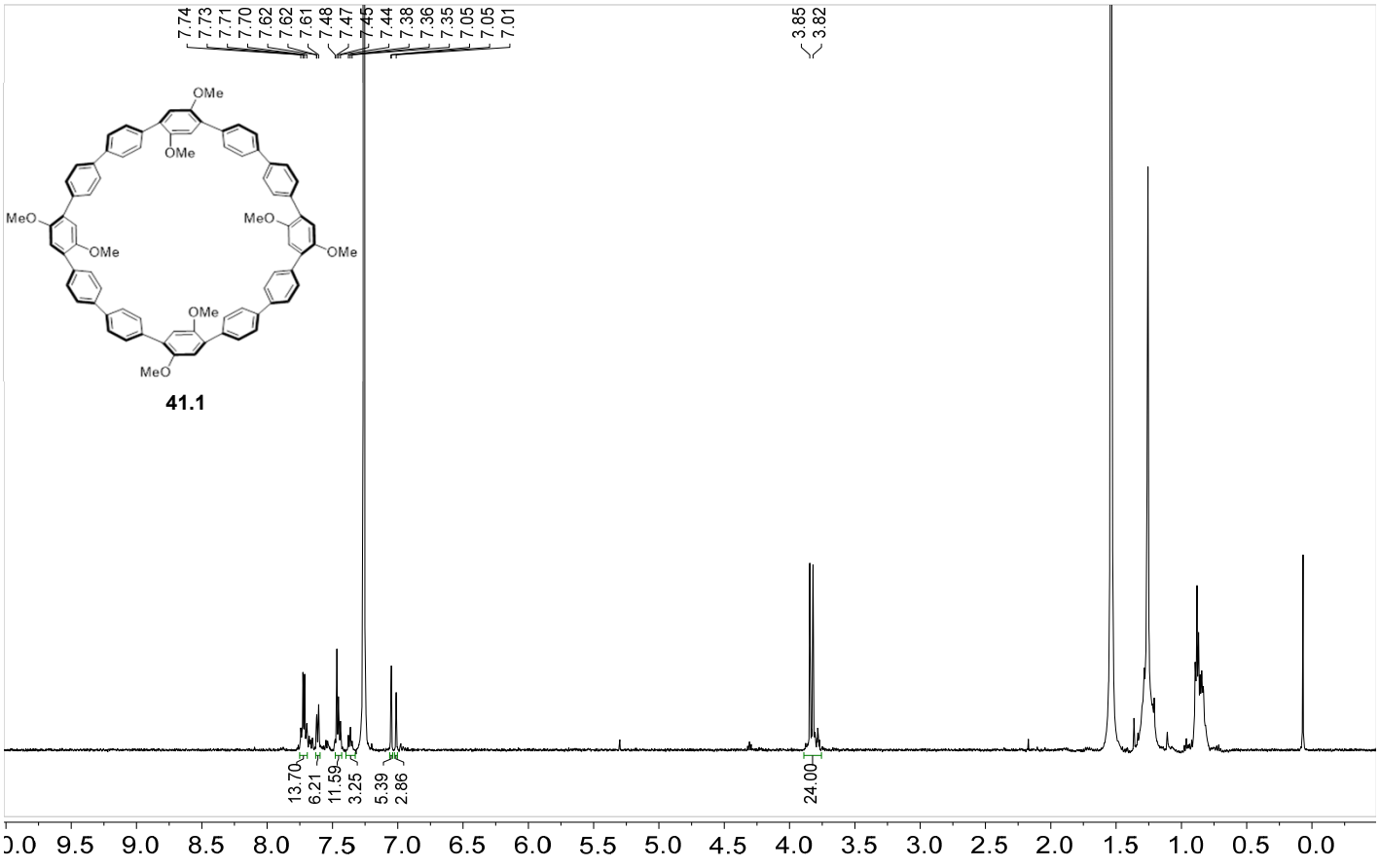
7.74
7.73
7.71
7.70
7.62
7.62
7.61
7.48
7.47
7.45
7.44
7.38
7.36
7.35
7.05
7.05
7.01
3.85
3.82
OMe
OMe
MeO
OMe
MeO
OMe
OMe
MeO
13.70
6.21
11.59
3.25
5.39
2.86
24.00
0.0 9.5 9.0 8.5 8.0 7.5 7.0 6.5 6.0 5.5 5.0 4.5 4.0 3.5 3.0 2.5 2.0 1.5 1.0 0.5 0.0

41.1

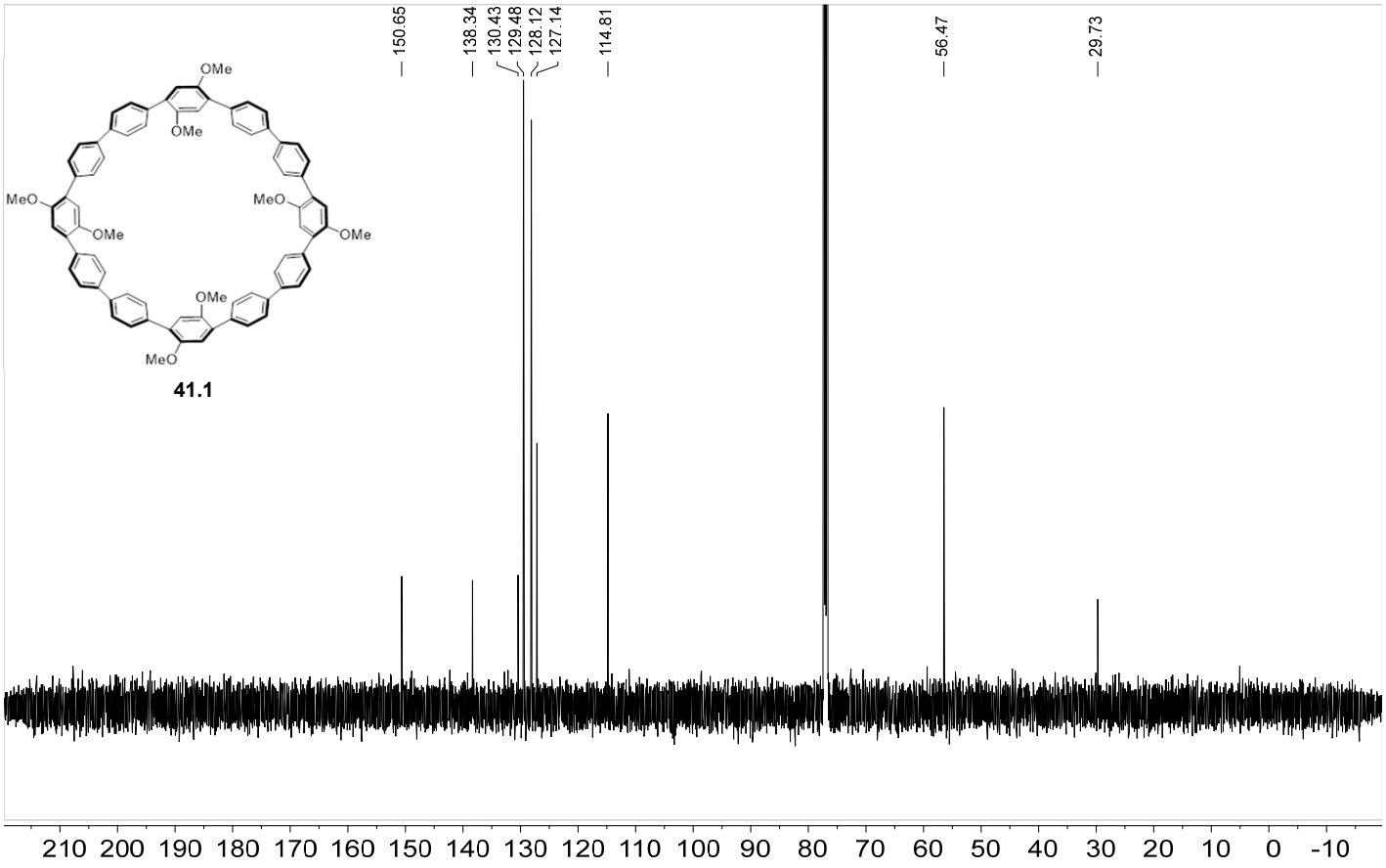
150.65
138.34
130.43
129.48
128.12
127.14
114.81
56.47
29.73
OMe
OMe
MeO
OMe
MeO
OMe
OMe
MeO
210 200 190 180 170 160 150 140 130 120 110 100 90 80 70 60 50 40 30 20 10 0 -10

41.1